New Tripodal Ligands for Asymmetric Catalysis

Sarah Resouly

Thesis Presented for the Degree of Doctor of Philosophy

The University of Edinburgh

2003

Acknowledgements

There are so many people to whom I am greatly indebted to for all their help and support, without which, life would have been so very much harder.

Firstly I would like to thank my supervisor Dr. Philip Bailey for all his help, encouragement and eternal optimism. In particular, for giving me the opportunity to experience some organic chemistry in Stockholm.

A special thank you goes to Dr. Tim Higgs, for his endless supply of advice, ideas and assistance.

Thanks to the crystallography service, and in particular Iain, for all their expertise, and support whilst I learnt to deal with rejection. Thanks must also go to the technical staff of the Chemistry Department for their skill and helpfulness. In particular John Millar for running NMR spectra, Alan Taylor for mass spectroscopy and Lorna Eades for elemental analysis.

Away from Edinburgh, I would like to thank Prof. Christina Moberg for letting me come and work in her lab and showing me a different aspect of C_3 chemistry.

Jag skulle också vilja tacka alla Ki, Fredrik Lake, Fredrik Rahm och Erik Risberg utan som, jag kunde inte sluta min avhandling.

Finally, a special thank you goes to all my friends and family for all their support and for keeping me smiling, without whom I definitely would not have reached this stage.

Abstract

The design and synthesis of novel tripodal ligands are considered. The ligands contain a central (bridgehead) atom connected to three donor atoms by two linker atoms and have the potential to form C_3 symmetric metal complexes, suitable for use as asymmetric catalysts. Systems with different bridgehead atoms (phosphorus, carbon, nitrogen and tin), donor atoms (oxygen, sulphur, nitrogen and phosphorus) and degrees of flexibility of the linker groups (sp^2 and sp^3) are described.

Tris(2-mercaptophenyl)phosphine oxide and tris(2-hydroxyphenyl)phosphine oxide were synthesised and characterised. The X-ray crystal structure of the latter is reported. Attempts to form complexes with titanium, vanadium, molybdenum, ruthenium and cobalt in which the ligand functions in a tridentate mode were unsuccessful, possibly as a consequence of the coordination of the phosphorus oxide group and, in the case of tris(2-mercaptophenyl)phosphine oxide, oxidation resulting in the formation of inter- and / or intra-molecular disulphide bridges.

Reactions of tris(2-pyridyl*N*-oxide)methanol with $CoCl_2$, $FeCl_3$ and $ZnCl_2$ also failed to generate complexes containing a tridentate ligand. Attempts were made to change the fourth group on the central atom. The hydroxyl group of the ligand precursor tris(2-pyridyl)methanol was exchanged for a chloride and the structure determined by X-ray crystallography. Tris(2-pyridyl)chloromethane was readily converted to tris(2-pyridyl)methane but the selective oxidation of only the three pyridine nitrogen atoms was unsuccessful.

Attempts to alkylate the bridgehead nitrogen atom in tris(benzimidazolylmethyl)amine to prevent this coordinating to the metal as a tetradentate ligand were unsuccessful. The ligand precursor $N(CH_2CO_2H)_3$ was successfully alkylated to form $MeN(CH_2CO_2Me)_3BF_4$ and $EtN(CH_2CO_2Me)_3CF_3SO_3$ and the X-ray structures were determined of both. It was not possible to form the imidazole rings from these precursors without loss of the alkyl group from the bridgehead nitrogen atom.

The structure of [(tris(benzimidazolylmethyl)amine)CoNCS]Cl formed from a material which was assumed to contain *N*-methyltris(benzimidazolylmethyl)amine and confirmed that the un-alkylated ligands readily acts as a tetradentate ligand.

The synthesis of the tripodal tetradentate C_3 symmetric amine, $N(CH_2CH^iPrNHMe)_3$, was optimised and attempts were made to convert this to the phosphoramidite derivative $N(CH_2CH^iPrNPX)_3$, where X is the cyclic diester derived from 2,2'-binaphthol, but only partial conversion was achieved.

The novel tripodal ligand $^n BuSn(C_6H_4PPh_2)_3$, QSn, has been shown to coordinate to tungsten as a bidentate ligand, providing two phosphorus donor atoms in a *pseudo*-octahedral complex [$^n BuSn(C_6H_4PPh_2)_3W(CO)_4$]. Reaction with $Mo(CO)_6$ forms a very unusual complex $^n BuSn(C_6H_4PPh_2)_2(C_6H_4COPPh_2)Mo(CO)_2$, a complex in which the ligand has partially broken down. This provides the first example of a carbonyl group bridging a transition metal – main group metal bond. QSn coordinates to manganese to form $^n BuSn(C_6H_4PPh_2)_2Mn(CO)_3$, a tricarbonyl compound in which two of the tripod arms are coordinated to the metal and the third arm has completely cleaved off. The remaining coordination site on the manganese ion is occupied by the tin atom. X-ray crystal structures of the three complexes were obtained. Reaction between QSn and silver ions led to the formation of the salt $^n BuSn(C_6H_4PPh_2)_3AgBF_4$, which is potentially C_3 symmetric in solution. Attempts to develop the ligand further by changing the central tin atom to silicon were unsuccessful.

Contents

Abbreviations

° C	degrees centigrade
Å	angstrom
Ar	aromatic
atm	atmospheres of pressure
br	broad
bz	benzyl
cf.	compare with
cm^{-1}	reciprocal centimetre
C_n	n-fold rotational axis
C_{nv}	n-fold rotational axis with n vertical mirror planes
COD	1,5-cyclooctadiene
Cp	cyclopentadienyl
Cp*	pentamethylcyclopentadienyl
d	doublet
DCM	dichloromethane
DMF	dimethylforamide
DMSO	dimethylsulphoxide
e.e.	enantiomeric excess: $(e_1-e_2)/(e_1+e_2)$; e_1 is the percentage of the major stereoisomer and e_2 is the percentage of the minor stereoisomer
eq	equivalents
Et	ethyl
et al.	et alli (and others)
fac	facial (coordination geometry)
g	gram
h	hour
IR	infra-red spectroscopy
J	spin-spin coupling constant
L	ligand
M	mol dm^{-3}
m	multiplet
M.P.	melting point
m-CPBA	*m*-chloroperbenzoic acid
Me	methyl
MeCN	acetonitrile
mmol	millimoles
NMR	nuclear magnetic resonance spectroscopy
ppm	parts per million
pz	pyrazolyl
q	quartet
R	alkyl group

R_{int}	independent reflections
s	singlet
t	triplet
THF	tetrahydrofuran
TLC	thin layer chromatography
Tm	hydrotris(methimazolyl)borate
TMEDA	tetramethylethylenediamine
Tp	tris(pyrazolyl)hydroborato
Tp*	tris(2,4-methyl-pyrazolyl)hydroborato
TREN	tris(2-aminoethyl)amine
δ	chemical shift (relative to tetramethylsilane)

Formulae Numbers for Ligands and Complexes

1 Thiophenol

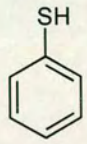

2 2-Lithiothiophenol

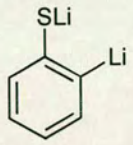

3 Tris(2-thiophenyl)phosphine

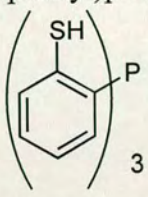

4 Tris(2-thiophenyl)phosphineoxide

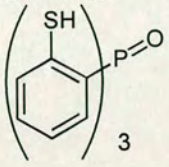

5 Bis(2-thiophenyl)phosphineoxide

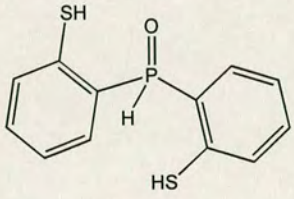

6 2-Methoxyphenylbromide

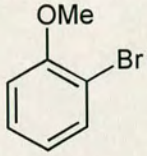

7 2-Methoxyphenylmagnesium bromide

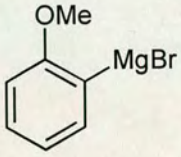

8 Tris(2-methoxyphenyl)phosphine oxide

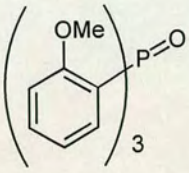

9 Tris(2-hydroxyphenyl)phosphine oxide

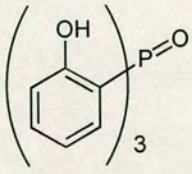

10 Tris(2-methoxyphenyl) phosphine

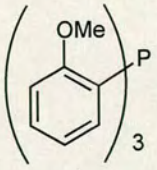

11 Tris(2-thalliumoxyphenyl) phosphineoxide

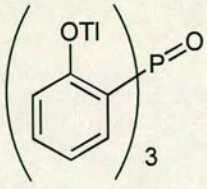

12 2-Lithiopyridine

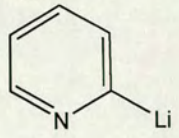

13 Bis(2-pyridylketone)

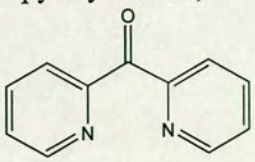

14 Tris(2-pyridyl)methanol

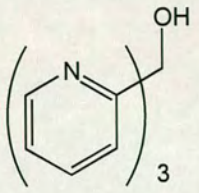

15 Tris(2-pyridyl*N*-oxide)methanol

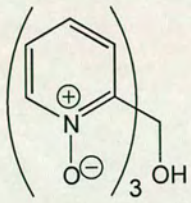

16 Tris(2-pyridyl)methoxide

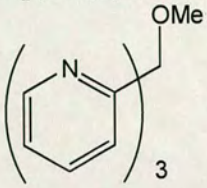

17 Tris(2-pyridyl)chloromethane

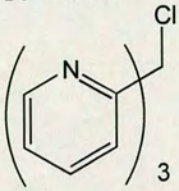

18 Tris(2-pyridyl)methane

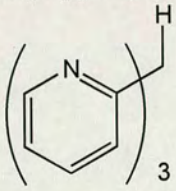

19 2-Lithiopyridine*N*-oxide

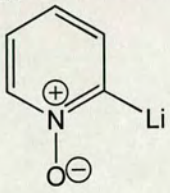

20 Tris(5-methyl-1(3)H-2-benzimidazolylmethyl)amine

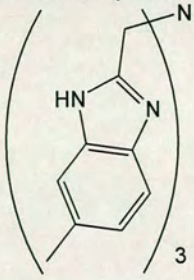

21 Trimethylnitrilotriacetate

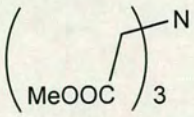

22 *N*-Methyltrimethylnitrilotriacetate tetrafluoroborate

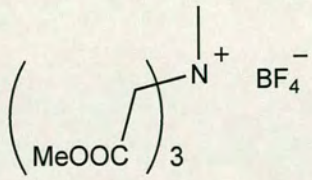

23 *N*-Ethyltrimethylnitrilotriacetate trifluoromethanesulphonate

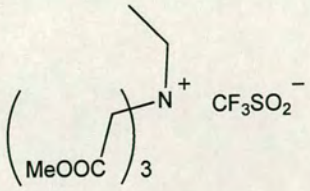

24 *N*-Methyl tris(benzimidazolylmethyl)amine

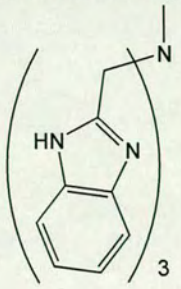

25 [Co(**24**)NCS]Cl

26 [Zn(**20**)Cl]

27 **20** + 4 $CF_3SO_3C_2H_5$

28 (*R*)-*N*-valine

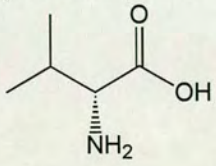

29 (*R*)-*N*-tosylvaline

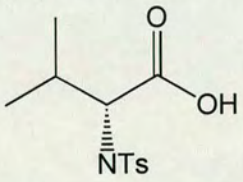

30 (*R*)-*N*-tosylvalinol

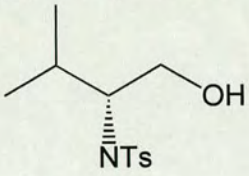

31 (*R*)-*N*-tosyl-2-isopropylaziridine

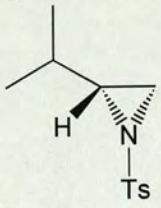

32 (*R,R,R*)-tris(*N*-tosyl-2-amino-3-methylbutyl)amine

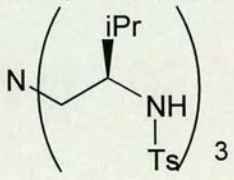

33 (*R,R,R*)-tris(*N*-tosyl-2-methylamino-3-methylbutyl)amine

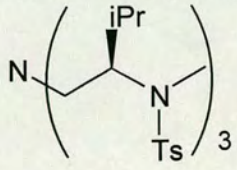

34 (*R,R,R*)-tris(2-methylamino-3-methylbutyl)amine

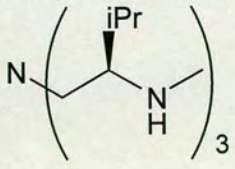

35 Binaptholphosphorylchloride

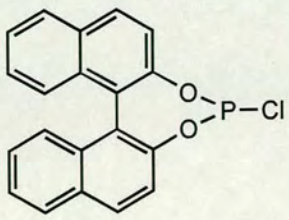

36 $^{n}BuSn(C_6H_4PPh_2)_3$, QSn

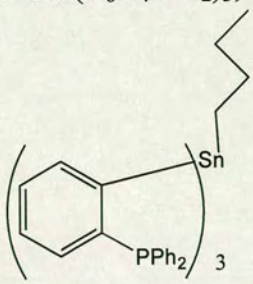

37 1-bromo-2-(diphenylphosphino)benzene

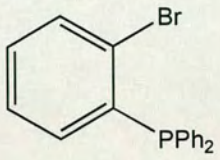

38 2-(diphenylphosphino) phenyllithium

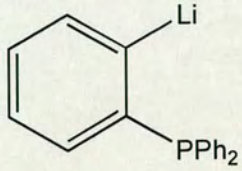

39 $[W(CO)_4QSn]$

40 $[Mo(CO)_3QSn]$

41

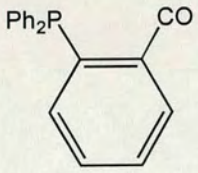

42

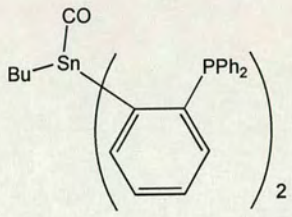

43 $[^{n}BuSn(C_6H_4P(C_6H_5)_2)_2Mn(CO)_3]$

44 $[QSnAg]BF_4$

45 $[QSnAg]CF_3SO_3$

46 $[QSnCuMeCN]BF_4$

47

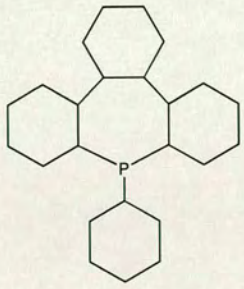

1 Introduction

1.1 Chiral Molecules

The ultimate aim of this work is to develop an asymmetric catalyst that facilitates the synthesis of enantiomerically pure chiral compounds. Chiral compounds are those that are non-superimposable mirror images of each other.[1] The two mirror images are known as enantiomers. Enantiomers have identical properties (except for optical rotation of plane polarised light) in an achiral environment. Many natural systems are homochiral, *i.e.* they are built up from amino acids and sugars that exist in only one enantiomeric form in the cell. Therefore enzymes and other proteins will exist in one enantiomeric form, as will carbohydrates and nucleic acids such as DNA and RNA. The basic building blocks of life are homochiral. Due to their chirality, enzymes and receptors are extremely selective and will preferentially bind to one enantiomer over the other. Therefore, the two enantiomers of a chiral molecule may have distinctly different biological activities.

One example is the molecule limonene. The receptors in our noses are chiral and so will interact differently with the two enantiomers, which are shown in Figure 1.1. *(S)*- limonene smells of lemons while *(R)*-limonene smells of oranges.

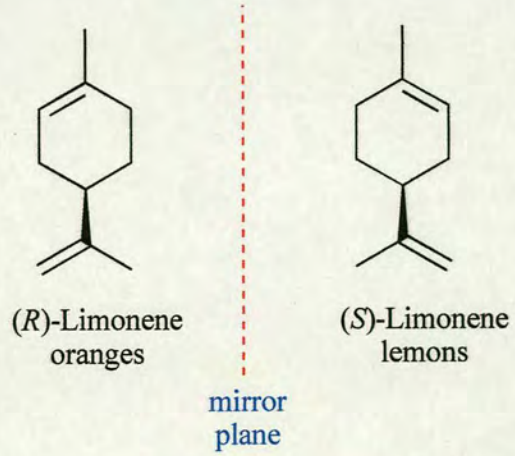

Figure 1.1 The two enantiomers of limonene

For pharmaceuticals, this difference may be in terms of potency and toxicity. For example, all of the biological activity of the drug may reside in one enantiomer. Therefore if the racemic mixture is separated into a single enantiomer, the drug will be more potent and in principle less toxic. One example where this was not considered is thalidomide, which led to disastrous consequences. One enantiomer is responsible for the desired therapeutic affects of being a sedative and an antinausea agent whilst the other is tetragenic and causes defective foetuses to be born. This tragedy led to a new set of rules in 1988 by the US Food and Drug Administration explicitly requiring the effects of both enantiomers of a new drug to be studied before it is marketed.[2]

Obtaining single enantiomeric forms is vitally important for many other industrial areas, especially for the production of agrochemicals including flavours, fragrances and sweetening agents. For example, for the molecule carvone, one half is responsible for the distinctive odour of spearmint whilst the other enantiomer is that of caraway. Another example is the molecule contained in neutrasweet, where one half is responsible for the sweet taste, the corresponding enantiomer has a bitter taste. In the agricultural industry, it may be that only one enantiomer of a pesticide is effective. If the chemical can be sprayed in an enantiomerically pure form, the undesirable impact on the environment will potentially be minimised.

There is now a worldwide market for chiral materials and new companies are being set up all the time to obtain single enantiomeric forms of molecules.[3]

There are a number of techniques for obtaining single enantiomers.[4] It is possible to separate the two enantiomers at the end of the synthesis. However, this is extremely wasteful, as it is often not possible to racemise and reuse the unwanted enantiomer. Other methods involve transformation or derivatisation of readily available, naturally occurring chiral compounds; or using naturally occurring enzymes to carry out specific transformations.

1.2 Asymmetric Catalysis

One approach to separating out the two enantiomers is to use an asymmetric catalyst that can produce one enantiomer in high excess.[4, 5] This method is particularly attractive to industrial companies who need to be able to produce large quantities of product as pure as possible. They are particularly concerned with minimising the amount of unwanted product that has to be disposed of and also with the inefficiency and costs involved in the chemical process.

Asymmetric catalysis is an extremely effective synthetic method since a small amount of man made catalyst can be used to produce chiral materials in large quantities. Furthermore, since the catalyst is unchanged after the reaction is complete, it can be recovered and used again. Such reactions are highly productive and economical.

The two products of the reaction, being enantiomeric, are of equal energy and so if the reaction is reversible, *i.e.* under thermodynamic control, the result will be a racemate (an equal mixture of the two enantiomers). If the reaction is effectively irreversible, *i.e.* under kinetic control, then the difference between the rates of the reactions leading to the products will determine the level of enantioselectivity.

For asymmetric catalysis, a chiral catalyst present as a single enantiomer is used. The chiral environment will provide different steric interactions with the possible orientations of the prochiral substrate when bound, leading to diastereotopic transition states. This is illustrated in Figure 1.2. Diastereoisomers usually have different energies, which consequently results in an energy difference, $\Delta\Delta G^{\ddagger}$ in Figure 1.2, between the transition states leading to the two product enantiomers. The ratio of the two products will be directly related to this difference in transition state energies, therefore it should be possible to produce one enantiomer in excess.

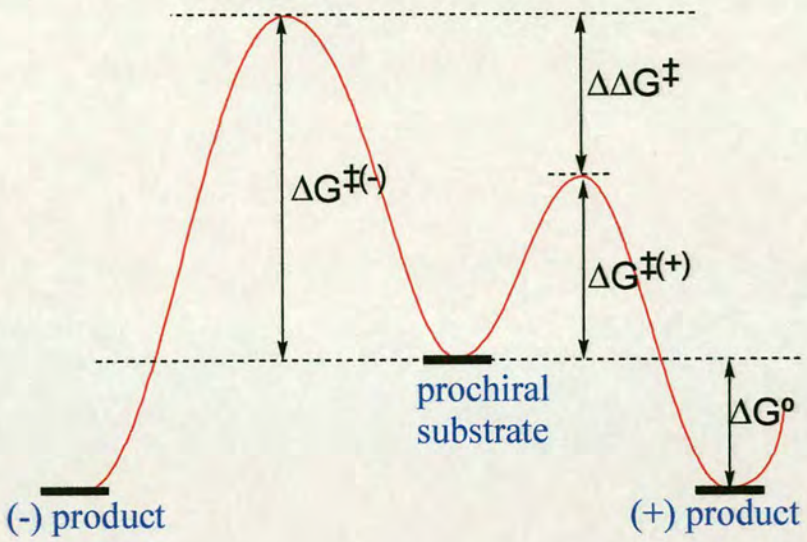

Figure 1.2 Energy profile for asymmetric catalysis

There is an exponential relationship between the activation energy and the reaction rate. Therefore even a small change in energy of the transition state will lead to a large change in the rate of the reaction. For example, a difference in energy between the two diastereotopic transition states, $\Delta\Delta G^{\ddagger}$ = 8.37 kJ mol^{-1} leads to an enantiomeric excess of 95 %. This energy difference corresponds to the magnitiude of the carbon-carbon rotation barrier in ethane. It follows that very small changes in the reaction system, such as the steric bulk of a ligand, may have a profound influence on the enantioselectivity of the reaction.

To achieve the greatest chiral multiplication, the energy difference between the two diastereotopic transition states needs to be maximised. Catalytic systems that precisely discriminate between enantiotopic atoms, groups, or faces in achiral molecules need to be designed. The use of chiral metal complexes that act as homogeneous molecular catalysts is one of the most successful strategies. Organometallic catalysts are able to exert efficient and flexible control over the stability and reactivity of reagents and substrates used. They have the distinct advantage over enzymes in that they can be used for a much wider range of reactions and can use substrates not accepted by enzymes.[3, 4, 6]

One way to increase the probability of achieving a high degree of asymmetric induction is to decrease the number of diastereotopic transition states and so reduce the number of competing reaction pathways leading to the same product. This can be achieved by removing non-equivalent co-ordination sites in the chiral metal complex. One approach to this is by introducing symmetry into the catalyst in such a way that the overall chirality is maintained.[7]

The steric environment of the metal complex used as the catalyst is controlled by the ligands. For example, for a square-planar metal complex containing a bidentate C_2 symmetric ligand (*i.e.* a ligand with two-fold rotational axis), the two remaining sites on the metal are equivalent and are said to be homotopic (see Figure 1.3).

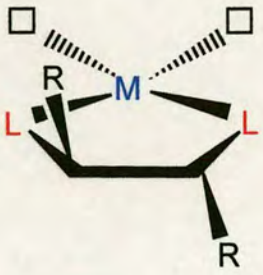

Figure 1.3 Square-planar metal complex containing a bidentate C_2 symmetric ligand

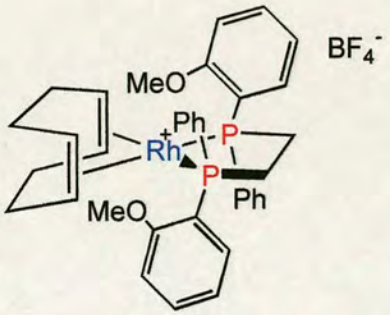

Figure 1.4 DIPAMP bound to rhodium

This approach has been utilised by Halpern's group in the case of asymmetric hydrogenation of alkenes[8] in which the C_2 symmetric ligand DIPAMP is used, (shown bound to rhodium in Figure 1.4). The first step of the reaction is the displacement of two solvent molecules in the catalyst precursor by the olefinic substrate to form a rhodium chelate complex. Hydrogen is oxidatively added to the metal to form a Rh(III) dihydride intermediate. The two hydrogen atoms on the metal are successively transferred to the olefinic carbon atoms. The secondary binding of the carbonyl oxygen of the amide functionality results in a ring system that stabilises the reactive intermediate.

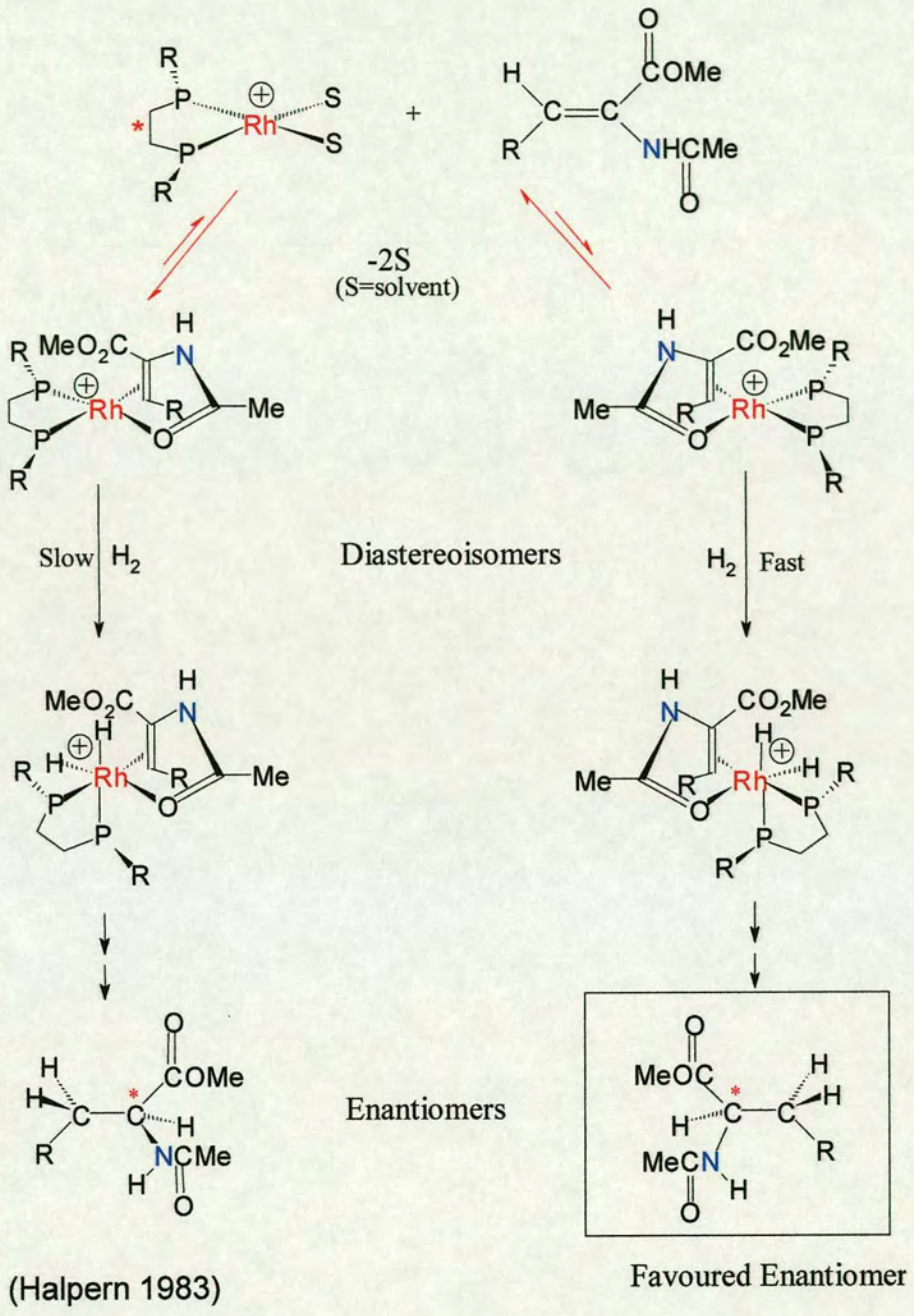

Figure 1.5 Catalytic cycle for the asymmetric hydrogenation of alkenes

There are two possible ways in which the alkene can bind to rhodium, as shown in Figure 1.5. Kinetic data suggests that the oxidative addition of hydrogen is the rate-limiting step. The steric interactions between the substituents and the chiral environment of the ligand will be different for the two orientations. The transition states will be of different energies resulting in a selective addition of hydrogen to one

face of the alkene. The two binding sites are equivalent and so co-ordination to either site will result in an identical set of complexes. There are only two diastereotopic transition states and so high optical yields can be obtained. Using the *R,R*-DIPAMP complex of rhodium, up to 94 % enantiomeric excesses could be achieved in the asymmetric hydrogenation of alkenes. A large amount of work has been carried out on C_2 symmetric ligands, particularly phosphine donors.[9]

Many transition metal catalysed reactions are known to involve octahedral intermediates. In an octahedral environment, a bidentate C_2 symmetric ligand results in a complex where the four remaining sites on the metal are of two non-equivalent types, as shown in Figure 1.6. The two axial sites are equivalent to each other but are different to the two equatorial sites. It is extremely difficult to block two of the sites selectively so that the two remaining sites are equivalent. For the vacant sites to be rendered homotopic requires the co-ordination of a chiral tridentate C_3 symmetric ligand (one with a three fold rotational axis), as shown in Figure 1.7. It is also essential that the C_3 ligand is facially co-ordinating as opposed to meridianal.

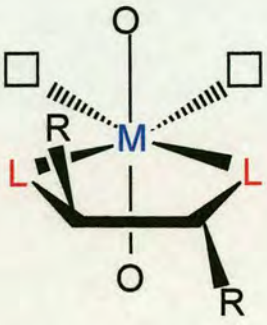

Figure 1.6 Octahedral metal complex containing a bidentate C_2 symmetric ligand

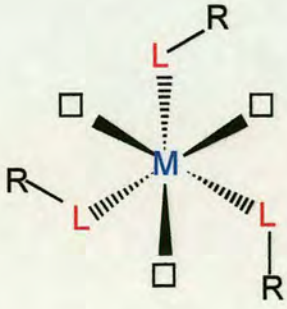

Figure 1.7 Octahedral metal complex containing a tridentate C_3 symmetric ligand

Control of the stereochemistry of the catalyst is dependent upon the ligand remaining co-ordinated to the octahedral complex throughout the reaction. Such a system will only be suitable for processes that do not involve square-planar / octahedral interconversions such as for oxidative-addition / reductive-elimination steps. An example where this system would be applicable is for the transfer hydrogenation of ketones to form secondary alcohols.[10] A typical catalytic cycle for this type of reaction, involving isopropyl as the hydrogen donor is shown in Figure 1.8.

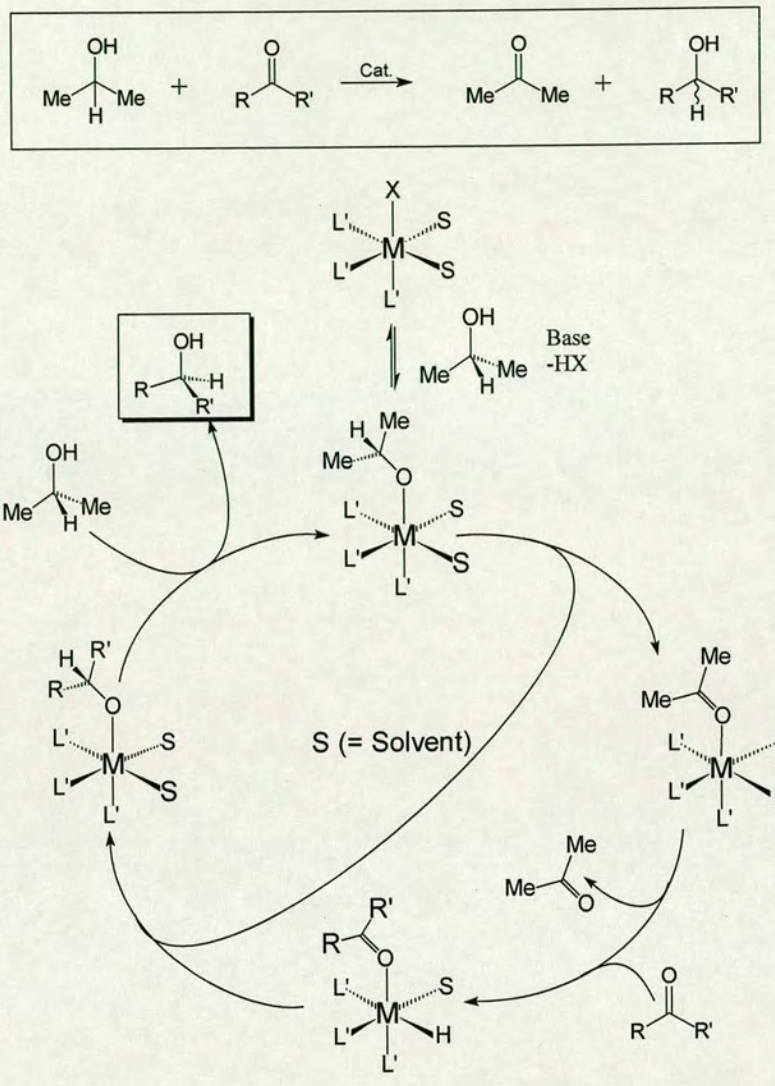

Figure 1.8 Catalytic cycle for transfer hydrogenation

If the three ligands L' represent the co-ordination by a C_3 symmetric tripod ligand, the transformations take place in a chiral environment and the possible sites for coordination of the prochiral substrate are equivalent.

The aim of this project is to develop ligands that will co-ordinate to transition metals and provide octahedral complexes with C_3-symmetry.

1.3 C_3 Symmetry

A complex possesses C_3 symmetry due to the presence of a three-fold principal rotation axis in the absence of mirror planes containing this axis. This can arise either by the co-ordination of an enantiopure C_3 symmetric ligand or by the co-ordination of a ligand in such a way that the overall symmetry of the complex is C_3. The ligands considered in this project are tripodal ligands, of the type illustrated in Figure 1.9, in which there are m linker atoms (L) between the central atom (E) and the donor atoms (D). By varying, L, E and D there is potentially a huge range of ligands that can be utilized.

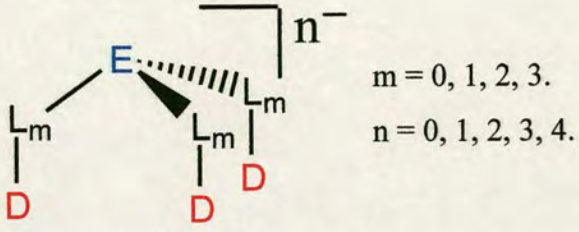

Figure 1.9 Basic structure of tripodal ligands

There are two principal means by which chirality can be introduced into the ligand. Either chiral groups can be incorporated into the ligand backbone (at the E or L positions) or they can be attached to the terminal donor substituents. In either case, the incorporation of such stereogenic groups must not disrupt the C_3 symmetry of the system. For example, if chiral substituents are introduced by substitution at the L positions, all three of the tripod arms must be substituted equivalently.

The design of C_3 symmetric ligands is a rapidly growing area and there are examples of all of the above types of ligands. Here follows a brief review of the literature, providing examples to illustrate the types of ligands described above.

1.3.1 Chiral Substituents

The most common strategy for creating C_3 symmetric chiral ligands is to attach a chiral substituent to each of the three donor functionalities. This places the chirality close to the metal centre in complexes containing the ligand. A large number of chiral analogues of well-established tripods have been synthesized in this way. A disadvantage of this type of ligand system is that the substituents may provide too much steric hindrance and prevent the formation of a metal complex, or the binding of a substrate to any metal complex that did form.

1.3.1.1 Phosphorus Donor Ligands

Phosphane ligands are one of the most popular systems for study in co-ordination chemistry. A wide range of monodentate and polydentate phosphane ligands are known and their co-ordination chemistry has been researched extensively, mainly by the groups of Sacconi,[11] Meek,[12] Venanzi[13] and Bianchini.[14] Phosphorus is a soft, polarisable donor atom, giving polyphosphines excellent bonding abilities. They are able to form stable complexes with most *d*-block metals in a variety of oxidation states, particularly Group VIII and the later transition metals. Phosphines are primarily donors and so on complexation, there is an increase in nucleophilicity of the co-ordinated metal centre due to the increase in electron density. They exert a strong *trans* influence on other ligands, which can be used to activate the complex. They are able to adapt to many different co-ordination numbers. The steric and basic properties can be varied easily through specific alterations at the backbone and to the substituents at the phosphorus, making polyphosphine ligands extremely versatile.[14] Such properties have made phosphine ligands ideal for use in homogeneous catalysis and many are utilised in industry.[8] By using chiral phosphine ligands, asymmetric transformations can be carried out with high enantiomeric excesses. For example, the chiral phosphine ligand DIPAMP was used by Halpern for asymmetric hydrogenation (see Section 1.2).

The first chiral, optically pure C_3 symmetric tripodal phosphine was reported by Burk and Harlow.[15] The chirality of the ligand is built into the terminal substituents of the phosphorus atoms. The ligands can be prepared starting from enantiomerically pure

disubstituted phospholanes, as illustrated in Figure 1.10. Upon treatment with lithium metal, the P-Ph bond is cleaved, yielding the cyclic lithiophosphane. Reaction with 1,1,1-tris(chloromethyl)ethane yielded the C_3 symmetric triphospholane – a tripod ligand with one methylene group linking each phosphine moiety to a central carbon atom. Analogously, the triphospholanamine could be prepared from the reaction with tris(2-chloroethyl)amine. This tripod ligand is potentially tetradentate, with a central nitrogen atom connected to the three phosphine groups *via* two methylene groups.

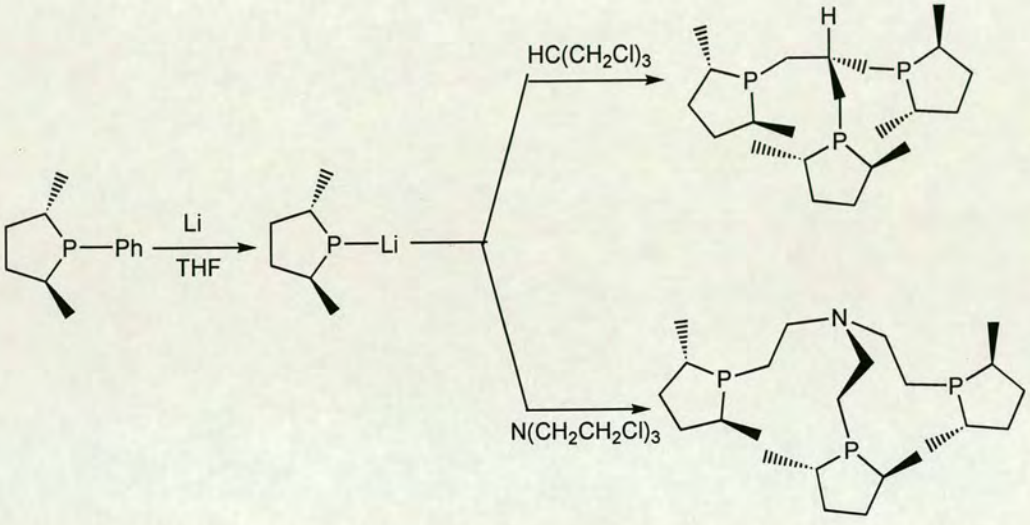

Figure 1.10 Synthetic routes to tripodal phosphine ligands

Both ligands form trigonal bypramidal complexes upon co-ordination to rhodium.[16] The structures were ascertained by X-ray crystallography studies and are shown in Figure 1.11 and Figure 1.12. The C_3 symmetric ligands confer a highly asymmetric environment around the metal centre. Both complexes contain a crystallographic C_3 symmetry axis that coincides with the axis defined by the central ligand atom and the metal centre.

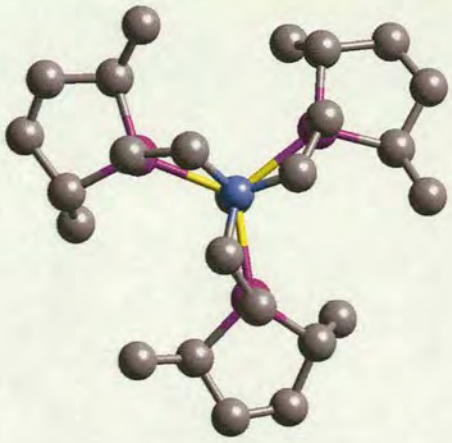

Figure 1.11 Rhodium complex of triphospholanamine

Figure 1.12 Rhodium complex of triphospholane

The rhodium complex of triphospholanamine was tested for asymmetric catalytic activity in enantioselective hydrogenation reactions.[17] The complex acts as a catalytic precursor for the hydrogenation of methyl (z)-α-acetamidocinnamate. A reaction time of 72 h at 50 °C results in an 89 % e.e. The hydrogenation of dimethyl itaconate is carried out at the same temperature for 20 h, giving a 95 % e.e. Activation of the catalyst is through hydrogenation of the COD ligand, which occurs at 25 °C and 2 atm H_2. Hydrogenation of the substrate under these conditions is very slow – a much higher temperature is required for reasonable reduction rates. This was postulated to be due to the formation of a five coordinate intermediate under the reaction conditions. In order for further reaction with hydrogen to occur, one arm of the chelating substrate or of the ligand would have to dissociate from the metal centre. However this argument would mean a loss of the three-fold symmetry of the complex, which is required for the maximum induction of asymmetry in the product.

The chirality of the ligand can be incorporated directly on to the phosphorus atoms, as opposed to on the carbon atoms as in the two ligands described previously. Ward and co-workers have reported the enantiomerically pure (*R,R,R*)-siliphos ligand.[16] This is a tridentate ligand, with a central silicon atom connected to the three phosphorus donors by a methylene group, as shown in Figure 1.13.

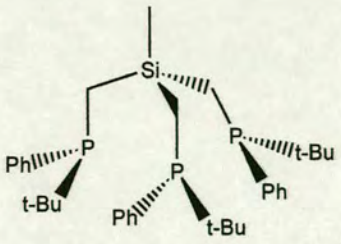

Figure 1.13 (*RRR*)-siliphos

The ligand is synthesised from the deprotonation of (*R*)-(*tert*-butyl)(methyl)(phenyl)phosphineborane, followed by the coupling to the electrophilic $MeSiCl_3$ and finally deprotection using morpholine.

The ligand co-ordinates to rhodium to yield the cationic complex [Rh(NBD)((*R,R,R*)-siliphos].[16] The X-ray crystal structure, shown in Figure 1.14, clearly shows the distorted square pyramidal geometry about the rhodium centre and the overall C_3 symmetry of the complex. No studies have yet been reported on the ability of the ligand to act as an asymmetric catalyst.

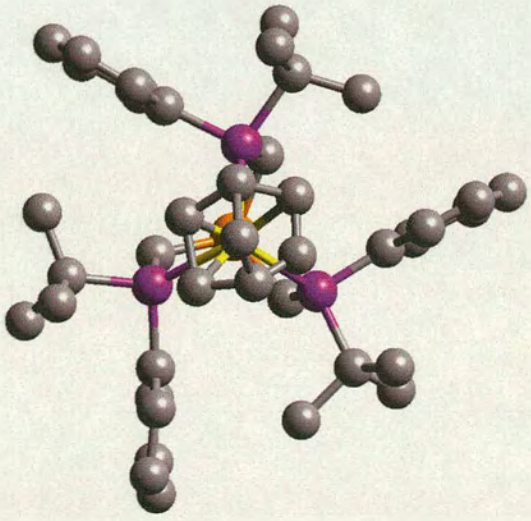

Figure 1.14 Rhodium complex of (*R,R,R*)-siliphos

1.3.1.2 Aliphatic Nitrogen Donor Ligands

1.3.1.2.1 Amido Ligands

Early transition metals require highly charged ligands, with hard donors, to stabilize the formally high valent metal centres. Tripodal amido ligands have several characteristics that make them ideal for studying a range of metal complexes. Amido nitrogen atoms have excellent σ. and π. donor abilities, enabling them to partially fulfil the electronic demands of high valent, extremely Lewis acidic metal centres. Amido functions are disubstituted at the donor atom and so groups can be added easily to the donor nitrogen atoms to fine-tune both the ligand periphery and the ligand framework. This provides a convenient route to introducing chiral substituents into the tripodal ligands. In this way, the ligand systems can be finely controlled to provide a rigid co-ordination environment that shields most of the coordination sphere around the metal. Therefore the size of the binding site offered by the ligand, as well as the geometry and size of the active site at the metal centre can be highly controlled.[18]

Most of the work investigating C_3 complexes involves tripodal ligands co-ordinated to late transition metals, with very little work involving early transition metal complexes. For this reason, Gade's group have extensively studied tripodal amido ligands. A wide range of tripodal amido ligands, based on carbon or silicon frameworks have been developed to enable the investigation of some interesting and varied chemistry.

Gade's group has looked at trianionic ligands based on a neopentane framework and used them to stabilise mixed valent M^{I} / M^{II} (M = In, Tl) compounds.[19] By replacing some of the framework atoms with bigger silicon atoms, more flexible ligands are obtained which allows the complexation of larger metal ions. Trisilylmethane frameworks with various substituents on the nitrogen atoms have been developed. These ligands are shown in Figure 1.15.

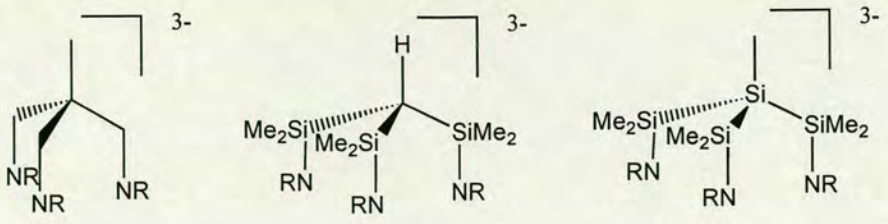

Figure 1.15 Tripodal amido ligands

The amine ligand precursors are prepared easily by the aminolysis of $HC(SiMe_2Br)_3$ with primary amines, in the presence of triethylamine as an auxiliary base. The secondary amines form in good yield provided that the primary amine is sufficiently nucleophilic. Steric factors do not appear to be an influential factor in this synthesis in that the reaction occurs readily with the sterically bulky *t*-$BuNH_2$.[18]

The preferred conformation of the ligand in solution depends on the nature of the nitrogen substituent. They generally lie between the two extremes shown in Figure 1.16, which accounts for the differing spectroscopic properties of the ligands.[18] This is also the case in the solid state, as confirmed by X-ray crystallographic studies on the ligands.

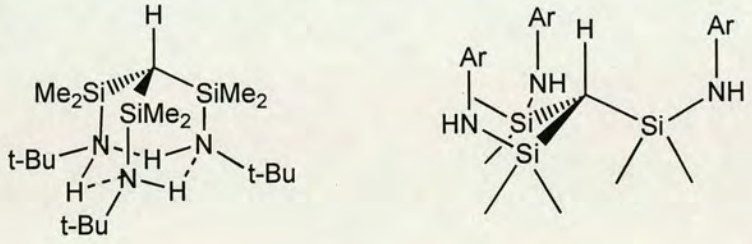

Figure 1.16 The two conformational extremes postulated for the structure of amido ligands in solution

With alkyl groups, the ligand is prearranged for complexation and has an adamantane type structure that is enhanced by weak N-H···N hydrogen bonding. For aryl substituents, the preferred conformation has the trisilylmethane backbone folded inside out relative to the adamantane structure. The $SiMe_2$ groups are not completely inverted with respect to those in the adamantane type structure, but are significantly twisted. This is probably due to the steric repulsion of the methyl groups. Three of the methyl groups occupy 'equatorial' positions, with the remaining three assuming

'axial' positions. Both possess idealised C_3 symmetry. The co-ordination of these ligands to a number of metals has been carried out.[18, 20, 21]

It is possible to prepare chiral tripodal amines from the reaction of an alkyl silicon bromide with a chiral primary amine. The reaction of $HC(SiMe_2Br)_3$ with three molar equivalents of *(R)*-1-aminotetralene, *(S)*-1-phenylethylamine or *(R)*-1-indanylamine in the presence of three equivalents of triethylamine yielded the tripodal amines $HC(SiMe_2NHR^*)_3$ where R^* = *(R)*-tetrahydronaphthyl,[22] *(S)*-1-phenylethyl, (shown in Figure 1.17), and *(R)*-1-indanyl[23] respectively.

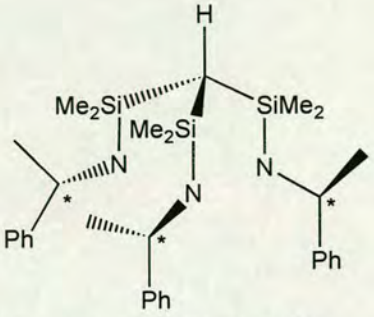

Figure 1.17 $HC(SiMe_2NHR^*)_3$ R*=*(S)*-1-phenylethyl

The X-ray structures of all three ligands show an adamantane type structure with a three-fold symmetry. The ligands are pre-arranged for binding to a metal effectively.

The free ligands are readily isolated as crystalline solids, however in solution, the ligands are not stable. The triamine ligands are in equilibrium with the cyclic diamine molecules, generated through elimination of one molecule of the primary chiral amine, resulting in a loss of C_3 symmetry. This was established from the ^1H and ^{13}C NMR spectroscopy data. This equilibrium, shown in Figure 1.18, lies almost entirely to the side of the tripodal amine at room temperature.

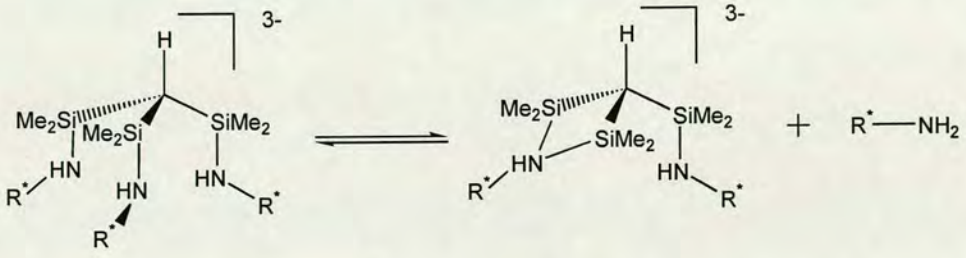

Figure 1.18 Solution equilibrium of triamine and diamine ligands

The amido ligand transfer reagents used in the formation of metal complexes are the corresponding trilithium triamides. These are readily prepared from the addition of three equivalents of *n*-BuLi to the chiral tripodal amines. The trilithium triamides

form as crystalline solids that have been fully characterized. They all have virtual C_3 symmetry and are based on a heteroadamantane cage structure. Unusually, the two co-ordinate lithium ions are 'internally solvated' by the peripheral aryl groups, so that the mainly ionic core $(LiN)_3$ is almost completely encapsulated.

Zirconium complexes of the ligands were formed by treating the trilithium triamides with $ZrCl_4$ in toluene. X-ray crystallography studies on the complexes $[Zr(CH_3)\{HC\{SiMe_2N[(S)\text{-1-phenylethyl}]\}_3\}]$ and $[Zr(CH_3)\{HC\{SiMe_2N((R)\text{-1-indanyl}])_3\}]$ showed that in the solid state, the ligand is distorted with respect to the ideal C_3 symmetric arrangement. This is due to the unsymmetrical arrangement of the chiral amine groups. The distortion is most pronounced for the *(S)*-1-phenylethyl substituted complex. Two of the aryl groups are arranged close to the $Zr\text{-}CH_3$ unit with the ipso-carbon atoms located at 3.29 and 3.46 Å from the metal centre. The third aryl group points away, almost horizontally, to the virtual molecular axis. The *(R)*-1-indanyl substituted complex is less distorted, although one of the aryl groups lies even closer to the metal centre, with an ipso-carbon lying at only 3.19 Å from the zirconium centre.

The close contact of one or two of the aryl units to the zirconium results in steric crowding at the metal centre. To minimize this, the remaining peripheral units are pushed away from the metal centre. One explanation for this is that the intramolecular π-interactions between the metal centre and the aryl unit(s) may help to stabilize the co-ordinatively unsaturated metal centre. This is a well-known feature of amidozirconium chemistry,[24] in particular of low-coordinate cationic species.

Gade *et al.* have carried out initial studies on the effect of chiral induction of the tripodal ligand and its efficacy as an asymmetric catalyst. The alkylamidozirconium species were shown to act as asymmetrical alkylating agents for aryl aldehydes. This reaction is shown in Figure 1.19. The highest stereoselectivities were obtained when the two substituents at the carbonyl function are of very different sizes. The maximum enantiomeric excess obtained was for the insertion of 2-naphthalene into

the *(R)*-1-indanyl substituted complex. After hydrolysis and workup, *(R)*-naphthylethanol was isolated in an enantiomeric excess of 82 %.

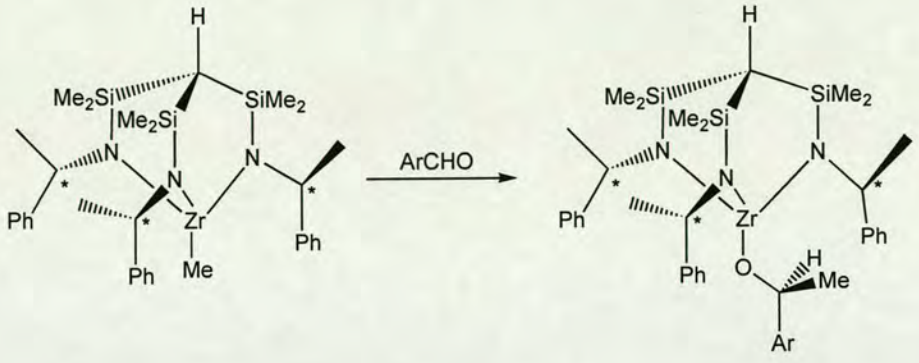

Figure 1.19 Insertion of aryl aldehydes into the Zr-C bond

The ligand periphery of the *(R)*-1-indanyl substituted complex is more rigid than that of the *(S)*-1-phenylethyl substituted complex and so there will be reduced conformational degrees of freedom in the alkylating agent. Despite this, there is no significant increase in the stereoselectivity of the *(R)*-1-indanyl substituted complex towards which orientation the prochiral ketone co-ordinates to the metal.

To investigate the degree to which the stereoselectivity originates from the chirality of the substrate or from the chirality of the alkylating agent, the chiral alkylamidozirconium complexes were reacted with chiral carbonyl compounds. This was compared to the reaction of the chiral carbonyl compounds with the nonchiral alkylamidozirconium complex $[Zr(CH_3)\{HC\{SiMe_2N(p\text{-}Tol)\}_3\}]$. The selectivity increases significantly upon use of a chiral alkylating complex, leading to diastereoselectivities of up to 94 % with *(R)*-myrtenal. However, this stereoselectivity originates from the chirality of the substrate. The increase in stereoselectivity observed is probably due to the greater steric shielding of the reaction site in the 1-phenylethyl substituted complex in comparison to the tolyl substituted complex. This slows down the speed of the reaction and favours alkyl transfer from one of the diastereotopic faces of the carbonyl group.

Ligands based on a trisilylsilane backbone, shown in Figure 1.15, are even more flexible.[25, 26] These ligands will be more suited to binding to larger metals. However, no chiral analogues of these systems have been reported to date.

1.3.1.2.2 Amido Amine Ligands

Schrock and Verkade have extensively studied triamidoamine ligands. These are tripod ligands based on a central nitrogen atom connected *via* two sp^3 methylene groups to amido donor groups. The co-ordination of these ligands to a variety of transition metal or main group elements, generally in oxidation states greater than, or equal to +3 has been reported.[27-32] The trianionic ligands usually bind to a transition metal in a tetradentate manner, giving rise to a relatively rigid, trigonal bipyramidal geometry. This leaves three orbitals available for bonding to additional ligands. There are two π orbitals (d_{xz} and d_{yz}) and one σ orbital, as illustrated in Figure 1.20.

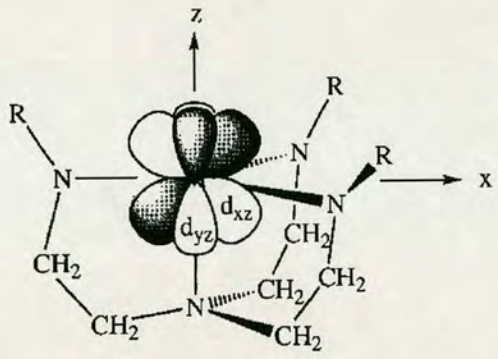

Figure 1.20 Triamidoamine ligands

If bulky substituents are placed on the nitrogen atoms, (R in Figure 1.20), a sterically protected, 3-fold symmetric pocket is formed which is ideal for protecting transition metals with relatively low *d* electron counts. Schrock has focused on looking at trialkylsilyl and pentafluorophenyl N-substituents. The nature of the nitrogen substituent is important in determining the overall stability of the complex. Although very effective at forming a sterically protected, symmetric pocket, silylated TREN ligands can easily decompose due to abstraction of a proton. For instance, with

reactive alkyl second or third row metal complexes, the ligands decompose when heated to give compounds in which a C-N_{ax} bond has been cleaved.[29]

Cyclometalation reactions have been observed with titanium alkyl complexes. These decomposition reactions will obviously limit the applicability of these ligands for forming some complexes.[28]

Ligands with pentafluorophenyl groups have the advantage of being synthesised easily and in a much higher yield.[33] The planar aryl rings form a pronounced geometry around the apical site. An X-ray crystal structure of $[Mo(N_3N_F)]Cl$, (where $(N_3N_F)^{3-} = ((C_6F_5NCH_2CH_2)_3N)^{3-}$), (Figure 1.21) shows that the aryl rings are orientated approximately perpendicular to the Mo-N-*ipso* C plane and so create a bowl shaped cavity around the apical Cl.

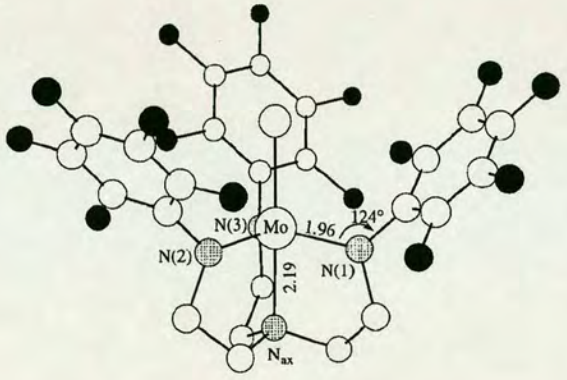

Figure 1.21 X-ray crystal structure of $[Mo(N_3N_F)]Cl$

This structure is not always observed; in $[(N_3N_F)V]$, the co-ordinatively unsaturated vanadium may form weak interactions with the fluorides.[34] To accommodate this, the C_6F_5 rings turn so that the *o*-fluorides approximately fill the apical cavity. This further illustrates the ability of the ligand to provide an active periphery, as observed with some of Gade's ligands.[35]

The high electron withdrawing power of the flouro substituted ligands enables complexes with higher co-ordination numbers to be isolated. Six-coordinate complexes with tungsten have been obtained, for example, $[(N_3N_F)W(CNR)_2]OTf$.[30]

The C_3 symmetry of the TREN based ligand is maintained and the two additional ligands occupy the apical pocket. Such complexes may have use as catalytic species.

Verkade has looked at alkyl substituted TREN ligands and the co-ordination of these ligands to form atranes. Atranes are of general formula, $Z\text{-}E(NRCH_2CH_2)_3N$, (shown in Figure 1.22) and a large amount of work has been carried out on investigating reactions at E, Z, Y and N and the structural changes that accompany them.[31,36]

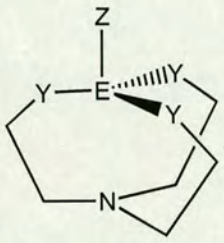

E = group 4, 5, 6, 13, 14 or 15 element
most common for E = P, Si, Sn
Y = N, OR
Z = nothing, lone pair, R, O, NR, SR, NR_2

Figure 1.22 Structure of atranes

The extent to which the central nitrogen atom takes part in the complexation to E can vary considerably. The distance between N and E can vary between the sum of the Van der Waals radii of the atoms N and E, through intermediate distances to full transannular bonds. The transannular bond length and the degree of delocalisation of the central nitrogen lone pair into a three centre, four electron bond system along the molecular axis depends upon the electron-withdrawing power of the Z substituent and upon the steric properties of the E substituents. In some cases it has even been possible to alkylate the central nitrogen atom, but only with E = P or Si.

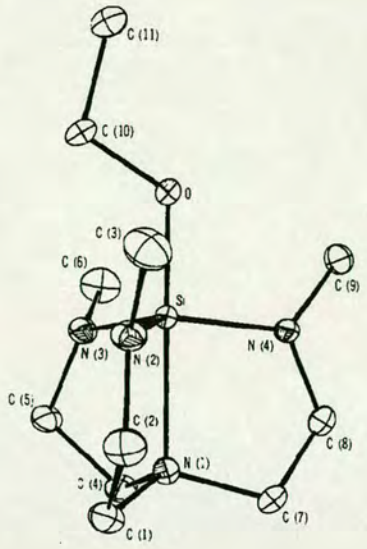

Figure 1.23 X-ray crystal structure of *N,N',N''*-Trimethyl-1-ethoxy-azasilatrane

An X-ray crystallographic study of the nitrogen substituted atrane *N,N',N''*-Trimethyl-1-ethoxy-azasilatrane, a complex in which the triamidoamine ligand is co-ordinated to silicon shows that the tricyclic skeleton has virtual C_3-symmetry with an envelope configuration for each of the five membered rings.[27] The X-ray crystal structure is shown in Figure 1.23. The disadvantage of using alkyl substituted TREN ligands is that they will be considerably more electron donating than silyl groups, which may lead to facile reduction of the metal in the initial synthesis. Furthermore, they may decompose easily due to the presence of one or more hydrogen atoms on the substituent α to the nitrogen atom. These could be deprotonated, leading to the formation of imine complexes and the loss of three-fold symmetry.

Following on from Verkade and Shrock's work, there have been reports of asymmetric versions of some of their triamido ligands. For example, Yamamoto has synthesised the C_3 symmetric triamidoamine, shown in Figure 1.24.[37]

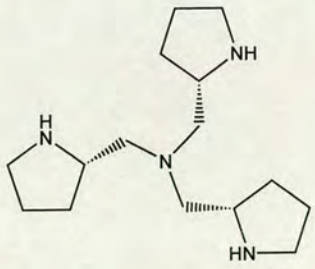

Figure 1.24 C_3 symmetric triamidoamine

Yamamoto *et al.* have also synthesised protetraazaphospatrane.[37] An X-ray crystal structure of protetraazaphospatrane has been obtained, but not for the C_3 symmetric triamidoamine. This is illustrated in Figure 1.25.

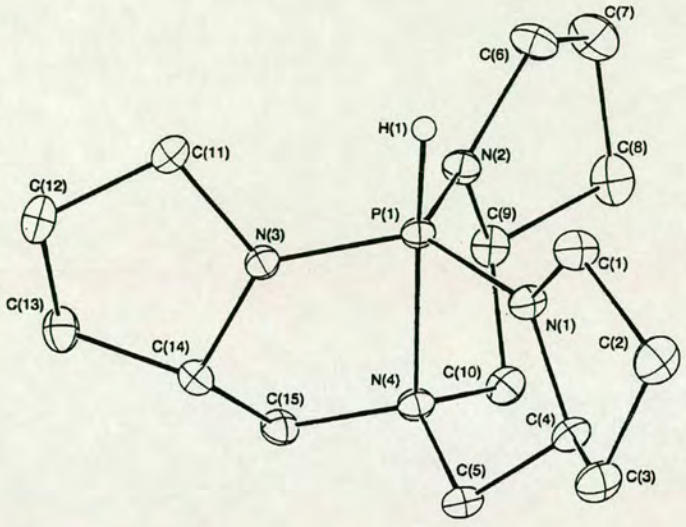

Figure 1.25 X-ray crystal structure of protetraazaphospatrane

No complexation studies of the ligands have been carried out. Protetraazaphospatrane has been tested for catalytic activity and asymmetric induction in the ethylation of benzaldehyde with diethyl zinc.[37] The yield was increased to 49 % compared with a yield of 26 % when no catalyst is present. The degree of asymmetric induction was very small – an enantiomeric excess of only 15 % was obtained.

1.3.1.2.3 Amidate Ligands

Tripodal ligands derived from nitrilotriacetamide, $[(RNHC(O)CH_2)_3N]$ have been studied by Rheingold *et al.*[38-40] These ligands contain three deprotonated amide moieties (amidates) and one tertiary amine. Tris((*N*-*t*-butylcarbamoyl)methyl)amine, containing optically active ^{t}Bu groups on the nitrogen atoms has been investigated. A schematic of this ligand bound to a metal ion is shown in Figure 1.26. Amidates are strong σ-donors and bind to metal ions *via* co-ordination of the nitrogen atoms.[41, 42]

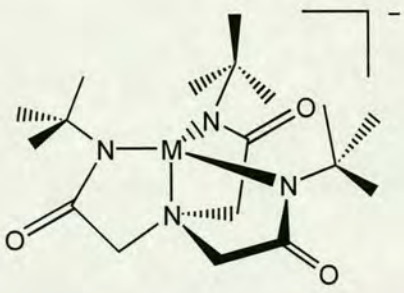

Figure 1.26 C_3 symmetric amidate ligand coordinated to a metal ion

This ligand is more rigid than the other nitrogen donors discussed so far in that there is one sp^2 and one sp^3 linker atom in each of the tripod arms (compared with two sp^3 linker atoms in the other ligands). This results in the formation of three relatively rigid, five-membered chelate rings upon complexation to a metal center.

The ligand is easily synthesized from *t*-butylamine and trinitrilotriacetic acid in pyridine using triphenylphosphite as a dehydrating agent. The ligand acts in a tetradentate manner and forms trigonal monopyramidal complexes with Co, Zn and Ni.[38, 40] NMR studies support the formation of C_3 symmetric species in solution. X-ray crystal structures show that the tripodal ligand co-ordinates in an identical manner to each of the metal ions. The three amidate nitrogen atoms are co-ordinated in the trigonal plane. The metal ion in each complex lies slightly above the trigonal plane and towards the vacant site. The vacant axial position is encompassed by the appended chiral substituents that wrap around the site to form a chiral cavity. The chiral substituents are not quite arranged symmetrically in the solid state.[40] This is attributed to the crystal lattice, where intermolecular aryl-methylene interactions are observed and so hinder a totally symmetrical arrangement of the chiral groups within the complex. This slight distortion illustrates that the ligand is still relatively flexible.

Trigonal monopyramidal complexes are relatively uncommon. However, the relatively rigid, five membered chelate rings enforce trigonal co-ordination of the amidate nitrogen atoms to the metal and prevent distortion towards a tetrahedral geometry. Furthermore, the ^{t}Bu groups provide enough steric hindrance around the vacant co-ordination site to allow the isolation of co-ordinatively unsaturated complexes. This ligand is unable to stabilize higher oxidized metal centers, and no complexes with trivalent (or higher) metal ions have been observed, unlike for Shrock's tripodal ligands $[(XNCH_2CH_2)_3N]^{3-}$, (X = trialkylsilyl or pentafluorophenyl

substituents). This difference may be due to the more flexible chelate rings formed with Shrock's ligands, which contain two sp^3 linker atoms.

The ligands have been investigated with respect to an interest in crystal engineering and no catalytic studies of the complexes have been reported.

1.3.1.3 Aromatic Nitrogen Donor Ligands

1.3.1.3.1 Pyrazolyl Ligands

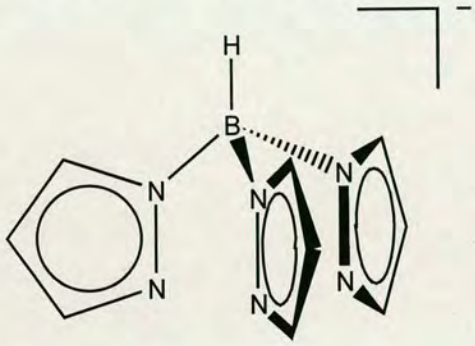

Figure 1.27 Tris(pyrazolyl)hydroborate

The poly(pyrazolyl)borate ligand system was first introduced by Trofikmenko[43, 44] in the 1960s and has been studied extensively since then. The ligand, shown in Figure 1.27, consists of pyrazolyl rings, containing an imine nitrogen donor atom in the two positions, linked to a central boron atom.

It is synthesised by the simple thermal dehydrogenation of an alkali metal borohydride with pyrazole. Up to four pyrazolyl rings can be substituted on to the boron atom, enabling the number of nitrogen donor atoms to be varied. The tris(pyrazolyl)borate ligands, abbreviated to Tp, are uni-negative and potentially tridentate. They can complex to a wide range of metals from throughout the periodic table. They are formally six electron donor systems and in this respect can be considered analogous to the Cp ligand. Trofikmenko has described them as scorpionate ligands.[45] On complexation to the metal, three six-membered chelate rings are formed, which almost always assume a boat structure. The metal generally assumes an octahedral geometry and the ligands can be considered to be of local C_{3v} symmetry.

The ligand systems are extremely versatile. Substitution on the pyrazole ring by groups with different steric and electronic properties can be used to vary the characteristics of the ligand system, enabling great control of the chelated metal

environment. These substituted systems are known as 'second generation Trofimenkos'.[45] In general, the unsubstituted systems form six co-ordinate, bis 'sandwich' complexes with bivalent metal ions.

Substitutions at the three positions have the most direct impact on the accessibility of the co-ordinated metal to other reactants. Parkin and co-workers have looked at the more sterically demanding ligand systems, *eg.* with a ^{t}Bu or phenyl substituent at the three position of the pyrazole ring. This hinders the formation of the bis complex and monomer species are favoured. The tripodal ligand provides a well-defined co-ordination environment, enabling an investigation of the synthesis and reactivity of monomeric Zn(II) and magnesium alkyl (MgR^+) and hydride (MgH^+) derivatives,[46, 47] which would otherwise be too unstable to isolate. For example, incorporation of a phenyl group at the three positions has enabled the isolation of lithium and thallium derivatives.[48]

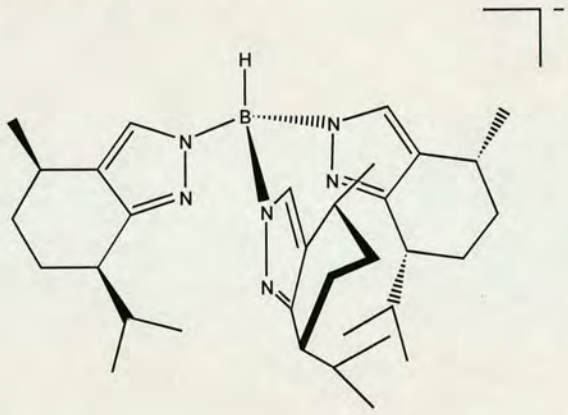

The chiral analogues of these ligands can be formed by attaching optically active centres to the ligand frame at the pyrazolyl ring's three position. Tolman *et al.* were the first to report enantiomerically pure tris(pyrazolyl)hydroborate (Tp^*) ligands, which have C_3 symmetry.[49]

Figure 1.28 A C_3 symmetric Tp* ligand

The general approach taken to synthesise optically active Tp^* ligands is to link together three identical enantiomerically pure pyrazoles (Hpz^*). Annulated pyrazoles are favoured because the stereogenic centre attached to the pyrazole carbon α to the free N, (the nitrogen not attached to the central ligand atom), is held in a relatively rigid conformation. B-N bond formation during the synthesis of the tripod ligand is known to occur at the least hindered nitrogen atom of the substituted pyrazoles. Therefore, the synthesis is extremely selective at forming just the desired ligand containing the stereo centre, of fixed orientation, distal to the central ligand atom.

Two optically active Tp^* ligands have been synthesised, HB((2*R*,5*R*)-menthylpz)$_3$, (abbreviated to Tp^{Menth}),[49] and HB((2*R*,5*S*)-Mementhylpz)$_3$, (abbreviated to $Tp^{Mementh}$).[50] The crystal structures of the ligands complexed to thallium(I) have been reported. The ligands are tridentate and show a propeller shaped geometry formed by the alternating bulky substituent groups and the hydrogen atoms fixed at the periphery of the metal centred ligand cavity. This results in a C_3 symmetric environment at the metal centre.[50]

Interestingly, although the configuration at the 4-carbon (containing the methyl group) is *R* in both cases, the 7-isopropyl substituent is cis to the 4-methyl (*R* configuration) in Tp^{Menth}, whilst the 7-tert-butyl group is in a trans position (*S* configuration) in $Tp^{Mementh}$. This results in the C_3 symmetric array of sterically bulky substituents having opposite rotational stereochemistry in the two complexes. The steric interactions between the *t*-Bu groups are greater than between *i*-Pr groups, resulting in a greater degree of distortion. This distortion results in a loss of coincidence of the bonding lone pairs on the pyrazolyl nitrogen atoms with their N-Tl bonds. This lack of directionality may reflect ionic character in the bonding.

The complexation of these C_3 symmetric ligands to transition metals has been explored. Four co-ordinate complexes; [$Tp^*M^{II}Cl$], (M = Zn^{II}, Ni^{II}, Co^{II}, Cu^{II}, Mn^{II}, Fe^{II}) were obtained from the metathesis reaction between the thallium salt of the ligand and the appropriate divalent metal halide.[49, 51] X-ray structure analysis confirmed the tridentate binding of the ligand to the metal centres to yield pseudotetrahedral metal geometries. Spectroscopic analysis was consistent with the complexes having a C_3 symmetric structure in solution.

Five co-ordinate complexes, [$Tp^*M(NO_3)$] and [$Tp^*M(OAc)$], (M = Cu, Zn), were formed in which there is a symmetrical binding of nitrate and acetate to form distorted square-pyramidal complexes.[51] The five co-ordinate $Tp^{Menth}Rh(CO)_2$ complex could also be isolated. However, the C_3, η^3 coordinated, 18 electron species is in equilibrium with a C_1, η^2 coordinated, 16 electron species. Despite this, the photolysis of the Rh complex leading to cyclometalation exhibits a high degree of

regio- and stereocontrol in the activation of the C-H bond.[52] The η^2 : η^3 ratio largely depends on the size of the 3-pyrazolyl substituents, with larger substituents favouring the formation of the η^2 isomer.[51] Six co-ordinate complexes, Tp^*TiCl_3, could be obtained. The spectroscopic data was consistent with a C_3 symmetric, octahedral complex. However, there was also ~10 % of another isomer present. This is believed to be due to an asymmetric form in which one pyrazolyl ring is bound by its less hindered N atom to the octahedral Ti ion.

Tolman has looked at the analogous ligand systems containing a central phosphorus oxide moiety, instead of borohydride. They can be synthesised by the substitution of the chlorides in $POCl_3$ by the appropriate pyrazole in the presence of triethylamine.[50] Rabinovich and co-workers have recently looked at the more flexible tris(pyrazolyl) ligands based on a central silicon atom.[53]

The effect of an aryl or alkyl substituent on the central boron atom has also been looked at. This enables the ligand to be used in situations where the reactivity of the B-H bond may prove problematic. This may provide a route to obtaining an optically pure ligand system by attaching an enantiomerically pure chiral group to the central atom.

1.3.1.3.2 Pyridine Ligands

Tris(2-pyridyl)methanol was first reported by Wibaut and co-workers in 1951.[54] The ligand consists of three pyridine rings attached to a central non-coordinating carbon atom. It acts as a symmetric, tridentate ligand and its co-ordination to a wide variety of metals has been reported. In general, it facially co-ordinates to a single metal centre through the three pyridyl nitrogen atoms to form stable metal complexes.

In comparison to the analogous tris (pyrazolyl) tripod ligands, the majority of pyridyl ligands are neutral. The pK_a values of the conjugate acids of pyrazole and pyridine are very different, suggesting that pyridine is a better sigma donor than pyrazole. Pyridine is also reported to be a better π-acidic donor than pyrazole. These properties ensure that metal complexes with tris(pyridyl) tripod ligands are very different to those with tris(pyrazole)tripod ligands in terms of overall charge, solubility and redox properties.

Chiral analogues of the tris(2-pyridyl)methanol ligands, shown in Figure 1.29, have been prepared by attaching a chiral group to the 6-position of each pyridine ring.[55] This removes the vertical mirror planes associated with the parent compound and the resulting ligand will have C_3 symmetry. The chiral substituent will be placed next to the catalytically active metal ion in any metal complex that may form.

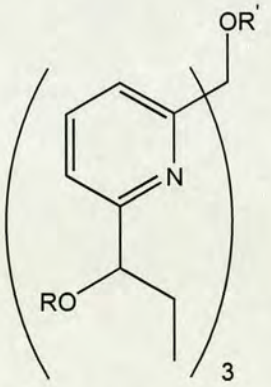

Figure 1.29 Chiral tris(2-pyridyl)methanol ligands

There are several ways in which chirality can be incorporated into the ligand. The ligand can be synthesized from three identical asymmetric monounits; or from achiral tris(2-pyridyl)methane derivatives and the centres of asymmetry added later. The latter approach was taken. The tripodal unit tris(2-pyridyl)methanol was built up

first. Prochiral ketone substituents were introduced at the 6-position, and were enantioselectively reduced using the chiral reagent (-)-DIP-Cl to yield the C_3 symmetric tetraalcohol.[56] Co-ordination of this ligand to $RhCl_3$ leads to a C_3 symmetric complex, but no crystal structure has been reported.

1.3.1.4 Oxazoline Ligands

Chiral (2,2'-bisoxazolino)alkanes are used as ligands in a wide variety of metal catalysed asymmetric reactions. Katsuki has developed the synthesis of enantiomerically pure tris(oxazoline) ligands.[57] The ligands can be prepared in two steps starting from amino alcohols and trimethyl nitrilotriacetic acid. Tris(β-hydroxy amides) are synthesized from trimethyl nitrilotriacetate and the corresponding amino alcohols. These are then cyclised using triphenylphosphine and triethylamine to form the desired tris(oxazoline). This is illustrated in Figure 1.30.

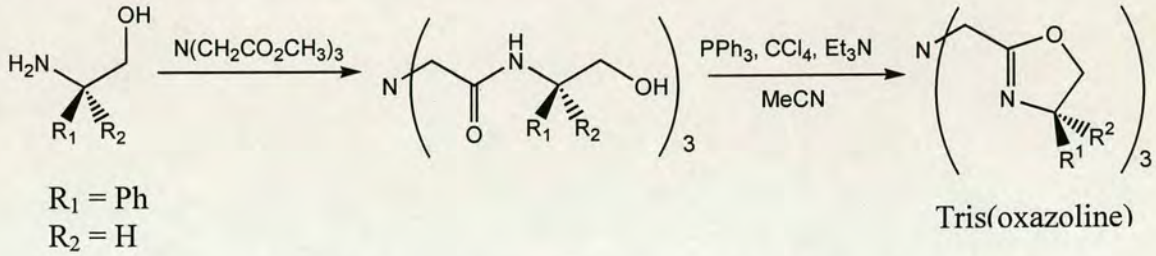

Figure 1.30 Synthesis of tris(oxazoline) ligands

Comprehensive complexation studies have not yet been carried out on the ligands. The iron complexes [$Fe(ClO_4)_2$tris(oxazoline)] and [$Fe(ClO_4)_3$tris(oxazoline)]; and the copper complexes [Cu(OTf)tris(oxazoline)] and [$Cu(OTf)_2$tris(oxazoline)] have been synthesized but not extensively characterized. The FAB mass analysis of the Fe(III) and Cu(II) salts shows that the ligands complex the metal in a ratio of 1:1.

The ligands were tested for their ability to induce asymmetric catalytic induction by examining the allylic oxidation of cyclopentene using iron or copper complexes of tris(oxazoline) as a catalyst. Neither of the iron complexes showed any signs of catalytic induction. Both copper complexes showed catalytic activity with the Cu(II) complex showing higher asymmetric induction. Using ^{t}Bu peroxybenzoate as a co-oxidant gave the oxidation product (*S*)-2-cyclopentenyl benzoate in 68 % yield and

74 % e.e. Further studies carried out showed that enantioselective allylic C-H hydroxylation is limited to cycloalkenes.

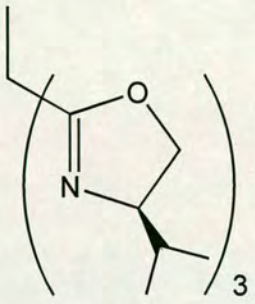

Figure 1.31 trisox-(*S*)-*i*Pr

Gade *et al.* have looked at synthesising a more rigid tris(oxazoline) ligand.[58, 59] They have replaced the central nitrogen atom with a carbon atom. This is linked directly to the three oxazoline rings and so the ligand no longer contains the flexible sp^3 methylene linker groups. One example of this type of ligand is trisox-(*S*)-*i*Pr, shown in Figure 1.31.

Synthesising the ligand *via* the same route as Katsuki *et al.*,[57] i.e. starting from the triester led to the formation of the bis(oxazoline) ligand. The tris(oxazoline) could be made by reacting the bis(oxazoline) ligand with a monomeric oxazoline.

Reaction of the ligand with rhodium trichloride forms the octahedral complex [$RhCl_3$-(trisox-(*S*)-*i*Pr)]. NMR spectroscopic data in solution indicated the expected 3-fold symmetric structure. X-ray diffraction studies confirmed that this was also the case in the solid state.

The (trisox-(*S*)-*i*Pr) ligand was employed in a first test for Cu(I) based asymmetric catalysis, in the cyclopropanation of styrene with *t*Bu diazoacetate. A strong preference was shown for the trans diastereomer (cis : trans = 22 : 78), which was obtained with a 65 % e.e.

1.3.2 Chirality in the Backbone

An alternative approach to obtaining C_3 symmetric ligands is to incorporate the chirality into the backbone of the ligand so that the stereocentres reside in the chelate framework. It is thought that this structure will be conformationally more rigid and hence more efficient at exerting stereocontrol over catalytic processes.[60]

1.3.2.1 Aliphatic Nitrogen Donor Ligands

Chiral analogues of the TREN ligand in which the chirality resides in the backbone have been prepared by Moberg's group.[60] The ligands have a central nitrogen atom, connected *via* two methylene groups to three amine donors.

The ligands can be synthesized by the nucleophilic ring opening of chiral aziridines, using ammonia as the nucleophile. The chiral aziridines can be prepared from the readily available chiral alcohols, as shown in Figure 1.32.

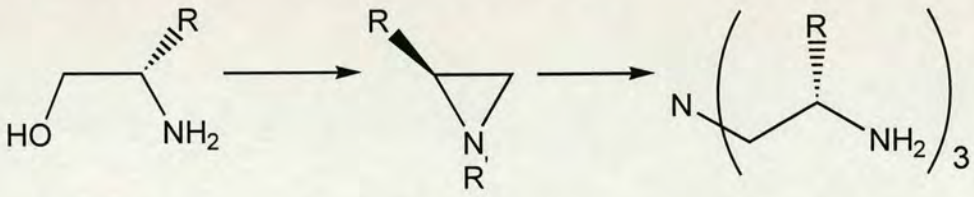

Figure 1.32 Synthesis of chiral TREN analogues

Initial complexation studies have been carried out with the ligands in which there is a tosylate or triflate group attached to the terminal nitrogen substituents. Mononuclear, tetradentate complexes have been obtained with titanium, aluminium and zirconium, however no crystal structures have been obtained. Preliminary investigations into the ability of these species to show asymmetric catalytic activity have been carried out. For the titanium complexes, the apical ligand is only partially exchanged and only in the presence of acidic amines such as pyrrole. The complexes generally show low catalytic activity and low stereoselectivity. It is thought that the co-ordination of the substrate is inhibited by the sterically hindered cavity.

The incorporation of large groups on the terminal amine functionalities has developed the ligands further. Ligands containing the pentafluorophenyl-substituted

moieties have been synthesized, shown in Figure 1.33. The chiral aminoamines have also been coupled with 2-DPPBA, a carboxylic acid. This ligand is illustrated in Figure 1.34. The catalytic activity of these ligands has not yet been assessed.

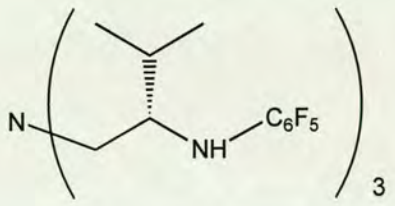

Figure 1.33 pentafluorophenyl substituted ligand

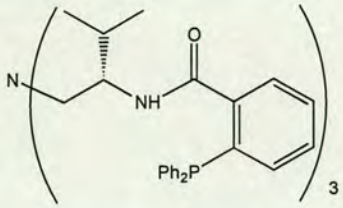

Figure 1.34 2-DPPBA substituted ligand

1.3.2.2 Alkoxide Ligands

Early transition metal complexes bearing chiral alkoxide ligands are used widely in asymmetric catalysis. Perhaps the most famous example being the asymmetric epoxidation reaction of Sharpless[61] – recognized by the noble prize for chemistry in 2001. The most successful cases studied have involved titanium as the early transition metal and have utilized diols or polyols so that the catalytic species is stabilized by chelation.

Nugent's group has investigated trialkonolamine ligands.[62] These ligands are analogous to those studied by Moberg *et al.* but contain oxygen donor atoms instead of nitrogen donor atoms. The parent ligand, triethanolamine is easily synthesised and is known to stabilize titanium alkoxides towards hydrolysis in aqueous environments. Early transition metal complexes co-ordinated by the trianion of this ligand have been synthesised. Nugent's group has looked at introducing chirality into the ligand by incorporating chiral groups into the ligand framework.[62]

The homochiral ligand (*S,S,S*)-triisopropanolamine is easily synthesised from ammonia and *(S)*-propylene oxide,[63] as illustrated in Figure 1.35. This can be extended to make other alkyl analogues. The synthesis of the ligand has been improved in terms of both higher yields and faster reaction times by the use of microwaves for the ring opening of the epoxide ring.[64]

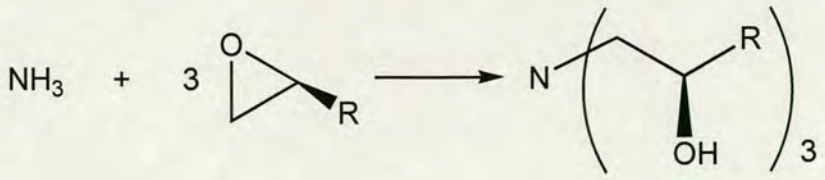

Figure 1.35 Synthesis of (*S,S,S*)-triisopropanolamine

The ligands form oligomeric species with zirconium.[65] Discrete hydroxo-bridged dimers formed upon partial hydrolysis. Although their exact structures have not been determined, the zirconium complexes have been shown to act successfully as asymmetric catalysts for the enantioselective addition of azides to meso epoxides. Under certain conditions, ring opened products are obtained with high selectivity (up to 93 %).[65] The partially hydrolysed zirconium species can also be used to catalyse the asymmetric sulphoxidation of alkyl aryl sulphides using alkyl hydroperoxides as the stoichiometric co-oxidant.[66]

Upon treatment with tri-*n*-propyl vanadate, the ligands form C_3 symmetric, trigonal bipyramidal structures.[62] The X-ray crystal structure of the R = ^{t}Bu complex shows that the vanadium centre is distorted towards a tetrahedral structure, with the vanadium displaced from the plane of the three oxygen donor atoms. The three ^{t}Bu groups are located distal to the vanadium centre and so have no direct influence on the steric environment of the metal co-ordination sphere. The asymmetry of the co-ordination sphere is due to the O-C-H hydrogen atoms, which are arranged in a clockwise array around the equatorial plane of the complex. This theory is supported further by the fact that altering the steric bulk of the alkyl substituents has no effect on the co-ordination sphere.

With niobium and tantalum, the ligands form discrete monomeric species.[62] Reaction of the ligand with Ti(IV) isopropoxide forms a stable trigonal bipyramidal titanium complex. The subsequent treatment of this species with acetyl chloride yields crystals of the chloro complex. X-ray analysis shows this complex to have a similar structure to the previously described complexes, with a trigonal bipyramidal structure and a pseudo 3-fold axis. The short Ti-N distances confirm the presence of a Ti-N bond.

This complex is able to catalyse the asymmetric sulphoxidation of alkyl aryl sulphides. In the presence of alkyl hydroperoxides, enantiomeric excesses of up to 84 % with a catalytic efficiency of 50-100 turnover numbers can be achieved.[67] A more detailed investigation into the exact titanium species involved in the catalytic cycle has been carried out. The tetradentate ligation of the titanium core provides a stable core whilst the apical site is labile in comparison. The nature of the complex depends upon the stoichiometry of the reaction mixture. An exact 1:1 ligand / Ti(IV) ratio results in a mononuclear species. Excess ligand leads to polynuclear titanium species in which the excess trialkonlamine bridges multiple titanatrane units. In the presence of excess *t*-butyl hydroperoxide, all of the precatalyst species are converted to a mononuclear Ti(IV) peroxo complex, which acts as the active catalytic species.[68]

Knochel's group has looked at a similar ligand system but with a central carbon atom that will be non-coordinating and so potentially the ligand will be tridentate. One such ligand is shown in Figure 1.36. The chiral C_3 symmetric triols can be prepared *via* the iterative catalytic asymmetric alkylation of aldehydes by organozinc reagents, followed by diastereoselective hydroboration.[69]

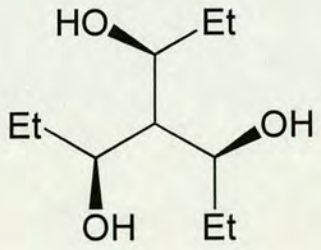

Figure 1.36 C_3 symmetric triol ligand

The triol ligands form oligomeric species upon complexation to titanium.[69]

Figure 1.37 shows a suggested structure for these species. NMR spectroscopy suggests that there are dynamic processes of ligand exchange *via* bridging alkoxide species. These equilibration processes will render the complexes useless for chiral induction, as the C_3 symmetric environment will not be maintained.

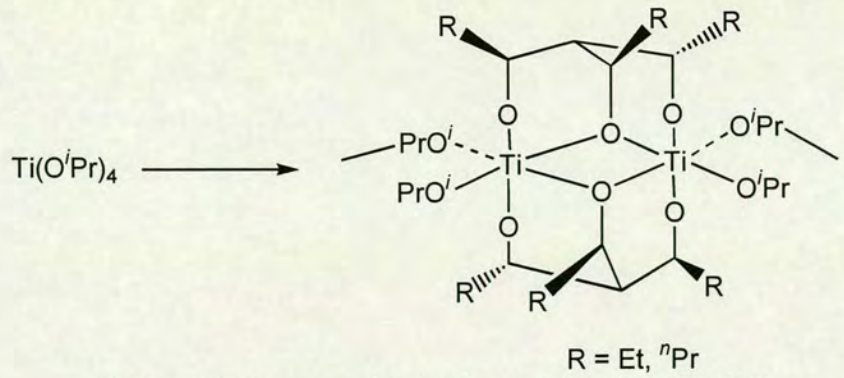

Figure 1.37 C_3 symmetric triol coordinated to titanium

Non-dynamic metal species can be obtained upon complexation to vanadium.[69] X-ray crystal structures were obtained and these show that the complexes do not have C_3 symmetry. The complexes are binuclear with two vanadium centres bridged by two triolato ligands. Both vanadium centres are penta-coordinated in a distorted tetragonal pyramidal fashion. Figure 1.38 shows a sketch of the structure of the vanadium complex.

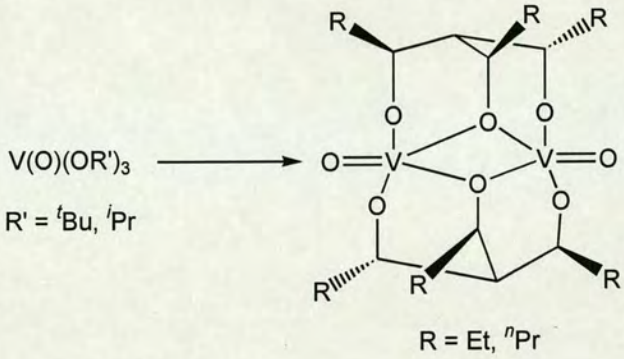

Figure 1.38 C_3 symmetric triol coordinated to vanadium

A series of model reactions were carried out to test the catalytic properties of the titanium and vanadium complexes.[69] However no synthetically useful asymmetric inductions could be obtained. This is not really surprising, given that none of the complexes have true, non-dynamic C_3 chirality.

1.3.2.3 Aromatic Nitrogen Donor Ligands

Canary's group has altered the ligand backbone using a slightly different approach to introduce C_3 symmetry to metal complexes.[70-73]

They have investigated modifications to tris(2-pyridylmethyl)amine, TPA, shown in Figure 1.39. TPA is a ligand system consisting of one sp^2 carbon atom and one methylene linking group between the nitrogen donor atom of the pyridine ring and a central nitrogen atom.[74]

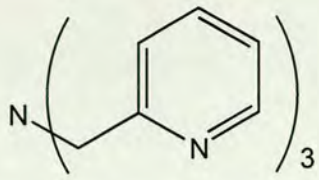

Figure 1.39 Structure of TPA

It has many potential binding modes, depending on the number of atoms through which it co-ordinates and can confer certain geometries on metal complexes containing it. Its complexation to many metals has been investigated.[75] The ligand generally forms mono or binuclear complexes, depending on the size of metal atom involved. There are two possible ligand conformations observed in the complexes. Trigonal bipyramidal complexes display C_3 symmetry, whereas octahedral and square pyramidal complexes possess a plane of symmetry and have C_σ symmetry.

In C_3 symmetric complexes, the ligand is tetradentate with the tertiary amine nitrogen atom occupying the axial site and the pyridine nitrogen atoms occupying equatorial positions. The three pyridine rings are tilted in the same direction with respect to the central axis of the molecule resulting in the ligand having a three-fold symmetric twist with a propeller like geometry. This twist is caused by a mismatch between the size of the metal ion and that of the coordination pocket provided by the four nitrogen donor atoms in the ligand. For a precisely matched metal-ligand combination, C_{3v} symmetry may be envisaged.

Various studies have been carried out on the effect of substituents on the pyridine rings. TPA derivatives containing more sterically bulky substituents show an increase in the degree of twist. For example, the ligand TPPA, shown in Figure 1.40, containing phenyl substituents in the 6-positions of the pyridine rings was investigated by Canary *et al.*[71]

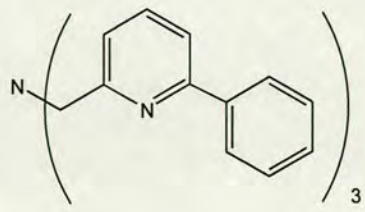

Figure 1.40 Structure of TPPA

The ligand forms complexes with both Cu(I) and Cu(II) and their crystal structures have been obtained. In both cases, the ligands are tetradentate with all four nitrogen atoms co-ordinating to the copper. Space filling models, generated from X-ray coordinates, shown in Figure 1.41, show that the Cu(I) is completely encapsulated by the ligand. The Cu(II) complex contains an additional acetonitrile molecule that is co-ordinated to the apical site of the trigonal bipyramidal complex. The ligand undergoes a helical twist to form a cavity defined by the phenyl substituents, which encase the additional solvent molecule. The twist is achieved solely through the rotation about the 2-pyridyl-CH_2 bonds and results in a more pronounced propeller shaped geometry compared to the Cu(I) complex. The average angle between the axis of the pyridine arms and the Cu-N bond is 14.8° in the Cu(I) complex, compared with 36.6° in the Cu(II) complex.

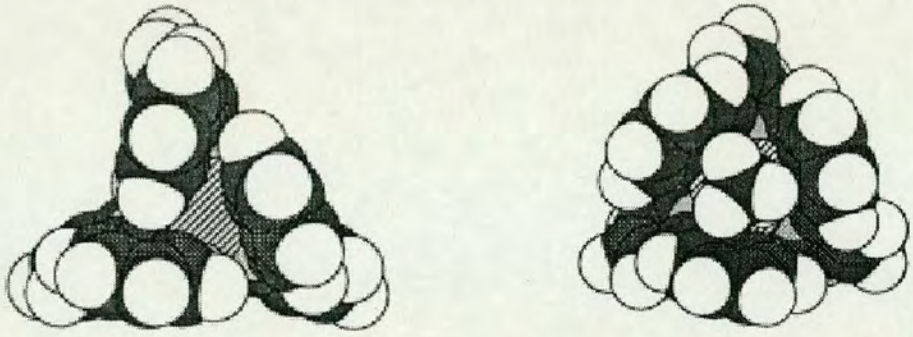

[Cu(TPPA)]BPh_4 [Cu(TPPA)(MeCN)]$(ClO_4)_2$

Figure 1.41 Space-filling models of Cu(I) and Cu(II) complexes with TPPA

Canary's group has tried to control the direction of twist by adding a single chiral centre to one of the tripod arms, two such ligands are illustrated in Figure 1.42.[70, 73]

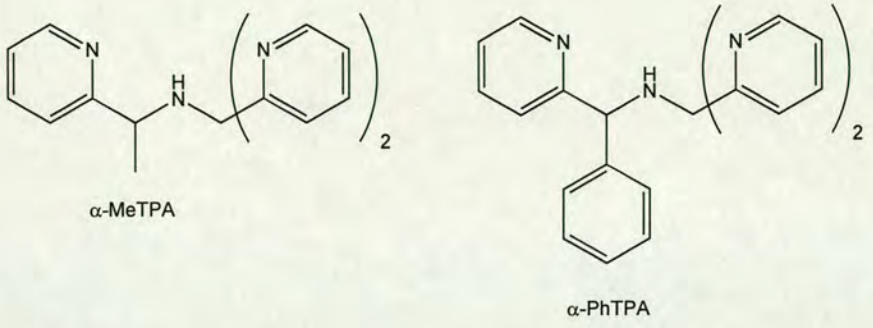

α-MeTPA

α-PhTPA

Figure 1.42 Structure of C_3 symmetric directing tripod ligands

Although the ligands are of C_1 symmetry, they wrap around the metal centre to form chiral, *pseudo* C_3 symmetric complexes. The ligand can wrap around the metal to form right or left handed propeller-like stereoisomers, which have opposite axial chirality and are conformational enantiomers. The absolute configuration of the centre dictates which conformation of propeller will form as a result of minimising steric interactions between the substituent group and the pyridyl groups. In the anti isomer, the α-substituent points away from the pyridine rings whilst in the syn conformation, the α-substituent points towards one of the pyridine rings.[73]

Molecular mechanics calculations of $[Zn(\alpha\text{-MeTPA})Cl]^+$ and $[Zn(\alpha\text{-PhTPA})Cl]^+$ indicate that the anti conformation would be more stable than the syn conformation by 1.5-2.5 kcal/mol.[73] This is seen from the X-ray crystal structures with the anti conformation observed in all cases. Although the arms are quite mobile in solution, they remain in a similar orientation to that observed in the solid-state structures. This is shown by strong anisotropic absorptions in circular dichroism studies.

In an attempt to determine what effect the nature of the chiral substituent on the tripod arm has, a range of ligands and their complexes were synthesized.[73] There appears to be no apparent trend for the effect of the substituent on the degree of the

twist. This can be seen from the average twist angle between the planes of the pyridine rings and the apical nitrogen–metal bond, shown in Table 1.1.

Complex	Twist angle / °
$[Zn(TPA)Cl]^+$	11.9
$[Zn(\alpha\text{-MeTPA})Cl]^+$	8.3
$[Zn(\alpha\text{-PhTPA})Cl]^+$	12.3

Table 1.1 The effect of the substituents on the average twist angle

The magnitude of the twist in the solid state is most likely to be affected by crystal packing forces. For instance, even for the unsubstituted ligand TPA, in $[Zn(TPA)Cl]^+$, one of the angles is double the other two. (17.2, compared to 9.7 and 8.9°).[73]

However, if a more bulky substituent than those discussed above is used, for example isopropyl, the pyridine arm is no longer able to co-ordinate to the metal ion.[72] This is accompanied by a rotation about the tertiary carbon-nitrogen bond to position the isopropyl substituent away from the steric crowding.

The distorted trigonal bipyramidal geometry of these compounds and the tetradentate nature of these ligands make them unsuitable for catalysis, however, they could be used as chiral Lewis acids.

1.3.3 Twisted Ligands

The third way in which C_3 symmetric complexes can be formed is when the ligand (not necessarily of C_3 symmetry) co-ordinates to the metal in such a way that the overall complex has C_3 symmetry. One example is when co-ordination of the tripodal ligand results in the formation of eight membered chelate rings. The larger chelate ring size is thermodynamically less favourable and molecular modelling shows that the lowest energy conformation for the resulting tricyclic metal-ligand framework possesses a distinct twist that minimises the angle strain within the structure. Such eight membered chelate ring structures form when a tripod with a non-coordinating

central atom and two linker atoms connecting the donor atoms co-ordinates to an octahedral or tetrahedral metal centre in a tridentate manner.

Alternatively, a tripod consisting of a co-ordinating central atom with three linker atoms may also coordinate to metals to form C_3 symmetric complexes. Coordination of the ligand results in the formation of six membered chelate rings that adopt a chair conformation. Provided the ligand coordinates to the metal in a tetra dentate manner, the conformation of the chelate rings will provide a C_3 symmetric structure.

1.3.3.1 Tripod Ligands with a Non-Coordinating Central Atom and n=2

Huttner carried out a study on the tris-pyrazolyl donor ligand $CH_3C(CH_2Pz)_3$.[76] This ligand has a non-coordinating central carbon atom connected *via* two linker atoms to the donor nitrogen atoms. He found that on treatment with $[Mo(CO)_3(NCMe)_3]$, only two of the three donor atoms were coordinated, while the third one acts as a dangling arm, as illustrated in Figure 1.43. This was shown from the X-ray crystal structure. The conclusion was drawn that the formation of three eight-membered chelate rings required for η^3 coordination is thermodynamically unfavourable.[76]

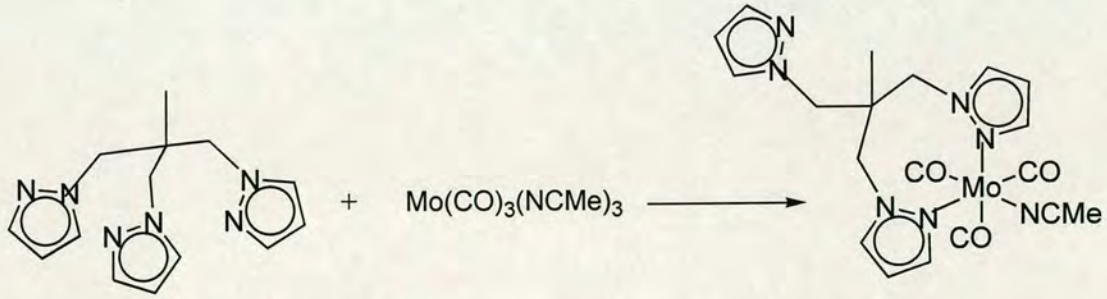

Figure 1.43 Formation of a complex with one 'dangling' arm

This cannot be generalized to all tripod-based systems with two linker atoms connecting the central atom to the three donor atoms and does not rule out η^3 coordination in all cases. Since then, there have been several reports in the literature of examples to challenge Huttner's hypothesis.

1.3.3.1.1 Sulphur Donor Ligands

Reglinski *et al.* have shown that this mode of coordination is possible with the formation of the ligand tris(methyimazolyl) η^3 coordinated to various octahedral and tetrahedral metal centres.

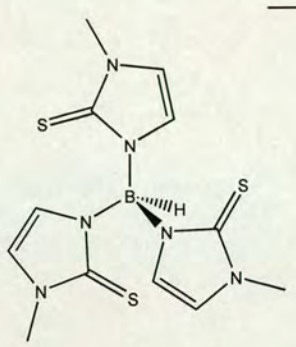

Figure 1.44 Tm

Hydrotris(methimazolyl)borate, (abbreviated to Tm) was developed by Reglinski and co-workers[77-80] as a soft analogue of the hydrotris(pyrazolyl)borate anion. They have looked at attaching a different organic ring system to the boron central atom to replace the hard nitrogen donors of Tp with softer sulphur donors. Tm is a soft, monoanionic, six-electron donor ligand and is isoelectronic with Cp and Tp.

The central boron atom is separated from the sulphur donor atoms by two linker atoms in Tm (compared to one in Tp). This results in eight membered chelate rings forming on complexation to the metal, compared with the six membered chelate rings formed with the analogous Tp ligand. Tm is synthesised in an analogous manner to Tp *via* the thermal dehydrogenation of sodium borohydride and methimazole, as shown in Figure 1.45.

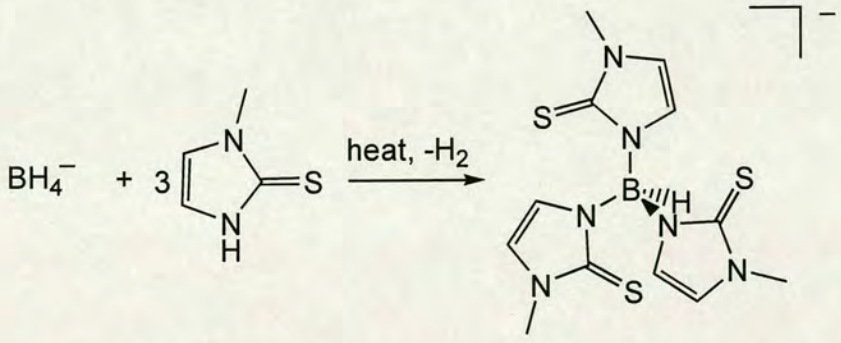

Figure 1.45 Synthesis of Tm

The co-ordination chemistry of Tm has been studied extensively. All of the complexes containing a metal ion coordinated to at least one Tm ligand are listed in Table 1.2.

Ligand	Metal	Complex	Group	Reference
Tm	Zn	ZnTmBr	Reglinski	78
		ZnTmCl ZnTmI		80
		ZnTmBr		81
	Cd	CdTmBr		
	Hg	HgTmBr		
	Tl(I)	TlTm		77
	Tl(III)	$TlTm_2I$ $[TlTm_2][TlI_4]$		80
	Ru	$[RuTm(CO)(PPh_3)]$	Hill	82
	Bi	$[Tm_2Bi][Tp_2Na]\cdot 4CH_2Cl_2.Cl(CH_2)_2Cl$ $[TmBiCl(\mu\text{-}Cl)]_2$	Reglinski	79
	Cu(I)	CuTm		78
		$(R_3P)CuTm$ $R'Ph_2PCuTm$ $[CuTm]_2$ pyCuTm $(m\text{-tolyl}_3P)CuTm$ $(p\text{-tolyl}_3P)CuTm$	Lobbia	83
	Ag(I)	$TmAgPPh_3$ $[TmAg]_2$		84
		$TmAg[PCy_3]$ $TmAgPR_3$ $[TmAg]_2$		85 86
	Mo	$TmMo(CO)_3\eta^3\text{-}C_3H_5$	Reglinski	87
	W	$TmW(CO)_3I$		
Tm^{Ph}	Zn	$Tm^{Ph}ZnNO_3$ $Tm^{Ph}ZnI$ $Tm^{Ph}ZnSPh$ $[Tm^{Ph}Zn(NCMe)][ClO_4]$ $Tm^{Ph}ZnOH$	Parkin	88 89 90
	Tl(I) Tl(III)	$[Tm^{Ph}Tl]_2$ $(Tm^{Ph})_2TlClO_4$		91
	Co	$(Tm^{Ph})_2Co$		92
	Fe	$(Tm^{Ph})_2Fe$ $(Tm^{Ph})_2FeClO_4$		
	Pb	$(Tm^{Ph})_2Pb$ $Tm^{Ph}PbClO_4$		93 94
$Tm^{t\text{-}Bu}$	Zn	$Tm^{t\text{-}Bu}ZnCl$ $Tm^{t\text{-}Bu}ZnF$ $Tm^{t\text{-}Bu}ZnONO_2$ $(Tm^{t\text{-}Bu})_2Zn$ $Tm^{t\text{-}Bu}ZnOClO_3$ $[Tm^{t\text{-}Bu}ZnEtOH]ClO_4\cdot EtOH$	Vahrenkamp	95

Tm^{Cum}	Cd	$Tm^{t\text{-}Bu}ZnBr$	Rabinovich	96
		$Tm^{t\text{-}Bu}CdBr$	Rabinovich Vahrenkamp	96 95
	Hg	$Tm^{t\text{-}Bu}HgBr$		
	Zn	$Tm^{Cum}Zn(o\text{-}C_6H_4\text{-}pNO_2)$		
Tm^{Bz}	Zn Cd	$Tm^{Bz}ZnBr$ $Tm^{Bz}CdBr$	Rheingold	97
$Tm^{p\text{-}Tol}$	Zn Cd	$Tm^{p\text{-}Tol}ZnBr$ $Tm^{p\text{-}Tol}CdBr$ $Tm^{p\text{-}Tol}CdSR$	Reglinski	80
Tbz	Tl	TlTbz		

Table 1.2 Metal complexes formed with Tm type ligands

These examples illustrate how versatile the Tm ligand is, in that it can coordinate to a range of different sized metals through one, two or all three of the sulphur donor atoms and can also act as a bridging ligand. The ligand can support tetrahedral, octahedral and a range of other metal coordination geometries.

Tm tends to forms mono ligand complexes with small metal cations such as zinc.[78, 80] The X-ray crystal structure of [ZnTmBr] has been obtained. Tm acts as a tridentate ligand and coordinates through all three sulphur atoms to form eight membered chelate rings. The larger chelate ring results in a different metal binding geometry. The strain associated with the larger chelate rings is minimised by the methimazole fragments of the ligand twisting to form a propeller geometry, resulting in the complexes being C_3 symmetric overall. In [ZnTmBr], the methimazole fragments adopt a propeller twist of 45.6° measured along the imaginary torsion angle S-N···B-N, giving the molecule C_3 symmetry. The zinc ion has a slightly distorted tetrahedral geometry with the S-Zn-S angles compressed to 105.35(8)°. The Tm ligand is much more flexible than Tp. In [ZnTmBr], the zinc ion moves much further into the plane of the donor atoms (S-Zn-S 105°) compared to the analogous Tp complex [η^3-HB(3-Bupz)$_3$}ZnBr], (N-Zn-N 95°).

By varying the degree of twist, the metal can move further out of the ligand co-ordination pocket while maintaining optimal sulphur-metal bond distances and geometry. To illustrate this Reglinski has compared the complexes [TmMBr] (M = Zn, Cd, Hg)[81] in which the increasing size of the metal ion results in a progressive

'opening up' of the twisted conformation of the TmM unit while maintaining optimal Zn-S distances. This can be seen from the H-B-N-C torsion angles, which have values of 31.8° for the Zn structure and 40.1 and 40.3° for the Cd and Hg structures respectively. The Cd and Hg complexes are crystallographically isomorphous and both have highly distorted tetrahedral geometries. The metal and B-H unit are no longer collinear and the halide is markedly displaced so that the structure tends towards a trigonal bipyramid. This is a mode of flexibility unavailable to ligands of the conventional Tp design. They also investigated the effect of changing the size of the halide ion but found there to be little influence on the overall structure.

Tetrahedral, monoligand complexes are also formed with Cu(I). Reglinski reported the formation of the copper complex [Cu(Tm)].[78] Lobbia *et al.* have synthesised and characterised a number of triorganophosphine Cu(I) complexes containing the Tm ligand.[98] The X-ray structures of [(*m*-tolyl$_3$P)CuTm] and [(*p*-tolyl$_3$P)CuTm] were obtained. Tm acts as a tridentate facially capping ligand coordinating through all three sulphur atoms to the copper ion. The ^{1}H NMR spectra indicate that these species are highly fluxional at room temperature. It is proposed that one or two of the Cu-S bonds dissociate, yielding complexes that are partially stabilised by a B-H···Cu agostic interaction. Diagrams of these structures are shown in Figure 1.46.

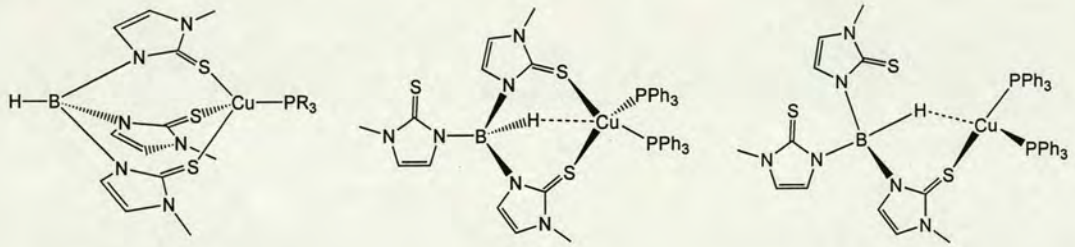

Figure 1.46 Proposed fluxional structures for triorganophosphine Tm copper(I) complexes

A B-H···M agostic interaction is reported in the triorganophosphine Ag(I) complexes containing the Tm ligand.[84, 85] [TmAgPCy$_3$] (PCy$_3$ = tricyclohexylphosphine) was characterised by X-ray crystallography. The ligand acts in a bidentate manner. Two methimazole sulphur atoms and a phosphorus atom are coordinated to the Ag(I) atom to form a distorted trigonal planar geometry. The loss of one of the methimazole

sulphur atoms from the coordination sphere is partially compensated for by the arrangement of the B-H unit to form an agostic interaction with the silver ion, as shown in Figure 1.47.

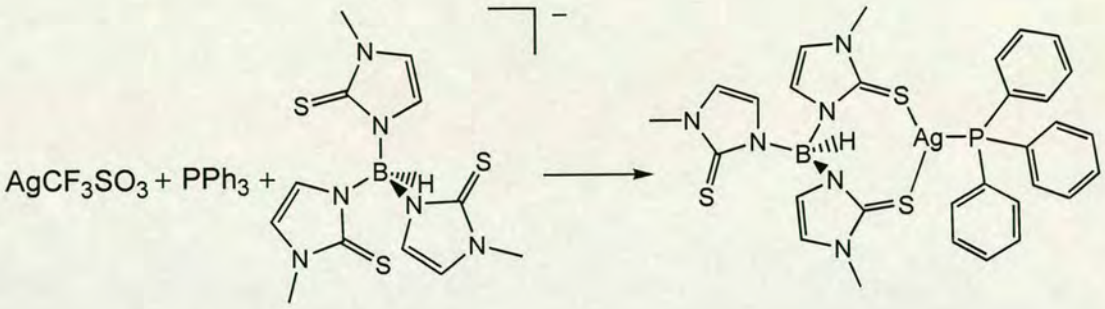

Figure 1.47 Triorganophosphine Tm Ag(I) complex

The Tm ligand is inverted at the boron atom with the B-H hydrogens pointing towards the silver(I) centre; in comparison to the tricoordinated ligand (e.g. in the TmZnBr complex[78]) in which the B-H hydrogen atoms point away from the metal centre. The complexes are fluxional in solution at room temperature, as illustrated by the ^{1}H NMR spectrum. This is proposed to be due to the complete dissociation and reassociation of the methimazole sulphur atoms.

Tm can act as a bridging ligand, as illustrated in the binuclear Ag(I) complex $[TmAg]_2$.[84, 86] The core of the dimer is a four membered $Ag(\mu\text{-}S_2)Ag$ ring. The sulphur atom bridges the two silver atoms unsymmetrically and the central borohydride moiety is orientated so that the hydrogen atom projects into the ring. The Tm ligand can also coordinate to octahedral metal ions. Reglinski *et al.* have formed complexes with group six metals molybdenum and tungsten.[87] X-ray crystal structures of $[TmMo(CO)_3\text{-}(\eta^3\text{-}C_3H_5)]$ and $[TmW(CO)_3I]$ were obtained. In both cases, Tm acts as a facially capping tridentate ligand. The molybdenum complex is octahedral and the seven coordinate tungsten complex can be described as a capped octahedron.

To compare directly the donor properties of the Tm ligand with those of the isoelectronic Cp and Tp ligands, the tungsten carbonyl compounds were

synthesised.[87] The ν(CO) value in the infrared spectra acts as a probe of the effects of the different face capping ligands, these are listed in Table 1.3.

Complex	ν(CO)/cm^{-1}		
[CpW(CO)$_3$I]	2030	1944	1936
[TpW(CO)$_3$I]	2021	1942	1904
[TmW(CO)$_3$I]	2004	1916	1902

Table 1.3 Carbonyl stretching frequencies for selected tungsten carbonyl complexes

The ν(CO) value moves to a lower frequency along the series Cp →Tp→Tm. This is indicative of a progressive change in donor properties of the facial ligand. Cp is able to act as a π-acceptor and competes with CO for electron density, resulting in a higher ν(CO) value. The Tp and Tm ligands have successively lower values, suggesting progressively greater electron density at the metal. This can be explained by the fact that Tp acts as a strong σ-donor with little or no π-interaction from the heterocycle π-system, while the lone pairs on the sulphur donors of Tm will overlap efficiently with the metal orbitals, giving strong π-donation.

An analysis of the η^3-allyl fragment in the series [(L)Mo(CO)$_2$(η^3-C$_3$H$_5$)] (L=Cp, Tp, Tm) was also carried out.[87] In each case the allyl group adopts an exo conformation with respect to the M(CO)$_2$ fragment. The M-C distances decrease slightly along the series Cp, Tp, Tm, suggesting a progressively tighter binding of the allyl fragment, which could correspond to a greater reactivity towards substitution.

A mononuclear octahedral metal complex could also be obtained with ruthenium.[82] The increased ring size of the chelate enables the metal ion to move deeper into the plane of the donor ligands. This occurs to such an extent in the ruthenium metal complex that there is an activation of the B-H bond resulting in the formation of a direct metal – boron bond to provide a metalloboratrane structural motif. This is illustrated in Figure 1.48. The more expansive chelation of HB(mt)$_3$ renders the complex more flexible and labile compared to the HB(pz)$_3$ ligand. The dissociation of one Tm arm followed by agostic B-H co-ordination and ultimately oxidative

addition of the B-H bond could provide a *cis*-hydrido-alkyl complex that would form the metalloboratrane structure upon alkene reductive elimination.

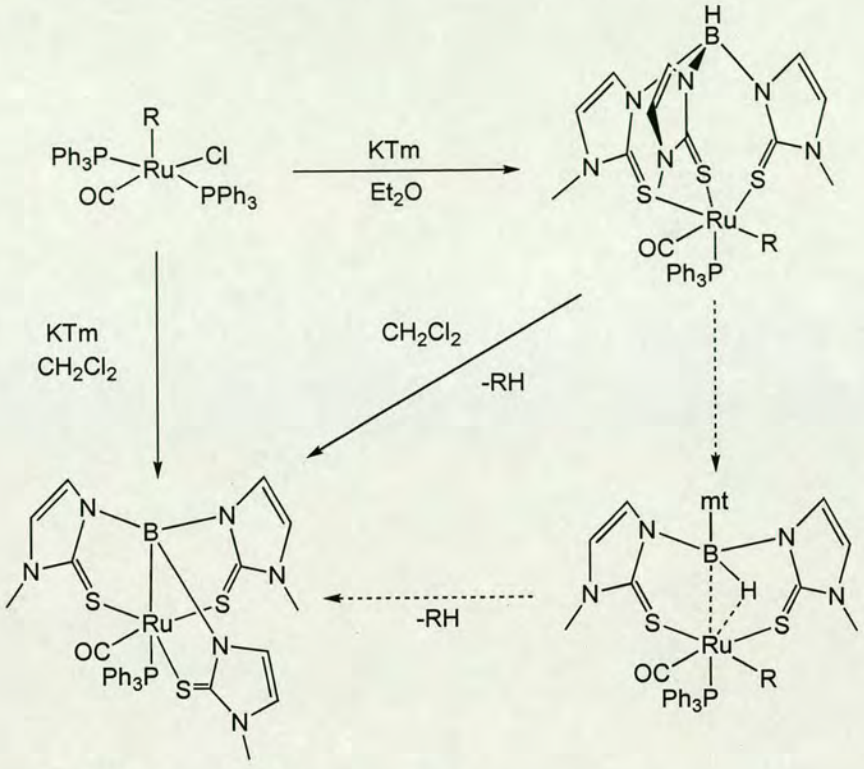

Figure 1.48 Formation of a mononuclear octahedral Tm ruthenium complex

Tm tends to form bis sandwich type complexes with larger, softer metal ions such as bismuth.[79] For example, Reglinski treated $BiCl_3$ with NaTm and obtained crystals that were structurally analysed by X-ray crystallography. The crystals were shown to be $[TmBiCl(\mu\text{-}Cl)]_2$. This binuclear complex is bridged by two chloride ions. However, the solid was found to be composed mostly of the salt $[Tm_2Bi][Tp_2Na]\cdot 4CH_2Cl_2.Cl(CH_2)_2Cl$. This consists of an octahedral Bi^{3+} coordinated by two Tm ligands. The ligands assume a propeller like configuration and exhibit local C_3 symmetry. This complex further illustrates the flexible nature of the Tm ligand as very little strain is required to accommodate the large Bi^{3+} cation.

Bis ligand complexes are also formed with Tl(III).[80] Crystals of $[Tl(Tm)_2]TlI_4$ have been analysed by X-ray diffraction. The large cation allows the repulsion between the peripheral methyl substituents to be minimized and the two ligands coordinate to form an approximately octahedral environment about the Tl(III) cation.

In a bid to extend this series of soft, tripodal ligands, Reglinski and Spicer have looked at using alternative imine-thiones as precursors of new thiazolylborate anions. They have synthesised the analogues Tz (from the thione 2-mercaptothiazoline) and Tbz (from the thione 2-mercaptobenzothiazoline).[83] These are illustrated in Figure 1.49.

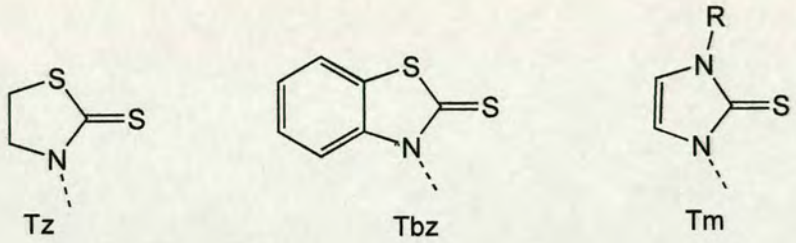

Figure 1.49 Structures of Tz, Tbz and Tm

Crystals of [TlTbz] have been grown and structurally analysed.[80] The monomeric unit consists of Tbz acting in a tridentate manner, coordinating through all three sulphur atoms to a Tl(I) metal. The ligand assumes a propeller like conformation. The monomeric units are associated *via* bridging thiones to give infinite one-dimensional polymeric chains consisting of a zigzag array of Tl and S atoms.

R	Ligand Abbreviation
Me	Tm
t-Bu	$Tm^{t\text{-}Bu}$
Ph	Tm^{Ph}
Mes	Tm^{Mes}
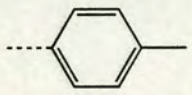	$Tm^{p\text{-}Tol}$
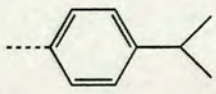	Tm^{Cum}
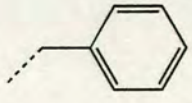	Tm^{Bz}

Table 1.4 Variations of the Tm ligand

A number of other groups have looked at increasing the steric bulk of the alkyl substituent at the 3-position of the imidazole ring. The phenyl- and mesityl- substituted ligands have been prepared by Parkin[88] to model zinc enzymes. A number of monomeric, tetrahedral zinc complexes have been isolated as shown in Table 1.4.[88-90] The molecular structure of $[(Tm^{Mes})Zn(HOMe)]^+$ has been determined by X-ray crystallography and is illustrative of the other zinc complexes containing Tm^{Ph} and Tm^{Mes}. The solid-state structure is similar to zinc complexes with Tm.

The ligand twists to adopt a propeller configuration and the complex has local C_3 symmetry. Solution ^{1}H NMR studies indicate that this configuration is rigid on the NMR time scale at room temperature.

The complexation of Tm^{Ph} to thallium has been investigated.[91] Tl(I) forms the binuclear complex $[Tm^{Ph}Tl]_2$. Tl(III) forms the species $[(Tm^{Ph})]_2Tl]ClO_4$ that has as an almost identical solid-state structure to $[(Tm^{Me})_2Tl][TlI_4]$ described above. The ^{1}H NMR spectra suggest that the structure in solution is different as there are two distinct types of Tm^{Ph} fragment.

Tm^{Ph} can form both mono and di ligand complexes with lead. Lead readily displaces zinc in the complexes $[Tm^{Ph}ZnX]$ to yield the monomeric, trigonal pyramidal $[Tm^{Ph}Pb]^+$ cation.[94] All three sulphur donor atoms coordinate to the lead. Unlike zinc, which is generally in a tetrahedral coordination in the solid state, lead has a reduced tendency to bind an additional ligand. $[(Tm^{Ph})PbClO_4]$ can also be synthesised by adding one equivalent of $Tm^{Ph}Li$ to $Pb(ClO_4)_2$. If two equivalents of ligand are used, the dinuclear complex $[(Tm^{Ph})]_2Pb$ forms.[93] This has been characterised by X-ray crystallography. The structure is very different to the other di-ligand complexes such as $[(Tm^{Ph})_2Tl]^+$ and $[Tm_2Bi]^+$. One ligand is η^3 coordinated whilst the other adopts an inverted η^4 configuration. The lead centre interacts with six sulphur donor atoms and with the H-B unit of the η^4 coordinated ligand. The X-ray crystal structure shows that the Pb-S bond lengths are much shorter for the η^3 coordinated ligand (2.848(1) Å) compared with the η^4 coordinated ligand (3.471(5) Å). This difference in length has led to the suggestion that $(Tm^{Ph})_2Pb$ is better described as a close contact ion pair, i.e. $[(Tm^{Ph})Pb][Tm^{Ph}]$. In direct contrast, the *tris*(pyrazolyl)borato complexes $[Tp_2Pb]$ and $[(Tp^{Me})_2Pb]$ both have a six coordinate geometry in which the lead ion is coordinated only by nitrogen donor atoms.[99] This further illustrates the greater flexibility conferred on the Tm^R ligand as a result of an extra linking atom in each of the tripod arms.

Tm^{Ph} forms sandwich complexes $[(Tm^{Ph})]_2Co$ and $[(Tm^{Ph})_2Fe]$ when FeI_2 and CoI_2 are treated with two equivalents of $Tm^{Ph}Tl$.[92] The X-ray structure analysis of the

complexes shows them to be virtually identical. The metal is in an approximately tetrahedral environment, being coordinated by only two of the sulphur donors from each ligand. The coordination sphere of the metal is completed by an interaction with the B-H unit of each ligand. This type of interaction results in the Tm^{Ph} ligand adopting a boat like eight membered ring configuration. One factor that may favour the formation of a tetrahedral structure is the more obtuse bite angle that is possible for the Tm^{Ph} ligand due to the extra flexibility of the tripod arms.

Higher valent metal centres favour tridentate binding and so the Fe(III) complex $[(Tm^{Ph})_2FeClO_4]$ adopts an octahedral structure in which both ligands coordinate to the metal through all three sulphur atoms.[92] This is analogous to the octahedral complexes $[Tm^{Ph}{}_2Tl]^+$ and $[Tm_2Bi]^+$, all of which contain an M^{3+} cation.

Vahrenkamp *et al.* have looked at the ^{t}Bu and cumyl substituted ligands $Tm^{t\text{-}Bu}$ and Tm^{Cum} and studied their complexation to zinc.[95] Monodentate zinc complexes combining the very soft $[(Tm^R)Zn]$ (R= ^{t}Bu, Cum) unit with harder, typically oxygen-containing co-ligands were synthesised and X-ray crystal structures were obtained. The complexes have a clearly defined propeller-like arrangement. However, the *t*-Bu groups point away from the zinc atom and do not really encapsulate it. They are not bulky enough to prevent the formation of the bis(Tm) complex. For example, the addition of zinc perchlorate to a solution of $KTm^{t\text{-}Bu}$, followed by extraction with non polar solvents yielded the bis complex $[(Tm^{t\text{-}Bu})_2Zn]$. In this complex, one arm of each tripod ligand remains uncoordinated.

In parallel, Rabinovich has investigated the $Tm^{t\text{-}Bu}$ ligand and looked at the Group 12 metal derivatives.[96] Complexes with each member of the triad have been structurally characterized by X-ray crystallography. The ligand forms four coordinate complexes, $[(Tm^{t\text{-}Bu})MBr]$ (M = Zn, Cd, Hg) that each have distorted tetrahedral geometries in the solid state. The three mercaptoimidazolyl groups adopt a propeller like arrangement about the approximate three-fold axis. Comparing the bond angles in the three complexes, it can be seen that the average Br-M-S angles increase down the triad, whilst the average S-M-S angles follow the opposite trend, (shown in Table

1.5). This results in a progressive elongation of the tetrahedral molecules along the approximate three-fold axis as the metal increases in size.

Metal	Average Br-M-S angle / °	Average S-M-S angle / °
Zn	112.4	106.3
Cd	115.9	102.1
Hg	117.4	100.4

Table 1.5 Selected bond angles for group 10 metal complexes with Tm^{t-Bu}

Rheingold and Rabinovich have contributed with the benzyl- and *p*-tolyl substituted Tm ligands which they have complexed to zinc and cadmiuim to form $(Tm^R)MBr$, (M = Zn, Cd; R = Bz, *p*-Tol).[97] The benzyl substituted derivatives were characterised by X-ray crystallography and shown to have a mononuclear, slightly distorted, tetrahedral geometry resembling the other $[(Tm^R)ZnX]$ complexes described previously.

Bailey and co-workers have developed a ligand that contains a different ring system attached to the central borohydride functionality. They have used thioxotriazolyl to construct hydridotris(thioxotriazolyl)borate, Tt, a ligand that combines the properties of the Tp and Tm ligands.[100] Tt is synthesised by the same route as Tm, (Figure 1.50).

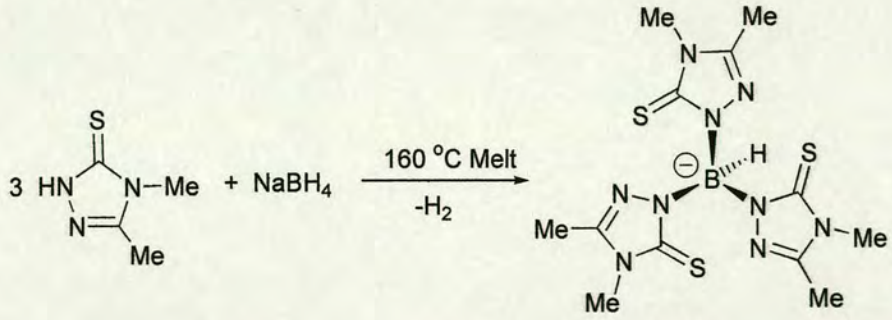

Figure 1.50 Synthesis of Tt

The ligand can co-ordinate through the sulphur (as for Tm) or nitrogen atoms (as for Tp). Co-ordination through all three nitrogen atoms will result in six membered chelate rings and C_{3v} symmetry whilst co-ordination through all three sulphur atoms

will result in eight membered chelate rings and C_3 symmetry. These mixed properties make the ligand viable for complexation with a very wide variety of metals. For instance, the ligand co-ordinates to the harder sodium and magnesium metals through the harder nitrogen atoms, but co-ordinates to the softer metals bismuth and tin *via* the softer nitrogen donors.[100] Alternatively, a combination of the different donor types could be obtained, allowing the co-ordination properties of the ligand to be finely tuned according to the precise electronic and steric requirements of the metal. However, examples of these mixed modes of co-ordination have yet to be observed.

1.3.3.1.2 Phosphinine Donor Ligands

The phosphinine based tripodal ligands recently reported by Le Floch's group[101] provide a different example of this type of ligand. They have synthesized two extended tripodal ligands each containing three phosphinine moieties. Each donor function is connected to a central carbon atom by means of a dimethylsilyl group and an sp^2 carbon atom.

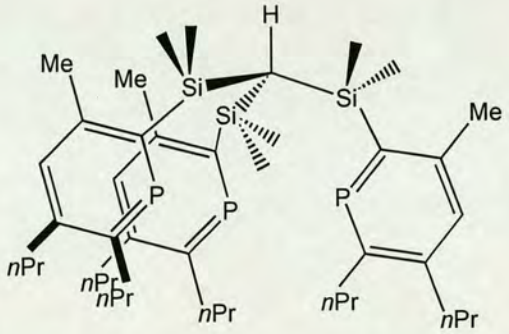

Figure 1.51 Phosphinine-based tripod ligand

Phosphinine based tripodal ligands have excellent π-acceptor abilities which significantly increases the Lewis-acidity of the metal centre to which they are co-ordinated.[102] They are also able to stabilise very electron-rich metal centres.[103] The ligands can be synthesized from the precursor tris(propynyldimethylsilyl)methane. This is formed by the reaction of three equivalents of propynyllithium with tris(bromodimethylsilyl)methane. Reaction of this precursor with excess 1,3,2-diazaphosphinine yields the corresponding tris(dimethylsilyl-1,2-azaphosphinine)methane intermediate. Reacting the intermediate with excess trimethlsilylacetylene or 4-octyne can form the phosphinine ligands L*1 and L*2.[101]

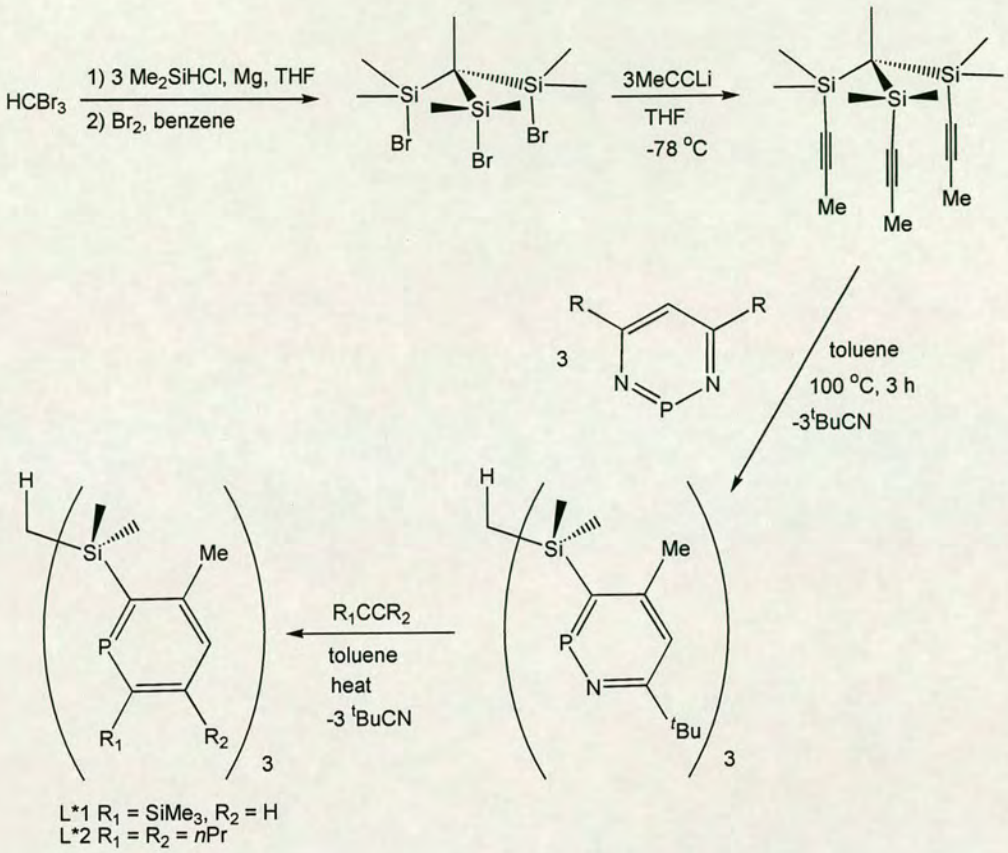

Figure 1.52 Synthesis of Phophinine ligands

Despite the large size of the cavity and the relative flexibility of L*1, the $SiMe_3$ groups are too sterically bulky to allow the approach of $M(CO)_3$ fragments, preventing the formation of metal complexes. The bulky $SiMe_3$ groups are replaced by linear alkyl groups in L*2. This allows the complexation of the ligand to a metal carbonyl fragment. Reaction of L*2 with $[W(CO)_5(THF)]$ in toluene at 110 °C for 20 h yields the complex $[(L*2)W(CO)_3]$. A schematic of the product is shown in Figure 1.53.

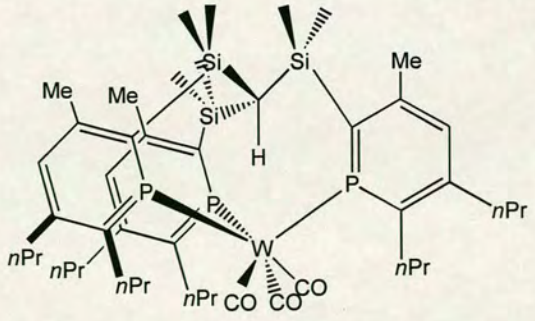

Figure 1.53 Schematic of tripod phosphinine L*2 bound to tungsten

The structure of the complex was verified by X-ray diffraction analysis, and is shown in Figure 1.54.[101]

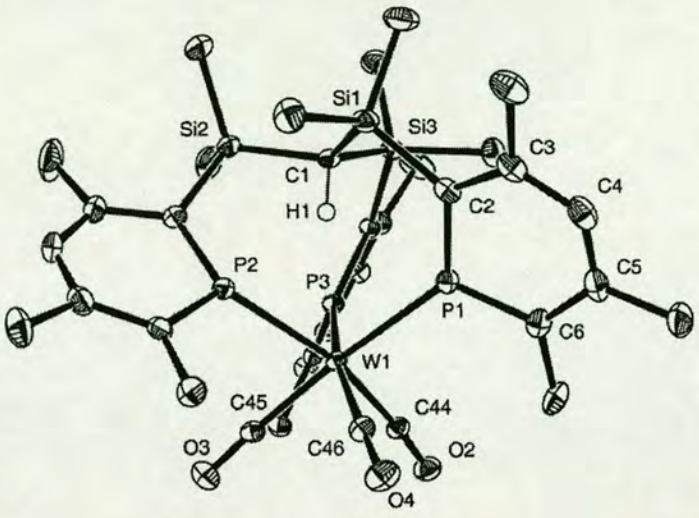

Figure 1.54 X-ray crystal structure of phospnine L*2 coordinated to tungsten

The ligand is tridentate and co-ordinates to the tungsten through all three phosphorus atoms. The tungsten has an octahedral geometry and the remaining sites are blocked by three equivalent carbonyl groups. The apex carbon is very flattened and the three Si-C-Si angles range between 114.93 and 118.17°. The sum of these angles at the central carbon atom is 349.76°, which is much closer to an sp^2 hybridised carbon than expected. The apical hydrogen atom is located inside the cavity, which explains the strong downfield shift of the C-H observed in the ^1H NMR (a quadruplet, $\delta = +6$, $^4J_{H\text{-}P} = 8.5$ Hz; compared to $\delta = 0$ in the free ligand). Although the apical hydrogen is located within the cavity, the C-H bond is not elongated (0.979 Å) and the H···W distance is 2.683 Å, indicating only a very weak interaction between the metal centre and the hydrogen. The complex is highly strained as illustrated by the dihedral angles C_{ring} - C_{ring} – P –W that lie between 145 and 160°, compared to the expected value of 180°. This strain is confined to the chelate rings and the three phosphinine rings are not significantly distorted. The eight membered chelate rings twist to minimize the strain, inducing a three-fold propeller shaped geometry.

1.3.3.2 Tripod Ligands with a Coordinating Central Atom and n=3

1.3.3.2.1 Aliphatic Nitrogen Donor Ligands

Schrock has investigated extended versions of the silyated TREN ligands described in Section 1.3.1.2.2. The symmetry of the chelate complexes can be decreased from C_{3v} to C_3 by using larger triamidoamine ligands with an extra methylene carbon in the tripodal arms. There are now three sp^3 atoms linking the central nitrogen atom to the donor atoms. The central atom is still potentially co-ordinating but will be more prone to dissociation than with analogous TREN derivatives. The ligand forms tetradentate, C_3 symmetric complexes with titanium(IV) ions.[29] The X-ray structure of [{$(Me_3SiNCH_2CH_2CH_2)_3N$}TiCl] shows it has a trigonal bipyramidal geometry. A top view of the structure is shown in Figure 1.55.

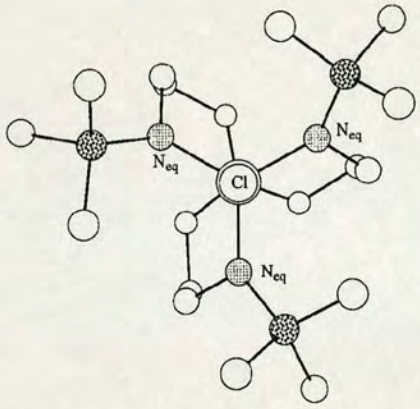

Figure 1.55 A top view of the structure of $[Me_3SiNCH_2CH_2CH_2)_3N]TiCl$

The TiN_2C_3 rings are puckered in a pseudocyclohexane chair form with the trimethylsilyl groups adopting a propeller shaped orientation. NMR analysis showed that the ligand framework is rigid on the NMR timescale so the methylene protons on a given carbon atom cannot interconvert readily by flipping of the six membered TiN_2C_3 ring. This more flexible ligand is potentially more compatible for use with larger second or third row metals, especially if bulkier N-substituents are utilised.

1.3.3.2.2 Aromatic Nitrogen Donor Ligands

Brunner has designed a ligand, shown in Figure 1.56, with three linker atoms between a central phosphorus atom and the donor imine functionalities.[104]

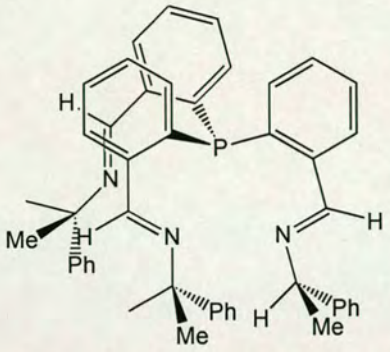

Figure 1.56 Brunner's tripodal ligand

In contrast to the previous systems, all three linker atoms are sp^2 carbons and so the ligand will theoretically be more rigid. The C_3 symmetry of the ligand will come about from the twist induced upon forming the six membered chelate rings that adopt a chair conformation and from the chiral substituents attached to the donor functionalities.

1.3.3.2.3 Oxygen Donors

Koch has designed the oxygen donor ligand tris(2-hydroxybenzyl)amine, shown in Figure 1.57.[106, 107] The ligand consists of a central nitrogen atom connected to phenolate rings *via* a methylene group. In other words there is one sp^3 linker atom and two sp^2 linker atoms.

The ligand is potentially tetradentate but due to the extra linking group will form eight membered chelate rings upon complexation to the metal. The metal / ligand chelate rings will twist to alleviate the strain associated with the less thermodynamically favourable sized rings to give a complex with C_3 symmetry.

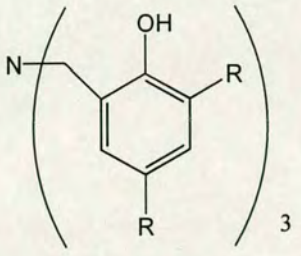

Figure 1.57 tris(2-hydroxybenzyl)amine

The phenolate ligand is able to form five and six co-ordinate complexes with Fe^{3+}. A trigonal bipyramidal complex forms with imidazole as the axial ligand and an octahedral complex forms when the remaining sites on the metal are blocked by a phen ligand.[106]

1.3.3.2.4 Sulphur Donors

Koch has designed the analogous sulphur donor ligand tris(2-mercaptobenzyl)amine, shown in Figure 1.58. The thiol donor ligand forms a four co-ordinate tetrahedral complex with Fe^{2+}, shown in Figure 1.59, that has idealised C_3 symmetry.[108] Ligands such as imidazole can be added to the vacant axial site opposite the amine nitrogen atom to give a trigonal bipyramidal geometry. Both the thiol and the phenolate ligands form stable complexes with Ga^{3+} and In^{3+} and are able to support a range of different co-ordination numbers and geometries depending upon the size of the metal donor and the other ligands present.[107] The overall structures of the complexes are chiral and have C_3 symmetry. This is reflected in the diastereotopic nature of the benzyl protons.

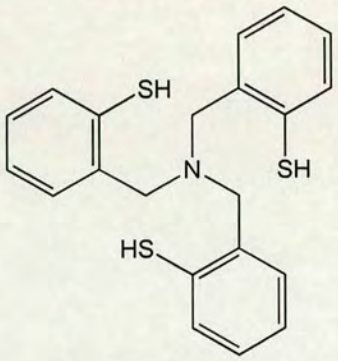

Figure 1.58 Tris(2-mercaptobenzyl)amine

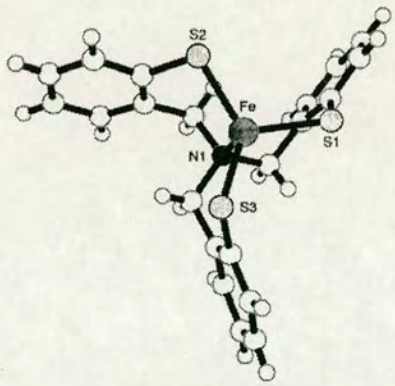

Figure 1.59 $[Fe^{II}(N(CH_2\text{-}o\text{-}C_6H_4S)_3)]^-$

The complexes were studied for their ability to act as diagnostic imaging probes[107] and so no investigations into their ability to induce asymmetric catalysis have been carried out yet.

1.4 Design Approach

The ligands that will be investigated in this thesis are tripods in which there are two linking atoms between the central, non-coordinating atom and the three donor atoms. Ligands fulfilling these criteria are predicted to form C_3 symmetric complexes upon coordination to metal fragments by virtue of the helical twist induced to minimize the strain, as described previously.

Upon complexation to the metal, two enantiomers can form, depending upon which direction the chelate rings twist. The resulting complexes will be of identical energy, and so will form as a racemic mixture. If chirality is introduced into the ligand prior to coordination, the complex will form as diastereoisomers, which then can be separated to give a single diastereoisomer with an enantiomerically pure metal center. Chirality can be introduced in two ways; either through placing a chiral group on the three fold rotational axis, i.e. attaching it to the central atom, as shown in Figure 1.60, or by attaching three identical chiral groups at equivalent points on each of the three tripod arms, as shown in Figure 1.61. The first method is preferable since introducing chiral substituents that are intrinsically bulky close to the metal center may produce too much steric hindrance about the substrate binding site and render the complex catalytically inactive.

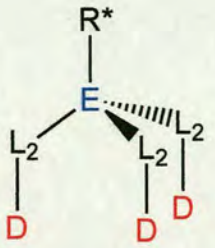

Figure 1.60 Chiral group attached to central atom

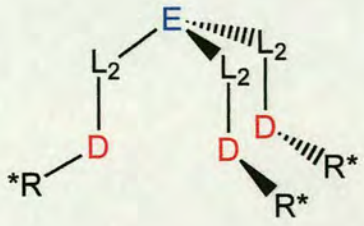

Figure 1.61 Chiral groups on each tripod arm

Interconversion between the two enantiomeric complexes can be achieved by a conformational change involving the relative twisting of the metal and the central ligand atom, as shown in Figure 1.62, and as such does not involve bond cleavage.

Molecular modelling suggests that this is a high-energy process, and introducing a bulky chiral substituent at the central ligand will hinder this process further.

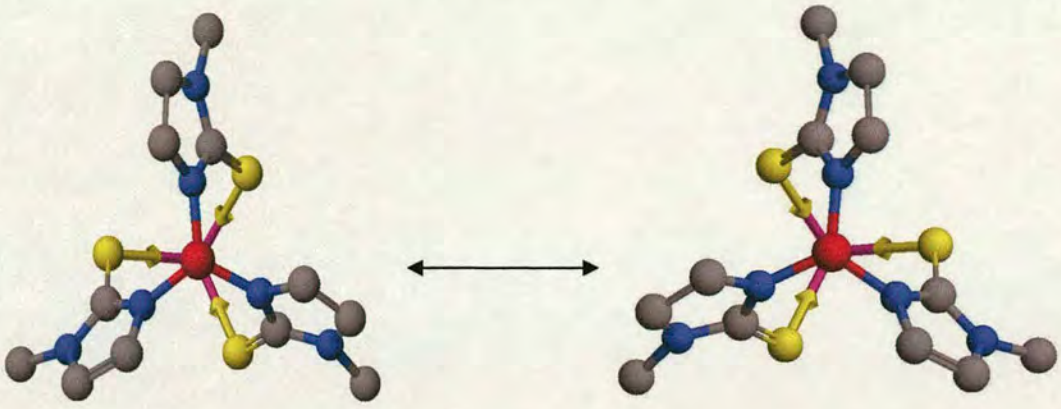

Figure 1.62 Interconversion between enantiomeric complexes

There are many other variables that need to be considered in designing the ligand. By altering the central ligand atom, the size and flexibility of the framework can be controlled. By incorporating larger atoms such as silicon into the framework, the ligand will be able to encompass larger metal fragments. The hybridization of the linker atoms controls the flexibility of the ligand. Ligands containing sp^2 hybridised linker atoms will be more rigid than those containing sp^3 hybridised atoms. The rigidity of the ligands may contribute significantly to the coordination properties of the ligand and to the range of metals with which it will form complexes. Flexible systems acting as a tridentate ligand will have a less favourable entropic term upon coordination to a metal compared to rigid ligands where the loss in entropy will be lower.

Modifying the type of donor atoms will enable the electronic character of the ligands to be controlled, and so increase the range of metals to be investigated. Metal coordination complexes can be considered as the combination of a Lewis acid (the central metal atom) with a number of Lewis bases (the ligands). Hard/soft acid/base theory holds for these complexes so that hard acids prefer to bind to hard bases and soft acids prefer to bind to soft bases. Early transition metals are hard acids and so

will be stabilized by π-donor ligands with hard donor groups. Late transition metals are soft acids and so will be stabilized by π-acceptor ligands with soft donor groups.

To determine the effects of altering the ligand design on its coordination properties, six novel tripodal ligand systems are presented within this thesis. The ligands vary in terms of the central atom, the donor atoms and the nature of the linker atoms. Fairly rigid ligands were studied to favour coordination to the metal through all three of the tripod arms. The design and synthesis of the ligands are described in the following chapters. Coordination studies of the successfully formed systems are also described.

1.5 References

1. F. A. Carey and R. J. Sundberg, *Advanced Organic Chemistry*. 1990, Plenum Press, 67

2. W. A. Nugent, T. V. RajanBabu and M. J. Burk, *Science*, 1993, **259**, 479

3. R. T. Morrison and R. N. Boyd, *Organic Chemistry*, Prentice-Hall International

4. G. Procter, *Stereoselectivity In Organic Synthesis*. 1998, Oxford University Press

5. D. F. Shriver, P. W. Atkins and C. H. Langford, *Inorganic Chemistry*. 1994, Oxford University Press, 723

6. R. Noyori, *Asymmetric Catalysis in Organic Synthesis*. 1994, John Wiley & Sons

7. C. Moberg, *Angew. Chem. Int. Ed.*, 1998, **37**, 248

8. Kagan, Halpern and Koeing, *Asymmetric Synthesis*. Vol. 5. 1985, New York, Academic Press

9. J. K. Whitesell, *Chem. Rev.*, 1989, **89**, 1581

10. J. March, *Advanced Organic Chemistry*. 1992, Wiley-Interscience, 775

11. L.Sacconi and F. Mani, *Transition Met. Chem.*, 1982, **8**, 179

12. W. H. Hohman, D. J. Kountz and D. W. Meek, *Inorg. Chem.*, 1986, **25**, 616

13. L. F. Rhodes, C. Sorato, L. M. Venanzi and F. Bachechi, *Inorg. Chem.*, 1988, **27**, 604

14. C. Bianchini, A. Meli, M. Peruzzini, F. Vizza and F. Zanobini, *Coord. Chem. Rev.*, 1992, **120**, 193

15. M. J. Burk and R. L. Harlow, *Angew. Chem. Int. Ed. Engl*, 1990, **29**, 1462

16. T. R. Ward, L. M. Venanzi, A. Albinati, F. Lianza, T. Gerfin, V. Gramlich and G. M. Ramos Tombo, *Helv. Chim. Acta*, 1991, **74**, 983

17. M. J. Burk and R. L. Harlow, *Tetrahedron:Asymmetry*, 1991, **2**, 569

18. H. Memmler, L. H. Gade and J. W. Lauher, *Inorg. Chem.*, 1994, **33**, 3064

19. K. W. Hellmann, L. H. Gade, A. Steiner, D. Stalke and F. Moeller, *Angew. Chem., Int. Ed. Engl.*, 1997, **36**, 160

20. K. W. Hellmann, P. Steinert and L. H. Gade, *Inorg. Chem.*, 1994, **33**, 3859

21. L. H. Gade, C. Becker and J. W. Lauher, *Inorg. Chem.*, 1993, **32**, 2308

22. P. Renner, C. Galka, L. H. Gade, S. Radojevic and M. McPartlin, *J. Chem. Soc., Dalton Trans.*, 2001, 964

23. L. H. Gade, P. Renner, H. Memmler, F. Fecher, C. H. Galka, M. Laubender, S. Radojevic, M. McPartlin and J. W. Lauher, *Chem. Eur. J.*, 2001, **7**, 2563

24. C. Pellecchia, A. Immirzi and D. Pappalardp, *Organometallics*, 1994, **13**, 3773

25. B. Findeis, M. Schubart, L. H. Gade, F. Moeller, I. Scowen and M. McPartlin, *J. Chem. Soc., Dalton Trans.*, 1996, 125

26. L. H. Gade, M. Schubart, B. Findeis, S. Fabre, I. Bezougli, M. Lutz, I. J. Scowen and M. McPartlin, *Inorg. Chem.*, 1999, **38**, 5282

27. J. G. Verkade and D. Gudat, *Organometallics*, 1989, **8**, 2772

28. R.R. Schrock, C.C. Cummins, T. Wilhelm, S. Lin, S. Reid, M. Kol and W.M. Davis, *Organometallics*, 1996, **15**, 1470

29. R. R. Schrock, *Acc. Chem. Res.*, 1997, **30**, 9

30. G.E. Greco, M.B. O'Donoghue, S.W. Seidel, W. M. Davis and R.R. Schrock, *Organometallics*, 2000, **19**, 1132

31. J. Pinkas, J. Tang, Y. Wan and J.G. Verkade, *Phosphorous, Sulfur and Silicon*, 1994, **87**, 193

32. M. Becker, F. W. Heinemann and S. Schindler, *Chem.Eur. J.*, 1999, **5**, 3124

33. M. Kol, R. R. Schrock, R. Kempe and W. M. Davis, *J. Am. Chem. Soc.*, 1994, **116**, 4382

34. K. Nomura and R. R. Schrock, *Inorg. Chem.*, 1996, **35**, 3695

35. H. Memmler, K. Walsh, L. H. Gade and J. W. Lauher, *Inorg. Chem.*, 1995, **34**, 4062

36. J. G. Verkade, *Acc.Chem.Res.*, 1993, **26**, 483

37. K. Ishihara, Y. Karumi, S. Kondo and H. Yamamoto, *J. Org. Chem*, 1998, **63**, 5692

38. M. Ray, B. S. Hammes, G. P. A. Yap, L. Rheingold and A. S. Borovik, *Inorg. Chem.*, 1998, **37**, 1527

39. D. Ramos-Maldonado, B. S. Hammes, G. P. A. Yap, A. L. Rheingold, A. S. Borovik and J. Young, V.G, *Co-ord. Chem. Rev.*, 1998, **174**, 241

40. D. Ramos-Maldonado, B. S. Hammes, G. P. A. Yap, A. L. Rheingold, A. S. Borovik, L. Liable-Sands and J. Young, V.G, *Inorg. Chem.*, 1997, **36**, 3210

41. D. W. Margerum, *Pure Appl. Chem.*, 1983, **55**, 23

42. T. J. Collins, *Acc. Chem. Res.*, 1994, **27**, 279

43. S. Trofimenko, *J. Am. Chem. Soc.,*, 1967, **89**, 3170

44. S. Trofimenko, *J. Am. Chem. Soc.,*, 1967, **89**, 6288

45. S. Trofimenko, *Chem.Rev*, 1993, **93**, 943

46. I. B. G. R. Han, A.G. Looney and G.Parkin, *J. Chem. Soc., Chem. Commun.*,1991, 717

47. R. H. A. Looney, I.B. Gorrell, M.Cornebise, K. Yoon, and G. Parkin, *Organometallics*, 1995, **14**, 274

48. T. H. J. L. Kisko, C. Kimblin, and G. Parkin, *J. Chem. Soc., Dalton Trans.*, 1999, 1929

49. D. D. LeCloux and W. B. Tolman, *J.Am.Chem.Soc.*, 1993, **115**, 1153

50. D. D. LeCloux, W. B. Tolman, M. Keyes, M. Osawa, R. P. Houser and C. J. Tokar, *Organometallics*, 1994, **13**, 2855

51. D. D. LeCloux, W. B. Tolman, M. Keyes, M. Osawa and V. Reynolds, *Inorg. Chem.*, 1994, **33**, 6361

52. W. B. Tolman, M. Keyes and J. Young, V.G., *Organometallics*, 1996, **15**, 4133

53. A. R. E. Pullen, D. Rabinovich, *Inorg. Chem. Commun.*, 1999, **2**, 194

54. J. P. Wilbaut, A. P. d. Jonge, H. G. P. V. d. Voort and H. L. Otto, *Recl. Trav. Chim. Pays-Bas*, 1951, **70**, 1054

55. H. Adolfsson, K. Waernmark and C. Moberg, *J. Chem. Soc., Chem. Commun.*, 1992, 1054

56. H. Adolfsson, K. Wärnmark and C. Moberg, *J. Chem. Soc., Chem. Commun.*, 1992, 1054

57. K. Kawasaki and T. Katsuki, *Tetrahedron*, 1997, **53**, 6337

58. S. Bellemin - Laponnaz and L. H. Gade, *Angew. Chem. Int. Ed. Engl*, 2002, **41**, 3473

59. S. Bellemin - Laponnaz and L. H. Gade, *Chem. Comm.*, 2002, **12**, 1286

60. M. Cernerud, H. Adolfsson and C. Moberg, *Tetrahedron-Asymmetry*, 1997, **8**, 2655

61. Y. Gao, R. Hanson, J. M. Klunder, S. Y. Ko, H. Masamune and B. Sharpless, *J. Am. Chem. Soc.*, 1987, **109**, 5765

62. W. Nugent and R. L. Harlow, *J. Am. Chem. Soc.*, 1994, **116**, 6142

63. J. D. Morrison, E. R. Grandbois and G. R. Weisman, *Asymmetric Reactions and Processes in Chemistry*.Vol. acs symposium series 185. 1982, Washington DC, American Chemical Society.

64. L. Favretto, W. Nugent and G. Licini, *Tet. Lett.*, 2002, **43**, 2581

65. W. Nugent, *J. Am. Chem. Soc.*, 1992, **114**, 2768

66. M. Bonchjo, G. Licini, F. Di Furia, S. Mantovani, G. Moderna and W. Nugent, *J.Org. Chem.*, 1999, **64**, 1326

67. F. Di Furia, G. Licini, G. Moderna, R. Motterle and W. Nugent, *J.Org. Chem.*, 1996, **61**, 5175

68. M. Bonchjo, G. Licini, G. Moderna, O. Bortolini, S. Moro and W. Nugent, *J.Am.Chem.Soc.*, 1999, **121**, 6258

69. H. Lutjens, G. Wahl, F. Moller, P. Knochel and J. Sundermeyer, *Organometallics*, 1997, **16**, 5869

70. J.W. Canary, C.S. Allen, J.M. Castagnetto and Y. Wang, *J. Am. Chem. Soc.*, 1995, **117**, 8484

71. C.-L. Chuang, K. Lim, Q. Chen, J. Zubieta and J. W. Canary, *Inorg. Chem.*, 1995, **34**, 2562

72. Y. Chiu, O. dos Santos and J. W. Canary, *Tetrahedron*, 1999, **55**, 12069

73. J. W. Canary, C. S. Allen, J. M. Castagnetto, Y. Chiu, P. J. Toscano and Y. Wang, *Inorg. Chem.*, 1998, **37**, 6255

74. G. Anderegg and F. Wenk, *Helv. Chim. Acta*, 1967, **50**, 2330

75. A. Hazell, J. McGinley and H. J. Toftlund, *Chem. Soc., Dalton Trans.*, 1999, 1271

76. G. Huttner, A. Jacobi, U. Winterhalter and S. Cunskis, *Eur. J. Inorg. Chem.*, 1998, 675

77. J. Reglinski, M. Garner, I. D. Cassidy, P. A. Slavin, M. D. Spicer and D. R. Armstrong, *J. Chemy. Soc., Dalt. Trans.*, 1999, 2119

78. M. Garner, J. Reglinski, I. Cassidy, M. D. Spicer and A. R. Kennedy, *Chem. Commun. (Cambridge)*, 1996, 1975

79. J. Reglinski, M. D. Spicer, M. Garner and A. R. Kennedy, *J. Am. Chem. Soc.*, 1999, **121**, 2317

80. P. A. Slavin, J. Reglinski, M. D. Spicer and A. R. Kennedy, *J. Chem. Soc., Dalton Trans.*, 2000, 239

81. I. Cassidy, M. Garner, A. R. Kennedy, G. B. S. Potts, J. Reglinski, P. A. Slavin and M. D. Spicer, *Eur. J. Inorg. Chem.*, 2002, 1235

82. A.F. Hill, G.R. Owen, A. J. P. White and D.J. Williams, *Angew. Chem. Int. Ed.*, 1999, **38**, 2759

83. J. F. Ojo, P. A. Slavin, J. Reglinski, M. Garner, M. D. Spicer, A. R. Kennedy and S. J. Teat, *Inorg. Chim. Acta*, 2001, **313**, 15

84. C. Santini, G. G. Lobbia, C. Pettinari, M. Pellei, G. Valle and S. Calogero, *Inorg. Chem.*, 1998, **37**, 890

85. C. Santini, C. Pettinari, G. G. Lobbia, R. Spagna, M. Pellei and F. Vallorani, *Inorg. Chim. Acta*, 1999, **285**, 81

86. Effendy, G. G. Lobbia, C. Pettinari, C. Santini, B. W. Skelton and A. H. White, *Inorg. Chim. Acta*, 2000, **308**, 65

87. M. Garner, M.-A. Lehmann, J. Reglinski and M. D. Spicer, *Organometallics*, 2001, **20**, 5233

88. C. Kimblin, B. M. Bridgewater, D. G. Churchill and G. Parkin, *Chem. Commun. (Cambridge)*, 1999, 2301

89. B. M. Bridgewater, T. Fillebeen, R. A. Friesner and G. Parkin, *J. Chem. Soc., Dalton Trans.*, 2000, 4494

90. B. M. Bridgewater and G. Parkin, *Inorg. Chem. Commun.*, 2001, **4**, 126

91. C. Kimblin, B. M. Bridgewater, T. Hascall and G. Parkin, *J. Chem. Soc., Dalton Trans.*, 2000,1267

92. C. Kimblin, D. G. Churchill, B. M. Bridgewater, J. N. Girard, D. A. Quarless and G. Parkin, *Polyhedron*, 2001, **20**, 1891

93. B. M. Bridgewater and G. Parkin, *Inorg. Chem. Comm.*, 2000, **3**, 534

94. B. M. Bridgewater and G. Parkin, *J. Am. Chem. Soc.*, 2000, **122**, 7140

95. M. Tesner, M. Shu and H. Vahrenkamp, *Inorg. Chem*, 2001, **40**, 4022

96. D. Rabinovich, J. M. Tanski and J. L. White, *J. Chem. Soc., Dalton Trans.*, 2002, 2987

97. S. Bakbak, V. K. Bhatia, C. D. Incarvito, A. L. Rheingold and D. Rabinovich, *Polyhedron*, 2001, **20**, 3343

98. G. G. Lobbia, C. Pettinari, C. Santini, N. Somers, B. W. Skelton and A. H. White, *Inorg. Chim. Acta*, 2001, **319**, 15

99. D. L. Reger, M. F. Huff, A. L. Rheingold and B. S. Haggerty, *J. Am. Chem. Soc.*, 1992, **114**, 579

100. P. J. Bailey, M. Lanfranchi, L. Marchio and S. Parsons, *Inorg.Chem*, 2001, **40**, 5030-5035.

101. U. Rhörig, N. Mézailles, N. Maigrot, L. Ricard, F. Mathey and P. Le Floch, *Eur. J. Inorg. Chem.*, 2000, 2565

102. C.Elschenbroich, M. Nowotny, A. Behrendt, W. Massa and S. Wocadlo, *Angew. Chem. Int. Ed. Engl*, 1992, **104**, 1343

103. F. Mathey and P. L. Floch, *Chem. Ber.*, 1996, **129**, 263

104. H. Brunner and A. F. M. M. Rahman, *Chem. Ber.*, 1984, **117**, 710

105. M. T. Powell, A. M. Porte and K. Burgess, *Chem. Comm.,* 1998, 2161

106. J. Hwang, K. Govindaswasmy and S. Koch, *Chem. Comm.*, 1998, 1667

107. R. J. Motekaitis, A. E. Martell, S. Koch, J. Hwang, J. Quarless, D and M. J. Welch, *Inorg. Chem.*, 1998, **57**, 5902

108. N. Govindaswasmy, J. Quarless, D and S. Koch, *J. Am. Chem. Soc.*, 1995, **117**, 8468

2 Phenolate and Thiolate Donor Ligands

2.1 Ligand Design

The first ligand systems chosen for study are based upon the ligand framework shown in Figure 2.1.

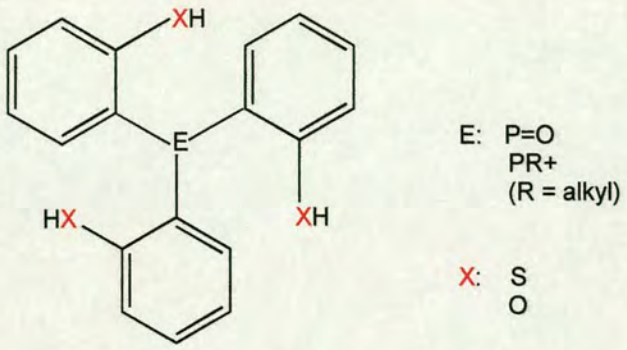

Figure 2.1 Basic framework of tripod ligands

The ligands studied in this Chapter are based on a non-coordinating phosphorus atom linked, in the 2-position, directly to three phenolate or thiophenolate rings. Coordination of the central phosphorus atom can be prevented either by alkylation or oxidation of the phosphorus atom. Both linker atoms in each tripod arm are sp^2 carbon atoms and so the framework will be fairly rigid. These systems will be potentially tridentate and will form eight member chelate rings upon complexation to a metal. Co-ordination of the ligand through all three donor atoms should lead to complexes with C_3 symmetry by nature of the helical twist induced to minimise the strain associated with an eight membered chelate ring. This has been demonstrated through simple molecular modelling using the cache programme. This uses an MM3 force field and molecular dynamics to optimise the molecular geometry and so finds the most energetically favourable structure. Figure 2.2 shows the results of looking at the co-ordination of $O{=}P(2\text{-}SHC_6H_4)_3$ in an octahedral iron complex with the remaining sites occupied by a Cp ligand.

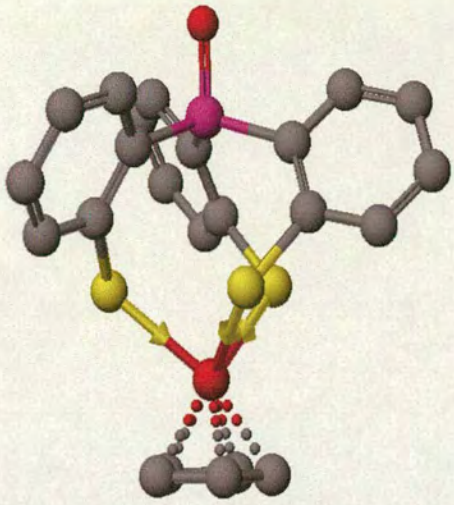

Figure 2.2 Co-ordination of O=P(2-$SHC_6H_4)_3$ to an octahedral iron complex

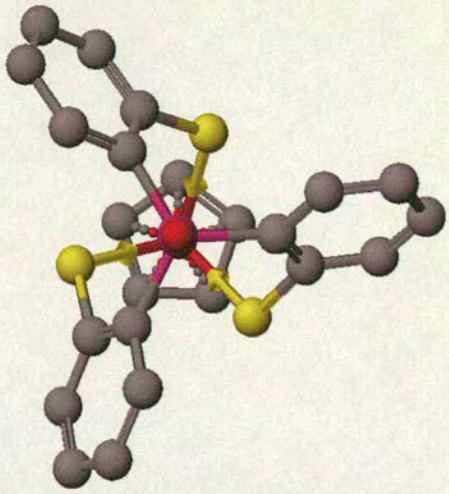

Figure 2.3 View down C_3 axis

Looking down the axis defined by the central atom and the metal ion, as shown in Figure 2.3, the three-fold rotational symmetry can be seen clearly. The planar aromatic groups take on a propeller shaped geometry and the complex has C_3 symmetry.

It is essential that the central atom remains non-coordinating in these ligands in order to maintain the C_3 symmetry. If the ligand is tetradentate with the central atom co-ordinating to the metal, the geometry becomes trigonal bipyramidal and the symmetry increases to C_{3v}. This can be seen in Figure 2.4, which shows the tetradentate co-ordination of $[P(2\text{-}SHC_6H_4)_3]^{3-}$ to a ruthenium metal ion. The three vertical mirror planes can be seen clearly from the view down the central C_{3v} axis, shown in Figure 2.5.

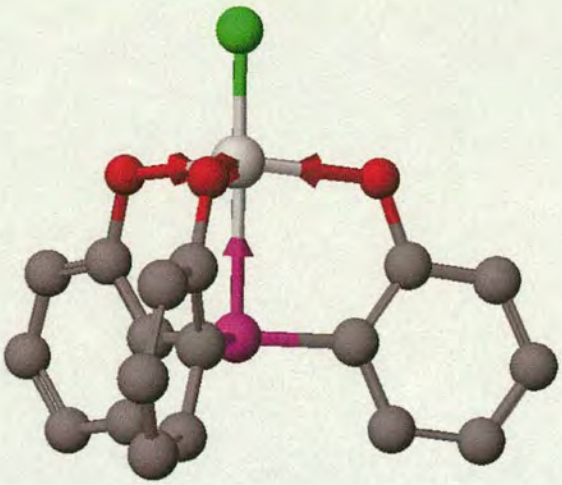

Figure 2.4 $P(2\text{-}SHC_6H_4)_3$ coordinated to a ruthenium ion.

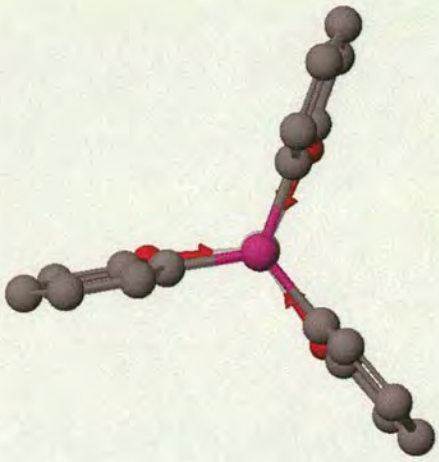

Figure 2.5 View down the central C_3 axis

There is now only one vacant site at the metal centre for the substrate to bind to. It would therefore be unsuitable for use as a catalyst as this requires at least two vacant sites for both substrate and reagent coordination. However, C_3 symmetric trigonal bipyramidal complexes could be used as chiral Lewis acids.

The chirality of the ligand could efficiently be transmitted to the remaining co-ordination sites through the use of the planar aromatic groups. These would provide a pronounced propeller geometry that would lead to a large energy difference between diastereotopic transition states.

By altering the central atom, the size and flexibility of the framework can be controlled. A similar ligand could be synthesised from trichloro-silicon to provide a system with a central silicon atom respectively. Nitrogen could be used as the central atom, provided that it is alkylated to prevent it from coordinating to the metal centre.

Modifying the type of donor atoms will enable the electronic character of the ligands to be controlled, and so increase the range of metals to be investigated. The phenolate ligands possess oxygen donors. Oxygen is a hard donor and so prefers to form complexes with hard metals, *i.e.* early transition metals or late transition metals in high oxidation states. In contrast, the thiophenolate donors possess sulphur donors.

Sulphur is a much softer, more polarisable donor and so prefers to co-ordinate to softer transition metals with higher *d*-electron counts. Thiolate groups are readily oxidised to disulphides. It is hoped that the sterically bulky aryl groups of these thiophenolate ligand systems will kinetically protect the thiolate sulphur atoms from facile oxidation.

2.2 Work Already Carried Out on Related Systems

Koch *et al.* have studied similar ligands. His group looked at tetradentate tripodal ligands in which three phenolate or thiolate rings are connected *via* a methylene group to a central nitrogen atom.[1-3] These ligands have already been discussed in Section 1.3.3.

Dinger and Scott have worked extensively with tris(3,5-dialkyl-2-hydroxyphenyl)methane ligands, shown in Figure 2.6. These ligands are very similar to the others discussed in this chapter, apart from having a central carbon atom and alkyl substituents on the phenyl rings.

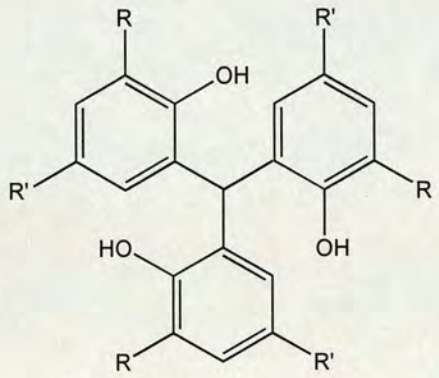

R, R' = *tert*-butyl
R, R' = phenyl
R = *tert*-butyl, R' = phenyl

Figure 2.6 Tris(3,5-dialkyl-2-hydroxyphenyl)methane ligands

The ligand can exist in two conformations: Type 1, in which the hydroxide groups are aligned with the central methine hydrogen; or Type 2, in which the hydroxide groups point away from the central methine hydrogen. Extensive solid and solution studies have confirmed that Type 1 is the preferred conformation, even when bulky substituents were introduced at the central carbon atom.[4-6]

The peripheral hydroxyl groups have been derivatised to form extended arms, producing systems similar to calix(*n*)arenes. These ligands are then able to present metals with an octahedral array of binding sites and may have potential for selective metal binding.[6]

The lithium, sodium and potassium salts of the ligand have been prepared and characterised.[4] They all form hexanuclear aggregates, composed of two triarylmethane units, in which the Type 1 conformation of the ligand is maintained.

Although no metal complexes, in which the ligand acts in a tridentate manner, have yet been reported, the C_3 symmetric phosphite, shown in Figure 2.7, in which the ligand exists in a Type 2 conformation, has been characterised.[7] The phosphite is formed by adding phosphorus trichloride to a solution of tris(3,5-di-phenyl-2-hydroxyphenyl)methane and triethylamine.

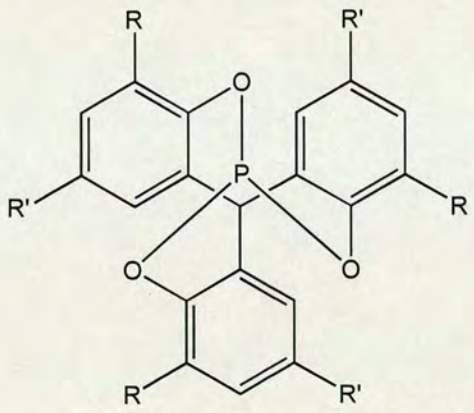

Figure 2.7 C_3 symmetric phosphites

Space filling models of the system show that the phosphorus atom occupies a sterically congested environment. X-ray crystal structures were obtained and show the twisting of the eight membered rings in the same manner as described in Section 1.3.3. The structure suggests that this ligand could form metal complexes with the ligand acting in a tridentate manner to form eight membered chelate rings which twist to give the complex an overall C_3 symmetry.

2.3 Thiolate Donors

Block described a synthesis for the phosphorus and silicon centred thiolate ligands (Figure 2.1, E = P, Si);[8] however their co-ordination chemistry has not been reported. The same synthesis has been used by Pascal in the formation of *in*-cyclophanes.[9]

The method described by Block, was used to synthesise ligand tris(2-mercaptophenyl)phosphine, **3**, as shown in Figure 2.8. The dilithiation of benzene thiol, **1**, to lithium2-lithiobenzenethiolate, **2**, was achieved by treating **1**, with two equivalents of *n*-butyllithium in cyclohexane. Tetramethylethylenediamine, (TMEDA) was added to chelate the lithium. Organolithium species exist as a mixture of aggregates in solution. *n*-Butyllithium exists as a tetramer-dimer mixture in THF, with the tetramer dominating. By chelating to the lithium atoms, TMEDA breaks up the clusters rendering the organometallic species more reactive.

The *ortho*-lithiated species, **2,** is then reacted with phosphorus trichloride in THF at –78 °C. A nucleophilic substitution reaction takes place with the more nucleophilic carbanion attacking the phosphorus centre. Carrying the reaction out at low temperatures may help to eliminate any competition between the thiolate and the carbanion centres. Three equivalents of the *ortho*-lithiated species are treated with one equivalent of phosphorus reagent, and **3** can be isolated following an acidic work-up and recrystallisation from toluene layered with hexane.

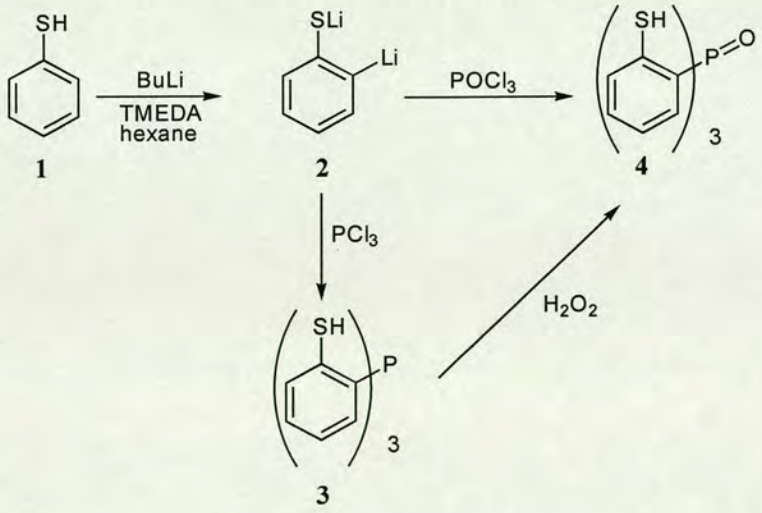

Figure 2.8 Synthesis of 3 and 4

Having made Block's phosphorous ligand, **3**, attempts were made to modify the ligand to be suitable for forming C_3 metal complexes. The alkylation of the central phosphorus atom proved non-trivial, with a mixture of alkylated species being formed. It was found that the softer sulphur atom was alkylated in preference to the phosphorus atom, when the alkylating agent $[OEt_3]BF_4$ was used. Treatment of the ligand with the milder alkylating agents methyl iodide, or $SO_2(OMe)_2$ resulted in no reaction, as followed by ^1H NMR analysis. In order to achieve selective methylation of the phosphorus, the sulphur atoms would need to be protected. One possibility for a protection group is to form a THP-thioether from each of the thiol groups.

Oxidation of the phosphorus atom could be achieved by treating the ligand with a solution of hydrogen peroxide. However, it was easier to treat the dilithiated thiol with phosphorus oxychloride, instead of phosphorus trichloride, to give tris(2-mercaptophenyl)phosphineoxide, **4**. The ^1H, ^{13}C and ^{31}P NMR, CHN analysis and mass spectrum all suggested that **4** had, indeed, formed. However, the X-ray crystal structure, illustrated in Figure 2.9, shows that **4** had not formed. Instead, only two thiol rings have been substituted on to the central phosphorus atom to give ligand **5**. A hydrogen atom has displaced the third chloride.

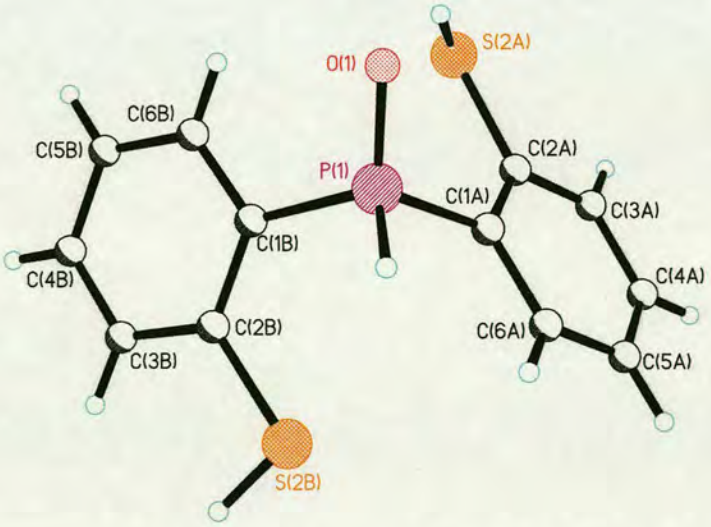

Figure 2.9 Crystal structure of $OPH(2\text{-}SHC_6H_4)_3$, 5

Selected bond lengths and angles in **5** are shown in Table 2.1. The lengths of the bonds connecting the thiol rings to the central phosphorus atom are equal, (P(1)-C(1A) = P(1)-C(1B)=1.802 Å). The two thiol rings are twisted with respect to

each other such that the thiol groups point in opposite directions. One of the thiol groups points up towards the phosphoryl oxygen and forms an intramolecular hydrogen bond with this oxygen, (O(1)···H(2) Å = 2.416 Å). The other thiol group points in the opposite direction and forms an intermolecular hydrogen bond with the phosphorus oxygen atom in an adjacent molecule, (O(1*)···H(2B) = 2.130 Å). This is illustrated in Figure 2.10. The phosphorus adopts an approximately tetrahedral geometry.

Bond	Length / Å
P(1)-O(1)	1.4896(16)
P(1)-C(1A)	1.802(2)
P(1)-C(1B)	1.802(2)
P(1)-H(1)	1.33(2)

Angle	Size / °
O(1)-P(1)-C(1A)	114.23(9)
O(1)-P(1)-C(1B)	112.33(9)
O(1)-P(1)-H(1)	114.1(9)
C(1A)-P(1)-C(1B)	108.83(9)
C(1A)-P(1)-H(1)	101.1(9)
C(1B)-P(1)-H(1)	105.3(9)

Table 2.1 Selected bond distances / Å and angles / ° for 5

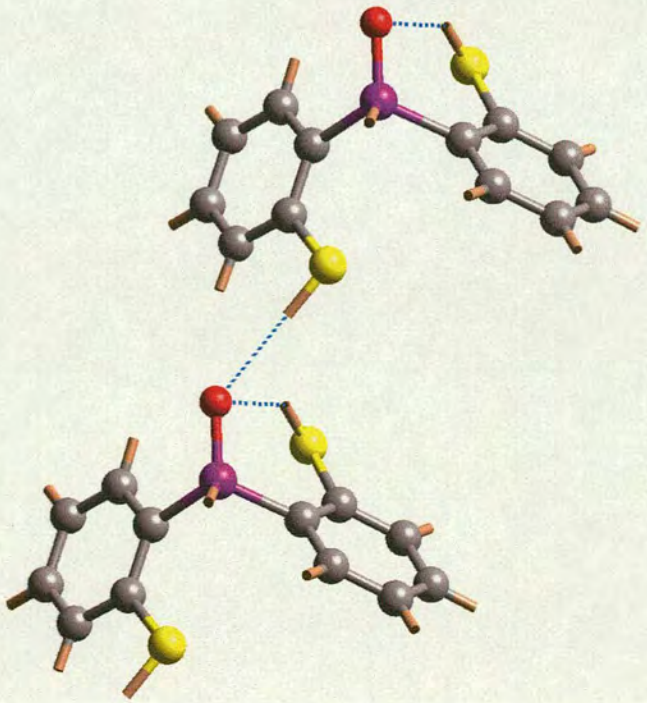

Figure 2.10 Crystal structure of $OPH(2\text{-}SHC_6H_4)_3$, 5, showing hydrogen bonds

It is likely that a mixture of substituted products is forming in the reaction. The di-substituted ligand, **5**, is likely to be less soluble than the tri-substituted ligand, **4**, as there are fewer possibilities for hydrogen bonding, and will crystallise out of

solution preferentially to the desired ligand. The X–ray structure may not be representative of the sample as a whole, and the di-substituted product may only represent a small side product. This is in accordance with the other data obtained.

It is interesting that a hydride as opposed to a hydroxide group replaces the chloride. This side reaction could be minimised in future preparations by adjusting the stoichiometries to ensure that **2** is in excess compared to the $POCl_3$. This is an unusual result. It is not possible to deduce how such a ligand has formed without further work.

2.4 Phenolate Donors

The synthesis of the phenolate analogue, **9**, of the thiolate ligand, **4**, was first reported in 1956 by Kennedy *et al.*[10] This ligand is based on a central phosphorus oxide moiety. This method was adapted to prepare the Grignard reagent *o*-methoxyphenyl magnesium bromide, **7**, by treating 2-bromoanisole, **6**, with magnesium as shown in Figure 2.11.

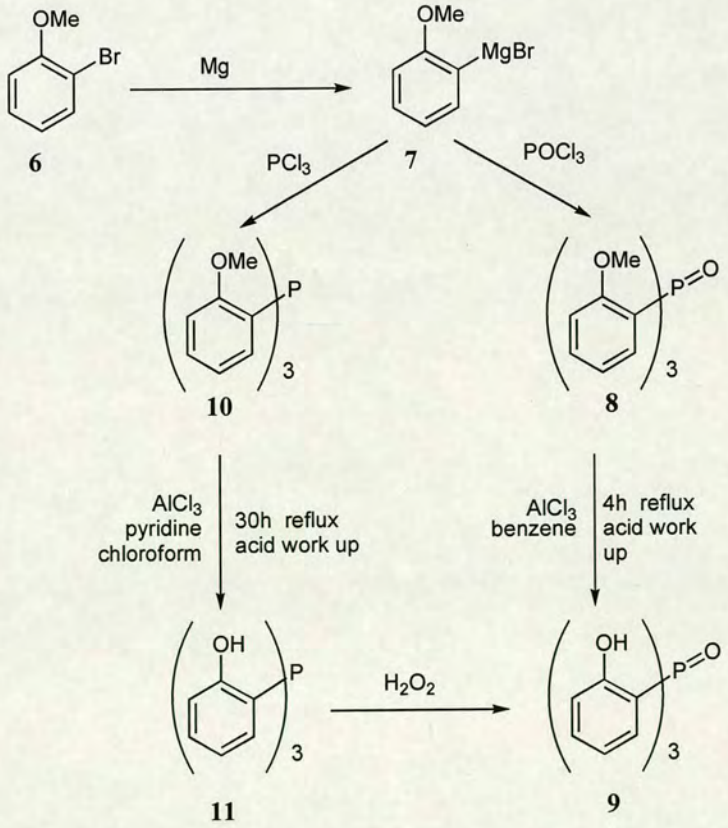

Figure 2.11 Synthesis of triphenolate ligands

The *in situ* reaction of **7** with phosphorus oxychloride yielded tri-(*o*-methoxyphosphine) oxide, **8**, as described by Nuenhoeffer *et al.*[11] Heating this under reflux with aluminium trichloride resulted in the cleavage of the methoxy group with the evolution of methyl chloride. After an acidic work-up and recrystallisation from dichloromethane-hexane, the tri-(o-hydroxyphosphine)oxide ligand, **9**, was isolated. **9** was fully characterised and an X-ray crystal structure obtained. This is shown in Figure 2.11.

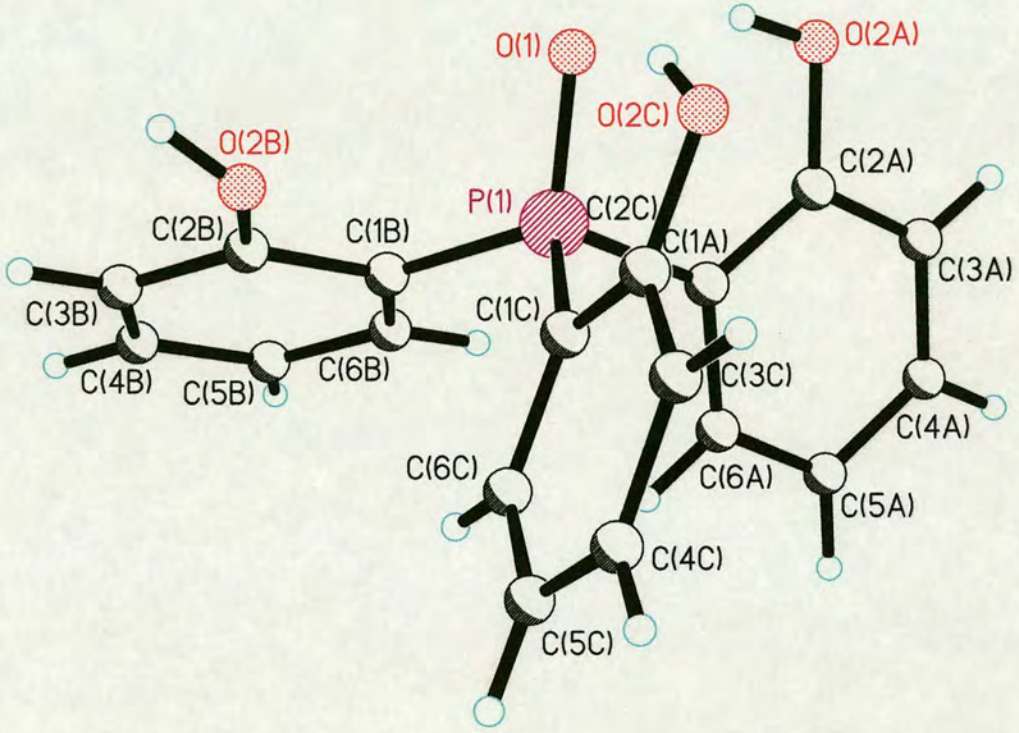

Figure 2.11 X-ray crystal structure of OP(2-OHC$_6$H$_4$), 9

Bond	Length / Å
P(1)-O(1)	1.5231(13)
P(1)-C(1B)	1.7834(19)
P(1)-C(1A)	1.7952(18)
P(1)-C(1C)	1.7982(19)

Angle	Size / °
O(1)-P(1)-C(1B)	114.75(8)
O(1)-P(1)-C(1A)	108.50(8)
O(1)-P(1)-C(1C)	110.58(9)
C(1B)-P(1)-C(1C)	107.93(9)
C(1A)-P(1)-C(1C)	106.14(8)
C(1B)-P(1)-C(1A)	108.57(9)

Table 2.2 selected bond distances / Å and angles / ° for 9

Table 2.2 shows selected bond lengths and angles for the ligand. The crystal structure confirms the formation of the desired ligand with all three phenol groups substituted on to the phosphorus at the 2-aryl positions. There are two intramolecular hydrogen bonds between two of the hydroxyl groups and the phosphorus oxygen, (O(1)···H(2C) = 1.961 Å, O(1)···H(2A) = 1.859 Å]. The third phenolate ring is twisted round and the hydroxyl group on this ring forms a hydrogen bond with the phosphorus oxygen on an adjacent molecule, (O(1*)···H(2B) = 1.891 Å). This can be seen in Figure 2.13. The geometry of the phosphorus atom is approximately tetrahedral. However, the phenolate ring hydrogen bonded to an adjacent molecule is slightly bent away from the axis defined by the phosphorus-oxygen bond, this can be seen from the slightly larger bond angle (O(1)-P(1)-C(1B) = 114.75(8)°).

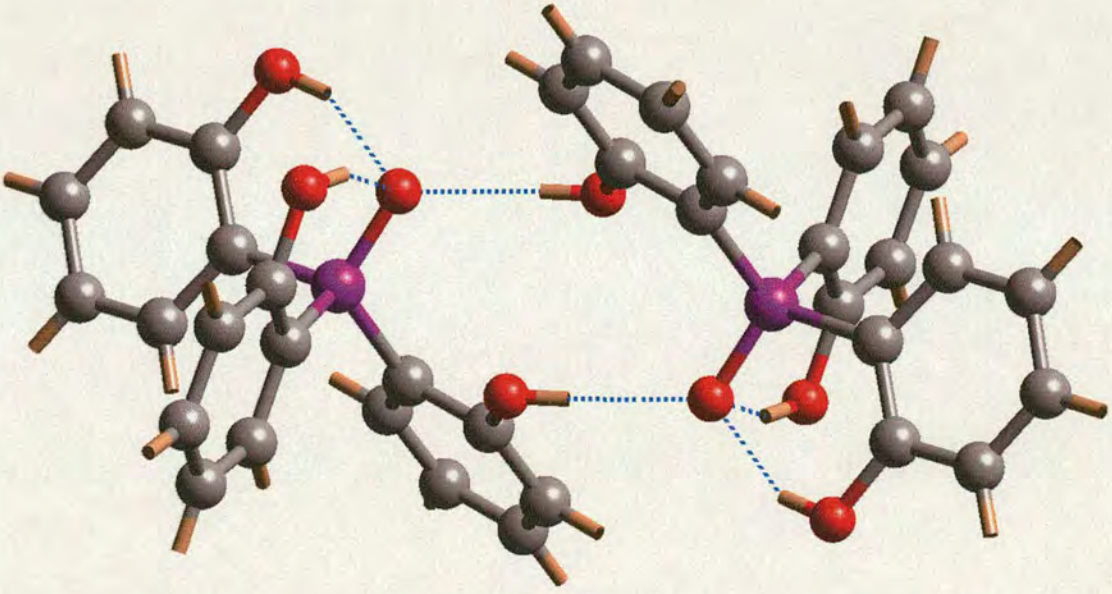

Figure 2.13 X-ray crystal structure of 9 showing hydrogen bonds

The synthesis of the phosphorus(III)-based ligand was attempted. Although it was possible to prepare the tri-*o*-methoxyphenylphosphine intermediate, **10**, cleavage with aluminium trichloride proved unsuccessful. The aluminium chloride works more effectively with the phosphorus oxide species, in which there may be a weak stabilising interaction between the aluminium and the oxygen atoms. This interaction may be necessary for the reaction to occur.

2.5 Complexation Studies

Having synthesised and characterised the ligands, attempts were made to investigate the co-ordination chemistry with various metal complexes. The metals chosen for study initially were those that would give complexes. The ligands are formally trianionic, and so complexes in which the metal is in a +3 oxidation state were selected as the most suitable for investigation, depending on the charge of the ancillary ligands.

To co-ordinate the ligand to the metal complex, the protons on the donor atoms were removed using three equivalents of butyl lithium in THF to form the lithiated species. One equivalent of metal compound was added *in situ* to facilitate the formation of the mononuclear complex.

2.5.1 Synthesis of Pentamethylcyclopentadiene

A number of the metal precursor complexes discussed in this chapter and in later chapters contain the ligand pentamethylcyclopentadiene (Cp*, C_5Me_5). This is available commercially but is extremely expensive, and so was synthesised following the three-step process, described by Fendrick *et al.*,[12] shown in Figure 2.14.

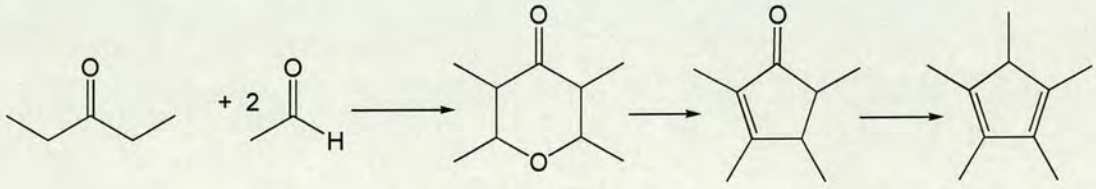

Figure 2.14 Synthetic route to Cp*

The first step was the formation of 2,3,5,6-tetrahydro-2,3,5,6-methyl-γ-pyrone, which was achieved by deprotonation at the β carbons of 3-pentanone, followed by the addition of one equivalent of acetaldehyde onto each β carbon. Ring closure accompanied by the loss of water yielded the product.

The next step was the formation of 2,3,4,5-tetramethylcyclopent-2-enone, which was made by a double acylation followed by dehydration. The acylation step was carried

out by combining formic and sulphuric acid to form an acid anhydride, which reacts with the 2,3,5,6-tetrahydro-2,3,5,6-methyl-γ-pyrone. The final step involved the alkylation of the α carbon, using the reagent methyl lithium, followed by dehydration to yield Cp* as a pale yellow liquid.

2.5.2 Coordination to Titanium

The first precursor investigated was $Ti^{IV}Cp^*Cl_3$, which was prepared from $TiCl_4$ and lithiated Cp^*. This compound contains three labile chloride ligands. The remaining co-ordination sites on the titanium are occupied by the Cp^* ligand. Titanium is an early transition metal and so will prefer to co-ordinate to hard donor atoms. On addition of the red compound to either **4** or **9**, there was a colour change to yellow. Crystals were obtained, however, these redissolved whilst waiting for analysis and repeated attempts to regrow crystals of suitable quality have proved unsuccessful.

A similar titanium precursor complex was made by treating $TiCl_4$ with hydrotris(pyrazole)borate, $[HB(pz)_3]K$. This is a ligand known to act in a tridentate manner and form stable complexes with many transition metals. The addition of $TiCl_4$ to a solution of $[HB(pz)_3]K$ in THF resulted in the solution turning bright yellow. After stirring at room temperature for 4 h, one equivalent of **9** was added to the solution. This resulted in the solution turning red and an orange precipitate forming. The solid was isolated by cannula filtration. Unfortunately it was not possible to crystallise the material or to obtain it in a sufficiently pure enough form to carry out further analysis.

A third titanium complex, $Ti^{IV}(O^iPr)_4$, was used. This is available commercially and contains four labile groups. On addition of the clear, colourless liquid to the ligand solution, there was a colour change from colourless to bright yellow. Attempts at isolating the product have proved unsuccessful with the only attainable material being an air sensitive powder precipitating out of solution. It was hoped that by substituting the remaining co-ordinated $^iPrO^-$ group with a ligand that is planar, such as PhS^-, pyrazole or imidazole, crystallisation would be more favourable. Unfortunately, neither substitution with pyrrole or pyrazole ligands proved successful.

2.5.3 Coordination to Ruthenium

The ruthenium metal complex precursor investigated was $(PhCN)_3RuCl_3$, which had been synthesised previously in the group. This contains three labile chloride groups that could be replaced by the tridentate ligand. On addition of the brick red solution to the lithium salt of **4**, there was a colour change to dark olive green. After removal of the lithium chloride by filtration, crystals of the product were obtained from toluene layered with diethyl ether, however they redissolved whilst waiting for analysis and repeated attempts to produce crystals did not yield any suitable for X-ray crystal analysis.

2.5.4 Coordination to Molybdenum

The metal complex $MoCl_3(MeCN)_3$ was used with **9**. On addition of **9**, a bright yellow solution was obtained. Unfortunately attempts at obtaining a tractable material to characterise were unsuccessful.

2.5.5 Coordination to Cobalt

Next, co-ordination of **4** to cobalt (in the II and III oxidation states) was investigated. The proton on the sulphur donor groups was removed using sodium hydride. To this was added the cobalt salt $Co(BF_4)_2.6H_2O$. The reaction was carried out in excess acetonitrile so that these groups could occupy the vacant sites on the Co(II) centre. The solution turned brown with the formation of a brown residue. PPh_4Cl was added to the solution to try and promote crystallisation. This is because PPh_4^+ is a bulky cation that should facilitate greater solubility in non co-ordinating solvents and thus assist in crystallisation attempts. This was unsuccessful, however, the reaction was not carried out in anhydrous, deoxygenated conditions. Co(II) is easily oxidised to Co(III) and so the experiment was repeated, using dry, deoxygenated conditions, and cobalt chloride as a starting material to see if a different product formed. Again a brown solid was obtained. Attempts at obtaining crystals for characterisation were unsuccessful.

2.5.6 Deprotonation of the Ligand Using Thallium Ethoxide

One reason for the inability to obtain metal complexes with the tripod ligands is that the lithiation reaction to remove the three protons of the thiol or phenol groups in **4** and **9** may not have gone to completion. An alternative reagent is thallium ethoxide. Thallium salts are very insoluble in THF and so can be isolated easily.

Three equivalents of thallium ethoxide were added to a solution of **9** in THF. The solution became warm and the thallium salt of the phenolate ligand, **11**, precipitated out of the solution as a white powder that was very insoluble in all common solvents.

2.5.7 Attempted Complexation using 11

2.5.7.1 Coordination to Vanadium

One equivalent of **11** was added to a dark pink solution of the vanadium chloride salt ($VCl_3 \cdot 3THF$). After stirring at room temperature in the dark, a purple precipitate formed under a dark green solution. The solid was isolated by filtration but proved to be extremely insoluble. The solvent was removed from the filtrate to yield a green solid. This was very air sensitive and turned black over 2 h.

2.5.7.2 Coordination to Titanium

The attempted synthesis of $HB(pz)_3TiP{=}O(2\text{-}OC_6H_4)_3$ was repeated, but using the thallium salt, **11** in place of **9**. This resulted in the formation of a white precipitate, presumably thallium chloride. A bright yellow, air stable residue was isolated from the solute but characterisation showed that no phenol ligand was present.

2.5.7.3 Coordination to Ruthenium

The chloro bridged *p*-cymene ruthenium dimer is a useful precursor for complexation reactions due to the ease with which the chloro bridge can be cleaved. Two equivalents of **11** were added to a brick red solution of $RuCl_2(\eta^2\text{-}C_{10}H_{14})]_2$. In order to try and make the complex more soluble, attempts were made to exchange the thallium counter ion for a tetraphenylphosphonium cation. This was done by adding one equivalent of PPh_4Cl. This reaction will be driven by the formation of the very insoluble thallium chloride salt. Analysis showed that the desired reaction had not occurred.

2.5.8 Possible Causes for Unsuccessful Complexation

There are a number of plausible reasons behind why no success has been made in synthesising tractable materials. It is possible that polymeric materials are forming. It is most likely that the ligands are coordinating to the metal *via* the phosphorus oxide oxygen atom. By doing so, the ligand will be able to form six membered chelate rings. Coordination of the ligand to the metal through all three arms of the tripod requires the formation of three eight membered chelate rings. These are more strained than six membered chelate rings and so it may be more favourable for the phosphorus oxide oxygen to coordinate to the metal compared to all three tripod arms. Coordination through the phosphorus oxide oxygen will then leave at least one of the tripod arms free for coordination, possibly to another metal. This will facilitate the formation of polymeric species.

One of the major difficulties of using thiol groups in co-ordination chemistry is the redox instability of metal-thiolate bonds. These bonds may readily undergo homolysis causing reduction of the metal ion and formation of a disulphide:

$$2Cu^{II} + 2RSH \rightarrow 2Cu^{I} + RSSR + 2H^{+}$$

Figure 2.15 Formation of a disulphide bridge

Incorporation of sulphur groups in co-ordination chemistry can cause severe problems due to facile oxidation of the sulphur ligand. This problem is usually solved by using sterically hindered thiol groups to try and prevent auto-oxidation. It may be that the phenyl groups in **4** are not sufficiently bulky to prevent this reaction from occurring. This will then inhibit the formation of metal complexes.

After the experimental work of this thesis had been completed, it was discovered that George *et al.* have also reported the use of tris(2-thiophenol)phosphine as a ligand.[13] They attempted to form a tin metal complex by treating the trilithiated ligand with *n*$BuSnCl_3$. Instead they isolated crystals that were shown to be the oxidised, dimerised ligand. This molecule contains two ligands that are coupled through a S-S bond. Within each original ligand the remaining two sulphur atoms form a S-S bond

and each phosphorous has been oxidised to a phosphine oxide. This molecule is shown in Figure 2.16.

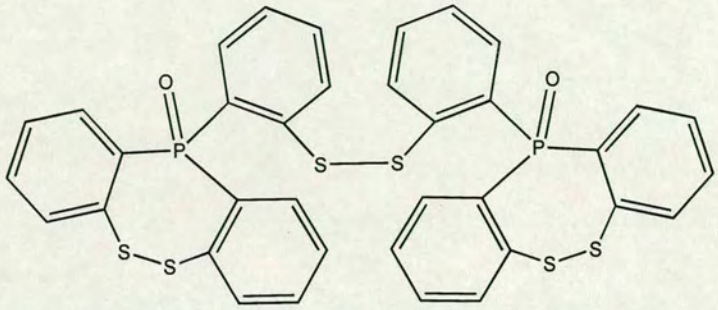

Figure 2.16 $(OP(C_6H_4S)_3)_2$

It is highly likely that a similar dimerisation process was occurring during the coordination studies of tris(2-thiophenol)phosphineoxide described in Section 2.5. This would provide a plausible explanation for the lack of formation of metal complexes.

2.6 Experimental

All air sensitive reactions were manipulated using Schlenk-type apparatus under an atmosphere of dry, dioxygen free dinitrogen, or under vacuum. All solvents were deoxygenated and dried before use by distillation from sodium / benzophenone for ethers, P_4O_{10} for acetonitrile and CaH_2 for hydrocarbons and dichloromethane.

Infrared spectra were recorded on a Perkin Elmer 1600 series FTIR spectrometer. Elemental Analysis was determined using a Perkin Elmer 2400 CHN Elemental Analyser. (+FAB) Mass spectra were obtained using a Kratos MS50TC spectrometer Nuclear Magnetic Resonance spectra were recorded on Bruker AC250 spectrometers and continuous wave spectra on a Joel PMX-60 with positive chemical shifts referenced to TMS.

These experimental conditions were adopted for all the work described within this thesis, unless stated otherwise.

2.6.1 Preparation of Ligands

2.6.1.1 Preparation of $P(2\text{-}SHC_6H_4)_3$, 3

The ligand was prepared as outlined by Block *et al.*[8]

Lithium 2-lithiobenzenethiolate, **2**, was prepared by the procedure of Martin and Figuly.[14] A solution of TMEDA (24.2 ml, 0.16 mol), and *n*-butyl lithium (65 ml of a 2.5 M solution, 0.1625 mol) in dry hexane (175 ml) was cooled to 0 °C. Thiophenol, **1**, (7.7 ml, 0.075 mol) was added slowly to the pale yellow solution. The solution was warmed to room temperature and stirred for 24 h, during which time a pale yellow solid, **2** formed. The solid was allowed to settle and the solvent was removed with a syringe. The residue was washed twice with dry hexane. Each time the suspension was stirred vigorously before being allowed to settle. The reaction mixture was cooled to –78 °C and the solid was dissolved in dry THF to give an orange solution. Phosphorus trichloride, (2.51 ml, 0.025 mol) was added slowly to the solution, with

vigorous stirring. The reaction mixture was warmed to room temperature overnight. The solution was acidified with ice cold, 10 % sulphuric acid. The mixture was concentrated *in vacuo* and the residue was taken up in ether. The ether solution was washed with water and dried over $MgSO_4$. The solution was concentrated to give the crude product as an off-white powder. This could be recrystallised from ether layered with hexane.

CHN: $C_{18}H_{15}S_3P$ requires C 60.34, H 4.19; found C 58.12, H 4.44

^{1}H NMR (360 MHz, $CDCl_3$): δ 4.09 (s, 3H, -SH), 6.76-7.42 (m, 12H, ArH)

^{13}C NMR (360 MHz, $CDCl_3$): δ 126.18, 129.79, 130.61, 132.48, 133.90, 138.02 (ArC)

^{31}P NMR (360 MHz, $CDCl_3$): δ -25.43

2.6.1.2 Attempted Alkylation of 3

2.6.1.2.1 With Methyl Iodide:

3 (0.895 g, 0.0025 mol) was dissolved in THF (50 ml). MeI (0.35 g, 0.0025 mol) was added slowly to this solution with vigorous stirring. The solution was stirred at room temperature for 2 h. The solvent was removed to yield a white powder.

^{31}P NMR analysis showed that no reaction had occurred.

The reaction was repeated on the same scale but heated under reflux for 2 h.

^{1}H and ^{31}P NMR analysis showed that the ligand had disintegrated.

2.6.1.2.2 With $SO_2(OMe)_2$

A solution of $SO_2(OMe)_2$ (0.126 g, 0.001 mol) in DCM (10 ml) was added slowly to a solution of **3** (0.358 g, 0.001 mol) in DCM (40 ml). The clear, colourless solution was stirred at room temperature under an atmosphere of nitrogen for 3 h. The solvent was removed to yield a white powder.

^{1}H and ^{31}P NMR analysis showed that no reaction had taken place.

2.6.1.2.3 With Triethyloxonium tetrafluoroborate

A solution of triethyloxonium tetrafluoroborate (0.126 g, 0.001 mol) in DCM (10 ml) was added slowly to a solution of **3** (0.358 g, 0.001 mol) in DCM (40 ml). The clear, colourless solution was stirred at room temperature under an atmosphere of nitrogen for 3 h. The solvent was removed to yield a white powder.

^{1}H and ^{31}P NMR showed a large number of peaks in the alkyl region that were not possible to identify, suggesting a large number of different products had formed.

2.6.1.3 Preparation of $O=P(2\text{-}SHC_6H_4)_3$, 4

2 was prepared as described in the procedure above. Phosphorus oxychloride, (2.3 ml, 0.025 mol) was added slowly to the solution while stirring vigorously. The reaction mixture was warmed to room temperature overnight. The solution was acidified with ice cold, 10 % sulphuric acid. The mixture was concentrated *in vacuo* and the residue was taken up in ether. The ether solution was washed with water and dried over $MgSO_4$. The solution was concentrated to give the crude product as an off white powder. This was recrystallised from toluene layered with ether.

MS (+ve FAB): m/z 375 (molecular ion), 357, ($P(2\text{-}SHC_6H_4)_3$); 341, ($O=P(2\text{-}SHC_6H_4)_2(C_6H_4)$); 307, ($O=P(2\text{-}SHC_6H_4)(C_6H_4)_2$); 267, ($O=P(2\text{-}SHC_6H_4)_2$); 233, ($O=P(2\text{-}SHC_6H_4)(C_6H_4)$); 154, ($O=P(2\text{-}SHC_6H_4)$).

CHN: $C_{18}H_{15}S_3OP$ requires C 57.75, H 4.03; found C 55.43, H 3.86

^{1}H NMR (360 MHz, $CDCl_3$): δ 4.59 (s, 3H, -S<u>H</u>), 7.30-7.70 (m, 12H, Ar<u>H</u>)

^{13}C NMR (360 MHz, $CDCl_3$): δ 126.47, 128.76, 129.92, 133.07, 134.01, 136.28, (Ar<u>C</u>)

^{31}P NMR (360 MHz, $CDCl_3$): δ -20.2

Crystal Data for $HP=O(2\text{-}SHC_6H_4)_2$, 5

Data were calculated using Mo-Kα radiation on a colourless block of dimensions 0.38x0.38x0.27 mm on a Stoe Stadi4 diffractometer in the range $2.97 \leq \theta \leq 25.2°$ using the ω-θ method. Of a total of 4264 reflections collected, 2133 (R_{int} = 0.0175) were independent. The structure was solved by direct methods (SHELXS-97 (Sheldrick, 1990)) and refined using SHELXL-97. Hydrogen atoms were geometrically fixed

and allowed to ride. The SH hydrogen was located by fourier synthesis. The largest difference between peak and hole in the final difference map was +0.313 and –0.292e $Å^{-3}$, with a final R of 0.0295 for 158 parameters.

Empirical Formula	$C_{12}H_{11}OPS_2$	γ / °	90
Formula Weight	266.3	Volume / $Å^3$	1187.7(5)
Crystal system	Monoclinic	Z	4
Space group	P21/n	Temperature / K	150(2)
a / Å	7.8136(18)	Wavelength / Å	0.71073
b / Å	12.698(3)	Density calc. / Mg/m^3	1.489
c / Å	12.041(3)	μ(Mo-Kα) / mm^{-1}	0.556
α / °	90	$R_1[F>4\sigma(F)]$	O.0295
β / °	96.20(3)	WR_2 (all data)	0.0680

Table 2.3 Crystallographic data for 5

2.6.1.4 Preparation of $O=P(2\text{-}OMeC_6H_4)_3$, 8

The Grignard reagent 2-methoxyphenylmagnesiumbromide, **7** was prepared from the slow addition of 2-bromoanisole, **6**, (18.68 ml, 0.15 mol) to magnesium turnings (3.64 g, 0.15 mol) in ether (200 ml) with a catalytic amount of iodine (2 mg). The mixture was heated slightly to initiate the reaction. The reaction was left until the mixture had stopped refluxing and all of the magnesium had reacted. A 70 % conversion rate was assumed.

The reaction was cooled to -10 °C using an ice / KCl bath. Phosphorus oxychloride (3.21 ml, 0.035 mol) was added slowly over a period of 1.5 h. On addition, a white precipitate formed (probably MgBrCl). The mixture was heated under reflux for 2 h to ensure that the reaction had gone to completion. It was then hydrolysed by the addition of saturated aqueous NH_4Cl solution. Dichloromethane (100 ml) was added and the mixture was filtered. The organic layer was separated, washed with water and dried with $MgSO_4$. The mixture was concentrated to yield a pale yellow solid. This was washed with methanol to yield **8** as a white powder.

^{1}H NMR (360 MHz, $CDCl_3$): δ 3.66 (s, 9H, MeO) 7.08-7.69 (m, 12H, ArH)

^{13}C NMR (360 MHz, $CDCl_3$): δ 55.63 (OMe), 110.13, 120.79 (ArC), 123.18 (Ar, quatC), 130.21, 133.75 (ArC), 161.30 (d, *J*=15.6Hz Ar, quatC attached to P)

^{31}P NMR (360 MHz, $CDCl_3$): δ 37.32

2.6.1.5 Preparation of $O=P(2\text{-}OHC_6H_4)_3$, 9 - $AlCl_3$ cleavage of 8

Benzene (150 ml) was added to **8** (1.0 g, 2.7 mmol) and anhydrous aluminium chloride (1.45 g, 0.01 mol) with stirring. Methyl chloride was evolved. The mixture was kept at 95-100 °C under reflux for 4 h until the evolution of methyl chloride had ceased. The solution was acidified with ice cold, 20 % hydrochloric acid. The organic layer was separated and washed with water. This was then dried with $MgSO_4$. Concentration of the solution *in vacuo* gave the crude product, **9** as a white solid. Recrystallisation from dichloromethane layered with hexane gave crystals of suitable quality for X-ray analysis.

MS (+ve FAB) m/z 327 (molecular ion), 309 ($O=P(2\text{-}OHC_6H_4)_2(C_6H_4)$), 293, ($O=P(2\text{-}OHC_6H_4)(C_6H_4)_2$), 215 ($O=P(2\text{-}OHC_6H_4)(C_6H_4)$),
199 ($P(2\text{-}OHC_6H_4)(C_6H_4)$), 141 ($O=P(2\text{-}OHC_6H_4)$.
CHN: $C_{18}H_{15}PO_4$ requires C 66.23, H 4.6; found C 66.51, H 4.5;
^{1}H NMR (360 MHz, $CDCl_3$): δ 6.83-7.50 (m, 12H, Ar<u>H</u>), 10.80 (s, 3H, O<u>H</u>)
^{13}C NMR (360 MHz, $CDCl_3$): δ 115.28, 116.54 (Ar, quat<u>C</u>), 118.76, 132.77, 134 (Ar<u>C</u>), 160.71 (d, *J*=3.1Hz Ar, quat<u>C</u> attached to P)
^{31}P NMR (360 MHz, $CDCl_3$): δ 37.32

Crystal Data for 9

Data were calculated using Mo-Kα radiation on a colourless plate of dimensions 0.58x0.31x0.08 mm on a Stoe Stadi4 diffractometer in the range $3.23 \leq \theta \leq 70.16°$ using the ω-θ method. Of a total of 3708 reflections collected, 2810 (R_{int} = 0.1156) were independent. The structure was solved by direct methods (SHELXS-97 (Sheldrick, 1990)) and refined using SHELXL-97. Hydrogen atoms were geometrically fixed and allowed to ride. The OH hydrogen was located using the difference map. The largest difference between peak and hole in the final difference map was +0.506 and –0.469e $Å^{-3}$, with a final R of 0.0412 for 212 parameters.

Empirical Formula	$C_{18}H_{15}O_4P$	γ / °	90
Formula Weight	326.27	Volume / $Å^3$	1539.7(4)
Crystal system	Monoclinic	Z	4
Space group	P21/c	Temperature / K	150(2)
a / Å	14.831(2)	Wavelength / Å	1.54184
b / Å	8.4991(13)	Density calc. / Mg/m^3	1.407
c / Å	13.2485(16)	μ(Mo-Kα) / mm^{-1}	1.747
α / °	90	$R_1[F>4\sigma(F)]$	0.0412
β / °	112.775(10)	wR_2 (all data)	0.1073

Table 2.4 Crystallographic data for 9

2.6.1.6 Preparation of $P(2\text{-}OMeC_6H_4)_3$, 10

The Grignard reagent **7** was prepared from the slow addition of **6**, (18.68 ml, 0.15 mol) to magnesium turnings (3.64 g, 0.15 mol) in ether (200 ml) with a catalytic amount of iodine (2 mg). The mixture was heated slightly to initiate the reaction. The reaction was left until the mixture was no longer in a state of reflux and all of the magnesium had reacted. A 70 % conversion rate was assumed.

The reaction was cooled to –10 °C using an ice / KCl bath. Phosphorus trichloride (3.52 ml, 0.035 mol) was added slowly over a period of 1.5 h. On addition, a white precipitate formed, (probably MgBrCl). The mixture was heated under reflux for 2 h to ensure that the reaction had gone to completion. It was then hydrolysed by the addition of saturated aqueous NH_4Cl solution. Dichloromethane (100 ml) was added and the mixture was filtered. The organic layer was separated, washed with water and dried with $MgSO_4$. The mixture was concentrated to yield **10** as a pale yellow solid. This was washed with methanol to yield a white powder.

CHN: $C_{21}H_{21}PO_3$ requires C 71.59, H 5.97; found C 68.92, H 6.33

^{1}H NMR (360 MHz, $CDCl_3$): δ 3.74 (s, 9H, Me), 6.68-7.36 (m, 12H, Ar<u>H</u>)

^{13}C NMR (360 MHz, $CDCl_3$): δ 55.61 (s, O<u>Me</u>) 110.11, 120.76, (Ar<u>C</u>) 123.75 (Ar, quatC), 130.01, 133.72, (Ar<u>C</u>), 123.75 (d, *J*=16.1Hz Ar, quat<u>C</u> attached to P)

^{31}P NMR (360 MHz, $CDCl_3$): δ -38.29

Attempted Preparation of $P(2\text{-}OHC_6H_4)_3$ - $AlCl_3$ cleavage of 9

Benzene (150 ml) was added to **10** (1.0 g, 2.7 mmol) and anhydrous aluminium chloride (1.45 g, 0.01 mol) with stirring. Methyl chloride was evolved. The mixture was kept at 95-100 °C under reflux for 4 h until the evolution of methyl chloride had ceased. The solution was acidified with ice cold, 20 % hydrochloric acid. The organic layer was separated and washed with water. This was then dried with $MgSO_4$. Concentration of the solution *in vacuo* gave a white solid. Unfortunately, ^{13}C NMR showed that the OMe group was still present and that the desired product had not formed.

2.6.2 Preparation of Metal Precursor Complexes

2.6.2.1 Large Scale Preparation of Cp^*H[12]

The first two steps were carried out with the assistance of Tony Barrett.

2.6.2.1.1 Synthesis of 2,3,5,6-tetrahydro-2,3,5,6methyl-γ-pyrone

Under an atmosphere of nitrogen, potassium hydroxide (152 g, 2.71 mol) was dissolved in methanol (950 cm^3) then the solution was cooled to 0 °C. Following the addition of 3-pentanone (7.56 mol, 800 cm^3), acetaldehyde (30.2 mol, 1698 cm^3) was added slowly at 0 °C, over a period of 15 h. During this time, the reaction mixture darkened in colour and after a further 12 h stirring had turned a dark brown-red colour. Cold concentrated hydrochloric acid, (HCl), (240 cm^3) was then added slowly over the period of 1 h. The organic and aqueous layers were separated and the organic layer washed with HCl (2 M, 1000 cm^3). The aqueous layer was then back-extracted with diethyl ether (2 x 500 cm^3) and the organic layers were combined. The ether was then removed and the residue was washed with sodium chloride, (NaCl), (2 M, 500 cm^3) and finally the remaining methanol was removed *in vacuo* to leave a viscous red oil. The product was obtained by fractional distillation to yield a clear, yellow liquid, (555.80 g, 47 %).

BP = 69–85 °C / 15 mmHg

IR (thin film): ν_{max} 1712, (s), (C=O) cm^{-1}

^{1}H NMR (250 MHz, $CDCl_3$): δ 0.92 (d, J = 7 Hz, 6 H, α $C\underline{H}_3$), 1.28 (d, J = 7 Hz, 6 H, β $C\underline{H}_3$), 2.24 (m, 2 H, α $\underline{H}$), 3.30 (m, 2H, β $\underline{H}$)

2.6.2.1.2 Synthesis of 2,3,4,5-tetramethylcyclopent-2-enone

Formic acid (2600 cm^3) and concentrated sulphuric acid (900 cm^3) were placed in a flask precooled to 0 °C and stirred rapidly. After warming to room temperature, 2,3,5,6-tetrahydro-2,3,5,6-methyl-γ-pyrone (555 g, 3.56 mol) was added slowly over 2 h. After addition was complete, the solution was warmed to 50 °C for 24 h, during which time the mixture turned dark brown. After cooling, portions (500 cm^3) of the reaction mixture were poured into conical flasks containing ice (1000 g), and then ether (500 cm^3) was added to each flask. The aqueous layers were separated and back extracted with ether (2 x 200 cm^3), then the combined extracts were washed with NaCl (2 M, 2 x 250 cm^3) portions followed by sodium hydroxide (10 % w/v) until the aqueous layer becomes alkaline. Finally, the organic layer was washed with NaCl (2 M, 2 x 250 cm^3), dried over anhydrous sodium sulphate, filtered and the ether removed by rotary evaporation. The brown residue was fractionally distilled to yield the product as a colourless liquid, (335.55 g, 68 %).

BP = 80 – 97 °C / 15 mmHg

IR (thin film): ν_{max} 1670, (s); 1651, (s), (C=O); 1623, (m), (C=C) cm^{-1}

^{1}H NMR (200 MHz, $CDCl_3$): δ 1.06 (d, J = 7 Hz, 3 H, βCH-C$\underline{H}_3$), 1.08 (d, J = 7 Hz, 3 H, αC-C$\underline{H}_3$), 1.79 (q, d, q, J = 7, 3, 0.5 Hz, 1 H, β C$\underline{H}$-CH_3), 1.89 (q, J = 0.7 Hz, 3H, β C-C$\underline{H}_3$), 2.17 (q, br, J = 7 Hz, 1H, α C$\underline{H}$-CH_3)

2.6.2.1.3 Synthesis of pentamethylcyclopentadiene

MeLi (0.178 mol, 127.2 cm^3 of 1.4 M in ether, 1.2 eq.) was transferred *via* cannula into a flask and cooled to 0 °C. 2,3,4,5-tetramethylcyclopent-2-enone (0.148 mol, 20.50 g) was added slowly over 30 minutes with rapid stirring. The solution was allowed to warm to room temperature and was stirred for 18 h. Excess MeLi was destroyed by the careful addition of methanol (50 cm^3), then water (100 cm^3). The resulting solution was washed with the following solution: ammonium chloride (120 g), concentrated HCl (100 cm^3) and water (500 cm^3) until the aqueous layer became acidic and the combined aqueous layers were back extracted with diethyl ether (200 cm^3). After removal of most of the ether *in vacuo* the concentrate was stirred with HCl (6 M, 2 cm^3) for 1 h to ensure water elimination from the intermediate. Finally

the ether concentrate was washed with sodium hydrogen carbonate (5 % w/v, 100 cm^3), dried over anhydrous potassium carbonate and filtered. The remaining ether was then removed and the product was obtained by fractional distillation yielding a pale yellow liquid, (12.54 g, 62 %).

BP = 65 – 70 °C / 15 mmHg

IR (thin film): ν_{max} 1659, (s), (C=C) cm^{-1}

^{1}H NMR (250 MHz, $CDCl_3$): δ 1.02 (d, J = 7.5 Hz, 3 H, βCH-C$\underline{H}_3$), 1.79 (2 d, q, J = 0.8 Hz, 6 H, C-C$\underline{H}_3$), 1.83 (2 d, J = 0.4 Hz, 6H, C-C$\underline{H}_3$), 2.5 (q, J = 8 Hz, 1H, C$\underline{H}$=CH_3)

^{13}C NMR (62.9 MHz, $CDCl_3$): δ 10.90 (C-$\underline{C}H_3$), 11.39 (C-$\underline{C}H_3$), 13.91 (CH-$\underline{C}H_3$), 51.34 ($\underline{C}$H-CH_3), 134.00 ($\underline{C}$-CH_3), 137.58 ($\underline{C}$-CH_3)

2.6.2.2 Preparation of Cp^*TiCl_3[15]

Cp^*H (1.36 g, 0.01 mol) in dry hexane was treated with *n*-butyl lithium (12.5 ml of a 1.6 M solution in hexane, 0.02 mol). Titanium tetrachloride (2.42 g, 0.0128 mol) was added to the pale yellow suspension of $LiCp^*$. The mixture was stirred at room temperature for two days to yield a dark brown mixture. This was filtered using a filter stick to yield a bright red, clear solution. The brown residue was washed with benzene (two 20 ml portions). The solvent was removed *in vacuo* to leave a dark red powder.

2.6.2.3 Preparation of $Cp^*Sn^nBu_3$[16]

n-Butyllithium (7.7 ml of a 2.5 M solution, 1.92 mmol) was added slowly over a period of 0.5 h to a well stirred solution of Cp^*H (2.6 g, 1.92 mmol) in THF. Butane was evolved and a white suspension of $LiCp^*$ formed. The mixture was stirred for 2 h after complete addition of the *n*-butyllithium.

Tributyltinchloride (5.2 ml, 1.92 mmol) was syringed onto the suspension. The white suspension dissolved, forming a yellow solution. After stirring for 1 h, the THF solvent was removed *in vacuo* leaving a mixture of white LiCl and yellow, oily Bu_3SnCp^*. Hexane (20 ml) was added and the mixture was stirred for 0.5 h. It was

then filtered through a filter stick under nitrogen. The hexane solvent was removed from the filtrate under vacuum to leave a clear colourless solution.

2.6.2.4 Preparation of $MoCl_4(MeCN)_2$[17]

$MoCl_5$ (5 g, 0.0183 mol) was placed in a rigorously pre-dried thimble and extracted with hot acetonitrile using a soxhlet apparatus under an atmosphere of dinitrogen. The initial exothermic reaction provided a light brown coloured solution that turned a very dark brown colour over a period of 3 h. The solution was cooled to room temperature to yield dark purple crystals.

2.6.2.5 Attempted Preparation of $Cp^*MoCl_3(MeCN)_2$

A solution of $Cp^*Sn^nBu_3$ (1.07 g, 3.0 mmol) in toluene (10 ml) was added slowly to a chilled (0 °C) and stirred solution of $MoCl_4(MeCN)_2$ (0.86 g, 3.0 mmol) in toluene (15 ml) under an atmosphere of nitrogen. This resulted in a dark red / brown solution. This was stirred at room temperature over 24 h. This resulted in the formation of a dark red / brown precipitate. The solution was reduced in volume by a third to yield more solid. The solids were washed with dichloromethane (3 x 20 ml) and hexane (2 x 10 ml). Boiling acetonitrile was added to dissolve the solid. The solution turned a dark green brown and had decomposed.

2.6.2.6 Preparation of $MoCl_3(MeCN)_3$

$MoCl_4(MeCN)_2$ (1 g, 3.2 mmol) was added to anhydrous acetonitrile (20 ml). To the vigorously stirred mixture was added tin powder (0.18 g, 1.6 mmol). The mixture was stirred at room temperature for 30 minutes. On addition of the tin, the brick red solution turned lime green, with a fine yellow precipitate. The precipitate was allowed to settle. The solution was removed using a cannula filter. The precipitate was washed with cold, anhydrous acetonitrile to give the product as a yellow solid. The product is air sensitive, turning grey on exposure to the air.

2.6.2.7 Preparation of Di-μ-chloro-bis[chloro(η^6-1-isopropyl-4-methyl-benzene) ruthenium(II), $RuCl_2(\eta^2\text{-}C_{10}H_{14})]_2$ [18]

α-Terpine (20 ml, 0.123 mol) was added slowly to a solution of hydrated ruthenium trichloride (4.0 g, 0.015 mol) in ethanol (200 ml). The dark red solution was heated under reflux, under an atmosphere of dinitrogen for 4 h. The solution was left to cool to room temperature. The dark red microcrystalline product was isolated by filtration. The orange filtrate was reduced in volume and placed in the fridge to yield more product. (4.025 g, 86 %)

^{13}C and ^{1}H NMR in $CDCl_3$ showed that the desired product had formed.

2.6.3 Complexation of Ligands to Metal Complexes

2.6.3.1 Attempted Synthesis of $TiCp^*P{=}O(2\text{-}SC_6H_4)_3$

4 (0.1 g, 3.1 mmol) was ground to a fine powder and dissolved in anhydrous THF (20 ml) in a degassed Schlenk tube at –78 °C. ^{n}BuLi (0.58 ml of a 1.6 M solution in hexane, 0.93 mmol) was added. The solution was warmed to room temperature and stirred for 2.5 h. The solution remained clear and colourless. $TiCp^*Cl_3$ (0.09 g, 0.31 mmol) was added to the solution, causing the colour to turn yellow / pale orange. The solution was stirred at room temperature overnight with no further colour change. The THF was removed *in vacuo* to leave a yellow oily solid. This was redissolved in hexane to give a yellow solution and a pale yellow precipitate. The precipitate was removed by filtration. The solution was reduced in volume by a half *in vacuo* and the solution was left to crystallise. Small yellow crystals were formed but were unsuitable for X-ray analysis. Recrystallisation was reattempted from cyclohexane but without success.

2.6.3.2 Attempted Synthesis of $HB(pz)_3TiP{=}O(2\text{-}OC_6H_4)_3$

$HB(pz)_3K$ (1.261 g, 0.005 mol) was dissolved in THF (50 ml) and $TiCl_4$ (0.55 ml, 0.005 mol) was added slowly with rapid stirring. A lot of fumes were produced and the solution turned bright yellow. **4** (1.141 g, 0.0035 mol) was added to the solution. This was stirred at room temperature for 24 h. During this time, an orange precipitate formed and the solution turned red. The solid was isolated by cannula filtration and

washed with THF. The solid was very insoluble and it was not possible to recrystallise or characterise.

2.6.3.3 Attempted Synthesis of Ti(O^iPr)P=O(2-OC_6H_4)$_3$

P=O(2-OHC_6H_4)$_3$ (0.33 g, 1.0 mol) was ground up to a fine powder and dissolved in dry THF (20 ml) in a degassed Schlenk tube at –78 °C. ^{n}BuLi (0.58 ml of a 1.6 M solution in hexane, 9.3 mmol) was added. The solution was warmed to room temperature and stirred for 2.5 h. The solution remained clear and colourless. Ti(O^iPr)$_4$ (0.285 ml, 1.0 mmol) was added to the solution, which became yellow in colour. The solution was stirred at room temperature overnight with no further colour change. The THF was removed *in vacuo* to leave a yellow oily solid. This was redissolved in toluene (only partially soluble) to give a yellow solution and a yellow precipitate that went into solution on warming. The solution was filtered whilst hot and left to cool in an attempt to grow crystals. A yellow powder crashed out of solution to leave a bright yellow saturated solution above it. The solution was removed by cannula filtration crystallisation was attempted by layering with hexane. Again, a powder crashed out of solution. This was air sensitive, turning brown within seconds of exposure to air.

2.6.3.3.1 Substitution of O^iPr in Ti(O^iPr)P=O(2-OC_6H_4)$_3$ for Pyrrole

The synthesis of Ti(O^iPr)P=O(2-OC_6H_4)$_3$ was repeated, taking great care to keep the reaction under air-free conditions. **9** (0.33 g, 1.0 mol) was ground to a fine powder and dissolved in dry THF (20 ml) in a degassed Schlenk tube at –78 °C. ^{n}BuLi (0.58 ml of a 1.6 M solution in hexane, 9.3 mmol) was added. The solution was warmed to room temperature and stirred for 2.5 h. The solution remained clear and colourless. Ti(O^iPr)$_4$ (0.285 ml, 1.0 mmol) was added to the solution, which became yellow in colour. The solution was stirred at room temperature for 4 h. Pyrrole (0.02 ml, 0.31 mmol) was added to the solution and the solution stirred for 24 h. During this time, the solution turned orange and a bright yellow precipitate formed. Both of these were extremely air sensitive, turning brown on exposure to air and it was not possible to characterise them.

2.6.3.3.2 Substitution of O^iPr in $Ti(O^iPr)P{=}O(2\text{-}OC_6H_4)_3$ for Hydrotris(pyrazole)borate

The synthesis of $Ti(O^iPr)P{=}O(2\text{-}OC_6H_4)_3$ was repeated on the same scale as described above. The THF was removed *in vacuo* to yield a bright yellow residue. This was partially redissolved in toluene. Acetyl chloride (0.033 ml, 0.92 mmol) was added to the solution and stirred for 4 h. After this time, the solution had turned yellow and some yellow precipitate had formed. The toluene was removed *in vacuo* and the solid redissolved in THF to give a clear yellow solution. Potassium Hydrotris(pyrazole)borate (0.039 g, 0.15 mmol) was added and the solution stirred at room temperature for 16 h. During this time, a white precipitate (presumably KCl) under a bright yellow solution formed. The solution was filtered, reduced to half its volume *in vacuo* and layered with hexane to encourage crystallisation. Repeated recrystallisation attempts only led to the formation of a yellow precipitate crashing out of solution. It was not possible to characterise this material before it decomposed.

2.6.3.4 Attempted Synthesis of $(PhCN)_3RuP{=}O(2\text{-}SC_6H_4)_3$

4 (0.2 g, 0.54 mmol) was ground up to a fine powder and dissolved in anhydrous THF (20 ml) in a degassed Schlenk tube at –78 °C. ^{n}BuLi (1 ml of a 1.6 M solution in hexane, 1.6 mmol) was added and the solution turned a clear yellow colour. The solution was warmed to room temperature and stirred for 2.5 h. This resulted in the formation of a pale yellow solution and a fine white precipitate. $(PhCN)_3RuCl_3$ (0.276 g, 0.54 mmol) was added to the well-stirred solution, to give a dark red solution. This was left to stir overnight to yield a pale olive green precipitate and a dark brown / green solution. The THF was removed *in vacuo* and the residue was redissolved in toluene. The solution was filtered through celite and concentrated *in vacuo* to one third of its original volume. Layering with ether yielded block crystals. Unfortunately, these re-dissolved whilst waiting for analysis. Repeated attempts have resulted in crystals but not of sufficient quality for X-ray analysis.

2.6.3.5 Attempted Synthesis of $Mo(MeCN)_3P{=}O(2\text{-}OC_6H_4)_3$

9 (0.16 g, 0.5 mmol) was ground up to a fine powder and dissolved in dry THF (20 ml) in a degassed Schlenk tube at –78 °C. ^{n}BuLi (0.93 ml of a 1.6 M solution in hexane, 1.5 mmol) was added. The solution was warmed to room temperature and stirred for 2.5 h. The solution remained clear and colourless. $MoCl_3(MeCN)_3$ (0.16 g, 0.5 mmol) was added to the well-stirred solution. This resulted in the formation of an olive green solution. The mixture was slowly warmed to room temperature and stirred overnight, resulting in a colour change to yellow- brown. The solvent was removed *in vacuo* and the resulting solution was redissolved in toluene. The solution was filtered through celite to yield a clear yellow solution. This was reduced in volume by a half and left in the freezer to crystallise but without success.

2.6.3.6 Attempted Synthesis of $Co(MeCN)_3P{=}O(2\text{-}SC_6H_4)_3$ – Complexation with $Co(BF_4)_2{\cdot}6H_2O$

An excess of NaH (0.1 g, 0.004 mol) was added to dry THF (20 ml) in a degassed Schlenk at –78 °C to give a grey / white suspension. **4** (0.3 g, 0.8 mmol) was ground to a fine powder and added to this suspension. The suspension was warmed to room temperature and stirred for 2 h. This resulted in a pale yellow solution with a small amount of white precipitate (presumed to be unreacted NaH). The yellow solution was removed by cannula filtration to a clean Schlenk tube. Excess acetonitrile (approximately 10 ml) and $Co(BF_4)_2.6H_2O$ (0.273 g, 0.8 mmol) was added, resulting in the solution turning dark brown. PPh_4Cl (0.3 g, 0.8 mmol) was added to the solution to promote crystallisation. The solution was stirred at room temperature overnight. The THF was removed *in vacuo* to yield a dark brown residue. This was redissolved in dichloromethane. The solution was filtered through celite, leaving a dark brown solution. This solution was layered with hexane to try and promote crystallisation. A brown powder crashed out of solution.

Mass spectrometry and CHN analysis of the brown precipitate showed the compound to have decomposed.

2.6.3.7 Attempted Synthesis of $Co(MeCN)_3P{=}O(2\text{-}SC_6H_4)_3$ – Complexation with $CoCl_2$

4 (0.2 g, 0.54 mmol) was ground up to a fine powder and dissolved in degassed, anhydrous acetonitrile under a nitrogen atmosphere. To this was added sodium methoxide (0.087 g, 1.6 mmol) and PPh_4Cl (0.2 g, 5.4 mmol). This resulted in a pale yellow solution. Pale purple / pink anhydrous $CoCl_2$ (0.07g, 0.54 mmol) was dissolved in dry, degassed acetonitrile in a separate Schlenk tube to give an intense turquoise solution. This was transferred by cannula into the $Na_3P{=}O(2\text{-}SC_6H_4)_3$ - PPh_4Cl solution. The solution turned brown immediately. The solution was stirred at room temperature for three hours. After this time, some precipitate had formed. The solution was filtered and reduced in volume by a half. Crystallisation was attempted by layering with isopropyl ether, but was unsuccessful.

Mass spectrometry and CHN analysis of the brown precipitate showed the compound to have decomposed.

2.6.3.8 Synthesis of $P{=}O(2\text{-}OTlC_6H_4)_3$, 11

9 (1.0 g, 3.1 mmol) was dissolved in THF (50 ml) to yield a clear, colourless solution. Thallium ethoxide (2.18 g, 8.74 mmol) was added and heat was evolved. A white powder precipitated out of the solution. The reaction mixture was stirred at room temperature, in the dark, under an atmosphere of dinitrogen for two hours. The white powder was filtered and washed on the filter with THF and then with diethyl ether. It was then dried in the vacuum oven for 45 minutes.

2.6.3.9 Coordination to Vanadium

11 (0.468 g, 0.5 mmol) was added to a dark pink solution of the vanadium chloride salt, $VaCl_3{\cdot}3THF$ (0.190 g, 0.5 mmol) in THF (20 ml). After stirring at room temperature in the dark, a purple precipitate had formed under a dark green solution. The solid was broken up using a sonic bath and isolated by filtration but proved to be extremely insoluble. The solvent was removed from the filtrate to yield a green solid. This was very air sensitive and turned black over 2 h.

2.6.3.10 Coordination to Titanium

$HB(pz)_3K$ (0.631 g, 0.0025 mol) was dissolved in THF (20 ml) and $TiCl_4$ (0.275 ml, 0.0025 mol) was added slowly with rapid stirring to the solution at 0 °C. A lot of fumes were produced and the solution turned bright yellow. An off white precipitate formed (presumably KCl) and was removed by filtration using a filter stick. **11** (1.638 g, 1.75 mmol) was added to the solution. This was stirred at room temperature for 24 h. During this time, a yellow precipitate formed and the solution turned bright yellow. The solid was isolated by cannula filtration and washed with THF. The solid was very insoluble and it was not possible to recrystallise or characterise.

2.6.3.11 Coordination to Ruthenium

$RuCl_2(\eta^2\text{-}C_{10}H_{14})]_2$ (0.28 g, 0.46 mmol) was dissolved in THF to give a brick red solution. **11** (0.859 g, 0.92 mmol) was added to the solution and it turned orange. The solution was stirred at room temperature, under an atmosphere of dinitrogen for 16 h. During this time, the solution turned pale orange and an orange / yellow precipitate formed. PPh_4Cl (0.241 g, 0.64 mmol) was added to the solution and stirred for a further 4 h. The very pale yellow precipitate was removed by filtration with a filter stick. The dark orange solution was reduced in volume to yield an orange residue. This was redissolved in toluene, hot filtered and left to crystallise. Repeated attempts at recrystallisation only led to the formation of fine precipitates.

2.7 References

1. K. Govindaswamy, D. A. Quarless Jr. and S. A. Koch, *J. Am. Chem. Soc.*, 1995, **117**, 8468

2. J. Hwang, K. Govindaswamy and S. A. Koch, *Chem. Commun.*, 1998, 1667

3. R. J. Motekaitis, A. E. Martell, S. A. Koch, J. Hwang, D. A. Quarless Jr. and M. J. Welch, *Inorg. Chem.*, 1998, **3**, 5902

4. M. B. Dinger and M. J. Scott, *Inorg. Chem.*, 2000, **39**, 1238

5. M. B. Dinger and M. J. Scott, *J. Chem. Soc., Perkin Trans. 1.*, 2000, 1741

6. M. B. Dinger and M. J. Scott, *Eur. J. Org. Chem.*, 2000, 2467

7. M. B. Dinger and M. J. Scott, *Inorg. Chem.*, 2001, **40**, 856

8. E. Block, G. Ofori-Okai and J. Zubieta, *J. Am. Chem. Soc.*, 1989, **111**, 2327

9. R. P. L'Esperance, A. P. West Jr., D. V. Engen and R. A. Pascal Jr., *J. Am. Chem. Soc.*, 1991, **113**, 2672

10. J. Kennedy, E. S. Lane and J. L. Willans, *J. Chem. Soc., Perkin Trans. 1.*, 1956, 4670

11. O. Nuenhoeffer and L. Lamza, *Chem. Ber.*, 1961, **94**, 2515

12. C. M. Fendrick, L. D. Schertz, E. A. Mintz and T. J. Marks, *Inorg. Synth.*, 1992, **29**, 193

13. K. A. Clark, T. A. George, T. J. Brett, C. R. Ross, II and R. K. Shoemaker, *Inorg. Chem.*, 2000, **39**, 2252

14. G. D. Figuly, C. K. Loop and J. C. Martin, *J. Am. Chem. Soc.*, 1989, **111**, 654

15. R. B. King and M. B. Bisnette, *J. Organomet. Chem.*, 1967, 287

16. R. D. Sanner, S. T. Carter and W. J. Burton, *J. Organomet. Chem.*, 1982, 157

17. G. R. Willey, *J. Organomet. Chem.*, 1996, **510**, 213

18. M. A. Bennett and A. K. Smith, *J. Chem. Soc., Dalton Trans.*, 1974, 233

3 Pyridine *N*-Oxide Ligands

This chapter discusses the attempts made at synthesising a tripod ligand containing three pyridine *N*-oxide donor functionalities. The supporting framework of the ligand is based upon tris(2-pyridyl)methanol. There is a central non-coordinating carbon atom that is joined to three pyridyl rings. The hard oxygen donor functionalities are connected to the central carbon atom *via* two sp^2 atoms – one carbon and one nitrogen. This is a fairly rigid framework and so should provide a pronounced, static C_3 coordination environment upon complexation to a metal.

3.1 Introduction to Heterocyclic N-oxides

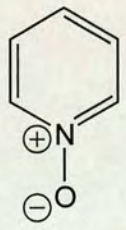

Figure 3.1 Pyridine *N*-oxide

Heterocyclic *N*-oxides are characterised by a donative or coordinate covalent bond from the nitrogen atom to the oxygen atom. This bond is the result of the overlap of the nonbonding electron pair on the nitrogen atom with an empty orbital on the oxygen atom and there is a formal positive charge on the nitrogen atom.

In aromatic systems, such as pyridine *N*-oxide, (Figure 3.1), the charge can be delocalised around the ring giving the mesomeric structures **2** (Figure 3.2). This results in the six membered ring in pyridine *N*-oxide being more regular and similar to benzene than to pyridine. All of the bonds in the ring are of similar length and the C-N-C angle is very close to 120 °C.

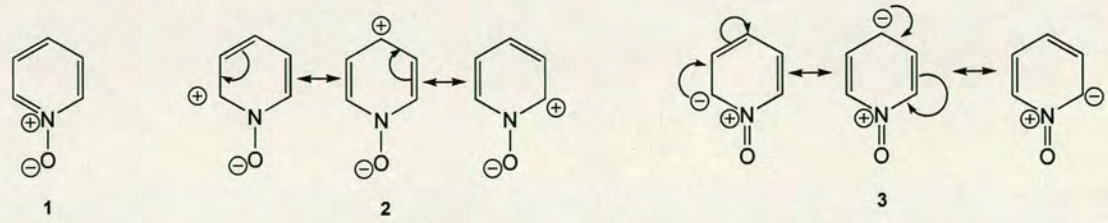

Figure 3.2 Mesomeric forms of Pyridine *N*-oxide

The negative charge is not confined to the oxygen atom and can be delocalised by π-bonding, giving the mesomeric forms **3**, (Figure 3.2). This results in the N-O bond having partial double bond character. This is supported spectroscopic evidence, including N-O stretching frequencies and crystal structure determinations. The N-O bond is relatively short at 1.28 Å and the bond order has been estimated to be 1.5.[1-3]

Substituents on the six membered ring will have a large influence on which of the canonical forms are favoured and so upon the nature of the N-O bond. Strong electron withdrawing substituents at *ortho-* and *para-* positions will favour the canonical forms **3** and so reduce the effective donor capacity of the ligand. In comparison, electron-donating substituents will enhance the importance of the canonical forms **2**, the N-O bond becomes longer and the effective donor capacity of the ligand is increased. This means that by varying the substituents on the pyridine rings the donor characteristics of the ligand can be controlled.

3.1.1 Heterocyclic *N*-oxides as Ligands in Metal Complexes

Heterocyclic *N*-oxide ligands readily form σ-complexes through the oxygen atom with metal ions. Upon coordination, the pyridine *N*-oxide oxygen atom can function as both a donor and an acceptor of electron density. If the metal possesses empty d-orbitals of correct symmetry, donation of electron density from the highest filled π-molecular orbital of the ligand occurs. The ligand also has the ability to act as a π-acceptor when coordinated to d-electron rich metals, with a filled metal d-orbital to an empty ligand π^*-orbital back bonding interaction occurring. These different bonding modes enable aromatic *N*-oxides to form complexes with metals from throughout the periodic table. They can be prepared by mixing alcoholic solutions of the ligand and a metal salt, with the resulting coordination compound often precipitating out of solution. The majority of complexes are decomposed by water through ligand displacement, although they are not necessarily sensitive to atmospheric moisture. For this reason, triethyl orthoformate or 2,2'-dimethoxypropane is often added to the reaction media to act as a desiccant.

The *N*-oxides generally form complexes with the maximum coordination number of the particular metal, although there are numerous exceptions. Most studies have been carried out using pyridine *N*-oxide as the ligand. The oxygen atom is much more polar than in other common oxo donors such as alcohols, ethers and amides. Reedijk *et al.* have prepared a large number of metal complexes with a wide variety of metals.[4] In the presence of weakly coordinating anions, such as perchlorate, tetrafluoroborate or nitrate, metal ions form complexes with the maximum coordination number of the metal ion. If anions more basic than perchlorate or tetrafluoroborate are present, metal complexes containing both the pyridine *N*-oxide ligands and the anion in the primary coordination sphere are formed.[5] According to infrared spectra, UV / vis spectra, magnetic measurements and X-ray powder diagrams, the MO_6^{n+} octahedral geometry is hardly distorted.

The ligand occurs very low in both the spectrochemical and nephelauxetic series, but rather high in the Dq / B series. Reedijk *et al.* measured the Dq and B values for octahedral solvates of formula $M(L)_6^{2+}$ (M = Co, Ni; L = PyNO, DMSO, H_2O and CH_3CN) and concluded that the spectrochemical series for these ligands is:

$$DMSO < PyNO < H_2O < CH_3CN$$

The nephelauxetic series has the sequence:

$$PyNO < CH_3CN < DMSO < H_2O$$

The sequence of Dq / B is:

$$DMSO < H_2O < PyNO < CH_3CN$$

Pyridine *N*-oxide generally acts as a monodentate ligand. However there are also some reports of it acting as a bridging group. This is observed in the Cu(II) complex $CuCl_2 \cdot 2pyNO$, as shown in Figure 3.3.

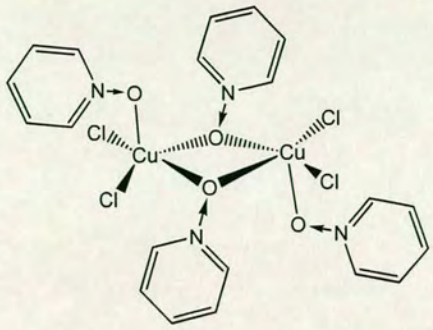

Figure 3.3 Pyridine *N*-oxide acting as a bridging ligand

Due to the oxidising abilities of *N*-oxide ligands, complexes containing metals in their lowest oxidation states are less common, though there are exceptions to this.[2] In some cases the *N*-oxide transfers the oxygen atom to the metal, for example in the preparation of oxo-bridged bimetallic samarium complexes, as shown in Figure 3.4.

$(C_5Me_5)_2Sm(THF)_2$ + pyridine *N*-oxide ⟶ $[(C_5Me_5)_2Sm]_2(\mu\text{-}O)$ + pyridine

Figure 3.4 Preparation of oxo-bridged bimetallic samarium complexes

The oxidising properties of the *N*-oxide ligands are also apparent in the reaction with palladium and platinum in the presence of organic halides, which results in the oxidation of the metal and yields pyridine complexes, as shown in Figure 3.5.

Pt + pyridine *N*-oxide + $CHBr_3$ ⟶ $[Pt(pyridine)_2Br_4]$

Figure 3.5 Metal oxidation by pyridine *N*-oxide

3.2 Attempted Synthesis of Tris(2-Pyridyl-N-Oxide) Tripod Ligands

There are two main approaches that can be taken in forming the ligand. The basic tris(2-pyridyl)methanol framework can be constructed and then the pyridine nitrogen atoms oxidised, or each tripod arm can be formed and then joined together. The initial approach taken was to form the tris(2-pyridyl)methanol framework.

3.2.1 Synthesis of Tris(2-Pyridyl)methanol

Tris(2-pyridyl)methanol, **14**, is a facially capping trinitrogen ligand and was originally reported by Wibaut and co-workers in 1951.[6] They were interested in its analogy with triphenylmethanol. It was first identified as a low yield by-product in the formation of bis(2-pyridyl)ketone, **13**, from the reaction between 2-pyridylmagnesiumiodide and ethylpicolinate.[7] Since then, several other groups have looked at this system and have modified the synthesis.

14 can be made from a number of different starting materials. These are shown in Figure 3.6. 2-Lithiopyridine, **12**, can be made *in situ* by treating 2-bromopyridine with ^{n}BuLi in THF at –78 °C. This step must be carried out at low temperature as **12** decomposes at –30 °C. Furthermore, at higher temperatures, the pyridine ring is susceptible to nucleophilic attack at the α-carbon and lithium reagents can add on to the C=N bond of the pyridine ring.

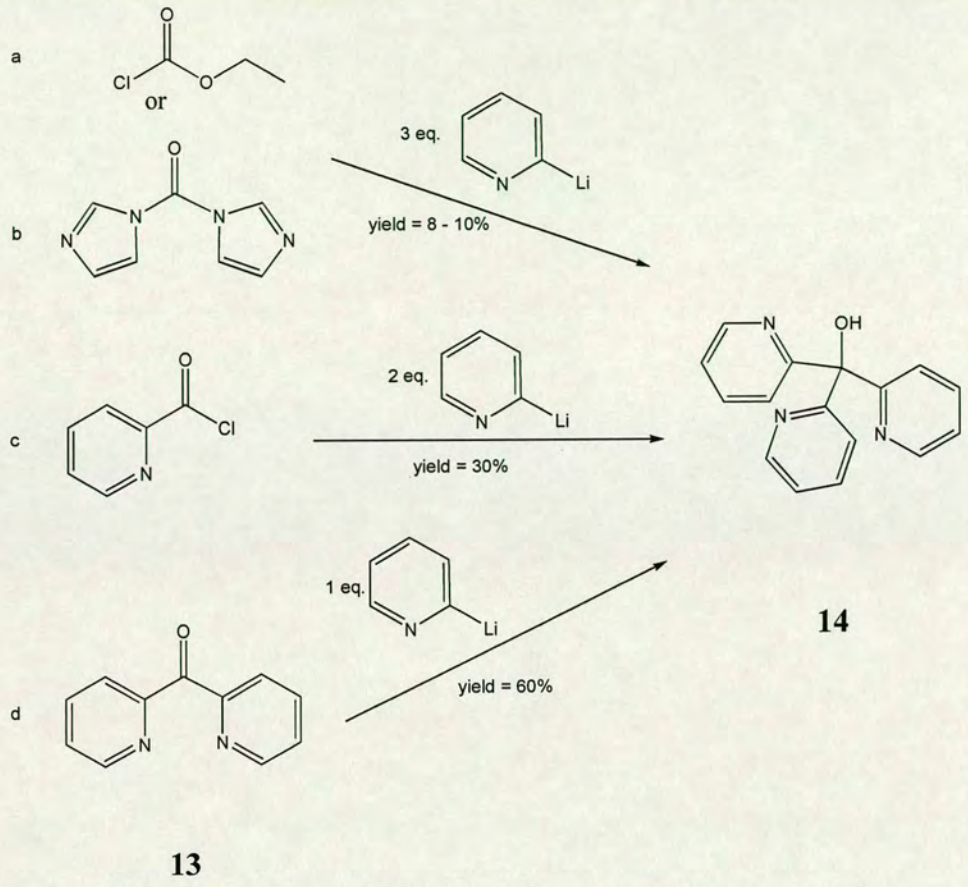

Figure 3.6 Synthesis of Tris(2-pyridyl)methanol

The reaction between three equivalents of 2-lithiopyridine and ethylchloroformate (a) or carbonyldiimidazole (b) occurs only in very low yield (< 10 %). A slightly higher yield (30 %) was obtained from the reaction between 2-lithiopyridine and picolinic acid chloride (c). The most efficient procedure, with a yield of 60 % is the nucleophilic attack of 2-lithiopyridine on **13** (d).

Although the precursor **13** can be synthesised from the nucleophilic attack of **12** on 2-cyanopyridine (f), or on ethylpicolinate (g), as shown in Figure 3.7, it is only obtained in low yield.[8] Fortunately **13** is commercially available, and so this resource intensive step could be avoided.

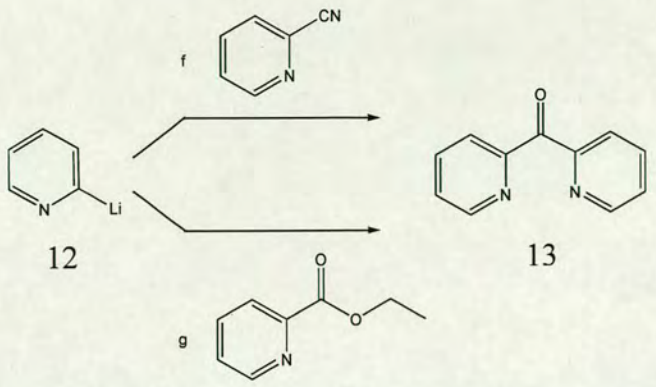

Figure 3.7 Synthesis of Bis(2-pyridyl)ketone

Hannon and Taylor reported a one pot synthesis for symmetrically tri-substituted tris(2-pyridyl)methanol compounds. Treatment of a substituted 2-bromopyridine with ^{n}BuLi and bis(trichloromethyl)carbonate yielded the desired products in moderate yields, (12 – 24 %). This is shown in Figure 3.8, where R = Me, Et, Ph. The yield obtained for the unsubstituted tris(2-pyridyl)methanol following this route is lower than the other methods reported, (16 %).[9]

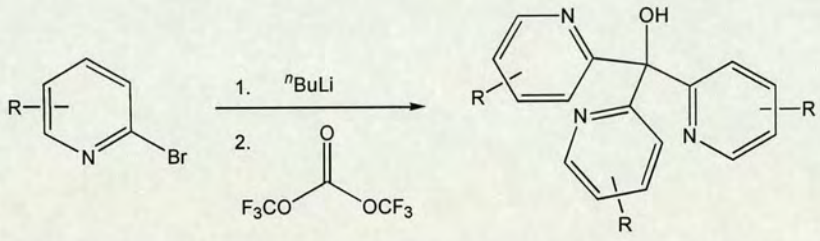

Figure 3.8 Synthesis of substituted tris(2-pyridyl)methanol ligands

The most efficient procedure for the synthesis of **14** is given by Jonas and Stack.[8] This procedure, route d shown in Figure 3.6, was adopted for the work of this thesis. **12** was prepared by lithiating 2-bromopyridine with ^{n}BuLi. A solution of **13** was added to **12** and a nucleophilic addition reaction yields **14**, which can be recrystallised from acetone as white crystalline blocks in 28 % yield.

3.2.2 Oxidation of Pyridine Nitrogen Atoms

Having obtained, **14**, the next stage was to oxidise the pyridine nitrogen atoms. Tertiary amines can be converted to *N*-oxides by oxidation with hydrogen peroxide. However, pyridine and its derivatives require the use of peracids.

Moberg *et al.* reported the *N*-oxidation of **14** as an intermediate in the synthesis of C_3 symmetric tripodal pyridine ligands.[10] **14** was reacted with three equivalents of *m*-chloroperbenzoic acid in chloroform. The resulting tris(*N*-oxide) was obtained in 100 % yield and was subsequently treated with *N,N*-dimethylcarbamoyl chloride and trimethylsilyl cyanide to yield the silyated trinitrile. The nitrile group was then manipulated to introduce a chiral group in this position, giving a C_3 symmetric pyridine ligand, as illustrated in Figure 3.9.

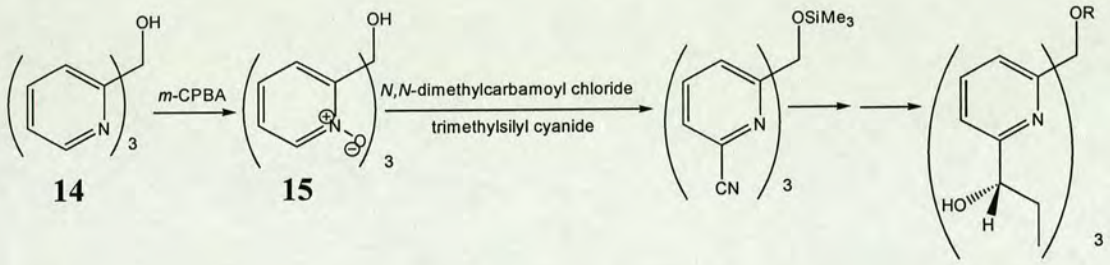

Figure 3.9 Synthesis of a C_3 symmetric pyridine ligand *via* a pyridine *N*-oxide intermediate

The oxidant Moberg *et al.* chose for this reaction was *m*-chloroperbenzoic acid, a convenient general reagent for *N*-oxidation.[11] The reaction can be carried out at room temperature in chloroform. The 3-chlorobenzoic acid formed during the reaction precipitates out and can be removed by filtration, making the work-up much simpler. This reagent was used for the work of this thesis. However, higher yields were obtained when the solvent was changed to DCM. (78 % compared with 60 % in chloroform).

14 was dissolved in DCM and stirred at room temperature in the dark for three days with *m*-chloroperbenzoic acid. After this time, the solution had turned yellow and a

white precipitate had formed. Gaseous ammonia was bubbled through the solution resulting in the formation of more white precipitate, which was identified as the product **15**. The IR showed an intense band at 1261 cm^{-1} that can be ascribed to the stretching of the N-O bond. The FAB+ mass spectrum confirmed the formation of **15**. Peaks could easily be assigned to the sequential loss of three oxygen atoms from the ligand.

3.2.3 Initial Complexation Studies of Tris(2-pyridyl*N*-oxide)methanol

Initial complexation studies were carried out with **15** and some first row transition metals. Ethanol solutions of the metal halide were added to ethanol solutions of **15**. The results are summarized in Table 3.1.

Metal halide	Colour of solution of metal halide in ethanol	Colour of precipitate formed upon addition of ligand
$ZnCl_2$	Colourless	White
$CoCl_2.6H_2O$	Blue	Pink
$FeCl_3$	Dark yellow	Yellow

Table 3.1 Complexation studies with tris(2-pyridyl *N*-oxide)methanol

Mass spectrometry analysis (FAB+) of the pink precipitate formed with Co(II) suggested that a complex had formed, with peaks representing Co(**15**)Cl and Co(**15**).

The most sensitive indication of coordination to metal ions is the shift in the NO stretch in the infrared vibrational spectrum, which has been discussed by Reedijk.[4] Bond formation between the oxygen of the *N*-oxide and the metal ion weakens the N-O bond, causing a smaller force constant and so a lowering of the stretching frequency. This can be seen from the values of the stretching frequencies listed in Table 3.2. The stretching frequency for **15** as a free ligand is at 1243 cm^{-1}. This decreases to 1211 cm^{-1} upon complexation to a cobalt ion. The size of the shift acts as an indication of the bond force between the metal ion and **15**.

Species	ν_{NO} / cm^{-1}
15	1243
Iron **15**	1205
Cobalt **15**	1211
Zinc **15**	1221

Table 3.2 NO stretching frequencies for the free tripodal ligand and Metal(15) species

These values compare favourably with the NO stretching frequencies reported previously for complexes with the monodentate ligand pyridine *N*-oxide, py*N*-O.[12] which are listed in Table 3.3.

Species	ν_{NO} / cm^{-1}
Pyridine*N*-oxide	1228
Fe(py*N*-O)$_6$(ClO_4)$_2$	1220
Co(py*N*-O)$_6$(ClO_4)$_2$	1221
Zn(py*N*-O)$_6$(ClO_4)$_2$	1225

Table 3.3 NO stretching frequencies for the free monodentate ligand and $ML_6(ClO_4)_2$ species

Pyridine *N*-oxides are hygroscopic and so it is not possible to conclusively determine if the central hydroxyl group is free or if it is coordinated to the metal, as any water present in the sample will dominate this region of the infrared spectrum. Unfortunately it was not possible to isolate the complexes in forms suitable for X-ray crystallography analysis and so their absolute structure cannot be determined.

One possibility is that **15** coordinates to the metal through the oxygen atom of the central hydroxyl group and not just through the pyridine *N*-oxide oxygen atoms, as shown in Figure 3.10.

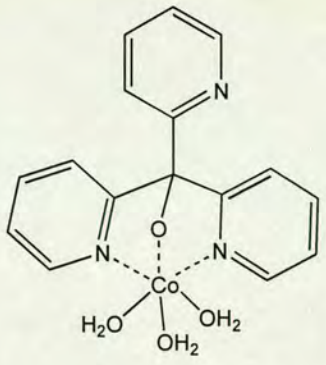

Figure 3.10 Coordination of the alkoxy oxygen in 15

Coordination of the bridgehead hydroxyl group in **15** will be thermodynamically more favourable as it will result in the formation of a six membered chelate ring, which is more stable than the eight membered chelate rings formed if the *N*-oxide oxygen atoms coordinate to the metal. Six membered chelate rings are more stable than eight membered chelate rings as less puckering of the ring is required to form suitable bond angles.

The formation of the six membered chelate ring is favoured entropically over an eight membered chelate ring as less freedom of movement is lost upon the ring closure. This is backed by the observations of White and Faller.[13] They looked at the coordination of **14** to cobalt. The X-ray structure of the Co(III) derivative formed contains each cobalt coordinated by two equivalents of **14**. One ligand is coordinated to the metal through all three pyridine nitrogens, the other ligand coordinates to the metal through two pyridine nitrogens and the alkoxy oxygen.[13]

In order to try and block the central hydroxyl group from coordinating to the metal, it was methylated. This was carried out prior to oxidation of the pyridine nitrogen atoms. The hydroxyl proton in **14** was removed with sodium hydride and then treated with iodomethane to give $(py)_3COMe$, **16**. However, this reaction occurred in low yield and the methoxy oxygen atom is still able to coordinate to metal ions and so a different approach was taken.

The next approach was to remove the central oxygen atom entirely. This was done before the pyridine nitrogen atoms were oxidised. **14** was reacted with thionyl chloride to give the chloromethane ligand, **17**. This was carried out following a modification of the method outlined by White and Faller.[13] It is thought that this reaction proceeds *via* the mechanism illustrated in Figure 3.11.

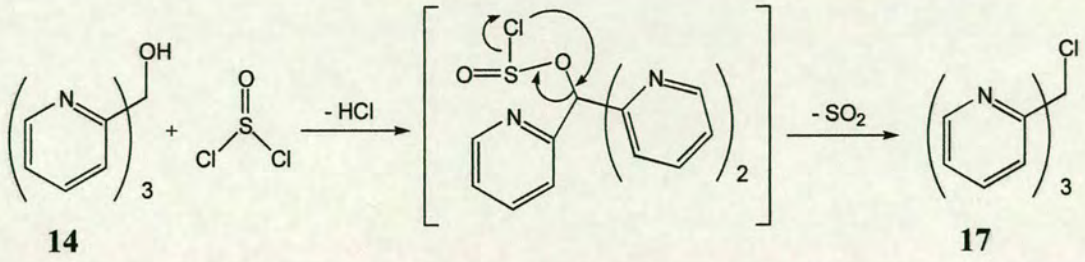

Figure 3.11 Formation of tris(2-pyridyl)chloromethane

Although the synthesis of **17** has been reported, its crystal structure has not, and consequently it has been obtained as shown in Figure 3.12. It is interesting to observe that the free ligand does not have three-fold symmetry in that the three nitrogen lone pairs do not all point in the same direction. There is a slightly distorted tetrahedral geometry at the central carbon atom. The three bonds linking this atom to the three pyridyl rings are approximately equal at 1.5277(19) - 1.533(2) Å, with the bond joining the chlorine atom to the central carbon atom being longer at 1.8155 (14) Å.

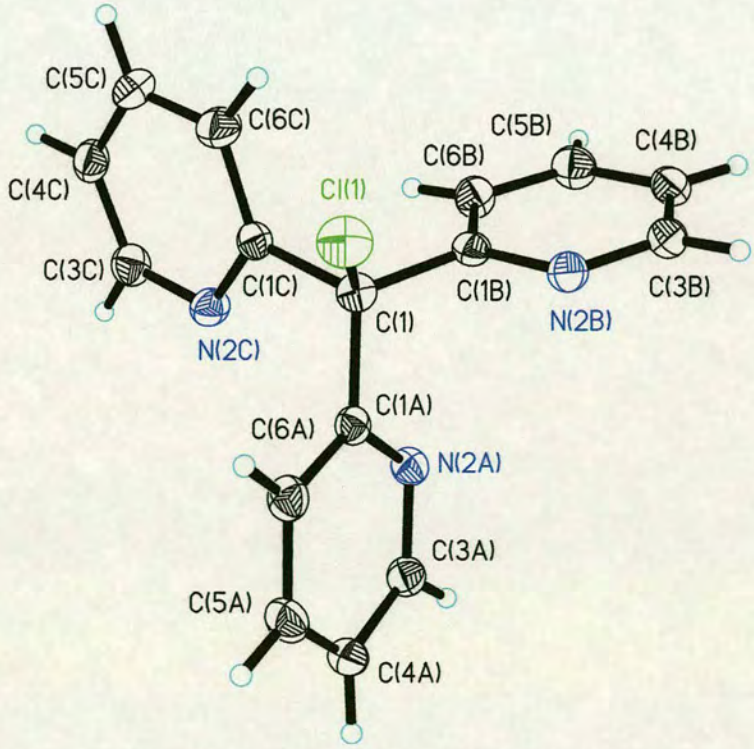

Figure 3.12 X-ray crystal structure of $ClC(C_5H_4N)_3$, 17

Bond	Length / Å
C(1)-C(1A)	1.5277(19)
C(1)-C(1C)	1.5320(19)
C(1)-C(1B)	1.533(2)
C(1)-Cl(1)	1.8155(14)

Angle	Size / °
C(1A)-C(1)-C(1C)	111.18(11)
C(1A)-C(1)-C(1B)	110.07(11)
C(1C)-C(1)-C(1B)	112.52(11)
C(1A)-C(1)-Cl(1)	108.81(9)
C(1C)-C(1)-Cl(1)	106.83(10)
C(1B)-C(1)-Cl(1)	107.23(9)

Table 3.4 Selected bond lengths / Å and angles / ° for 17

The halogen atom can be readily exchanged for lithium by treating **17** with methyl lithium. The reaction was initially carried out at –100 °C, however this was too low a temperature and starting material only was recovered after the work up. Raising the reaction temperature to –78 °C resulted in the formation of the lithiated tripod. Hydrolysis of this lithium reagent gave tris(2-pyridyl)methane, **18**, in which the central carbon atom is now attached to a proton only. This route may also provide a way by which a chiral group could be introduced on to the central atom.

Having ensured the central group had no possibility of coordinating to the metal, the ligand was treated with *m*-chloroperbenzoic acid. Unfortunately, the mass spectra showed that the central carbon atom had been oxidised, as well as the pyridine nitrogen atoms. It is very difficult to get the exact stoichiometry of three equivalents of *m*-chloroperbenzoic acid for every equivalent of tripod as the reagent comes as 57-86 % pure with the remainder as 3-chlorobenzoic acid and water, and is unstable in any purer form.

Despite the moderate yields of **14** reported by Jonas and Stack,[8] only lower yields of around 28 % could be obtained. The low yields, combined with the relatively high cost of **13** led to a new approach to the ligand synthesis being sought.

3.2.4 Synthesis of Tripodal *N*-Oxide Ligand Starting From Pyridine *N*-Oxide

An alternative route to forming **15** is to start with the pyridine nitrogen atoms already oxidized. A patent suggested that the formation of 2-pyridine *N*-oxide carbanion salts was possible by treating pyridine *N*-oxide with a strong base at low temperature.[14] The carbanion salt was then treated *in situ* with elemental sulphur to give 2-pyridinethiol *N*-oxides and related derivatives, which are of industrial importance.

Proton abstraction under basic conditions in heterocyclic *N*-oxides is greatly favoured at the *ortho-* position, the relative rate in pyridine 1-oxide being 2 >> 3 > 4.[2, 15] This is in direct contrast to the non-oxidised parent system, pyridine, where the relative rate is 4 > 3 > 2. The poor reactivity at the *ortho-* position of pyridine has been explained by the destabilisation of the developing carbanion by the lone pair of electrons on the nitrogen. This situation does not occur in *N*-oxides. The reaction proceeds *via* a carbanion intermediate. The reported stability of the alkali metal salts formed by the reaction between pyridine *N*-oxide is probably due to a chelating – directing effect of the oxygen lone pair, as shown in Figure 3.13.

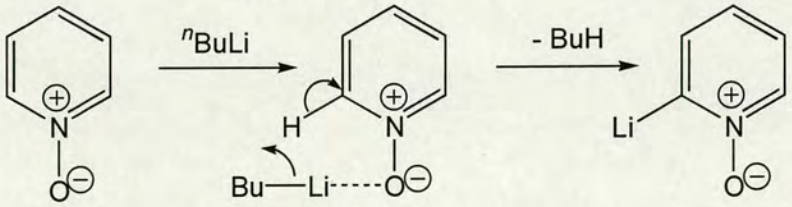

Figure 3.13 Proton abstraction of pyridine *N*-oxides

In the synthesis of the tripodal *N*-oxide ligand, the next step would be to react the carbanion salt, **19**, with diethylcarbonate to give the *N*-oxide tripod, as illustrated in Figure 3.14.

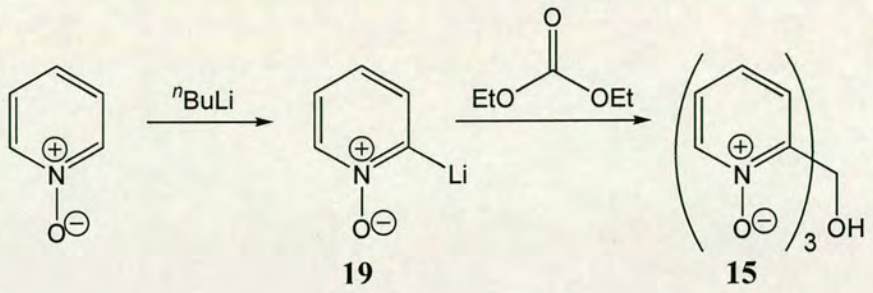

19 **15**

Figure 3.14 Synthesis of 15 starting from pyridine *N*-oxide

Pyridine *N*-oxide is extremely hygroscopic, becoming a liquid within seconds of exposure to the atmosphere, making it very difficult to handle. Pyridine *N*-oxide obtained from Aldrich was dried by azeotropic distillation in toluene using a Dean Stark apparatus set-up and then purified by vacuum sublimation. It was dried under high vacuum for one hour to try and remove all traces of water prior to each experiment.

Initial attempts at preparing **19** and reacting it with diethylcarbonate *in situ* failed. In order to confirm that **19** was actually being formed, the pyridine *N*-oxide was lithiated with one equivalent of ^{n}BuLi in THF at – 78 °C and then treated with one equivalent of an electrophile known to trap metal carbanion salts. Reactions were attempted with trimethylchlorosilane, methyl iodide and benzylbromide but all without success. It is most likely that the pyridine *N*-oxide was still not dry enough and that the lithiation step was not occurring smoothly.

This route was proving even less successful than the previous methodology and so was abandoned at this stage.

3.3 Experimental

3.3.1 Synthesis of Tris(2-pyridyl)carbinol, 14

14 was prepared as described by Jonas and Stack.[8]

A THF solution of 2-bromopyridine (2.50 ml, 4.14 g, 0.0262 mol) was cooled to –78 °C and ^{n}BuLi (2.5 M, 11.0 ml, 0.028 mol) was added slowly to maintain the temperature below –60 °C. A THF solution of bis(2-pyridyl)ketone, **13** (4.52 g, 0.0245 mol) at –78 °C was added slowly to give initially a dark red solution that eventually turned deep blue and finally a dull purple after 1 h. The reaction was quenched with MeOH (25 ml) and warmed to room temperature to give a light orange solution. After the addition of water (50 ml) and 10 % HCl (50 ml) the organic solvents are removed. **14** was extracted with DCM and recrystallised from acetone to yield white crystalline blocks. (1.81 g, 28 %).

^{1}H NMR (250 MHz, $CDCl_3$): δ, 7.20 (dt, J = 1.6, 4.9 Hz, 3H, 5-Hpy), 7.66 (m, 3H, 4-Hpy), 7.72 (m, 3H, 3-Hpy), 8.53 (td, J = 1.4, 5.9 Hz, 3H, 6-Hpy)

^{13}C NMR (62.9 MHz, $CDCl_3$): δ 81.15 (C-OH), 122.21 (3-Cpy), 122.84 (5-Cpy), 136.32 (4-Cpy), 147.71 (6-Cpy), 162.73 (2-Cpy)

IR (KBr disc): 3435, (br); 3045, (w); 1586, (s), 1465, (s); 1431, (s); 1351, (s); 1195, (s); 1116, (s); 1052, (s); 992, (s); 782, (s); 751, (s); 665, (s) cm^{-1}

MS (+ve FAB): *m/z* 264 ($HOCpy_3$), 246 ($HCpy_3$), 185 ($HOCpy_2$), 109 (HOCpy)

M.P. = 125-126 °C

3.3.2 Synthesis of Tris(2-pyridyl*N*-oxide)carbinol, 15

In Chloroform

3-Chloroperbenzoic acid (0.500 g, 2.9 mmol) was added to a well stirred solution of **14** (0.256 g, 0.97 mmol) in chloroform (30 ml). The solution was stirred at room temperature in the dark for four days. After this time, the pale yellow solution was shaken with an excess of 1 M aqueous sodium hydoxide solution, washed with further 1 M sodium hydroxide solution and then with saturated aqueous sodium chloride. The chloride layer became colourless and the aqueous layer turned yellow.

The organic layer was dried over magnesium sulphate, filtered and reduced in volume to yield **15** as a white powder. (0.183 g, 60 %).

In DCM

3-Chloroperbenzoic acid (2.550 g, 15 mmol) was added to a well stirred solution of **14** (0.863 g, 3.3 mmol) in DCM (30 ml). The solution was stirred at room temperature in the dark for four days. Over this time, the solution turned yellow and a white precipitate formed. More DCM was added (20 ml). Gaseous ammonia was bubbled through the well stirred solution for five minutes during which time more white precipitate formed. The yellow solution was filtered and the solid was washed several times with DCM. The filtrate was dried over magnesium sulphate, filtered and concentrated *in vacuo* to yield **15** as a yellow crystalline material. (0.8 g, 78 %).

^{1}H NMR (250 MHz, $CDCl_3$): δ 7.27 (m, 5-Hpy), 7.34 (dd, J = 2.1, 8.0 Hz, 3H, 4-Hpy), 7.51 (ddd, J = 0.4, 2.3, 8.0 Hz, 3H, 3-Hpy), 8.12 (ddd, J = 0.5, 1.8, 6.7 Hz, 3H, 6-Hpy)

^{13}C NMR (62.9 MHz, $CDCl_3$): δ 77.92 (C-OH), 125.17 (3-Cpy), 126.22 (5-Cpy), 127.18 (4-py), 139.95 (6-Cpy), 147.42 (2-Cpy)

MS (+ve FAB): *m/z* 312 (M+1), 296 ((M+1)-O), 280 ((M+1)-O)

IR (KBr disc): 3397 (br); 1607 (m), ν(CN); 1563 (m); 1485 (s); 1428 (s); 1291(s); 1243 (s), ν(NO); 1184(s); 1039, m, ν(C-O); 836 (s), 766 (s) cm^{-1}

3.3.3 Metal Complexation

3.3.3.1 With $CoCl_2$

15 (0.1 g, 0.32 mmol) was dissolved in ethanol (10 ml) to give a pale yellow solution. To this was added a bright blue ethanolic solution of Co(II) chloride (0.077 g, 0.32 mmol). Upon mixing, the solution turned green and a green solid formed. This was filtered and redissolved in methanol. After 2 days at –30 °C, the solution had turned pale pink over a bright pink solid. The pink solid was isolated by filtration and characterised. (0.12 g, 82 %).

MS (+ve FAB): *m/z* 405 (HOC(py*N*-O)$_3$CoCl), 369 (HOCpy*N*-O$_2$)$_3$Co

IR (KBr disc): ν_{max} 3332, (br); 1630, (m), ν(CN); 1485, (s); 1433, (s); 1289, (m); 1211, (s); 1173, (s); 1041, (m), ν(C-O); 930, (w); 848, (s); 831, (s); 781, (s), cm^{-1}

3.3.3.2 With $FeCl_3$

15 (0.1 g, 0.32 mmol) was dissolved in ethanol (10 ml) to give a pale yellow solution. To this was added an orange ethanolic solution of Fe(III) chloride (0.052 g, 0.33 mmol). Upon mixing, a bright yellow solid formed. This was isolated by filtration.

IR (KBr disc): ν_{max} 3398, (br); 2360, (m); 2341, (m); 1623, (m), ν(CN); 1485, (s); 1435, (s); 1287, (m); 1205, (s); 1174, (m); 1037, (m), ν(C-O); 850, (m); 832, (s); 774, (s); cm^{-1}

3.3.3.3 With $ZnCl_2$

15 (0.109 g, 0.35 mmol) was dissolved in ethanol (10 ml) to give a pale yellow solution. To this was added an ethanolic solution of anhydrous zinc chloride (0.048 g, 0.35 mmol). Upon mixing, a white solid formed immediately. This was filtered and recrystallisation attempted without success. (0.11 g, 76 %).

^{1}H NMR (200 MHz, $CDCl_3$): δ, 7.43 (m, 3H, 5-Hpy), 7.52 (m, 6H, 3,4-Hpy), 8.27 (m, 3H, 6-Hpy), 10.48 (C-OH)

IR (KBr disc): ν_{max} 3328, (br); 1632, (m); 1485, (m); 1433, (m), ν(CN); 1287, (m); 1221, (s); 1175, (m); 1040, (m), ν(C-O); 930, (w); 849, (m); 830, (s); 782, (s); cm^{-1}

3.3.4 Preparation of Tris(2-pyridyl)methoxymethane, 16

A solution of **14** (0.198 g, 0.75 mmol) was added slowly to a suspension of sodium hydride (0.072 g, 3.0 mmol) in THF at room temperature. Iodomethane (0.05 ml, 0.75 mmol) was added slowly and the cloudy white solution stirred at room temperature for 1.5 h. After this time, the reaction was quenched with a 1 : 1 mixture of acetone and 2- propanol. Water was added until the solution had turned clear. The

organic solvents were removed *in vacuo*. The product was extracted with DCM and recrystallised from acetone to give a white crystalline solid.

^{1}H NMR (200 MHz, $CDCl_3$): δ 3.74 (s, 3H, C-OMe), 7.16 (m, 3H, 5-Hpy), 7.62 (m, 6H, 3,4-Hpy), 8.47 (d, J = 3.9 Hz, 3H, 6-Hpy)

3.3.5 Preparation of tris(2-pyridyl)chloromethane, 17

A solution of **14** (1.266 g, 4.8 mmol) in THF (35 ml) was added slowly *via* an addition funnel to a rapidly stirred suspension of sodium hydride (0.144 g, 6.0 mmol) in THF (10 ml) resulting in the formation of a beige solution. Thionyl chloride (0.713 g, 6.0 mmol) in THF (5 ml) was added slowly to the beige solution. This was then stirred at room temperature for 2 h. During this time, the solution became a brighter yellow colour. The reaction mixture was quenched with a saturated solution of sodium hydrogen carbonate (17 ml). The two layers were separated. The organic solvent was removed *in vacuo* to yield a beige solid. The aqueous layer was washed with DCM (x 3) and the DCM washings used to redissolve the organic residue. This solution was washed with 1 M sodium hydrogen carbonate and saturated sodium chloride solution. The clear yellow solution was dried over sodium sulphate and filtered. The solvent was removed *in vacuo* to yield the product as a beige solid that could be recrystallised from acetone to give large colourless plate shaped crystals. (0.44 g, 32 %).

M.P. = 162 – 164 °C

^{1}H NMR (250 MHz, $CDCl_3$): 7.19 (ddd, 3H, py5-H, $J_{5,4}$ = 4.8, $J_{5,3}$ = 1.2, $J_{5,6}$ = 1.4 Hz), 7.50 (dt, 3H, py3-H, $J_{3,4}$ = 8.1, $J_{3,6}$ = 1.1 Hz), 7.67 (td, 3H, py4-H, $J_{4,6}$ = 1.9, $J_{3,5}$ = 7.5 Hz), 8.57 (ddd, 3H, py6-H, $J_{6,5}$ = 7.4, $J_{6,4}$ = 1.4, $J_{6,3}$ = 1.0 Hz)

^{13}C NMR (62.9 MHz, $CDCl_3$): δ 79.83 (C-OH), 122.27 (3-Cpy), 123.87 (5-Cpy), 136.19 (4-Cpy), 148.46 (6-Cpy), 161.31 (2-Cpy)

MS (+ve FAB): *m/z* 282 ($ClCpy_3$), 246 ($HCpy_3$), 91 (Cpy)

Crystal Data for **17**

Data were collected using Mo-Kα radiation on a colourless block of dimensions 1.5 x 1.0 x 0.5 mm on a Stoe Stadi4 diffractometer in the range $2.23 \leq 2\theta \leq 28.86^{\circ}$ using the ω-θ method. Of a total of 7923 reflections collected, 3115 (R_{int} = 0.0263) were independent. The structure was solved by direct methods (SHELXS-97). Hydrogen atoms were placed using a difference map and freely refined. The final difference-map extrema were 0.229 and –0.523 e $Å^{-3}$ with a final *R* of 0.0434 for 2589 parameters.

Empirical formula	$C_{16}H_{12}ClN_3$	γ / °	90
Formula weight	281.74	Volume / $Å^3$	1299.83 (15)
Crystal system	Monoclinic	Z	4
Space group	P2(1)/c	Temperature / K	150(2)
a/ Å	9.1895 (6)	Wavelength / Å	1.54178
b / Å	9.0650 (6)	Density calc. / Mg/m^3	1.440
c / Å	15.6957 (10)	μ(Mo-Kα) / mm^{-1}	0.286
α / Å	90	R_1 [$F>4\sigma(F)$]	0.0434
β / Å	96.2070 (10)	WR_2 (all data)	0.1121

Table 5 Crystallographic data for 17

3.3.6 Preparation of Tris(2-pyridyl)methane

A solution of **17** (0.296 g, 0.001 mol) in THF (20 ml) was cooled to – 78 °C. MeLi (1.66 M, 0.7 ml, 0.001 mol) was added slowly. The colourless solution turned yellow immediately and deepened to a bright orange. The solution was stirred at – 78 °C for 20 minutes with no further change in colour. The solution was allowed to warm to room temperature, during which time the solution turned a darker red colour and a precipitate formed. The reaction was quenched by the addition of water (3 ml) in THF (15 ml). The precipitate redissolved and solution turned yellow. The product was extracted into DCM and the solvent removed to yield a beige solid. (0.182 g, 72 %).

^{1}H NMR (200 MHz, $CDCl_3$): δ 5.96 (s, 1H, C<u>H</u>), 7.09 (ddd, 3H, py5-<u>H</u>, $J_{4,5}$ = 7.8, $J_{4,3}$ = 2.0, $J_{4,6}$ = 1.37 Hz), 7.27 (dd, 3H, py3-<u>H</u>, $J_{3,4}$ = 2 Hz), 7.58 (td, 3H, py4-<u>H</u>, $J_{4,5}$ = 7.8, $J_{3,4}$ = 2.0 Hz) 8.53 (dd, 3H, py6-<u>H</u>, $J_{5,6}$ = 4.3, $J_{4,6}$ = 1.37 Hz)

3.3.7 Attempted Preparation of Tris(2-pyridyl*N*-oxide)methane,

3-Chloroperbenzoic acid (3.371 g, 20 mmol) was added to a well stirred solution of **18** (1.068 g, 4.3 mmol) in DCM (30 ml). The solution was stirred at room temperature in the dark for four days. Over this time, the solution turned yellow and a white precipitate formed. More DCM was added (20 ml). Gaseous ammonia was bubbled through the well stirred solution for five minutes during which time more white precipitate formed. The yellow solution was filtered and the solid was washed several times with DCM. The filtrate was dried over magnesium sulphate, filtered and concentrated *in vacuo* to yield the product as a yellow crystalline material.

IR (KBr disc): ν_{max} 3042 (m), 1483 (s), 1428 (s), 1286 (s), 1258 (s), 1239 (s), 1181 (s), 1040 (s), 930 (s) cm^{-1}
MS (+ve FAB): *m/z* 312 (M^+ + 16), 296 (M^+ + 1)

3.3.8 Attempted Preparation of 15, Starting From Pyridine*N*-oxide

Pyridine*N*-oxide, (1.12 g, 0.012 mol) was placed in a Schlenk tube and dissolved in THF (40 ml). ^{n}BuLi (1.6 M, 9.4 ml, 0.015 ml) was added to the solution slowly at -78 °C, with vigorous stirring. The pale yellow solution turned orange and then dark red. After stirring at low temperature for 30 minutes, diethylcarbonate (0.46 g, 0.004 mol) was added slowly with further stirring. The solution was stirred and allowed to warm to room temperature over an hour. The reaction mixture was quenched with methanol (20 ml), followed by 10 % HCl (10 ml) and water (20 ml). The organic layer was separated and the aqueous layer extracted with diethyl ether (20 ml x 3). The combined aqueous layers were dried over $MgSO_4$, filtered and the solvent removed *in vacuo* to yield a dark residue.

IR (KBr disc) showed that the *N*-oxide group was no longer present.

3.3.9 Attempt to Confirm Formation of 2-Lithiopyridine*N*-oxide

3.3.9.1 Reaction with Benzylbromide

Pyridine*N*-oxide, (1.12 g, 0.012 mol) was placed in a Schlenk tube and dissolved in THF (40 ml). ^{n}BuLi (1.6 M, 9.4 ml, 0.015 ml) was added to the solution slowly at -78 °C, with vigorous stirring. The pale yellow solution turned orange and then dark red. After stirring at low temperature for 30 minutes, benzyl bromide (1.46 ml, 0.012 mol) was added slowly during which time, evolution of a gas was observed. The solution was stirred and allowed to warm to room temperature over an hour. The reaction mixture was quenched with methanol (20 ml), followed by 10 % HCl (10 ml) and water (20 ml). The organic layer was separated and the aqueous layer extracted with diethyl ether (20 ml x 3). The combined aqueous layers were dried over $MgSO_4$, filtered and the solvent removed *in vacuo* to yield a dark orange oil.

^{1}H NMR ($CDCl_3$) showed that the benzyl bromide had remained unreacted.

3.3.9.2 Reaction with Trimethylchlorosilane

The reaction was carried out as described above, using trimethylchlorosilane (1.50 ml, 0.012 mol) in place of benzyl bromide.

IR (KBr disc) showed that the *N*-oxide group was no longer present.

3.3.9.3 Reaction with Methyl Iodide

Pyridine*N*-oxide, (1.12 g, 0.012 mol) was placed in a Schlenk tube and dissolved in THF (40 ml). ^{n}BuLi (1.6 M, 9.4 ml, 0.015 ml) was added to the solution slowly at -78 °C, with vigorous stirring. The pale yellow solution turned orange and then dark red. After stirring at low temperature for 30 minutes, methyl iodide (0.73 ml, 0.012 mol) was added slowly, during which time, evolution of a gas was observed. The solution was stirred and allowed to warm to room temperature over an hour. The reaction mixture was quenched with ammonium chloride (0.63 g, 0.012 mol). After stirring at room temperature for 30 minutes, the mixture was reduced in volume to

yield a dark orange oily residue. This was extracted into DCM and dried over $MgSO_4$. The solution was filtered and the solvent removed *in vacuo* to yield a bright orange oil.

IR (DCM thin film) showed that the *N*-oxide group was no longer present.

3.4 References

1. A. R. Katritzky and J. M. Lagowski, *Chemistry of the Heterocyclic N-Oxides*.Vol. 19. 1971, London and New York, Academic Press

2. A. Albini and S. Pietra, *Heterocyclic N-Oxides*. 1991, Boca Raton, CRC Press

3. P. L. Goggin, ed. *Sulfoxides, Amides, Amine Oxides and Related Ligands*. Comprehensive Coordination Chemistry, ed. J. A. McCleverty. Vol. 2. 1987

4. J. Reedijk, *Recl. Trav. Chim. Pays-Bas*, 1969, **88**, 499

5. J. V. Quagliano, J. Fujita, G. Franz, D. J. Philips, J. A. Walmsley and S. Y. Tyree, *J. Am. Chem. Soc.*, 1961, **83**, 3770

6. J. P. Wibaut, A. P. De Jonge, H. G. P. Van der Voort and P. P. H. L. Otto, *Recl. Trav. Chim. Pays-Bas*, 1951, **70**, 1054

7. A. P. De Jonge, H. J. den Hertog and J. P. Wibaut, *Recl. Trav. Chim. Pays-Bas*, 1951, **70**, 989

8. R. Jonas and T. D. P. Stack, *Inorg. Chem.*, 1998, **37**, 6615

9. M. J. Hannon, P. C. Mayers and P. C. Taylor, *Tetrahedron Letters*, 1998, **39**, 8509

10. H. Adolfsson, K. Wärnmark and C. Moberg, *J. Chem. Soc., Chem. Commun.*, 1992, 1054

11. J. H. Markgraf and C. G. Carson, *J. Org. Chem.*, 1964, **29**, 2806

12. R. G. Garvey, J. H. Nelson and R. O. Ragsdale, *Coord. Chem. Rev.*, 1968, **3**, 375

13. D. L. White and J. W. Faller, *Inorg. Chem.*, 1982, **21**, 3119

14. R. A. Damico, U.S. patent 3700676, 1972

15. R. A. Abramovitch, M. Saha, E. M. Smith and R. T. Coutts, *J. Am. Chem. Soc.*, 1967, **89**, 1537

4 Benzimidazole Ligands

This chapter is concerned with the synthesis and characterisation of a new benzimidazole-containing tripodal ligand.

4.1 Rationale for Choosing Ligand System

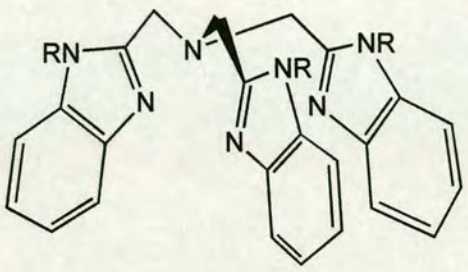

Figure 4.1 NTB

The ligand is based on tris(benzimidazole)methylamine, NTB, shown in Figure 4.1, studied by Thompson in the late 1970s.[1] It consists of three benzimidazole rings attached to a central nitrogen atom *via* methylene groups. The ligand is relatively flexible due to the sp^3 linker groups.

There are two linker atoms between the central amine nitrogen atom and the three donor atoms. Provided that the ligand acts in a tridentate fashion and the central nitrogen atom remains non-coordinating, eight membered chelate rings will form upon complexation to a metal. The ligand metal geometry will twist to reduce the strain associated with the rings, as described in Section 1.3.3, resulting in a complex of C_3 symmetry overall. In order to favour this form of coordination, the ligand has been designed with the central nitrogen atom alkylated so as to block the lone pair from coordinating to the metal. This is illustrated in Figure 4.2.

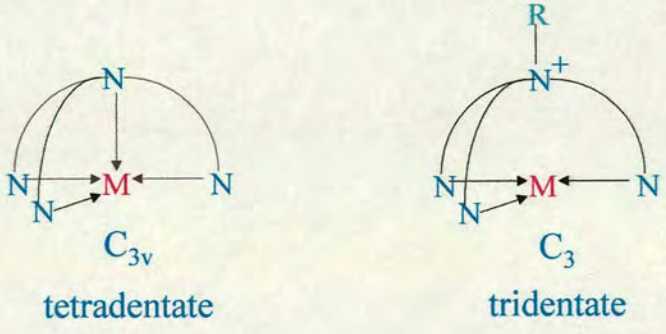

Figure 4.2 Diagram illustrating the control of symmetry by the design of the bridgehead

Imidazole rings contain both an amine and an imine nitrogen atom, making them interesting donor ligands. The ring is aromatic due to delocalisation of the lone pair from the amine nitrogen atom into the ring. Imidazoles have a $pK_a = 7.0$ and so are more basic than the isomeric pyrazole systems studied by Trofimenko that have a $pK_a = 2.5$.[2] This relative basicity is due to the formation of symmetrical resonance stabilised cations, as illustrated in Figure 4.3.

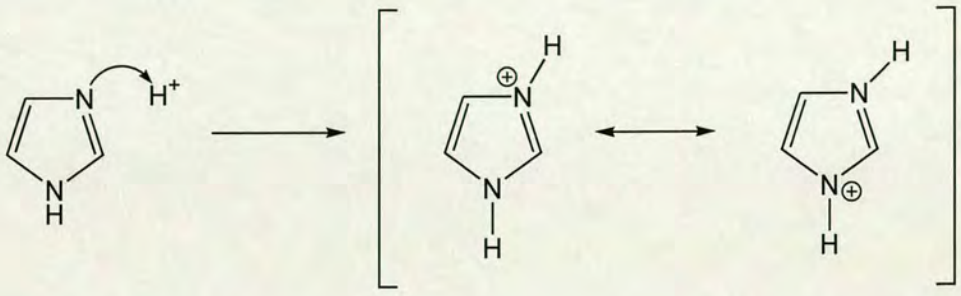

Figure 4.3 Illustration of resonance stabilised imidazole cations.

The advantage of using large planar aromatic benzimidazole groups is that they should provide the complexes with a pronounced propeller shaped geometry. This should efficiently transmit the chirality of the complex to the substrate binding site and so lead to a large energy difference between the diastereotopic transition states in a catalytic cycle. The donor atoms form part of the planar aromatic rings and so the transmission of chirality should be more effective for the benzimidazole ligands compared to those discussed in other Chapters.

Methylation of the heterocyclic amine nitrogen atoms will allow the electronic properties of the ligand to be finely controlled. No methylation of the central nitrogen atom will allow the ligand to be used as a neutral donor. Successive methylations result in the formation of a tri-, di-, or mono- anionic ligand, making this an extremely versatile ligand system.

4.2 Work Already Carried Out on Related Systems

4.2.1 Imidazole Ligands

The complexation of tripodal ligands, incorporating imidazole units, to transition metals has been well studied, in particular as models for the active site of metalloproteins. The enzyme carbonic anhydrase is used to catalyse the interconversion of CO_2 and HCO_3^-. X-ray crystallographic studies have shown the active site to consist of a tetrahedral Zn^{2+} ion coordinated by three histidine imidazoles and a H_2O or OH^- group.[3] Blue copper proteins contain a cupredoxin copper site coordinated by four amino acid residue ligands, two of which are known to be histidinyl-imidazoles.[4]

Breslow has investigated two isomeric tripodal tris-imidazole ligands, tris(2-imidazolyl)carbinol (2-TIC) and tris(4(5)-imidazolyl)carbinol (4-TIC).[5] The structure of these ligands is shown in Figure 4.4.

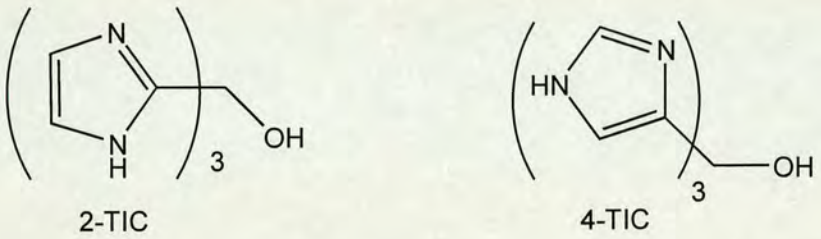

Figure 4.4 diagram of 2-TIC and 4-TIC

Both ligands are tridentate and co-ordinate to Zn^{2+}, Co^{2+} and Ni^{2+} through all three imidazole rings. The three imidazole rings are held in close proximity, which promotes an octahedral geometry. This results in the Zn^{2+} complex being relatively strained. The N-Zn^{2+}-N angles are about 95°. This is reflected in the way all three metals readily bind a second ligand to form an octahedral geometry. It is proposed that the second equivalent of ligand may coordinate through the hydroxyl group. In order to remove this ambiguity, Breslow investigated the reductive removal of the central hydroxyl group.[6] Several different methodologies were developed, the most successful being the use of lithium aluminium hydride and titanium trichloride to

reduce the *N*-ethoxymethyl protected 2-TIC and 4-TIC followed by a deprotection step to yield the new ligands 2-TIM and 4-TIM respectively, as shown in Figure 4.5.

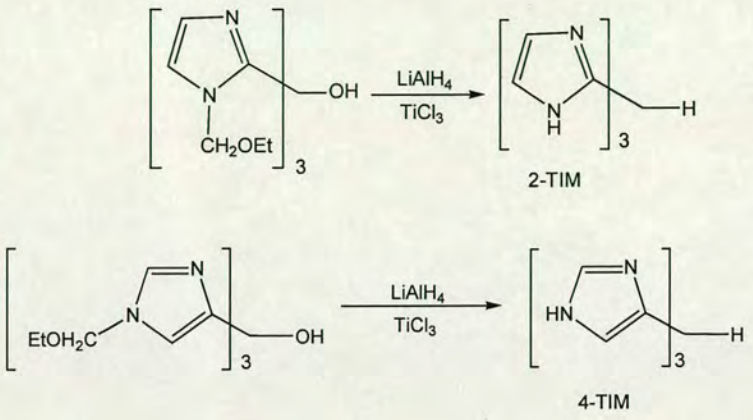

Figure 4.5 Formation of 2-TIM and 4-TIM

4-TIC is more basic and a stronger metal complexing agent compared with 2-TIC. One explanation proposed for this is that of charge separation. In the 2-isomer, the nitrogen atoms are much closer together than for the 4-isomer and protonation leads to strong electrostatic repulsion, to the extent that the third protonation cannot be detected. In comparison, in the 4-isomer, the positive charge is shared with a nitrogen atom that is further from the other rings. The same explanation can be invoked for the metal binding constants as complexation induces positive charge on both the coordinated and the non-coordinated nitrogen atoms.

Brown and Huguet have carried out a lot of work on synthesizing tripod ligands containing imidazole units to model the active site of carbonic anhydrase.[3, 7, 8] They have investigated the effect of methylating the amine nitrogen to give L_a shown in Figure 4.6, and found that N-methylation reduces the metal binding ability of the ligands by some 3-4 pK units. It is proposed that this is due to the better solvation of the non-methylated derivatives when bound to the metal.[8]

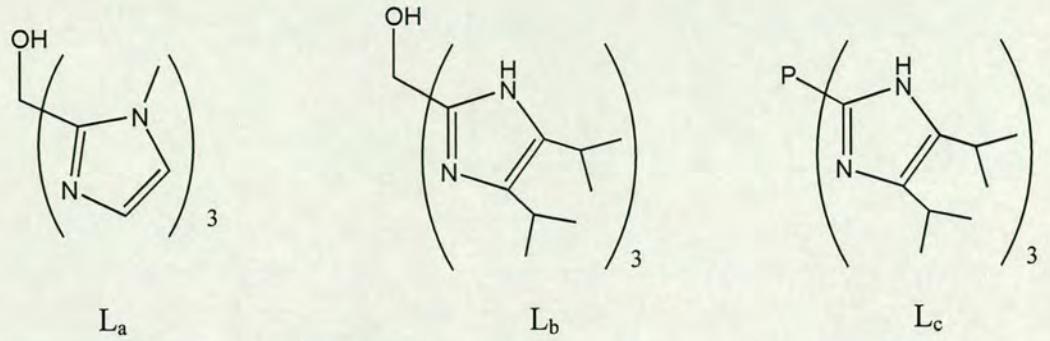

L_a L_b L_c

Figure 4.6 Imidazole tripod ligands studied by Brown and Huguet

Introducing sterically bulky groups at the 4 and 5 ring positions of tris(2-imidazole) ligands, to give L_b, shown in Figure 4.6, hinders the formation of 2:1 $L:Zn^{2+}$ complexes.[8] Measurements of the stability constants indicate that there is no second binding constant for 4,5-diisopropyl substituents. However, the carbinol system is quite unstable under basic conditions when coordinated to the metal. The substituted ligands tend to dehydrate to form highly coloured materials, probably due to the formation of extensive conjugated systems such as in the fulvene-like system shown in Figure 4.7.[8]

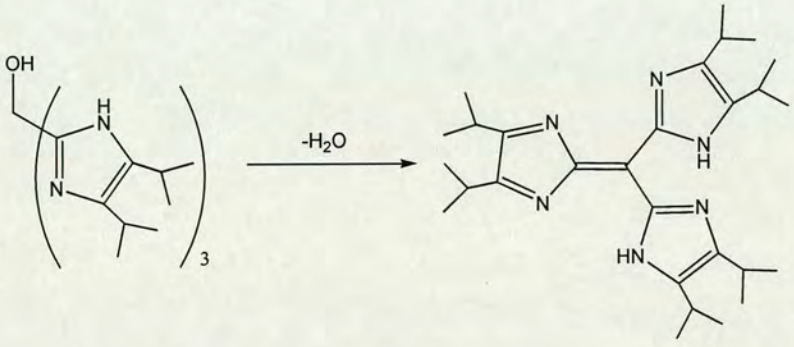

Figure 4.7 Dehydration of substituted imidazolyl ligands

In order to circumvent the problems of dehydration of the substituted ligands and the complex strain problems, Brown's group turned to the corresponding phosphine system, in which a phosphorus atom replaces the central carbon atom (Figure 4.6, L_c).[7] The P-C bond is longer than the HOC-C bond length (approximately 1.8 Å c.f. 1.5 Å), resulting in the imidazole rings being further apart and more suited for

coordination to a tetrahedral Zn^{2+}. This is reflected in the higher binding constant of the ligand to Zn^{2+} than to Co^{2+}. The X-ray crystal structure of the ligand coordinated to Zn^{2+} was obtained and shows the Zn^{2+} to adopt a distorted tetrahedral geometry.

Extending the imidazole rings out from the central phosphorus by incorporating methylene linker groups developed this system further to give ligands L_d and L_e.[3]

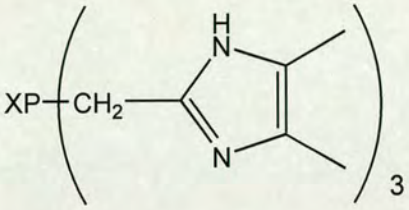

L_d X = lone pair
L_e X = O

Figure 4.8 Extended tris(imidazole)phosphine ligands

It was hoped that this ligand design would lead to an improved metal – ligand binding ability. Although the $pK_{Zn^{2+}}$ and $pK_{Co^{2+}}$ values are larger with L_e, there is no noticeable structural change. This has been attributed to an unfavourable interaction between the O-P dipole and the bound M^{2+} ion, which is illustrated in Figure 4.9.

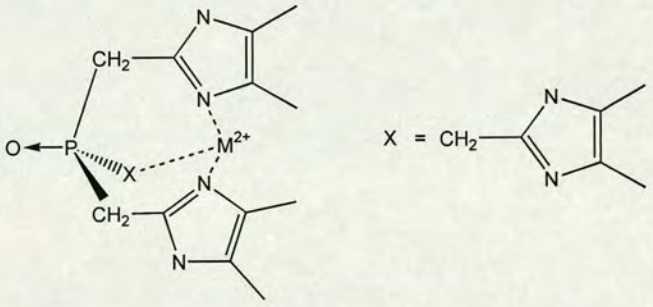

Figure 4.9 Interaction between the O-P dipole and the bound M^{2+} ion

The unoxidised phosphine ligand L_d proved too air sensitive to be isolated. Furthermore, zinc complexes formed with the phosphorus bridgehead systems were not stable for prolonged periods and underwent P-C cleavage to produce bis(imidazolyl)phosphinic acid·Zn^{2+} complexes, as illustrated in Figure 4.10.[9]

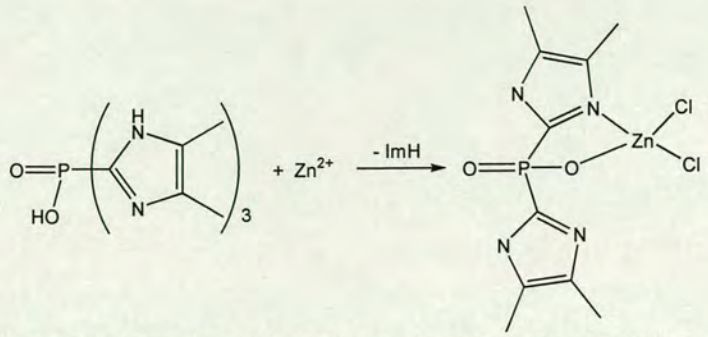

Figure 4.10 Decomposition of Zinc·Imidazoyl complexes

The lack of stability of these ligands renders them deficient as models for carbonic anhydrase. Brown *et al.* went on to investigate the synthesis of symmetric ligands with a CH_2 unit inserted between the imidazole unit and the central atom.[10] Tris(imidazolylmethyl)acetonitriles could be made by three sequential alkylations of acetonitrile using three equivalents of a N-protected 2- or 5- (chloromethyl)imidazole and a strong non-nucleophilic base such as LDA, as illustrated in Figure 4.11. Unfortunately the yields of these reactions were very low.

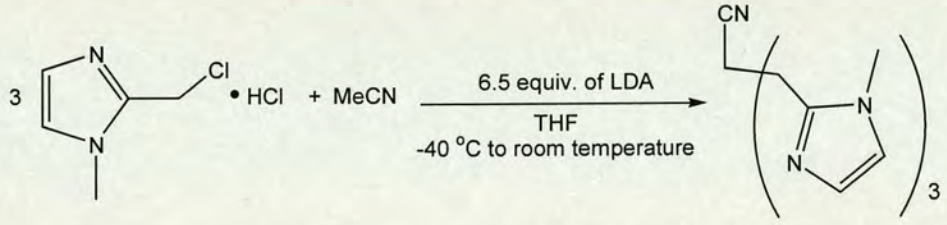

Figure 4.11 Formation of tris(imidazolylmethyl)acetonitriles

4.2.2 Benzimidazole Ligands

The synthesis and characterisation of a trisbenzimidazole derivative – tris(2-benzimidazolylmethyl)amine (NTB) was first reported by Thompson *et al.* in 1977.[1] NTB is the first example of a tetradentate tripod ligand involving three coordinating benzimidazole groups. It consists of three benzimidazole groups attached to a central nitrogen atom *via* a methylene linking group. NTB can be synthesised *via* the direct fusion of *o*-phenylenediamine with either trinitrilotriacetic acid, $N(CH_2CO_2H)_3$, or with nitrilotriacetonitrile, $N(CH_2CN)_3$, at high temperatures, followed by recrystallisation from methanol.

In the solid state, the free ligand possesses C_3 symmetry with the three benzimidazole arms lying on the same side, as illustrated in Figure 4.12 and Figure 4.13.

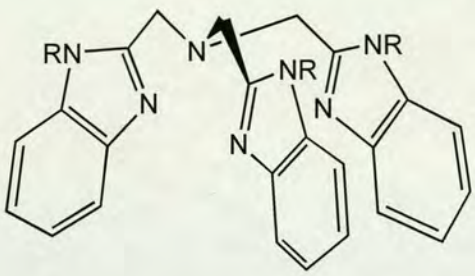

Figure 4.12 NTB *endo* conformation

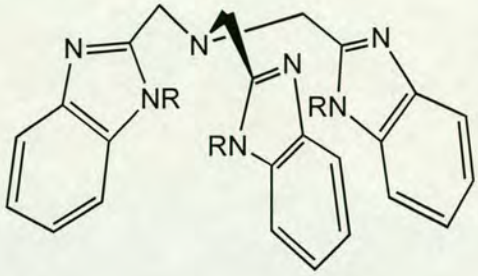

Figure 4.13 NTB *exo* conformation

The NMR spectrum of the ligand indicates that there is a single set of proton signals at room temperature. It was originally proposed that this is due to a plane of symmetry that bisects each imidazole unit.[1] This suggests that the imidazole ring proton is delocalised equally along the N-C-N framework. Su *et al.* have recently attributed this to the ligand existing in two conformations at room temperature,[11] – the endo conformation in which the three imine nitrogen atoms point inward at the lone pair of the apical tertiary nitrogen atom, as illustrated in Figure 4.12 or the exo conformation in which the three imine nitrogen atoms point outwards, as shown in Figure 4.13. Interconversion of the two conformations can take place through the rotation of the three benzimidazole arms about the respective N_{apical}-C bonds and / or through the inversion of the tetrahedral tertiary amine. Both of these represent low energy processes so interconversion would be facile at room temperature.

The ligand is stable in air and melts at 270 °C. It is stable in concentrated acid – heating with conc. HCl under reflux caused no degradation but simply formed the hydrochloride salt. The free ligand could be regenerated upon treatment with base. There is a strong association that exists between alcohols and NTB. A 1:3 solvate is formed upon recrystallisation from alcoholic solvents that requires prolonged drying under vacuum to desolvate.

Thompson *et al.* have studied the co-ordination chemistry of NTB with a variety of Co(II) and Zn(II) salts and obtained complexes that contain mixed stereochemistries.[1] Complexes of the general formula [M(NTB)X]X (M=Co; X=Cl, Br, NCS, NO_3 and ClO_4); [M(NTB)X]BPh_4 (M = Co; X = Cl, Br, NCS, NO_3, ClO_4; M = Zn; X = Cl, Br, I, NCS) and [M(NTB)X]$_2$[MX_4] (M = Co, Zn; X = Cl, Br, NCS) have been made and characterised. The first two classes consist of a pseudo-trigonal bipyramidal cation in which the NTB ligand acts as a tetradentate ligand. In the first class, the negative anion is capable of coordination that may help stabilise the cation. Tetraphenylborate is a relatively non-coordinating anion but is known for its ability to stabilise five-coordinate cations. The magnetic data indicate that these complexes are high spin, which is typical of systems of this type with hard donor atoms. The magnetic moments for the five co-ordinate tetraphenylborate derivatives fall in the range 4.3-4.7 BM, which is comparable with moments for typical trigonal bipyramidal systems with tripod ligands containing N, O, S, P donor atoms which lie in the range 4.4-4.7 BM. The latter class of compounds are metal complexes with mixed stereochemistry – containing two five coordinate, pseudo trigonal bipyramidal cations and a four coordinate, tetrahedral anion.

The electrical conductances of these complexes are somewhat lower than expected. This has been attributed to ionic association occurring in solution. This would lead to the formation of large bulky ions with low ion mobility. One possible associative mechanism could involve pseudo-hydrogen bonding of an axial halogen (or pseudo halogen) on one ion with one of the three imidazole hydrogen atoms on another. The NMR spectra of the zinc complexes indicate that one of the aromatic protons is shifted significantly downfield upon coordination to the metal. This significant downshield shift corresponds to a marked deshielding of one ring proton with respect to the others.

Vahrenkamp *et al.* have synthesised *N*-R-substituted NTB based ligands where R = H, Me, and Bz and looked at their complexation with various zinc salts.[12] Crystal structures were obtained for the more hindered complexes [L_bZnCl][pyZnCl_3] and

$[L_cZnONO_2]NO_3$ and show that the [LZnX] cations have a coordination geometry intermediate between tetrahedral and trigonal-bipyramidal in these structures.

Su *et al.* have looked at the coordination of NTB based ligands to copper salts.[1] They used NTB and the N-^{n}Pr substituted derivative PrNTB to form the Cu(I) complexes $[Cu(NTB)(PPh_3)]NO_3 \cdot H_2O$ and [Cu(PrNTB)]I, which have been characterised by X-ray crystallography. Both of these complexes are tetrahedral. In the NTB complex, the copper is coordinated by a phosphorus atom and three nitrogen atoms – the axial amine nitrogen atom (N_{amine}) and two from the benzimidazole side arms (N_{Bim}). In the PrNTB complex, the iodide and the three N_{Bim} coordinate the Cu(I) ion but the N_{amine} remains uncoordinated. This results in the formation of eight membered chelate rings. These rings pucker to minimise the strain, as predicted in Section 1.3.3.

The five coordinate Cu(II) complexes [Cu(NTB)Cl]Cl and [Cu(PrNTB)I]Cl were also prepared.[4] The NTB complex is square pyramidal with one of the N_{Bim} atoms in the axial site. The equatorial sites are occupied by the remaining two N_{Bim} atoms, the N_{amine} and a chloride ion. The PrNTB complex is trigonal bipyramidal. The PrNTB ligand is symmetrically coordinated with the N_{amine} in the axial site and the three N_{Bim} atoms in the equatorial plane. The remaining axial site is filled by the iodide. Both PrNTB complexes have C_3 symmetry. In the crystal lattice of both molecules, the benzimidazole arms stack so that they can interact *via* weak intermolecular π-π interactions. (π…π distance of about 3.6 Å).

NTB forms stable complexes with lanthanide(III) ions.[13-15] The formation of bis complexes is favoured and the ligands have a suitable cavity size to encapsulate completely the metal ion and shield it entirely from solvent molecules. The complexes $[Ln(NTB)_2](ClO_4)_3 \cdot 3Et_2O$ (Ln = La, Nd, Eu) have been made and characterised by X-ray crystallography. The lanthanide ion is eight coordinated and the geometry is approximately a distorted bicapped trigonal antiprism. Short interplane distances suggest that there are strong π-π interactions between the imidazole rings. This provides a strong enthalpic driving force for the formation of bis complexes.

Su's group have also used NTB and its alkyl-substituted derivatives to form a variety of silver aggregates.[11] Following on from their hypothesis that the ligand can exist in an endo- or exo- conformation, they predicted that the ligand should interact with metal ions in diversified forms. The nuclearity of the complex formed is dependent upon a number of factors, including the metal : ligand ratio, the coordinating nature of the anions, the benzimidazole nitrogen atom substituent R, and the conformation of the ligand. Four complexes from mono- to tetra- nuclear were formed with Ag(I) ions.

If the ligand is in an endo- conformation, it prefers to accommodate the metal ions in its own cavity. It can coordinate to one Ag(I) ion through all three of its arms (for PrNTB). A di- or tri- nuclear silver system can be accommodated if the three arms splay out; two tripodal ligands can support a Ag(I) dimer or trimer (for the N-alkylated derivatives MeNTB and EtNTB respectively). Alternatively, the non-alkylated ligand can coordinate in an exo- conformation to form a cage like complex. This can be considered as a six component cage comprised of two tripodal ligands bridged by four Ag(I) ions.

Rheingold *et al.* have investigated the selective deprotonation of the NTB ligand.[16] His group looked at Co(II)-NCS complexes of NTB and sequentially deprotonated the coordinated benzimidazole arms. The introduction of negative charge onto the tripodal ligand resulted in a shift in the electrochemical potential of the Co(II) ion from +0.98 to +0.47 V or an average of 0.17 V per proton. This shows that by modulating the ligand framework, the redox properties of the metal centre can be finely tuned.

4.3 Attempted Synthesis of Imidazole Ligands

4.3.1 Attempted Alkylation of Tris(benzimidazole) Central Nitrogen Atom

The initial approach taken to synthesise the desired ligand was to form the NTB ligand and then to alkylate the central nitrogen atom. This nitrogen atom has a highly exposed lone pair that should be very susceptible to nucleophilic attack. It is the most basic nitrogen atom in the ligand with a pK_a = 10-11[17] for the conjugate base, compared with the imidazole nitrogen atom that has a pK_a = 7 for its conjugate base.[18] These pK_a values correspond to the process shown in Figure 4.14.

$$R_3\overset{+}{N}H \overset{pK_a}{\rightleftharpoons} R_3N + H^+$$

Figure 4.14 pK_a process for tertiary amines

NTB was prepared as described by Thompson *et al.* by the condensation of *o*-phenylenediamine with nitrilotriacetic acid.[1] *o*-Phenylenediamine and nitrilotriacetic acid were heated together in a melt at 190 - 200 °C, followed by heating under reflux in methanol. Recrystallisation from methanol gave the desired product as fine white needles in 50 % yield.

NMR analysis was in agreement with the literature values reported for the ligand.[1] The methylene protons all appear equivalent and are shifted downfield only slightly compared to nitrilotriacetic acid. The aromatic protons appear as a symmetrical set of peaks typical of the *AA'BB'* spectrum generally observed for symmetrically *ortho*-substituted benzene rings. The symmetrical nature of this set of peaks indicates a plane of symmetry bisecting each benzimidazole ring suggesting that the imidazole ring proton is fully delocalised along the N-C-N framework.

Initial attempts to alkylate NTB were carried out by Richard Bailes, a project student in the group. NTB was treated with one equivalent of a variety of alkylating agents, all of which proved to be unsuccessful. The results are summarised in Table 4.1.

Alkylating Agent	Solvent	Product
MeI	MeOH	Dark green powder
	EtOH	White powder
	DMSO	Beige powder
	DMF	Bright yellow powder
EtI	THF	Gold crystals
Me_3OBF_4	MeOH	Green crystals
Et_3OBF_4	MeOH	Blue powder
$CF_3SO_3CH_3$	MeOH	Blue oil

Table 4.1 Initial attempts at alkylating NTB

The results were analysed by ^1H NMR and all were shown to be a mixture of products, with very complicated signals in the aromatic regions. This can be explained by the presence of a mixture of alkylated ligands containing different numbers of alkyl groups and with the alkyl groups on different nitrogen atoms. If only one of the heterocyclic nitrogen atoms has been alkylated, the ligand will no longer contain a three fold rotational axis of symmetry and so the number of NMR equivalent protons will be greatly reduced.

One of the drawbacks to the use of NTB is its limited solubility. It is only slightly soluble in methanol, requiring large sample volumes and heat to fully dissolve the ligand. This solvent system may be incompatible with some of the alkylating agents. A slight modification was made to the NTB ligand by placing a methyl group on to the benzene ring to form tris(5-methyl-1(3)H-2-benzimidazolylmethyl)amine, **20**. This serves the purpose of increasing the solubility of the ligand in organic solvents and to act as a spectroscopic handle on the ligand. Although the addition of this extra group will increase the steric bulk of the ligand, its presence should not block access to remaining coordination sites on a metal site to which the ligand is complexed, as the groups will be pointing outwards, away from the metal centre.

The modification could easily be achieved by using 3,4-diaminotoluene in place of *o*-phenylenediamine in the melt reaction. Reflux in methanol led to the formation of a dark cherry red coloured solution. The addition of ether led to a pale pink solid crashing out of solution. Repeated washing with acetonitrile led to the isolation of **20**

as a white powder. This could be recrystallised from methanol to give fine white needles in a comparable yield to NTB. This work was also carried out by Richard Bailes.

^{1}H NMR analysis of **20** shows a new singlet at δ 2.53 due to the nine methyl protons. The singlet representing the methylene protons remains unchanged from the NTB ligand. The introduction of the methyl substituent on the benzene ring reduces the symmetry of the aromatic rings and this is reflected in the splitting of the aromatic multiplet in the ^{1}H NMR spectrum. CHN elemental analysis and mass spectrometry confirm the formation of this new ligand.

An initial attempt to alkylate **20** was carried out by Richard Bailes. **20** was treated with one equivalent of the alkylating agent $CF_3SO_3CH_3$ in THF, to yield a black decomposition solid. The reaction was repeated in DCM, which led to the formation of a red solid that consisted of a mixture of alkylated products.

The reaction was then attempted using $CF_3SO_3CH_2CH_3$ as the alkylating agent in DCM. The addition of ethyl groups as opposed to methyl groups should allow for easier identification by ^{1}H NMR analysis. Thompson reported there to be a strong association between NTB and alcohols. NMR data indicated the presence of solvate molecules in the undried product in a ratio of 1: 3 (ligand : solvate molecule).[1] These solvate molecules are probably hydrogen bonded, one to each imidazole ring. In order to remove the possibility of any coordinated alcohol solvent molecules from reacting with the alkylating agent, the ligand was placed under high vacuum for several hours. **20** was then treated with one equivalent of $CF_3SO_3CH_2CH_3$ in freshly distilled, degassed DCM. Over forty eight hours, the clear yellow solution had turned cloudy with the formation a white precipitate. The ^{1}H NMR spectrum in DMSO showed the heterocyclic region to be similar to the spectrum of the unreacted ligand. However, the spectrum of the product showed there to be a large number of peaks in the ethyl region suggesting that a mixture of products had formed. This was confirmed by the FAB+ mass spectra that showed peaks representing molecules with one, two and three ethyl groups attached.

Alkylating Agent	Solvent	Product	Explanation
$CF_3SO_3CH_3$	THF	Black crystalline solid	Alkylation of solvent
	DCM	Dark red solid	Mixture of products
$CF_3SO_3CH_2CH_3$	DCM	White solid	Mixture of products

Table 4.2 Further attempts at alkylating 20

Again, it is likely that a mixture of alkylated products is formed.

4.3.2 Attempted Alkylation of Ligand Precursor

The second approach taken was to alkylate the initial tripod precursor, before forming the heterocycle. By doing this, there is only one nitrogen atom available for nucleophilic attack, avoiding the problem of competing side reactions at the heterocyclic nitrogen atoms.

4.3.3 Esterification of Nitrilotriacetic Acid

Nitrilotriacetic acid was esterified following Fisher's method of acid catalysis, as reported by Kawaski *et al.*[19] Acid catalysis enhances the carbonyl character by protonation of the carbonyl oxygen and promotes the loss of the leaving group. Nitrilotriacetic acid was heated under reflux in acidic methanol for 6 h to form trimethylnitrilotriacetate, **21**. The triester was purified by distillation to yield a colourless oil, which was fully characterised.

4.3.4 Alkylation of Central Nitrogen Atom

The next step was to alkylate the central nitrogen atom of **21**. A number of alkylating agents were tried and these are listed in Table 4.3. MeI, and the benzyl halides were not strong enough reagents to alkylate the central nitrogen atom. Following heating under reflux in a vast excess of the reagent for eight hours, there was no change in **21** according to ^{1}H NMR analysis. The stronger alkylating reagent $SO_2(OCH_3)_2$ was utilised without success. The reaction was carried out in toluene and refluxed at 140 °C for 48 h. The reaction was cooled to room temperature and quenched with the addition of water. The ^{1}H NMR spectrum suggested that the central nitrogen atom had been protonated with a large, broad signal at 10 ppm.

Alkylating Agent	Result
MeI	No reaction
BzCl	No reaction
BzBr	No reaction
$SO_2(OCH_3)_2$	N protonated
Me_3OBF_4	Colourless crystals
Et_3OBF_4	No reaction
$CF_3SO_3C_2H_5$	Colourless crystals

Table 4.3 Attempted alkylation of 21

The most successful alkylating agents were Me_3OBF_4 and $CF_3SO_3C_2H_5$ both of which resulted in the formation of the alkylated tripods. These are very strong alkylating agents due to the excellent leaving group ability of the oxonium and the triflate anions. **21** was treated with one equivalent of the alkylating agent in DCM, under nitrogen at room temperature. Anhydrous conditions are essential to avoid the cleavage of the oxonium ion to give an alcohol and ether, as shown in Figure 4.15.

Figure 4.15 Hydrolysis of trialkyloxonium tetrafluoroborate

After stirring the solution at room temperature under nitrogen for 48 h, the excess solvent was removed *in vacuo* to yield the desired alkylated tripod as a colourless oily residue in almost quantitative yields. Colourless block shaped crystals of $N(Me)(CH_2COOMe)_3BF_4$, **22**, and colourless rod shaped crystals of $N(Et)(CH_2COOMe)_3CF_3SO_3$, **23**, suitable for X-ray analysis could be obtained by layering an acetonitrile solution of the ligand with diethyl ether. The crystal structure of **22** is shown in Figure 4.16 and selected bond lengths and angles are summarised in Table 4.4. Crystals of **22** were found to contain two independent molecules per unit cell consisting of a tetrahedral $[N(Me)(CH_2COOMe)_3]^+$ complex with an associated BF_4^- counter ion. The tripod is tetrahedral with all four C-N bonds of similar length (average C-N = 1.514(2) - 1.515(2) Å).

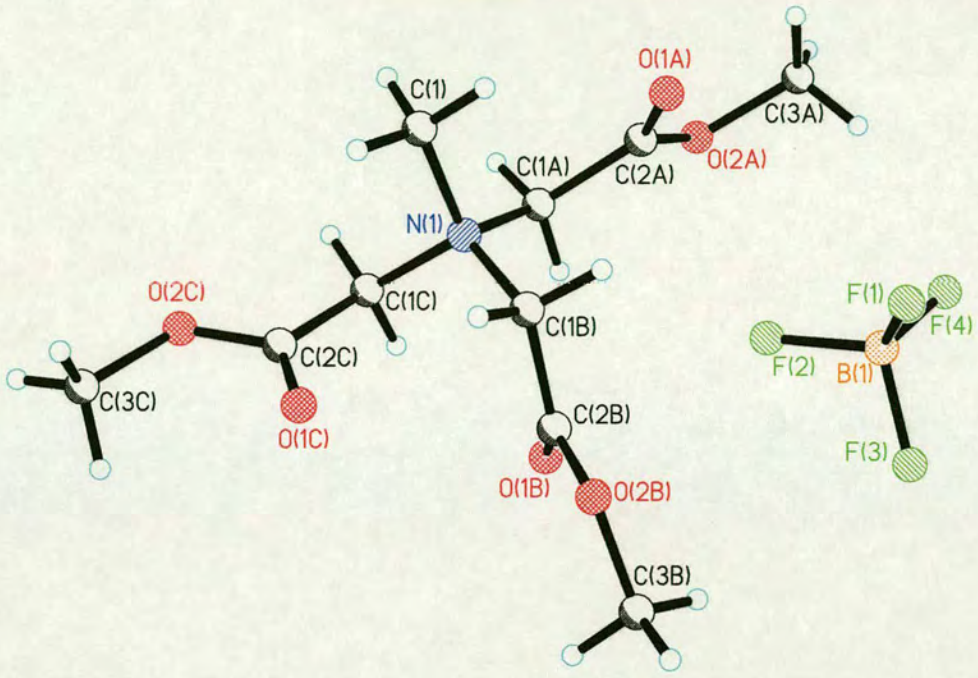

Figure 4.16 X-ray crystal structure of $CH_3N(CH_2CO_2Me)_3BF_4$, 22

Bond	Length / Å
N(1)-C(1B)	1.514 (2)
N(1)-C(1)	1.514 (2)
N(1)-C(1A)	1.515 (2)
N(1)-C(1C)	1.515 (2)

Angle	Size / °
C(1B)-N(1)-C(1)	106.57 (12)
C(1B)-N(1)-C(1A)	111.20 (14)
C(1)-N(1)-C(1A)	111.86 (14)
C(1B)-N(1)-C(1C)	114.93 (13)
C(1)-N(1)-C(1C)	107.96 (14)
C(1A)-N(1)-C(1C)	104.40 (12)

Table 4.4 Selected bond lengths / Å and bond angles / ° for 22

Crystals of **23** were found to contain two independent molecules per unit cell consisting of a tetrahedral $[N(Et)(CH_2COOMe)_3]^+$ complex with an associated $CF_3SO_3^-$ counter ion. Figure 4.17 shows a picture of the crystal structure of **23**, selected bond lengths and angles are listed in Table 4.5.

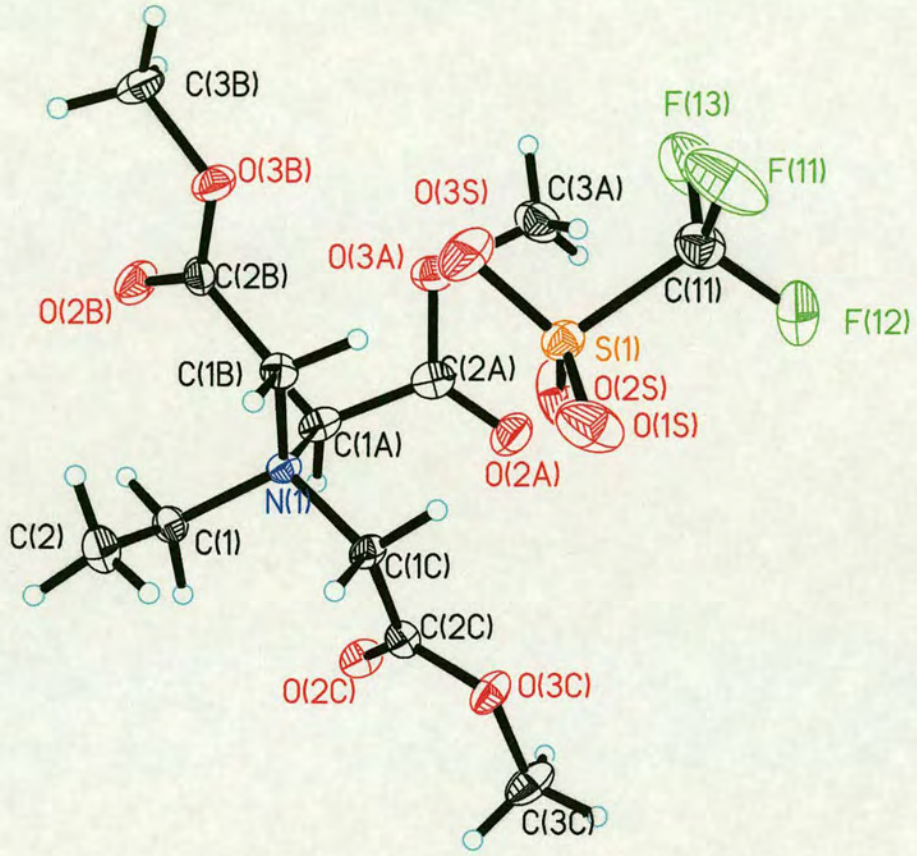

Figure 4.17 X-ray crystal structure of $CH_3CH_2N(CH_2CO_2Me)_3CF_3SO_3$, 23

Bond	Length / Å
N(1)-C(1C)	1.510(3)
N(1)-C(1B)	1.516(3)
N(1)-C(1A)	1.519(3)
N(1)-C(1)	1.546(3)

Angle	Size / °
C(1C)-N(1)-C(1B)	105.37(18)
C(1C)-N(1)C(1A)	111.57(18)
C(1B)-N(1)-C(1A)	110.07(18)
C(1C)-N(1)-C(1)	109.68(19)
C(1B)-N(1)-C(1)	112.34(18)
C(1A)-N(1)-C(1)	107.9(2)

Table 4.5 Selected bond lengths / Å and bond angles / ° for 23

23 is approximately tetrahedral with the three C-N bonds joining the arms of the tripod to the central nitrogen atom being of similar length to each other (C-N bond length = 1.510(3) – 1.519(3) Å) and to the corresponding bonds in **22**. Unlike for **22**, the C-N bond joining the added alkyl group is 0.031(3) Å longer than the other C-N bonds. This may be due to the increased steric bulk of the ethyl group relative to the methyl group.

The ^{1}H NMR analysis of the two tripods shows that the signal for the methylene protons has been shifted downfield with respect to the unmethylated triester. The values of the shift are shown in Table 4.6. The shift is greatest for the methyl amine nitrogen atom. This shift is due to the formation of a positive charge at the central nitrogen atom and so the methylene protons will be less shielded than in the unalkylated ester.

Tripod	δ ^{1}H for methylene protons
21	3.62
22	4.73
23	4.53

Table 4.6 δ ^{1}H for methylene protons in tripod triester precursors

The reaction was also carried out using Et_3OBF_4 under the same conditions as were successful for Me_3OBF_4. This reagent was probably unsuccessful due to the tertiary amine attacking the oxonium salt to form the acid, as illustrated in Figure 4.18.

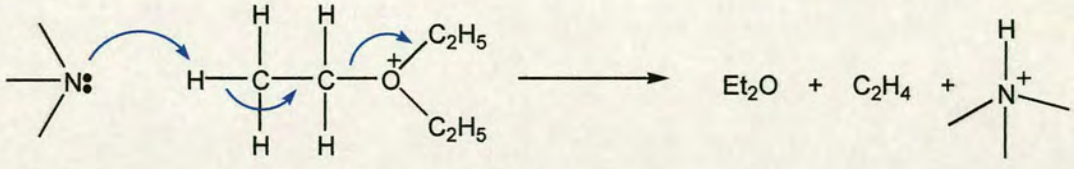

Figure 4.18 Decomposition of Et_3OBF_4

4.3.5 Formation of the Heterocycle

The next stage of the synthesis was to form the heterocycle. Initially the same condensation method as that reported by Thompson[1] was utilized but with the alkylated triester substituted for the nitrilotriacetic acid.

Reactions were carried out using **22** as the tripod precursor with both 3,4-diamino toluene and *o*-phenylenediamine as starting materials. The conditions were varied by using different melt reaction times, but without success. In each case, a gas was produced, which then condensed on the walls of the reaction flask. This was presumed to be methanol. In order to push the equilibrium towards the formation of the desired product, the methanol was distilled out of the reaction vessel during the melt process. Following the melt reaction the product was extracted into methanol to give a deep red coloured solution. Upon cooling, followed by the addition of diethyl ether, a small amount of pale pink solid could be isolated from the reaction solution. This was recrystallised from methanol to give white crystalline needles.

^{1}H NMR analysis showed that the heterocycle had formed in all of the reactions. For the reaction between *o*-phenylenediamine and **22**, it was originally believed that the desired ligand, **24**, had formed, with the methyl group on the central nitrogen atom intact. The ^{1}H NMR spectrum showed two peaks close together, one at 3.16 ppm and one at 3.18 ppm. One peak could be assigned to methanol and the assumption was made that the other represented the methyl group on the central nitrogen atom. This seemed plausible given that the peak representing the alkyl group on the central nitrogen atom in the ^{1}H NMR analysis of **22** resonated at 3.60 ppm. The ^{13}C NMR spectrum of **24** showed two peaks close together at 48.70 and at 50.32 ppm, backing this hypothesis further. The mass spectroscopic analysis (FAB+) showed the major peak to be at *m/z* 450, corresponding to NTB, but there was also a peak at *m/z* 464, corresponding to the alkylated ligand, **24**.

On the premise that **24** had been successfully synthesised, and whilst waiting on further analysis, attempts were made to complex **24** to a metal. Following the protocol outlined by Rheingold *et al.*[16] **24** was complexed to cobalt. The Co(II) complex was readily prepared by the direct reaction of **24** with $CoCl_2 \cdot 6H_2O$ in

methanol; addition of $NaBPh_4$ and KSCN gave the purple complex assumed to be [Co(**24**)(NCS)]Cl in good yield. The IR analysis (KBr disk) of the product suggested the complex had formed with peaks representing both the imidazole and the isothioyanate ligand. The mass spectrometry analysis (FAB+) showed peaks indicating the formation of **25**. Crystals of [Co(**24**)(NCS)]Cl, suitable for X-ray analysis were grown from MeCN. However, most unfortunately the structure showed no alkyl group was present. The structure of the complex is shown in Figure 4.19.

Rheingold *et al.* have reported a virtually identical structure for $[CoNTB(NCS)]BPh_4$, the only difference being the nature of the counter ion.[16] NTB is coordinated through all four nitrogen atoms to the Co(II) metal ion forming a trigonal bipyramidal complex. There are also two acetonitrile solvent molecules and a chloride counter ion in the unit cell. The central nitrogen atom is no longer bound to an alkyl group. Instead, the tetrahedral geometry of the central atom has inverted compared to the free ligand and the nitrogen atom is coordinated to the metal. The three benzimidazolyl nitrogen atoms define the trigonal plane with a Co-N_{benz} bond distance of 2.009(2) - 2.036(2) Å. The metal ion sits slightly out of the trigonal plane formed by the benzimidazolyl nitrogen atoms towards the isothiocyanato ligand. The terminal isothiocyanato ligand is positioned nearly trans to the central nitrogen atom.

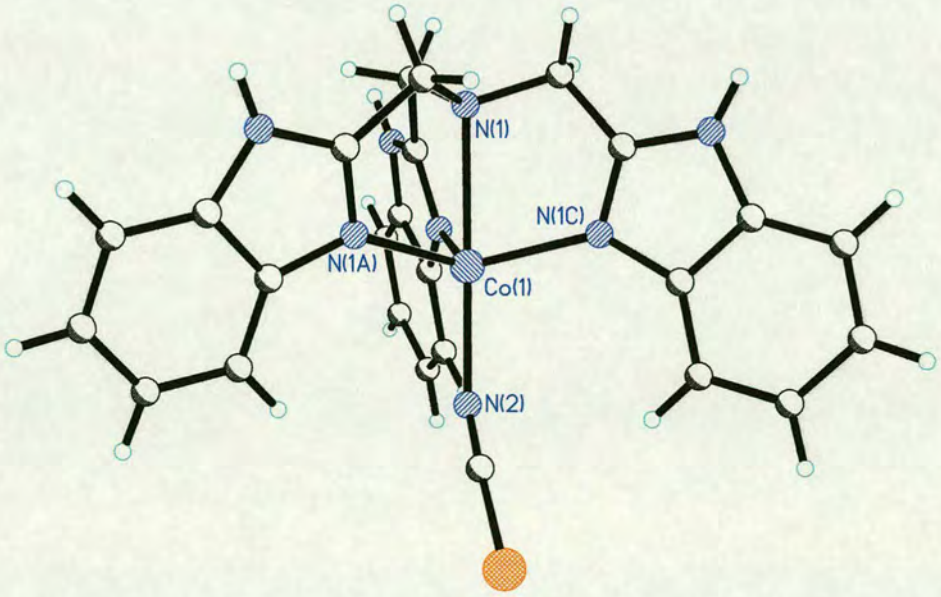

Figure 4.19 X-ray crystal structure of Co(NTB)(NCS)

Bond	Length / Å
Co(1)-N(1)	2.050(3)
Co(1)-N(1A)	2.036(2)
Co(1)-N(1B)	2.009(2)
Co(1)-N(1C)	2.031(2)
Co(1)-N(10A)	2.389(2)

Angle	Size / °
N(1B)-Co(1)-N(1C)	110.04(10)
N(1B)-Co(1)-N(1A)	106.43(10)
N(1C)-Co(1)-N(1A)	125.62(10)
N(1B)-Co(1)-N(1)	110.88(10)
N(1C)-Co(1)-N(1)	102.40(9)
N(1A)-Co(1)-N(1)	100.60(10)
N(1B)-Co(1)-N(10A)	75.76(9)
N(1C)-Co(1)-N(10A)	76.53(9)
N(1A)-Co(1)-N(10A)	74.99(9)
N(1)-Co(1)-N(10A)	173.05(9)

Table 4.7 Selected bond lengths / Å and bond angles / ° for 25

Looking down the axis defined by the central nitrogen atom, the cobalt ion and the isothiocyanato ligand, as shown in Figure 4.20, it can be seen that the ligand arms are very slightly twisted at the methylene carbon atom. This allows the central amine nitrogen to approach the metal ion more closely.

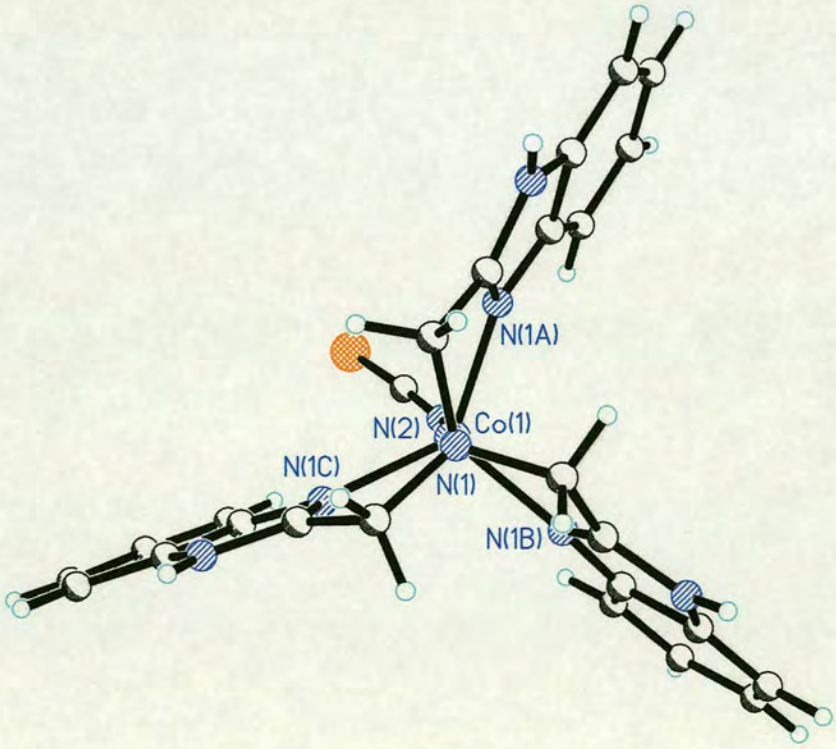

Figure 4.20 View of Co(NTB)(NCS) looking down the three fold axis.

Careful analysis of the products of the reactions between the alkylated triesters and the diamines ultimately revealed that the methyl group on the central nitrogen atom had been lost during the reaction and that **20** or NTB had formed, depending upon which diamine was used as the starting material. The peaks assigned to the methyl group on the nitrogen atom could be due to coordinated molecules of methanol. These may have slightly different shift values if they are in non-identical chemical environments. The small peaks representing the alkylated ligands in the mass spectrometry analysis could be due to trace amounts of the desired products forming. This result led to new approaches to alkylating the central nitrogen atom being considered.

The heterocycle forming reactions were repeated using **23** as the tripod precursor. It was hoped that the ethyl group would be more easily identifiable from the ^{1}H NMR traces than the methyl group. Unfortunately reactions carried out with **23** resulted in the formation of the unalkylated tris-benzimidazole ligands.

It was thought that the conditions of the melt may be too harsh for **22** and **23**. One possibility is that a transamination reaction is taking place. Baron and Hünig reported the dealkylation of quaternary salts with ethanolamine.[20] In this reaction, methyl groups are cleaved in preference to other saturated alkyl groups, as shown in Figure 4.21.

$$R_4N^+ + NH_2CH_2CH_2OH \longrightarrow R_3N^+ + RNH_2CH_2CH_2OH$$

Figure 4.21 Dealkylation of quaternary salts with ethanolamine

It may be that a transamination reaction is taking place in which the alkyl group is transferred to one of the free amine groups of the phenylenediamine during the reaction. This would explain the moderately low yields of product formation and the loss of the alkyl group in the final product.

The reaction was carried out in a more controlled manner by heating under reflux in a number of high boiling solvents, including triethylene glycol and diethylene glycol.

This reaction system did not provide the formation of the desired product, however it did result in a higher yield of **20** than when the melt process was used, suggesting that this is a more efficient procedure for the synthesis of **20**. This indeed was the case when the synthesis of **20** was carried out directly from nitrilotriacetic acid and 3,4-diaminotoluene in digol instead of using a melt. This method also resulted in a higher yield for NTB. In order to eliminate the possibility that the lack of success of the reaction was due to the use of the ester as opposed to the acid, NTB was prepared from **21** in place of nitrilotriacetic acid. This reaction resulted in the clean formation of NTB, using both the melt method and by using digol as the reaction media.

4.3.6 Attempted Exchange of the Counter ion

One reason for the heterocycle not forming completely is that there is some evidence supporting the possibility of the thermal decomposition of BF_4^-. At high temperatures, the anion could decompose to BF_3 and F^-, both of which are highly reactive species that could attack the ester or any preformed heterocyclic species at the high temperatures of the reaction. In order to try and overcome this, attempts were made to exchange the BF_4^- ion for a chloride ion. This could then be metathesised for virtually any other anion using silver salts.

Simple attempts at just heating **22** under reflux in 3M HCl proved unsuccessful, with **22** remaining unchanged. The next approach tried was to heat **22** under reflux in an aqueous solution of sodium hydroxide for four hours. The colourless solution was then cooled to room temperature and tetraethylammonium chloride was added to the solution. The product was extracted into DCM. This was reduced in volume to yield a white solid. ^{1}H NMR analysis showed the methyl ester groups to have remained unhydrolysed and the IR showed the BF_4^- anion to still be present.

An alternative approach tried was to use a strongly basic anion exchange column. A DOWEX-1X8-200 mesh in the chloride form was used. These meshes generally have quaternary amine functionalities and so the anion exchange would be statistically driven. BF_4^- is a large, non coordinating anion and so it was hoped that this would work with a good yield of the chloride salt forming.

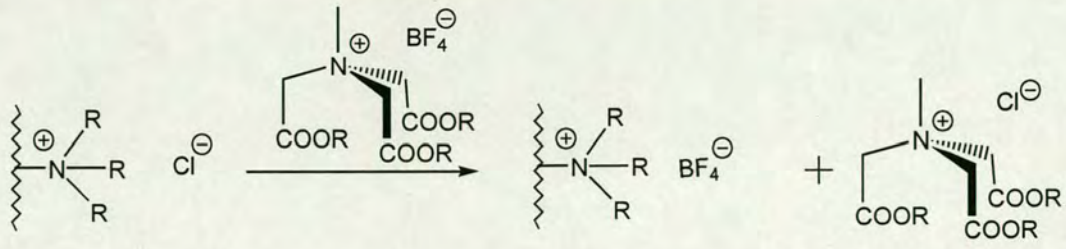

Figure 4.22 Schematic for anion exchange

After passing **22**, as an aqueous solution, through the column, thin film IR studies suggested that the BF_4^- was no longer present. Unfortunately, attempts to isolate the chloride salt in any significant quantity were unsuccessful and this method was abandoned.

4.3.7 Attempt at Selective Alkylation of the Central Nitrogen Atom Through Metal Complexation

A different approach to obtaining the selective alkylation of the central nitrogen atom was to co-ordinate **20** to a metal, thus blocking the heterocyclic nitrogen atoms from further reaction and leaving only the central nitrogen atom open to attack.

20 was added to a solution of anhydrous zinc chloride in methanol. The pale yellow solution was stirred at room temperature overnight, resulting in the formation of a white precipitate. Mass spectrometry and ^{1}H NMR data suggested that this was the mononuclear trigonal bipyramidal complex (**20**)ZnCl, **26**, which is very similar to the complex NTBZnCl first reported by Thompson.[1] **26** was dissolved in freshly distilled DCM and treated with one equivalent of Me_3OBF_4. The clear solution was stirred at room temperature for forty eight hours, during which time the solution turned cloudy with the formation of a white precipitate. The powder was isolated by filtration and ^{1}H NMR analysis showed that the complex had remained unreacted. The FAB+ mass spectrum confirmed this with strong peaks for **26** and for unbound **20**. This finding is not unexpected given that the geometry of the central nitrogen atom is tetrahedral in

the unreacted zinc complex. The nitrogen atom lone pair will be pointing downwards towards the zinc metal centre and so methylation would require the geometry of the nitrogen centre to invert, which would represent a relatively unfavourable, high energy process.

4.3.8 Attempted Alkylation of All Donor Nitrogen Atoms

In order to overcome the problem of selectively alkylating only the central nitrogen atom, and not the three heterocyclic nitrogen atoms, **20** was treated with four equivalents of alkylating agent in an attempt to alkylate all four nitrogen atoms. The drawback of this approach is that there is evidence that the methylation of the heterocyclic amine nitrogen atoms reduces the metal binding ability of the ligands.[8] The ligand was treated with four equivalents of Me_3OBF_4 in freshly distilled anhydrous DCM. After stirring for 48 h under nitrogen, at room temperature, the white suspension had dissolved to yield a clear colourless solution. Upon removing the excess solvent *in vacuo*, a white solid was obtained. The ^1H NMR spectrum suggested that a mixture of alkylated products had formed. Mass spectrometry analysis (FAB+) suggested that only a maximum of three nitrogen atoms had been alkylated with peaks representing three, two, one and no methylated nitrogen atoms present.

20 was treated with four equivalents of $CF_3SO_3C_2H_5$ in DCM. After stirring for 48 h under nitrogen, at room temperature, the white suspension had dissolved to yield a clear yellow solution. Upon removing the excess solvent, a yellow solid, **27**, was obtained. **27** was recrystallised from MeCN layered with diethyl ether to yield clear, colourless, block shaped crystals suitable for X-ray analysis. ^1H NMR analysis of the crystals dissolved in $CDCl_3$ showed the presence of one ethyl environment. Unfortunately, X-ray analysis of the crystals, (Figure 4.23), clearly showed that there was no coordinated ethyl group.

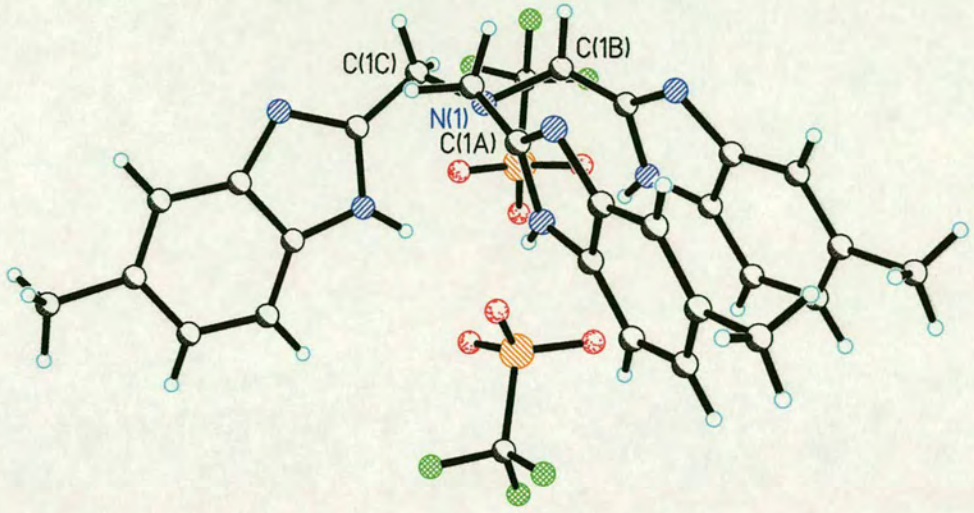

Figure 4.23 X-ray crystal structure of $C_{33}H_{30}F_9N_8O_9S_3$, 27

Three triflate counter ions are present. The structure no longer possesses three-fold symmetry, shown in Figure 4.24. Two of the arms lie parallel to each other and there may be weak π-π stacking interactions providing an extra stabilizing force for the structure.

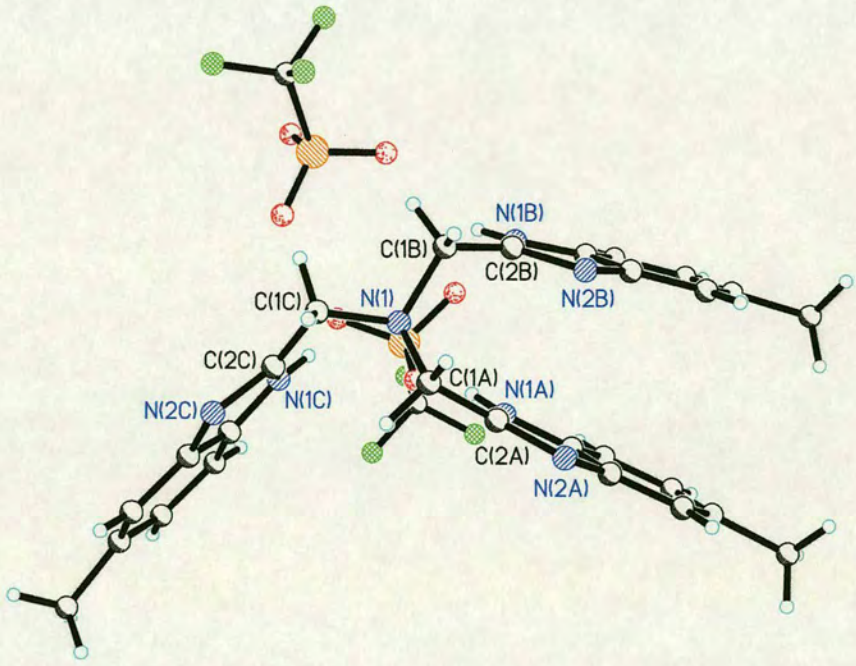

Figure 4.24 Crystal structure of 27 looking down the central axis.

The ethyl group identifiable from the solution ^{1}H NMR spectrum may be due to traces of ethanol in the solution. It is possible that the $CF_3SO_3C_2H_5$ reagent was hydrolysed by traces of water in the reaction, leading to the formation of triflic acid. This is one of the strongest Lowry – Brønsted acids known and so will protonate the nitrogen atoms very easily. Interestingly, it is the three heterocyclic nitrogen atoms that are protonated in preference to the central nitrogen atom. The other product of the hydrolysis reaction is ethanol, which may be responsible for the ethyl groups observed in the ^{1}H NMR data.

Although various mass spectra indicate peaks that may correspond to the alkylated ligand, they are always much less intense in comparison to the other peaks and there has been no ^{1}H NMR data confirming the existence of an alkyl group bound to the central nitrogen atom. At this point it was decided that the alkylation of the central nitrogen atom was not feasible and this ligand system was abandoned.

4.4 Experimental

4.4.1 Preparation of Tris(2-benzimidazolylmethyl)amine (NTB)

NTB was prepared as described by Thompson *et al.*[1]

Nitrilotriacetic acid (15.3 g, 0.08 mol) and freshly sublimed *o*-phenylenediamine (27.0 g, 0.25 mol) were finally ground, and then heated together at 190 – 200 °C for 1 h using an oil bath. The fused reaction mixture was removed and crushed into fine particles. This black / brown solid was then refluxed in methanol containing decolourising charcoal for 4 h. Following hot filtration of the resulting red solution, its volume was reduced until, on cooling, a pale pink solid was obtained. Recrystallisation from methanol yielded NTB as fine white needles. The crystals were dried under high vacuum to remove solvated methanol (16.12 g, 50 %).

M.P. = 269 °C (lit. 270)[1]

CHN: $C_{24}H_{21}N_7$ requires C 70.8, H 5.16, N 24.1; found C 70.4, H 5.3, N 23.5

IR (KBr disc): ν_{max} 3058 ν(NH), 1622 ν(CN) cm^{-1}

^{1}H NMR (200 MHz, DMSO): δ 4.25 (s, 6H, $C\underline{H}_2$), 5.4 (broad s, N$\underline{H}$), 7.27 and 7.65 (AA'BB' m, 12H, ArC$\underline{H}$)

MS (+ve FAB): *m/z* 408

4.4.2 Synthesis of 20

Nitrilotriacetic acid (3.82 g, 0.02 mol) and 3,4-diaminotoluene (7.64 g, 0.063 mol) were finely ground together and heated at 190 – 200 °C for 1 h using an oil bath. The fused reaction mixture was removed and crushed into fine particles. This black / brown solid was then refluxed in methanol containing decolourising charcoal for 6 h. Following hot filtration of the resulting red solution, its volume *in vacuo*. Diethyl ether was added and a pale pink precipitate formed. This was washed with acetonitrile and the white solid was recrystallised from methanol to yield **20** as fine white needles. The crystals were dried under high vacuum to remove solvated methanol (3.58 g, 40 %).

^{1}H NMR (250 MHz, DMSO): δ 2.40 (s, 9H, C$\underline{H}_3$), 3.16 (s, 3H, co-ordinated MeOH), 3.18 (s, 3H, C$\underline{H}_3$N), 4.06 (s, 6H, C$\underline{H}_2$), 6.99 (d, 3H, *J* = 8.2 Hz, ArC$\underline{H}$), 7.30 (s, 3H, ArC$\underline{H}$), 7.48 (d, 3H, *J* = 8.2 Hz, ArC$\underline{H}$), 12.35 (br s, 3H, N$\underline{H}$)

^{13}C NMR (62.9 MHz, DMSO): δ 21.37 (C$\underline{H}_3$), 48.69 (C$\underline{H}_3$N / Me$\underline{O}$H) 50.32 (Me$\underline{O}$H / C$\underline{H}_3$N), 51.49 (C$\underline{H}_2$), 111.11 (ArC$\underline{H}$), 118.2 (ArC$\underline{H}$), 122.72 (ArC$\underline{H}$), 123.43 (ArC$\underline{H}$), 130.1 (ArC$\underline{H}$), 131.28 (ArC$\underline{H}$), 134.56 (ArC$\underline{H}$)

IR (KBr disc): ν_{max} 3150, (br, s), (N-H); 1632, (m), (C=N); 1538, (m); 1448, (s); 1017, (m); 803, (s) cm $^{-1}$

MS (+ve FAB): *m/z* 449 (M^+)

4.4.3 Esterification of Nitrilotriacetic acid – preparation of 21

This was carried out by a modification Fisher's method.[19]

To a suspension of nitrilotriacetic acid (30 g, 157 mmol) in methanol (250 ml) was added concentrated sulphuric acid (9 ml). The resulting mixture was refluxed for ten hours. The reaction mixture was cooled to room temperature and potassium carbonate (20 g) was added as portions and stirred for one hour. The suspension was then filtered and concentrated *in vacuo* to give a yellow oil. The residue was distilled under reduced pressure (75 °C, 2.5 mmHg) to give **21** as a colourless oil. (21.3 g, 58 %).

IR (KBr disc): ν_{max} 3045 (s), 2360 (w), 1749 (vs) ν(C=O), 1445 (s), 1347 (s), 1226 (br) ν(C-O-C), 1062 (s), 905 (s) ν(BF) cm^{-1}

^{1}H NMR (200 MHz, $CDCl_3$): δ 3.68 (s, 9H, COOMe), 3.62 (s, 6H, NC$\underline{H}_2$)

4.4.4 Preparation of 20 from 21

21 (2.0 g, 0.0085 mol) and freshly sublimed 3,4-diaminotoluene (3.25 g, 0.027 mol) were heated to 200 °C under vacuum in a Schlenk tube fitted to another by means of a solids addition tube for three hours. A heat gun was used to drive the methanol produced over into the other Schlenk tube. The yellow solid melted to form a green solution that proceeded to turn dark orange. The solution was allowed to cool, forming a dark orange red solid. The orange solid was redissolved in methanol and heated under reflux for six hours. The solution was left to cool overnight. An off

white precipitate formed and the solution turned a dark red colour. The precipitate was filtered off. Recrystallisation from hot methanol led to the formation of thin white strand like crystals.

NMR and mass spectrometry analysis showed the product to be **20**.

4.4.5 Attempted alkylation of 20

4.4.5.1 Using Ethyl trifluoromethanesulphonate

20 (6.87 g, 0.015 mol) was placed in a Schlenk tube and dried under high vacuum for 2 h to ensure any solvated alcohol was removed. This was then partially dissolved in freshly distilled, anhydrous DCM (50 ml) to yield a pale yellow suspension. Ethyl trifluoromethanesulphonate (1.98 ml, 0.015 mol) was added slowly with a syringe. The solution turned clear yellow. The solution was stirred at room temperature under nitrogen, during which time a white precipitate formed. This was isolated by filtration.

^{1}H NMR (200 MHz, DMSO): δ 1.2 (br m), 2.4 (s), 4.2 (m), 4.5 (s), 7.2 (d), 7.5 (s), 7.6 (d)
MS (+ve FAB): *m/z* 535 ((**20**)+ 3 Et), 523 ((**20**) + 3Me + Et), 506 ((**20**) + 2 Et), 492 ((**20**) + Et + Me), 478 ((**20**) + Et), 464 ((**20**) +Me), 450 (**20**)

4.4.5.2 Using Methyl iodide

20 (1.0 g, 4.3 mmol) was heated under reflux in methyl iodide (40 ml) for 48 h. After this time, the clear, colourless solution had turned yellow. Addition of diethyl ether resulted in a pale yellow solid crashing out of solution. The solid was recrystallised from acetonitrile layered with diethyl ether.

4.4.5.3 Using Benzyl halides

20 (1.4 g, 6.0 mmol) was heated under reflux in either benzyl bromide or benzyl chloride (70 ml) for eight hours. After this time, the solvent was removed *in vacuo* to leave a dark orange oil.

^{1}H NMR showed that the triester had remained unreacted for both reaction mediums.

4.4.6 Preparation of 22

21 (7.5 g, 0.032 moles) was placed in a degassed Schlenk and dissolved in freshly distilled DCM (20 ml). Trimethyl oxonium tetrafluoroborate (4.76 g, 0.032 moles) was weighed out into a separate Schlenk in the glove box. This was dissolved in freshly distilled DCM (20 ml). The trimethyl nitrilotriacetate solution was transferred *via* cannula to the solution of trimethyl oxonium tetrafluoroborate. The solution was stirred at room temperature under nitrogen for three days, yielding a clear colourless solution. The solvent was removed *in vacuo* to yield a colourless oily residue. This was recrystallised from acetonitrile layered with diethyl ether to yield **22** as colourless block shaped crystals (11.78 g, 91 %).

MP = 88 °C

IR (KBr disc): ν_{max} 3045, (s); 1749, (vs), (C=O); 1445, (CH_2); 1347, (CH_3); 1266, (C-O-C); 1063; 905; 875 cm^{-1}

^{1}H NMR (250 MHz, DMSO): δ 4.73 (s, N$\underline{CH_2}$COOMe, 6H), 3.76 (s, COO$\underline{Me}$, 9H), 3.60 (s, N$\underline{CH_3}$, 3H)

^{13}C NMR (62.9 MHz, DMSO): δ 164.81 ($\underline{C}$OOMe), 61.04 (N$\underline{C}H_2$COOMe), 54.31 (N$\underline{C}H_3$), 53.20 (COO$\underline{Me}$)

CHN: $C_{10}H_{18}NO_6BF_4$ requires C 35.82, H 5.37, N 4.18; Found C 35.80, H 5.19, N 3.99.

MS (+ve FAB): *m/z* 248 (M^+)

Crystal Data for **22**

Data were collected using Mo-Kα radiation on a colourless block of dimensions 0.51 x 0.47 x 0.43 mm on a Stoe Stadi4 diffractometer in the range $5.04 \leq 2\theta \leq 69.93^\circ$ using the ω-θ method. Of a total of 2554 reflections collected, 1577 (R_{int} = 0.0145) were independent. The structure was solved by direct methods (SHELXS-97). Hydrogen atoms were geometrically fixed and allowed to ride. The final difference-map extrema were 0.229 and –0.186 e $Å^{-3}$ with a final *R* of 0.0247 for 1553 parameters.

Empirical formula	$C_{10}H_{18}BF_4NO_6$	γ / °	90
Formula weight	335.06	Volume / Å^3	1477.4 (2)
Crystal system	Orthorhombic	Z	4
Space group	P2(1)2(1)2(1)	Temperature / K	150(2)
a / Å	9.0078 (8)	Wavelength / Å	1.54178
b / Å	9.3431 (7)	Density calc. / Mg/m^3	1.506
c / Å	17.5548 (16)	μ(Mo-Kα) / mm^{-1}	1.338
α / Å	90	R_1 [F>4σ(F)]	0.0247
β / Å	90	WR_2 (all data)	0.0616

Table 4.8 Crystallographic data for 22

4.4.7 Preparation of 23

20 (2.0 g, 8.58 mmol) was placed in a degassed Schlenk and dissolved in freshly distilled DCM (20 ml). Ethyl trifluoromethanesulfonate (1.11 ml, 8.58 mmol) was added slowly with a syringe to the solution. The solution was stirred at room temperature under nitrogen for three days, yielding a clear colourless solution. The solvent was removed to yield a colourless oily residue. This was recrystallised from acetonitrile layered with diethyl ether to yield **23** as colourless block shaped crystals (2.01 g, 57 %).

^{1}H NMR (250 MHz, DMSO): δ 1.11 (t, 3H, $NCH_2C\underline{H}_3$, J = 7.2 Hz), 3.58 (s, 9H, COO<u>Me</u>), 3.77 (q, 2H, $NC\underline{H}_2CH_3$, J = 7.2 Hz), 4.53 (s, 6H, $NC\underline{H}_2COOMe$)
^{13}C NMR (62.9 MHz, DMSO): δ 7.79 ($NCH_2\underline{C}H_3$), 52.89 (COO<u>Me</u>), 58.21 ($N\underline{C}H_2CH_3$), 60.21 ($NC\underline{H}_2COOMe$), 164.51 ($NCH_2\underline{C}OOMe$)
CHN: $C_{12}H_{20}NSO_9F_3$ requires C 35.04, H 4.87, N 3.41; Found C 35.13, H 4.85, N 3.55.

Crystal Data for **23**

Data were collected using Mo-Kα radiation on a colourless rod of dimensions 0.31 x 0.12 x 0.10 mm on a Stoe Stadi4 diffractometer in the range $1.70 \leq 2\theta \leq 29.03°$ using the ω-θ method. Of a total of 10826 reflections collected, 4233 (R_{int} = 0.0560) were independent. The structure was solved by direct methods (SHELXS-97). Hydrogen atoms were geometrically fixed and allowed to ride. The final difference-map extrema were 0.381 and –0.380 e Å^{-3} with a final R of 0.0614 for 2800 parameters.

Empirical formula	$C_{12}H_{20}F_3NO_9S$	γ / °	90
Formula weight	411.35	Volume / Å^3	1748.0 (3)
Crystal system	Monoclinic	Z	4
Space group	P2(1)/c	Temperature / K	150(2)
a / Å	12.7089 (12)	Wavelength / Å	0.71073
b / Å	9.4609 (9)	Density calc. / Mg/m^3	1.563
c / Å	15.4612 (15)	μ(Mo-Kα) / mm^{-1}	0.263
α / Å	90	R_1 [F>4σ(F)]	0.0614
β / Å	109.903 (2)	WR_2 (all data)	0.1303

Table 4.9 Crystallographic data for 23

4.4.8 Attempted Alkylation of 21 Using Triethyl oxonium tetrafluoroborate

21 (0.58 g, 2.5 mmol) was placed in a degassed Schlenk and dissolved in freshly distilled DCM (20 ml). Triethyl oxonium tetrafluoroborate (1.0 M solution in DCM) (0.36 ml, 2.5 mmol) was added slowly with a syringe. The solution was stirred at room temperature under nitrogen for three days, yielding a clear colourless solution. The solvent was removed to yield a colourless oily residue.

^{1}H NMR showed that **21** had remained unreacted.

4.4.9 Preparation of 20 from 21

21 (2.0 g, 0.0085 mol) and freshly sublimed 3,4-diaminotoluene (3.25 g, 0.027 mol) were heated to 200 °C under vacuum in a Schlenk fitted to another by means of a solids addition tube for three hours. A heat gun was used to drive the methanol produced over into the other Schlenk. The yellow solid melted to form a green solution that proceeded to turn dark orange. The solution was allowed to cool, forming a dark orange red solid. The orange solid was redissolved in methanol and heated under reflux for six hours. The solution was left to cool overnight. An off white precipitate formed and the solution turned a dark red colour. The precipitate was filtered off. Recrystallisation from hot methanol led to the formation of thin white strand like crystals.

NMR and mass spectrometry analysis showed this product to be **20**.

4.4.10 Attempted Preparation of Methyl tris(5-methyl-1(3)H-2-benzimidazolylmethyl)amine tetrafluoroborate, 24 – melt reaction

22 (3.35 g, 0.01 mol) and freshly sublimed 3,4-diaminotoluene (5.0 g, 0.041 mol) were finely ground together. The pale yellow powder was heated to 200 °C under vacuum in a Schlenk fitted to another by means of a solids addition tube for three hours. A heat gun was used to drive the methanol produced over into the other Schlenk. The yellow solid melted to form a green solution that proceeded to turn dark orange. The solution was allowed to cool, forming a dark orange red solid. The orange solid was redissolved in methanol and heated under reflux for six hours. The solution was left to cool overnight. An off white precipitate formed and the solution turned a dark red colour. The precipitate was filtered off. Recrystallisation from hot methanol led to the formation of thin white strand like crystals (1.45 g, 32 %).

NMR and mass spectrometry analysis showed this product to be **20**.

The reaction was repeated using different times for the melt reaction. Reaction times of 2 and 3 h were used but with no change in product. The reaction was also carried out using **23** as the tripod precursor, and using *o*-phenylenediamine in place of 3,4-diaminotoluene.

4.4.11 Preparation of 25, the Co(II) Complex of '24'

'**24**' (1.0 g, 2.0 mmol) was dissolved in methanol (25 ml). To this was added the $CoCl_2 \cdot 6H_2O$ (0.47 g, 2.0 mmol) to yield a dark purple solution. This was stirred at room temperature for 1 h. $NaBPh_4$ (1.35 g, 4.0 mmol) was added and a large amount of purple solid ([Co'24'Cl]BPh_4) precipitated out of solution. The purple solid was isolated by filtration and redissolved in acetonitrile (30 ml). The solution was treated with potassium thiocyanate (0.19 g, 2.0 mmol) and stirred for 1 h at room temperature. A large amount of purple material precipitated out of solution. Crystals suitable for X-ray analysis were grown from acetonitrile. (0.58 g, 45 %).

IR (KBr disc): ν_{max} 3118, (br, s), (N-H); 2072, (vs), (NCS); 1656; 1629; 1600, (m), (benzimidazolyl) cm^{-1}

M^+ *m/z*: 539 ((**24**)CoNCS), 524 (NTBCoNCS), 481 (NTBCo)

Crystal Data for **25**

Data were collected using Mo-Kα radiation on a magenta plate of dimensions 0.51 x 0.29 x 0.20 mm on a Stoe Stadi4 diffractometer in the range $1.42 \leq 2\theta \leq 29.08^{\circ}$ using the ω-θ method. Of a total of 18044 reflections collected, 7079 (R_{int} = 0.0385) were independent. The structure was solved by direct methods (SHELXS-97). Hydrogen atoms were geometrically fixed and allowed to ride. The final difference-map extrema were 1.012 and –0.613 e $Å^{-3}$ with a final *R* of 0.0605 for 6229 parameters.

Empirical formula	$C_{29}H_{27}N_{10}SCoCl$	γ / °	90
Formula weight	642.05	Volume / $Å^3$	2917.6 (9)
Crystal system	Monoclinic	Z	4
Space group	P2(1) / c	Temperature / K	150(2)
a / Å	14.625 (3)	Wavelength / Å	0.71073
b / Å	13.882 (2)	Density calc. / Mg/m^3	1.462
c / Å	14.625 (3)	μ(Mo-Kα) / mm^{-1}	0.791
α / Å	90	R_1 [$F>4\sigma(F)$]	0.0605
β / Å	100.694 (3)	WR_2 (all data)	0.1418

Table 4.10 Crystallographic data for 25

4.4.12 Attempted Preparation of Methyl tris(5-methyl-1(3)H-2-benzimidazolylmethyl)amine tetrafluoroborate – using a high boiling temperature solvent

22 (11.14 g, 0.033 mol) and freshly sublimed 3,4-diaminotoluene (13.0 g, 0.11 mol) were finely ground together. The pale yellow powder was dissolved in either digol or triglyme (20 ml). The pale yellow solution was heated at 200 °C under nitrogen for 24 h. The dark red solution was allowed to cool. Water was added causing a large amount of material to precipitate out. This was titrated with DCM causing a large amount of white precipitate to form. The precipitate was filtered off. Recrystallisation from hot methanol led to the formation of thin white strand like

crystals (6.78 g, 46 % yield when carried out in digol; 5.64 g, 38 % yield when carried out in triglyme).

NMR and mass spectrometry analysis showed no presence of the central methyl group and that the product in both cases was **20**.

The reaction was also carried out using **23** as the tripod precursor.

4.4.13 Attempted Exchange of The BF_4^- Counter Ion:

4.4.13.1 Treatment with Hydrochloric Acid

22 was heated under reflux in 3 M hydrochloric acid (15 ml). The clear, colourless solution was concentrated *in vacuo* to leave an oily residue.

^{1}H NMR suggested that the ester groups still remained and had not been hydrolysed as would be expected.
IR showed that the BF_4^- ion was still present.

4.4.13.2 Treatment with Sodium hydroxide

22 was heated under reflux in 20 % sodium hydroxide (25 ml) for 4 h. The clear colourless solution was allowed to cool to room temperature. To this was added tetra ethyl ammonium chloride. The aqueous solution was washed with DCM twice. The solvent was removed to yield a white residue.

^{1}H NMR and IR showed that no reaction had occurred.

4.4.14 Coordination of 20 to Zinc, Formation of 26

Anhydrous zinc chloride was freshly prepared by refluxing zinc chloride in excess thionyl chloride under nitrogen for 20 minutes. The solution was evacuated to dryness, removing excess solvent, along with hydrochloric acid and water.
Anhydrous zinc chloride (3.12 g, 0.027 moles) was placed in a Schlenk and dissolved in freshly distilled anhydrous methanol (30 ml). **20** (1.33 g, 0.027 moles) was added to give a pale yellow, clear solution. This was stirred at room temperature under nitrogen for 72 h. During this time a white precipitate, **26** formed. Addition of

diethyl ether (30 ml) resulted in more precipitate coming out of solution. **26** was isolated by filtration and recrystallised from methanol.

^{1}H NMR (250 MHz, DMSO): δ 2.45 (s, 9H $C\underline{H}_3$), 4.53 (s, 6H, $C\underline{H}_2$), 7.18 (m, 3H, Ar$C\underline{H}$), 7.40 (m, 3H, Ar$C\underline{H}$), 8.51 (m, 3H, Ar$C\underline{H}$)
MS (+ve FAB): *m/z* 550 ((**20**)ZnCl), 450 (**20**)

4.4.14.1 Attempted Alkylation of 26

26 (0.125 g, 0.23 mmol) was added to a solution of trimethyl oxonium tetrafluoroborate (0.034 g, 0.23 mmol) in DCM (10 ml). The clear colourless solution was stirred at room temperature under nitrogen for 48 h. After this time, the solution had turned cloudy. The precipitate was isolated by filtration.

MS (+ve FAB): *m/z* 550 ((**20**)ZnCl), 450 (**20**)
^{1}H NMR showed that the zinc complex had remained unchanged after the reaction.

4.4.15 Attempted alkylation of 20

4.4.15.1 With Four Equivalents of Trimethyl oxonium tetrafluoroborate

20 (1.25 g, 2.8 mmol) was placed in a Schlenk and dried under high vacuum for 2 h to ensure any solvated alcohol was removed. This was then partially dissolved in freshly distilled, anhydrous DCM (20 ml) to yield a pale yellow suspension. Trimethyl oxonium tetrafluoroborate (1.65 g, 0.011 mol) was added slowly with a syringe. The solution turned clear yellow. The solution was stirred at room temperature under nitrogen. The excess solvent was removed *in vacuo* to yield a white solid.

^{1}H NMR (200 MHz, DMSO) was very messy suggesting a mixture of products had formed.
MS (+ve FAB): *m/z* 494 ((**20**)+ 3 Me), 479 ((**20**)+ 2 Me), 464 ((**20**)+Me), 450 (**20**)

4.4.15.2 With Ethyl trifluoromethanesulphonate

20 (2.0 g, 4.5 mmol) was placed in a Schlenk and dried under high vacuum for 2 h to ensure any solvated alcohol was removed. This was then partially dissolved in freshly distilled, anhydrous DCM (20 ml) to yield a pale yellow suspension. Ethyl trifluoromethanesulphonate (1.98 ml, 0.015 mol) was added slowly with a syringe. The solution turned clear yellow. The solution was stirred at room temperature under nitrogen. The excess solvent was removed *in vacuo* to yield an oily residue. Titration with diethyl ether yielded a white solid, **27**. This could be recrystallised from acetonitrile to yield clear colourless crystals suitable for X-ray analysis.

^{1}H NMR (250 MHz, DMSO): δ 2.31 (s, 9H), 4.37 (s, 6H), 7.2 (dd, J = 0.9, 6.8 Hz, 3H), 7.43 (s), 7.53 (d, J = 6.2 Hz, 3H)
^{13}C NMR (62.9 MHz, DMSO): δ 20.88 (CH_3), 49.52 (CH_2), 113.21 (ArCH), 113.55 (ArCH), 117.87 (quatC), 123.00 (quatC), 126.98 (ArCH), 131.39 135.64 (quatC)
MS (+ve FAB): *m/z* 535 ((**20**)+ 3 Et), 523 ((**20**) + 3Me + Et), 506 ((**20**) + 2 Et), 492 ((**20**) + Et + Me), 478 ((**20**) + Et), 464 ((**20**) +Me), 450 (**20**)

Crystal Data for **27**

Data were collected using Mo-Kα radiation on a colourless block on a Stoe Stadi4 diffractometer in the range $1.68 \leq 2\theta \leq 22.50°$ using the ω-θ method. Of a total of 16465 reflections collected, 5417 (R_{int} = 0.0846) were independent. The structure was solved by direct methods (SHELXS-97). Hydrogen atoms were geometrically fixed. The final difference-map extrema were 0.863 and –0.553 e Å^{-3} with a final R of 0.2197 for 2584 parameters.

Empirical formula	$C_{33}H_{30}F_9N_8O_9S_3$	γ / °	90
Formula weight	949.83	Volume / Å^3	4153.6 (18)
Crystal system	Monoclinic	Z	4
Space group	P2(1)/n	Temperature / K	150(2)
a / Å	13.925 (4)	Wavelength / Å	0.71073
b / Å	18.796 (5)	Density calc. / Mg/m^3	1.519
c / Å	15.937 (4)	μ(Mo-Kα) / mm^{-1}	0.280
α / Å	90	R_1 [F>4σ(F)]	0.2197
β / Å	95.305 (6)	WR_2 (all data)	0.5478

Table 4.11 Crystallographic data for 27

4.5 References

1. L. K. Thompson, B. S. Ramaswamy and E. A. Seymour, *Can. J. Chem.*, 1977, **55**, 878

2. D. T. Davies, *Aromatic Heterocyclic Chemistry*. 1992, Oxford Chemistry Primers

3. R. S. Brown, N. J. Curtis, D. Salmon and S. Kusuma, *J. Am. Chem. Soc.*, 1982, **104**, 3188

4. C.-Y. Su, B.-S. Kang, T.-B. Wen, Y.-X. Tong, X.-P. Yang, C. Zhang, H.-Q. Liu and J. Sun, *Polyhedron*, 1999, **18**, 1577

5. C. C. Tang, D. Davalian, P. Huang and R. Breslow, *J. Am. Chem. Soc.*, 1978, **100**, 3918

6. R. Breslow, J. T. Hunt, R. Smiley and T. Tarnowkski, *J. Am. Chem. Soc.*, 1983, **105**, 5337

7. R. S. Brown, N. J. Curtis and J. Huguet, *J. Am. Chem. Soc.*, 1981, **103**, 6953

8. R. S. Brown and J. Huguet, *Can. J. Chem.*, 1980, **58**, 889

9. R. G. Ball, R. S. Brown and J. L. Cocho, *Inorg. Chem.*, 1984, **23**, 2315

10. T. S. Manoharan and R. S. Brown, *J. Org. Chem.*, 1989, **54**, 1439

11. C.-Y. Su, B.-S. Kang, Q.-C. Yang and T. C. W. Mak, *Dalton*, 2000, 1857

12. U. Hartmann, R. Gregorzik and H. Vahrenkamp, *Chem. Ber.*, 1994, **127**, 2123

13. R. Wietzke, M. Mazzanti, J. M. Latour and J. Pecaut, *Chem. Commun. (Cambridge)*, 1999, 209

14. C.-Y. Su, B.-S. Kang, X.-Q. Mu, J. Sun, Y.-X. Tong and Z.-N. Chen, *Aust. J. Chem.*, 1998, **51**, 565

15. C.-Y. Su, Q. Zhou, W.-J. Zhang, Z.-L. Lu and B.-S. Kang, *Chemical Research in Chinese Universities*, 1999, **15**, 63

16. B. S. Hammes, M. T. Kieber-Emmons, R. Sommer and A. L. Rheingold, *Inorg. Chem.*, 2002, 1351

17. J. March, *Advanced Organic Chemistry*. 1992, Wiley-Interscience

18. D. Davies, *Aromatic Heterocyclic Chemistry*. 1992, Oxford University Press

19. K. Kawaski and T. Katsuki, *Tetrahedron*, 1997, **53**, 6337

20. Hünig and Baron, *Chem. Ber.*, 1957, **90**, 395

5 Phosphoramidite TREN Based Chiral Ligands

During the second year of my PhD, I studied in the organic chemistry department at the Kungl Tekniska Högskolan (Royal Institute of Technology) in Stockholm, Sweden for three months. I worked under the supervision of Prof. Christina Moberg investigating the synthesis of new C_3 symmetric, tripodal tetra-amine ligands. This chapter describes some of the work that was carried out during this period.

Moberg's group have developed chiral analogues of the TREN ligand in which the chirality resides in the ligand backbone. These ligands were introduced briefly in Chapter 1. Chiral analogues can be conveniently synthesised in high yields by the nucleophilic ring opening of chiral aziridines, using ammonia as the nucleophile.[1] I worked on improving some of the steps of this synthesis. The second part of the project was to look at the incorporation of a phosphoramidite functionality onto the terminal amine groups of the tetra-amine ligand.

5.1 Introduction to Phosphoramidite Ligands

Phosphoramidites [$P(NR_2)(OR')_2$] consist of a phosphorus atom connected to two oxygen groups and one nitrogen group. Phosphoramidites have electron donor – acceptor properties typically lying between those of arylphosphines and arylphosphites and so are an interesting class of ligands to study. Trivalent phosphines and phosphites are frequently used as ligands in asymmetric catalysis but phosphoramidites have received very little attention. This is presumably due to the sensitivity towards hydrolysis normally attributed to this class of compounds. However, Feringa *et al.*, amongst others, have reported chiral phosphoramidites based on binaphthol to be remarkably stable.[2] Feringa *et al.* have used chiral phosphoramidites based on 2,2'-binaphthol as ligands for Cu-catalysed 1,4-additions of R_2Zn to cyclic and acyclic enones.[3] They have investigated the effect of ligand modification on the reaction and found that adjustment of the amine moiety had a large affect on both the yield and the enantioselectivity of the reaction, whereas the effects of variation of the binaphthol unit are less prominent. The most successful results were obtained using a chiral amine moiety in the binaphthol based

phosphoramidite ligand. When the phosphoramidite ligand containing the sterically demanding (*R,R*)-bis-(1-phenylethyl)amine structural unit, shown in Figure 5.1, is employed, yields of up to 95 % and e.e. values exceeding 98 % are achieved for the enantioselective 1,4-addition of R_2Zn compounds to a range of cyclic enones (illustrated in Figure 5.2). Enantioselectivities of up to 90 % were obtained for acyclic enones.[4]

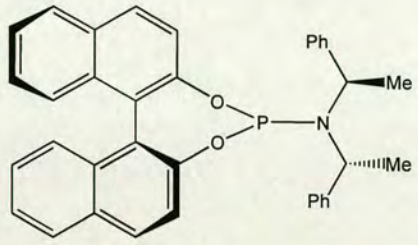

Figure 5.1 (*R,R*)-bis-(1-phenylethyl)amine phosphoramidite ligand

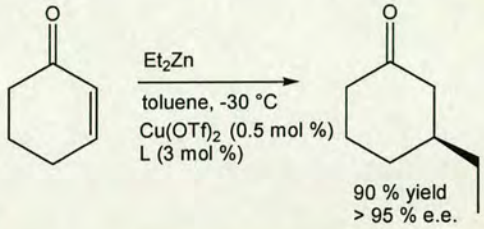

Figure 5.2 1,4 addition of Et_2Zn to a cyclic enone

Chiral phosphoramidites have also been utilised for palladium catalysed allylations,[5] and asymmetric Cu-catalysed Diels-Alder reactions.[6]

5.2 Synthesis of Chiral TREN Based Ligands

Chiral TREN based ligands can be synthesized by the nucleophilic ring opening of chiral aziridines, using ammonia as the nucleophile. The chiral aziridines can be prepared from the readily available chiral alcohols, as shown in Figure 5.3.

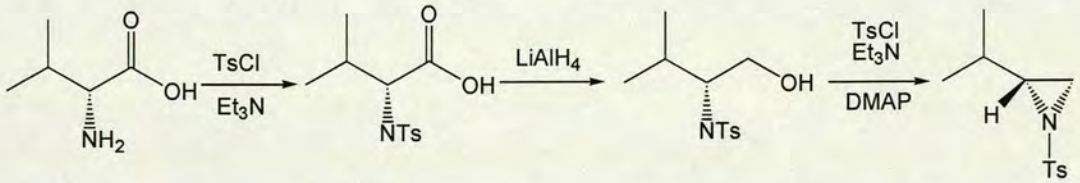

28 **29** **30** **31**

Figure 5.3 Synthesis of chiral aziridines

The introduction of an electron withdrawing substituent on the aziridine ring increases the rate of reaction for the ring opening. In this case, a tosyl group was attached to the nitrogen atom. Valinol, **28**, was treated with one equivalent of tosyl chloride in the presence of triethylamine and DMAP to form **29**. The carboxylic acid function was reduced to a hydroxyl group by treating with one equivalent of lithium

aluminium hydride to give **30**. Further reaction with triethylamine in the presence of tosylchloride afforded the aziridine, **31**. These intermediates are all highly crystalline and so are easily isolated from the reaction mixture in high yields by filtration. **31** can be ring opened by reacting with ammonia in methanol, to give **32**. This process requires heating for four days at 50 °C, followed by heating under reflux for two hours. In order to reduce this reaction time, I looked at the use of microwaves. Experiments were carried out varying both the length of the reaction and the temperature at which the reaction took place. The optimum reaction conditions were 60 seconds at 120 °C followed by 3540 seconds at 140 °C. Microwave irradiation on an organic reaction in the liquid state results in fast and homogenous *in situ* heating without creating sharp temperature gradients.[7] The disadvantage of using microwaves is that the machine can only take small, 10 ml reaction vessels, which limits the scale on which the reaction can be carried out. The reaction vessels are sealed Pyrex tubes and so the reaction could be carried out under an atmosphere of nitrogen. However, care had to be taken to avoid a build up of pressure.

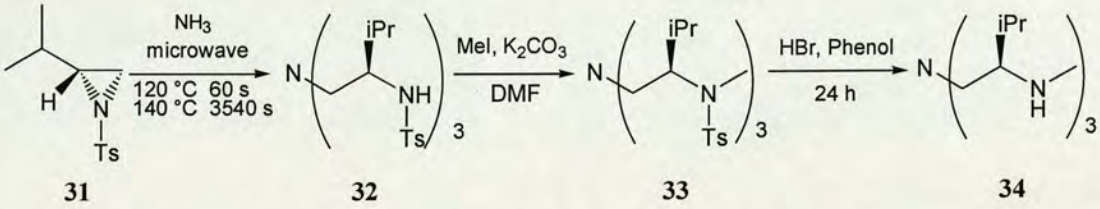

Figure 5.4 Formation of chiral tetra-amine ligands

All of the phosphoramidite ligands reported in the literature are synthesised from secondary amines. For this reason, the terminal amine groups in **32** were methylated. A method used previously in the group was to deprotonate the amine with sodium hydride in DMF and then to treat the ligand with methyl iodide. A simpler method was developed, using potassium carbonate to deprotonate **32** in place of sodium hydride, which is less easy to handle. The deprotection of the methylated product, **33** requires less harsh conditions than for the free amine ligand, **32**. This step was optimised by refluxing **33** in hydrogen bromide in the presence of phenol at 160 °C for 24 h. After an alkaline work-up, the product was purified by Kugelrohr distillation. These last three steps are illustrated in Figure 5.4.

5.3 Attempted Synthesis of Phosphoramidite Ligand

Feringa reports that phosphoramidites can be synthesised by the nucleophilic substitution of a phosphoryl chloride compound with a variety of secondary amines.[3] This method was adopted to try and convert the terminal amine nitrogen atoms of **34** into phosphoramidite functionalities, as shown in Figure 5.5. The phosphoryl chloride intermediate was generated *in situ* by treating enantiopure 2,2'-binaphthol with two equivalents of base and then one equivalent of phosphorus trichloride.

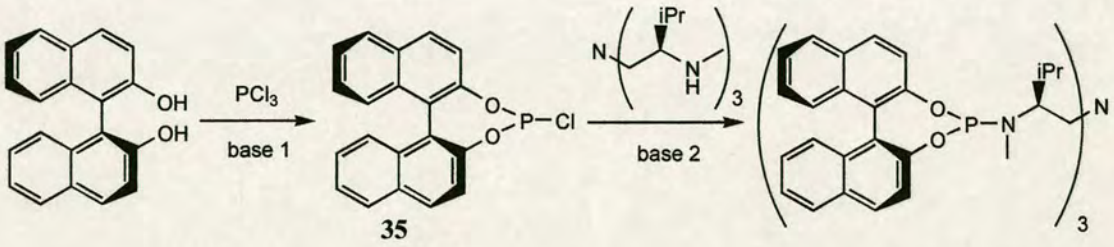

Figure 5.5 Synthesis of Phosphoramidite Ligands

The reaction conditions were varied by using different bases, different solvent systems, changing the reaction temperature and in the treatment of the phosphoryl chloride intermediate. These are listed in Table 5.1.

Reaction	Conditions for Deprotonation of Binaphthol	Treatment of **35**	Conditions for Deprotonation of **34**
1	NEt_3 / Toluene -78 °C	Filtered	NEt_3 / Toluene -40 °C
2	NEt_3 / Toluene -60 °C	Filtered	^nBuLi / THF -78 °C
3	NEt_3 / Toluene -60 °C	No Filtration	NEt_3 / Toluene -40 °C
4	NEt_3 / Toluene -78 °C	No Filtration	NEt_3 / Toluene -78 °C
5	^nBuLi / THF -78 °C	No Filtration	^nBuLi / THF -78 °C

Table 5.1 Reaction conditions for synthesis of phosphoramidite ligands

The reaction was followed by TLC and NMR analysis. The ^{1}H NMR spectra were generally very complicated due to the large number of phenyl protons. The ^{31}P NMR data was potentially more useful as the required ligand would have only one phosphorus environment. The phosphorus chemical shift typically observed for phosphoramidite phosphorus atoms lies in the region δ 140 – 150.[3]

The first reaction conditions resulted in one phosphorus environment but in totally the wrong region (δ 3.9). It was thought that the tetra-amine may be too hindered a nucleophile and so **34** was deprotected using the more reactive base ^{n}BuLi before mixing with the phosphoryl chloride intermediate. Again, the ^{31}P NMR data suggested that the desired product had not formed.

The failure of the reaction may be due to **35** decomposing during the filtration step. To try and circumvent this, the filtration step was omitted. Triethylamine was used as the base in both steps of the reaction. Different reaction temperatures were used. This reaction protocol proved more successful. The ^{31}P NMR spectrum showed several phosphorus environments, but these were in the region 140 – 150 ppm which is expected for phosphoramidite phosphorus atoms.[3] This suggests that the reaction is not going to completion and that a variety of products are being formed, with different numbers of arms successfully converted to phosphoramidite functionalities. The fifth reaction condition attempted was to use ^{n}BuLi as the base for both deprotonation steps. Unfortunately this was not successful either. The ^{31}P NMR spectrum showed a number of phosphorus environments had formed, and not all in the required region.

At this point, my time in Sweden came to an end and I was unable to make further progress with this ligand. The major drawback to this system is that the chiral TREN based tetra-amine framework is lengthy to synthesise, requiring many steps. More recent consultations between members of Moberg's lab and Feringa have revealed that the phosphoramidites are not as robust as the literature may lead one to believe and are best synthesised on a much larger scale than was used for these experiments.

5.4 Experimental

Chemicals were purchased from Lancaster and used as received. All solvents were distilled before use. CH_2Cl_2 was distilled from P_2O_5, THF from Na / benzophenone and triethylamine from CaH_2. DMF was dried over molecular sieves. ^1H and ^{13}C NMR spectra were recorded on a Bruker Aspec 3000 at 400.1 MHz and 100.6 MHz respectively. NMR measurements were carried out in $CDCl_3$ with $CHCl_3$ as an internal standard.

5.4.1 Synthesis of (R)-*N*-Tosylvaline, 29

Freshly ground tosyl chloride (28.6 g, 150 mmol), dry triethylamine (21.4 ml, 157 mmol) and acetone (72 ml) were added successively to a mixture of *(R)*-valine (16.75 g, 143 mmol), **28,** dissolved in aqueous NaOH 2 M (72 ml, 143 mmol) at 0 °C. This mixture was stirred at room temperature for 6 hours. Afterwards, it was washed with 2 x 100 ml Et_2O and the washings extracted with 20 ml NaOH 2 M. After acidifying with concentrated hydrochloric acid at –10 °C to pH = 1, the product was extracted from the mixture with 2 x 100 ml EtOAc. Evaporation yielded **29** as a white crystalline material. (36.04 g, 93 %)

^{1}H NMR (400.1 MHz, $CDCl_3$): δ 7.64 and 7.20 (AA'BB', 4H, J = 7.3, 7.0 Hz, aromatic), 5.18 (d, 1H, J = 9.8 Hz, N<u>H</u>), 3.71 (dd, 1H, J = 4.7, 9.8 Hz, <u>H</u>CCOOH), 2.33 (s, 3H, Ph-C<u>H</u>$_3$), 2.05 – 1.96 (m, 1H, <u>H</u>C(CH$_3$)$_2$), 0.87 (d, 3H, J = 6.8 Hz, (C<u>H</u>$_3$)$_2$CH), 0.79 (d, 3H, J = 6.8 Hz, (C<u>H</u>$_3$)$_2$CH)
^{13}C NMR (100.6 MHz, $CDCl_3$): δ 176.33 <u>C</u>OOH, 144.24, 137.85, 130.35, 127.58, <u>Ts</u>N, 61.88 <u>C</u>CCOOH, 31.33 <u>C</u>(CH$_3$)$_2$, 21.04 Ph<u>C</u>H$_3$, 19.41 C(<u>C</u>H$_3$)$_2$, 17.57 C(<u>C</u>H$_3$)$_2$

5.4.2 Synthesis of (R)-*N*-Tosylvalinol, 30

Lithium aluminium hydride (6 g, 158 mmol) was added under an atmosphere of N_2 to dry Et_2O (300 ml) and refluxed for 30 minutes. After allowing to cool to room temperature, **29**, (16 g, 60 mmol) dissolved in 30 ml of dry Et_2O / THF (1:1), was added *via* a cannula wire, under an atmosphere of N_2. The mixture was refluxed for 30 minutes. After cooling to room temperature, the reaction was quenched by the

careful addition of aq. NaOH 1 M (6 ml) followed by distilled water (18 ml) at 0 °C. HCl 4 M (150 ml) was added to dissolve the aluminates. The organic / aqueous phases were separated. The organic layer was washed with 2 x 45 ml brine followed by 2 x 45 ml saturated $NaHCO_3$ solution. The solution was dried over $MgSO_4$ for 30 minutes and then filtered. Removal of the solvent *in vacuo* yielded **30** as a pale yellow solid. (13.78 g, 91 %)

^{1}H NMR (400.1 MHz, $CDCl_3$): δ 7.72 and 7.23 (AA'BB', 4H, J = 8.3, 8.0 Hz, aromatic), 4.95 (d, 1H, J = 8.3 Hz, N<u>H</u>), 3.51 – 3.49 (m, 2H, C<u>H</u>$_2$OH), 2.99 (ddd, 1H, J = 1.7, 6.1, 12.4 Hz, Ph-C<u>H</u>$_3$), 2.05 – 1.96 (m, 1H, <u>H</u>C(CH$_3$)$_2$), 0.87 (d, 3H, J = 6.8 Hz, (C<u>H</u>$_3$)$_2$CH), 0.79 (d, 3H, J = 6.8 Hz, (C<u>H</u>$_3$)$_2$CH)

^{13}C NMR (100.6 MHz, $CDCl_3$): δ 143.41, 138.34, 130.39, 127.89 <u>Ts</u>N, 63.47 <u>C</u>H$_2$OH, 61.42 <u>C</u>COOH, 29.34 <u>C</u>(CH$_3$)$_2$, 21.96 Ph<u>C</u>H$_3$, 19.54 C(<u>C</u>H$_3$)$_2$, 18.53 C(<u>C</u>H$_3$)$_2$

5.4.3 Synthesis of (R)-*N*-Tosyl-2-isopropylaziridine, 31

Dry triethylamine (45.65 ml, 328 mmol) was added to a mixture of **30,** (28.15 g, 109 mmol), toluene sulphonyl chloride (25.03 g, 131 mmol) and DMAP (2.67 g, 22 mmol) in 200 ml dry CH_2Cl_2. The pale yellow solution turned orange and was stirred for 30 minutes at –78 °C and then at room temperature over night. During this time, the solution turned a dark orange / red colour. The mixture was separated between 300 ml EtOAc and 300 ml HCl (0.1 M). The two phases were separated and the organic phase washed with H_2O. The aqueous phases were combined and saturated with solid NaCl and then extracted with 200 ml EtOAc. The combined organic layers were washed with 2 x 150 ml saturated $NaHCO_3$ solution and 2 x 150 ml brine and dried over $MgSO_4$. The solution was filtered and the solvent removed *in vacuo* to yield an orange / pale brown solid. The solid was filtered over silica gel with a mixture of CH_2Cl_2 / hexane (1:3). The filtrate was then evaporated to yield **31** as a white crystalline solid. (18.362 g, 70 %)

^{1}H NMR (400.1 MHz, $CDCl_3$): δ 7.76 and 7.26 (AA'BB', 4H, J = 8.3, 8.0 Hz, aromatic), 2.55 (d, 1H, J = 7 Hz, $C\underline{H}_2$), 2.46 – 2.42 (m, 1H, $\underline{H}CN$), 2.38 (s, 3H, Ph-$C\underline{H}_3$), 2.03 (d, 1H, J = 4.6 Hz, $C\underline{H}_2$), 1.37 – 1.30 (m, 1H, $\underline{H}C(CH_3)_2$), 0.84 (d, 3H, J = 6.8 Hz, $(C\underline{H}_3)_2CH$), 0.73 (d, 3H, J = 6.7 Hz, $(C\underline{H}_3)_2CH$)

^{13}C NMR (100.6 MHz, $CDCl_3$): δ 144.826, 135.62, 130.00, 128.51 $\underline{Ts}N$, 46.70 $\underline{C}H_2NTs$, 33.13 $\underline{C}HNTs$, 30.54 $\underline{C}(CH_3)_2$, 22.05 $Ph\underline{C}H_3$, 19.97 $C(\underline{C}H_3)_2$, 19.48 $C(\underline{C}H_3)_2$

5.4.4 Synthesis of (R,R,R)-Tris(*N*-tosyl-2-amino-3-methylbutyl)amine, 32

NH_3.MeOH (c = 1.80 moldm^{-3}), (14.2 ml, 26 mmol) was added to a solution of **31** (18.36 g, 77 mmol) in MeOH (10 ml) in a dry 250 ml round bottomed flask under an atmosphere of N_2. The reaction vessel was sealed and stirred at 50 °C for four days. MeOH (100 ml) was added and the mixture heated under reflux for two hours. After cooling to room temperature, **32**, as a white solid, was removed by filtration and washed with cold MeOH. (11.95 g, 64 %)

^{1}H NMR (400.1 MHz, $CDCl_3$): δ 7.76 and 7.18 (AA'BB', 12H, J = 8.2, 8.1 Hz, aromatic), 6.13 (d, 3H, J = 7.0 Hz, $N\underline{H}$), 3.77 – 3.73 (m, 3H, $\underline{H}CN$), 2.89 (t, 3H, J = 12.1 Hz, $\underline{H}CH$), 2.31 (s, 9H, aromatic, $C\underline{H}_3$), 2.09 (dd, 3H, J = 4.6, 12.6 Hz, $\underline{H}CH$), 1.65 – 1.61 (m, 3H, $\underline{H}C(CH_3)_2$), 0.74 (d, 9H, J = 6.8 Hz, $(C\underline{H}_3)_2CH$), 0.71 (d, 3H, J = 6.8 Hz, $(C\underline{H}_3)_2CH$)

^{13}C NMR (100.6 MHz, $CDCl_3$): δ 142.89, 140.17, 130.06, 127.49 $\underline{Ts}N$, 55.58 $N\underline{C}H_2$, 52.42 $\underline{C}HNHTs$, 31.86 $\underline{C}(CH_3)_2$, 21.91 $Ph\underline{C}H_3$, 18.79 $C(\underline{C}H_3)_2$, 18.63 $C(\underline{C}H_3)_2$

5.4.5 Synthesis of 32– using microwaves

The reaction was conducted under continuous microwave irradiation (2450 MHz, MicroWell 10) in sealed 10 ml Pyrex tubes, under an atmosphere of nitrogen. NH_3.MeOH (c = 1.80 moldm^{-3}), (1.4 ml, 2.6 mmol) was added to a solution of **31** (1.84 g, 7.7 mmol) in MeOH (8.6 ml) in a dry 10 ml Pyrex tube under an atmosphere of nitrogen. The reaction vessel was placed in the microwave. Both the reaction time

and the temperature reached were controlled. The optimum conditions were found to be heating for 60 seconds at 120 °C followed by 3540 seconds at 140 °C. After this time, **32** had formed as a white solid. This was isolated by filtration and washed with cold MeOH. (1.53 g, 82 %)

The ^{1}H and ^{13}C NMR spectra were identical to that observed when using conventional heating methods.

5.4.6 Methylation of 32

32 (3.732 g, 5.08 mmol) was placed in a dry round bottomed flask and dissolved in dry DMF (60 ml) under N_2 at 0 °C. To the cloudy suspension was added K_2CO_3 (8.41 g, 60.93 mmol), which had been previously finely ground and dried in the oven over night. The suspension was stirred at 0 °C for 30 minutes. After this time, MeI (1.9 ml, 30.46 mmol) was added slowly *via* a syringe. The solution was kept at 0 °C for a further 30 minutes and then stirred at room temperature overnight. Water (50 ml) was added to the cloudy suspension to destroy the excess MeI. After stirring at room temperature for 30 minutes, the aqueous layer was extracted four times with CH_2Cl_2, washed with 2 x 20 ml saturated $NaHCO_3$ solution and 2 x 20 ml brine, and dried over $MgSO_4$. After filtration, the CH_2Cl_2 was removed by filtration and the DMF by vacuum distillation to yield **33** as a white solid (3.498 g, 92 %)

^{1}H NMR (400.1 MHz, $CDCl_3$): δ 7.69 and 7.17 (AA'BB', 12H, J = 8.2, 8.1 Hz, aromatic), 3.67 – 3.62 (m, 3H, HCN), 2.87 (t, 3H, J = 12.1 Hz, HCH), 2.62 (s, 3H, TsNMe), 2.31 (s, 9H, aromatic, CH_3), 2.03 (dd, 3H, J = 4.6, 12.6 Hz, HCH), 1.77 – 1.71 (m, 3H, $HC(CH_3)_2$), 0.90 (d, 9H, J = 6.8 Hz, $(CH_3)_2CH$), 0.79 (d, 3H, J = 6.8 Hz, $(CH_3)_2CH$)

^{13}C NMR (100.6 MHz, $CDCl_3$): δ 143.47, 137.59, 129.92, 127.78 TsN, 60.25 NCH_2, 55.46 CHNHTs, 30.73 $C(CH_3)_2$, 30.52 NTsMe, 21.92 $PhCH_3$, 20.83 $C(CH_3)_2$, 20.03 $C(CH_3)_2$

5.4.7 Deprotection of 33

33 (3.25 g, 4.2 mmol), phenol (3.96 g, 42 mmol) and HBr (ww 48% aq.) (194 ml, 1.71 mol) were heated under reflux at 160 °C overnight. After allowing to cool to room temperature, solid NaOH was added until the solution was pH = 3. The mixture was extracted between EtOAc and H_2O. The organic layer was washed with water. The aqueous fractions were made basic by the addition of solid NaOH to pH > 13, saturated with NaCl and then extracted with CH_2Cl_2. The solvent was removed *in vacuo* and the resulting oil purified by Kugelrohr distillation at 110 °C to give **34** as a very pale yellow oil. (0.910 g, 69 %).

^{13}C NMR (100.6 MHz, $CDCl_3$): δ 63.07 N<u>C</u>H_2, 56.76 <u>C</u>HNHTs, 35.35 <u>C</u>$(CH_3)_2$, 28.66 NtsMe, 19.58 C$(\underline{C}H_3)_2$, 17.44 C$(\underline{C}H_3)_2$

5.4.8 Attempted Formation of Phosphoramidite Ligand

5.4.8.1 Reaction 1

(S)-2,2'-binaphthol (0.144 g, 0.50 mmol) was dissolved in toluene (5 ml) and warmed to 60 °C to give a pale yellow solution. This was added to a cooled solution of phosphorus trichloride (0.44 ml, 0.50 mmol) and triethylamine (0.14 ml, 1.0 mmol) in toluene (5 ml). The reaction was stirred at –78 °C for 2 h. The reaction mixture was then warmed to room temperature and filtered through celite into a toluene solution of **34** (0.05 g, 0.16 mmol) and triethylamine (0.068 ml, 0.48 mmol) at – 40 °C. The solution was warmed to room temperature and stirred for 16 h. After this time, the solution was filtered and concentrated *in vacuo* to yield a pale yellow solid.

^{1}H NMR ($CDCl_3$): showed many peaks in the aromatic region.
^{31}P NMR (101 MHz, $CDCl_3$): δ 3.9

5.4.8.2 Reaction 2

(S)-2,2'-binaphthol (0.144 g, 0.50 mmol) was dissolved in toluene (5 ml) and warmed to 60 °C to give a pale yellow solution. This was added to a cooled solution of phosphorus trichloride (0.44 ml, 0.50 mmol) and triethylamine (0.14 ml,

1.0 mmol) in toluene (5 ml). The reaction was stirred at –60 °C for 2 h. After this time, the solution was yellow and a small amount of white precipitate had formed. The reaction mixture was then warmed to room temperature and filtered through celite. The solvent was removed *in vacuo* to yield a yellow solid. This was redissolved in THF. In a separate flask, ^{n}BuLi (0.19 ml of a 2.5 M solution in hexane, 0.48 mmol) was added slowly to a THF solution of **34** (0.05 g, 0.16 mmol) at –78 °C. The solution was stirred at low temperature for 10 minutes and then transferred *via* cannula to the phosphoryl chloride solution. The solution was allowed to warm slowly to room temperature over 24 h to yield a clear yellow solution. The solvent was removed *in vacuo* to yield a yellow solid.

^{31}P NMR (101 MHz, $CDCl_3$): δ 5.5, 6.3

5.4.8.3 Reaction 3

(S)-2,2'-binaphthol (0.273 g, 0.96 mmol) was dissolved in toluene (10 ml) and warmed to 60 °C to give a pale yellow solution. This was added to a cooled solution of phosphorus trichloride (0.83 ml, 0.96 mmol) and triethylamine (0.27 ml, 1.9 mmol) in toluene (10 ml). The reaction was stirred at –60 °C for 2 h. The reaction mixture was then warmed to room temperature and stirred for 30 minutes. A solution of the tetra-amine ligand (0.075 g, 0.24 mmol) and triethylamine (0.10 ml, 0.72 mmol) in toluene (5 ml) was precooled to – 40 °C and transferred to the phosphoryl chloride solution at –40 °C. The solution was warmed to room temperature and stirred for 16 h. After this time, the solution was filtered to remove a small amount of white precipitate and concentrated *in vacuo* to yield a pale yellow solid.

^{31}P NMR (101 MHz, $CDCl_3$): δ 142.9, 145.6, 148.2

5.4.8.4 Reaction 4

The previous reaction was repeated on the same scale, but using a reaction temperature of –78 °C for the formation of the phosphoryl chloride intermediate and for the addition of **34**.

^{31}P NMR (101 MHz, $CDCl_3$): δ 143.2, 144.9

5.4.8.5 Reaction 5

(S)-2,2'-binaphthol (0.144 g, 0.50 mmol) was dissolved in THF (8 ml) and warmed to 60 °C to give a pale yellow solution. This was added to a cooled solution of phosphorus trichloride (0.44 ml, 0.50 mmol) and triethylamine (0.14 ml, 1.0 mmol) in THF (8 ml). The reaction was stirred at –78 °C for 2 h. After this time, the solution was a brighter yellow colour. The reaction mixture was warmed to room temperature and stirred for 10 minutes. In a separate flask, ^{n}BuLi (0.19 ml of a 2.5 M solution in hexane, 0.48 mmol) was added slowly to a THF solution of **34** (0.05 g, 0.16 mmol) at –78 °C. The solution was stirred at low temperature for 30 minutes and then transferred *via* cannula to the phosphoryl chloride solution. The solution was allowed to warm slowly to room temperature over 24 h to yield a cloudy yellow solution. The solvent was removed *in vacuo* to yield a yellow solid.

^{31}P NMR (101 MHz, $CDCl_3$): δ 3.4, 138.9, 142.4

5.5 References

1. M. Cernerud, H. Adolfsson and C. Moberg, *Tetrahedron : Asymmetry*, 1997, **8**, 2655

2. B. L. Feringa, *Acc. Chem. Res.*, 2000, **33**, 346

3. L. A. Arnold, R. Imbos, A. Mandoli, A. H. M. De Vries, R. Naasz and B. L. Feringa, *Tetrahedron*, 2000, **56**, 2865

4. B. L. Feringa, *Angew. Chem., Int. Ed. Engl.*, 1997, **36**, 2620

5. G. Buono, J. M. Brunel and B. Del Campo, *Tetrahedron: Asymmetry*, 2000, **11**, 3585

6. G. Buono, J. M. Brunel and A. Tenaglia, *Tetrahedron Lett.*, 1998, **39**, 9663

7. U. Bremberg, M. Larhed, C. Moberg and A. Hallberg, *J. Org. Chem.*, 1999, **64**, 1082

6 QSn – A Novel Tripodal Ligand

This Chapter describes the synthesis of the novel tripodal ligand QSn, $^{n}BuSn(C_6H_4PPh_2)_3$, **36**.

6.1 Rationale for Choosing Ligand System

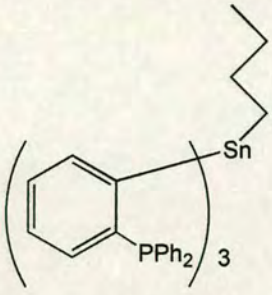

Figure 6.1 36

$^{n}BuSn(C_6H_4PPh_2)_3$, **36**, shown in Figure 6.1, has a central tin atom that is connected to three diphenylphosphinophenyl rings. The butyl group should block the central tin atom from coordinating to metals. The ligand is potentially tridentate and there are two sp^2 carbon atoms attaching the three donor phosphorus atoms to the central tin atom. Provided that the ligand coordinates through all three phosphorus atoms, the ligand metal geometry should twist to yield a C_3 symmetric complex, as described in Section 1.3.3.

Although the ligand appears to be fairly bulky, there are many examples in the literature of similar diphenylphosphine donor ligands forming stable complexes with a wide range of metals.

6.2 Work Previously Carried Out On Related Systems

36 is based on the ligand systems designed by Venanzi and co-workers. They have prepared a series of potentially tetradentate ligands containing a phosphorus, arsenic or antimony central atom and phosphorus or arsenic donor atoms.[1-3] They are based on the framework structure shown in Figure 6.2

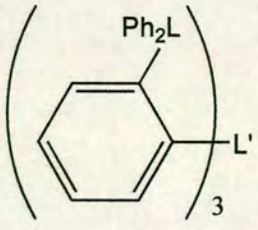

L'	Ligand	L
P	QP	P
As	QAS	As
As	ASTP	P
Sb	SBTP	P
P	PTAS	As
Sb	SBTAS	As

Figure 6.2 Tetradentate group (V) ligands

Metal - Group (V) donor ligand bonds are generally largely covalent. This is due to the high polarisability of the donor atoms, which use hybrid orbitals of the sp^3 type for σ-bond formation, and due to the contribution from π-bond formation, which involves the transfer of charge from filled d-orbitals of the metal atom to vacant orbitals on the ligand. This π-acidity has been used to explain the ability of phosphine donor groups to stabilize unusually low oxidation states. For example, the Co(I) complex $[Co(CO)(Q)]BPh_4$, (Q = QP, QAS), is stable towards air oxidation both in the solid state and in solution.[4] Phosphines generally bind very readily to metal complexes containing soft ligands that have a high tendency to form π-bonds, e.g. CO, NO, N_2, CN^-. In comparison, the tendency to form metal compounds with highly electronegative ligands such as F^-, OH^-, and H_2O is much less common. However, QP has been used to isolate hydroxo-phosphino complexes of the type $[M(OH)QP]Y$ (Y = BF_4, BPh_4) and aqua-phosphino complexes of the type $[M(H_2O)QP](BF_4)_2$ with metal ions (M = Co, Ni).[5]

Metal complexes formed with these ligands have been studied extensively.[6] There are two main types of complex in which the ligand coordinates in a tetradentate manner. The largest class of compounds is that where the ligand forms five coordinate, trigonal bipyramidal complexes of the type $[M^{n+}X(Q)]^{(n-1)+}$ (X= halogen, Q = QP or QAS). This has been confirmed by X-ray structural analysis. The preferential formation of trigonal bipyramidal geometries is due to the steric requirements of the ligand. After coordination, the bonds about the apical donor atom are tetrahedral so that the positions of the three donor atoms will lie around a three-fold axis of symmetry. For complexes of QP or QAS with transition metals, it is found that the donor-donor distances are too short for the formation of tetrahedral complexes but just right for the formation of trigonal bipyramidal complexes.

Trigonal bipyramidal complexes of QP and QAS ligands with d^7 metal ions often show an appreciable distortion towards a square pyramidal structure. For example, the Co(I) complex [CoH(QP)] has a d^8 configuration in which the d_{xy} and $d_{x^2-y^2}$ orbitals are fully occupied and the coordination geometry is almost regular

trigonal bipyramidal. In comparison, the Co(II) complex containing the same ligand $[CoCl(QP)]BPh_4$ has a d^7 configuration in which one of the two orbitals is singly occupied. The orbital degeneracy of this configuration is removed by a distortion towards square pyramidal.[7, 8] This can be explained by the Jahn-Teller effect.

The ligands form six coordinate, octahedral complexes of the form $[M^{n+}X_2(Q)]^{(n-2)+}$ (M = Rh, Pd, Pt; X = halogen; Q = QP or QAS). Fe(II) is interesting in that it can form both penta- and hexa- coordinate complexes with QP.[9] The penta- coordinate complexes are of the type $[FeX(QP)]^+$ (X = Cl, Br and I), have trigonal bipyramidal structures and two unpaired electrons; whilst the hexa- coordinate complexes are of the type $[FeX_2(QP)]$ (X = NCS and CN), have an octahedral structure and are diamagnetic. Ru(II) and Os(II) also form octahedral complexes with X = Cl and these are surprisingly stable to oxidation.

There has been report of the isolation of a seven coordinate complex of Ir(III), $[IrHBr(PPh_3)(QP)]BPh_4$.[10] All four phosphorus atoms of the QP ligand are bonded to the central iridium ion and the complex is hepta- coordinate. Seven coordinate complexes are also observed with molybdenum and tungsten, $[MX_2(CO)(QP)]$ (X = Cl, Br, I; M = Mo, W).[11]

QP can act as a tridentate ligand in six coordinate complexes such as $[M(CO)_3(QP)]$ (M = Cr or W).[3, 12] In these complexes, the central phosphorus atom and two of the ligand arms are coordinated with the other arm dangling free. QP and QAS act as bidentate ligands when coordinated to Hg(II) to form complexes of the type $[HgX_2(Q)]$ (X = Cl, Br or I; Q = QP or QAS).[6] The X-ray crystal structure of $[HgBr_2(QAS)]$ showed that the QAS ligand was acting as a bidentate donor coordinated through only two of its terminal donor atoms. An explanation for the occurrence of this coordination mode is that Hg(II) is d^{10} and so a coordination number of greater than four will place electrons in antibonding orbitals.

6.3 Synthesis of Ligands

QAS was the first of this series of ligands to be synthesized. It is prepared by treating arsenic trichloride with three equivalents of *o*-(diphenylarsino)phenyllithium under an atmosphere of nitrogen, followed by hydrolysis to yield the tripodal ligand in 24 % yield.[1] The other ligands can all be prepared in a similar way, using *o*-(diphenylphosphino)phenyl-lithium, **38**, for the ligands containing tripod arms with phosphorus donor atoms. This method was adopted for the synthesis of the novel ligand **36.**The reaction scheme is illustrated in Figure 6.3.

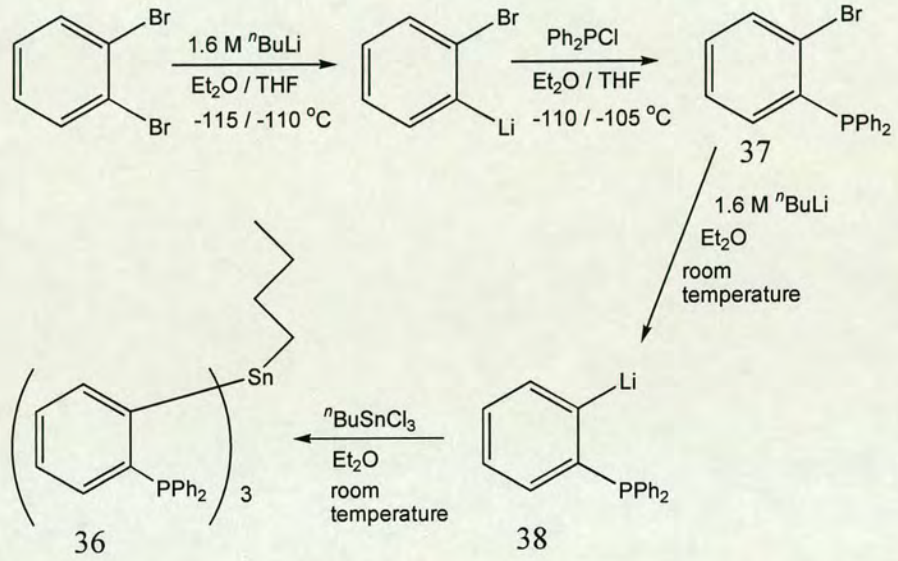

Figure 6.3 Reaction scheme for the synthesis of QSn

In this thesis, **38** was made following the procedure described by Harder *et al.*[13] from 1-bromo-2-(diphenylphosphino)benzene, **37**. This starting material is commercially available but is easily synthesized from dibromobenzene, at a lower cost. Dibromobenzene was treated with one equivalent of ^{n}BuLi to form 1-bromo-2-lithhiobenzene. This was treated with chlorodiphenylphosphine and after work-up, **37** was obtained as a pale yellow oil that solidified on standing. This could be recrystallised from dry ethanol to yield large white crystals in good yield, (75 %).

38 was prepared by lithium-bromine exchange between ^{n}BuLi and **37** in diethyl ether at room temperature. **38** forms as a crystalline material that consists of dimeric aggregates in which the lithium atoms are solvated by an additional diethyl ether molecule, making the lithiate relatively stable. **38** can be isolated or used *in situ* to generate the tripod ligand. **36** was synthesised by generating the **38** *in situ*, followed by treatment with butyltintrichloride. **36** was isolated as a pale yellow oil. Addition of ethanol led to the formation of a white crystalline material. Recrystallisation from DCM and ethanol yielded large colourless blocks suitable for X-ray crystal analysis, in moderate yield, (64 %). The crystal structure of **36** is shown in Figure 6.4

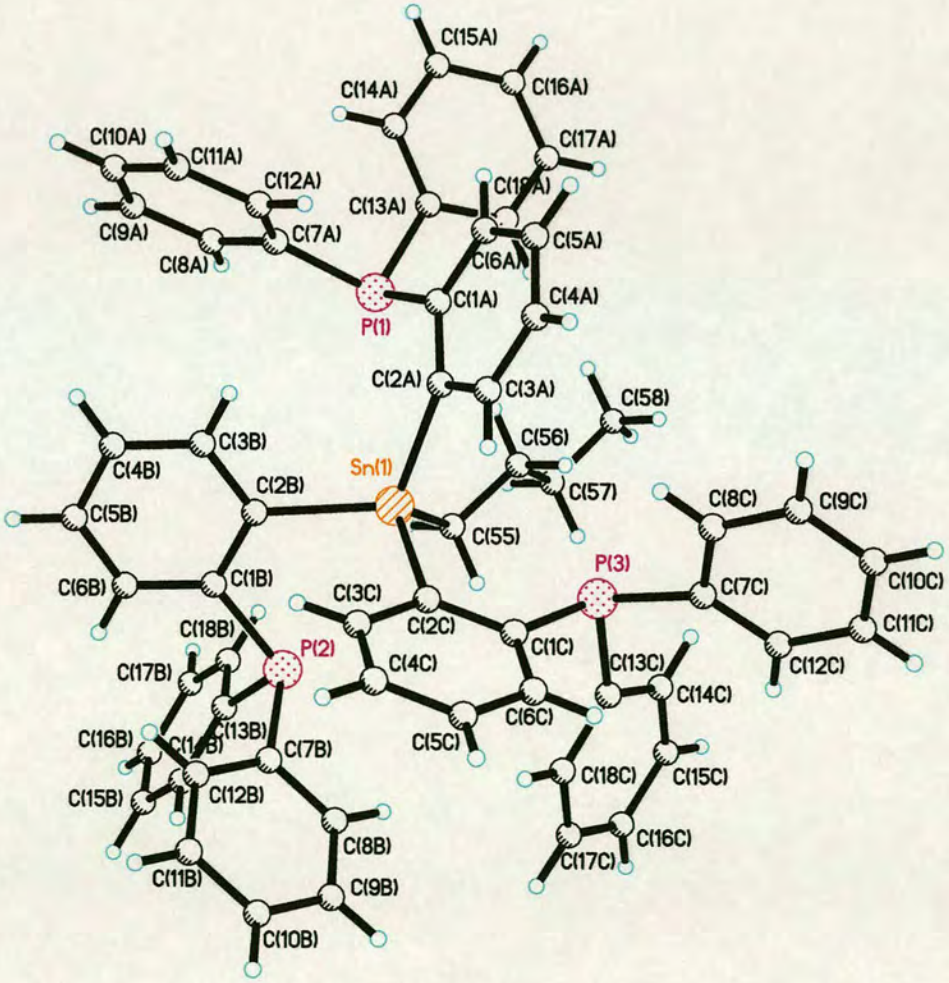

Figure 6.4 X-ray crystal structure of ^{n}BuSn($C_6H_4PPh_2$)$_3$

The geometry about the central tin atom is distorted tetrahedral. Table 6.1 shows some selected bond lengths and angles for the ligand. The bond connecting the central tin atom to the butyl chain is slightly shorter than the bonds connecting the tin atom to the phenyl rings. (2.151(3) Å compared with 2.166(3) Å).

Bond	Length / Å
Sn(1)-C(55)	2.151(3)
Sn(1)-C(2B)	2.159(2)
Sn(1)-C(2C)	2.170(3)
Sn(1)-C(2A)	2.170(3)

Angle	Size / °
C(55)-Sn(1)-C(2B)	112.94(9)
C(55)-Sn(1)-C(2C)	117.32(10)
C(2B)-Sn(1)-C(2C)	102.49(9)
C(55)-Sn(1)-C(2A)	111.63(9)
C(2B)-Sn(1)-C(2A)	111.75(9)
C(2C)-Sn(1)-C(2A)	99.75(9)

Table 6.1 Selected bond lengths / Å and bond angles / ° for $^{n}BuSn(C_6H_4PPh_2)_3$

The ^{31}P NMR spectrum shows one signal at δ –0.15 with three sets of satellite signals. One low intensity set of signals is seen at $J = 69.1$ Hz and is due to coupling to ^{13}C. There are two spin active tin isotopes, shown in Table 6.2, which exist in approximately the same abundance. They have similar gyromagnetic ratios and so will have similar coupling constants to the phosphorus atom. Therefore, it is unlikely that satellites due to the two different isotopes could be resolved. The set of satellite signals at $J = 30.83$ Hz can be ascribed to the two tin isotopes. There is also a pair of satellite signals at $J = 16.94$ Hz, but we are unable to assign these.

Isotope	Spin	Natural Abundance / %	Gyromagnetic Ratio
^{119}Sn	½	8.58	10.0318
^{117}Sn	½	7.61	9.589

Table 6.2 NMR active Sn isotopes

The ^{1}H NMR spectrum of **36** is very complicated in the aromatic region due to the large number of phenyl protons. The signals attributable to the butyl chain can easily be assigned and act as a spectroscopic handle for the ligand. The butyl chain also leads to characteristic stretches in the infrared spectrum: ν_{max} 2954 cm^{-1}, (CH_3 antisymmetric stretch); 2919 cm^{-1}, (CH_2 antisymmetric stretch); 2869 cm^{-1}, (CH_3 symmetric stretch); 2850 cm^{-1}, (CH_2 symmetric stretch).

6.4 Complexation Studies of QSn

Having synthesised the novel ligand, the next step was to investigate its coordination chemistry.

6.4.1 Coordination to Group VI Metals

Molybdenum and tungsten complexes with tripod ligands have successfully been synthesised starting from molybdenum and tungsten hexacarbonyls.[11] In order to favour the formation of a complex in which **36** coordinates to the metal through all three tripod arms, the hexacarbonyl complexes were refluxed in excess acetonitrile to exchange three of the carbonyl ligands for more labile acetonitrile ligands, prior to reacting with **36**. Molybdenum hexacarbonyl is more reactive than the tungsten analogue and only requires heating under reflux for four hours. In comparison, tungsten hexacarbonyl requires a reaction time of forty hours for the successful conversion to $[W(CO)_3(MeCN)_3]$. The generation of these nitrile derivatives was reported previously by Tate *et al.*[14]

6.4.1.1 Coordination to Tungsten

36 was added to a yellow solution of $[W(CO)_3(MeCN)_3]$ in benzene at room temperature. The solution was heated under reflux for eight hours. During this time, the solution turned a dark orange colour and then eventually dark red. The solvent was removed to yield a mixture of dark orange and yellow solids. To separate out the different complexes present, the mixture was redissolved in the minimum volume of benzene and filtered onto a column of silica. Two yellow bands were observed and subsequently eluted with benzene. The solvent was removed to yield an orange oil in both cases. Recrystallisation was attempted from benzene layered with *n*-heptane, which gave a pale orange crystalline material. The first band was identified as unreacted $[W(CO)_3(MeCN)_3]$. The second band was identified as $[W(CO)_4(QSn)]$, **39**. The mass spectrum (FAB+) showed a molecular ion at *m/z* 1256 and the sequential loss of four carbonyl groups. The crystals obtained from benzene layered with *n*-heptane were recrystallised from DCM and ethanol to yield colourless block shaped crystals suitable for X-ray analysis.

The X-ray crystal structure of **39**, illustrated in Figure 6.5, shows that two of the tripod arms are coordinated to the tungsten, whilst the third arm remains uncoordinated. This results in the formation of one eight membered chelate ring. The two phosphine atoms occupy cis positions in the equatorial plane and carbonyl groups occupy the remaining four coordination sites on the tungsten atom. It is interesting that the final product contains four carbonyl groups when the starting material contains only three. It is most likely that there is some form of carbonyl exchange occurring between different complexes in the reaction solution, however the exact mechanism cannot be explained.

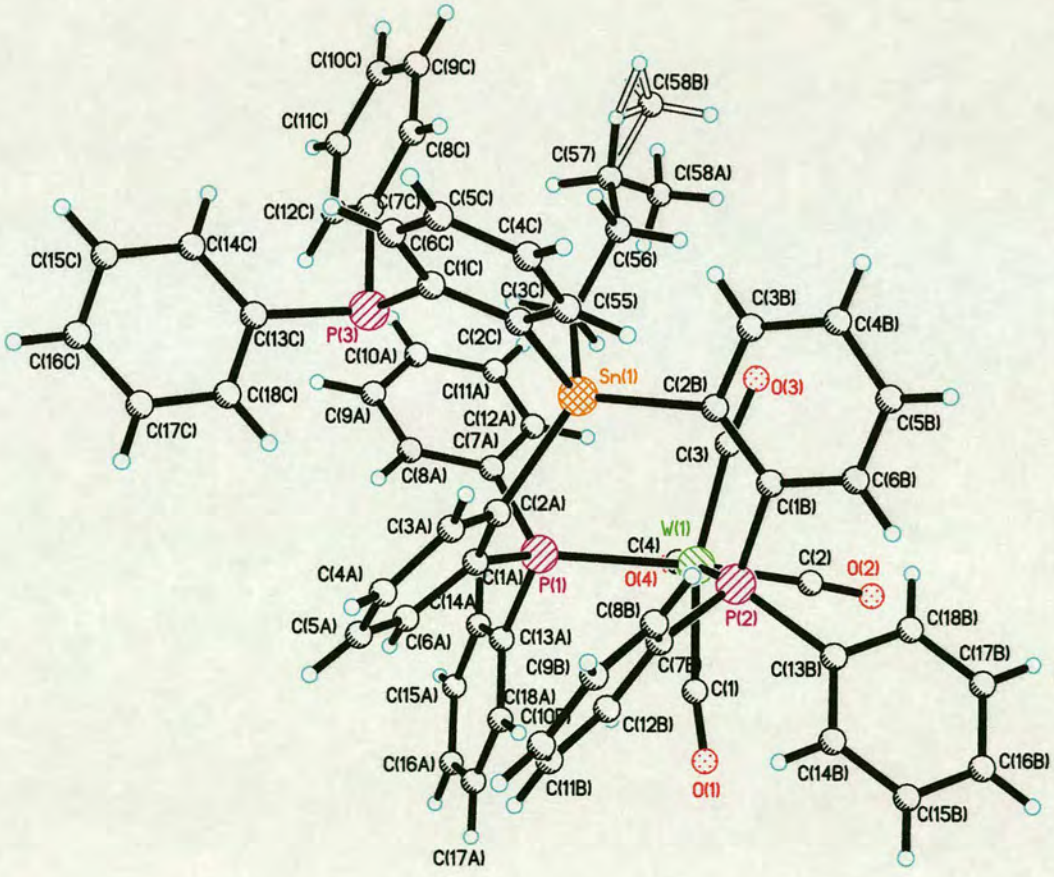

Figure 6.5 X-ray crystal structure of ^{n}BuSn(C$_6$H$_4$PPh$_2$)$_3$W(CO)$_4$

Table 6.3 shows some selected bond lengths and angles in **39.** The two phosphorus to tungsten bonds are of very similar length (W(1)-P(1) = 2.5441(7) and W(1)-P(2) = 2.5525(7) Å), whilst the four tungsten to carbon bonds are shorter (1.972(3) – 2.025(3) Å). There is a distorted octahedral environment about the tungsten atom. The sterically bulky diphenylphosphine groups occupy the most room in the equatorial plane and result in the carbonyl groups being compressed together ((P(1)-W(1)-P(2) = 101.83(2)°). The coordination geometry around the tin atom is virtually identical to that in the free ligand.

Bond	Length / Å
W(1)-C(2)	1.972(3)
W(1)-C(4)	1.978(3)
W(1)-C(3)	2.022(3)
W(1)-C(1)	2.025(3)
W(1)-P(1)	2.5441(7)
W(1)-P(2)	2.5525(7)
Sn(1)-C(55)	2.146(3)
Sn(1)-C(2A)	2.167(3)
Sn(1)-C(2B)	2.169(3)
Sn(1)-C(2C)	2.181(3)

Angle	Size / °
C(2)-W(1)-C(4)	81.77(12)
C(2)-W(1)-C(3)	85.19(12)
C(4)-W(1)-C(3)	93.65(12)
C(2)-W(1)-C(1)	81.54(12)
C(4)-W(1)-C(1)	89.47(12)
C(4)-W(1)-P(1)	83.22(9)
C(3)-W(1)-P(1)	100.57(8)
C(1)-W(1)-P(1)	93.57(8)
C(2)-W(1)-P(2)	92.78(9)
C(3)-W(1)-P(2)	89.82(8)
C(1)-W(1)-P(2)	85.79(8)
P(1)-W(1)-P(2)	101.83(2)
C(55)-Sn(1)-C(2A)	118.79(11)
C(55)-Sn(1)-C(2B)	109.19(11)
C(2A)-Sn(1)-C(2B)	118.07(10)
C(55)-Sn(1)-C(2C)	106.80(11)
C(2A)-Sn(1)-C(2C)	100.24(10)
C(2B)-Sn(1)-C(2C)	100.92(11

Table 6.3 Selected bond lengths / Å and bond angles / ° in $^{n}BuSn(C_6H_4PPh_2)_3W(CO)_4$

NMR analysis suggests that the complex has the same structure in solution. The ^{31}P NMR spectrum shows a peak at –4.12 ppm, in which satellites to Sn are absent, for the uncoordinated phosphorus arm and a doublet of doublets at 29.81 ppm for the two coordinated phosphorus atoms. Although in similar environments, these two coordinated phosphorus atoms are chemically distinct and coupling between the two is observed. Satellite signals at J = 234 and 237 Hz can be assigned to coupling to ^{183}W (I = ½), which has a natural abundance of 14.28 %. Further satellite signals due

to coupling with the central tin atom can also be observed. The peak for the uncoordinated phosphorus is shifted slightly upfield from the phosphorus resonance in the uncoordinated ligand (-4.12 compared with –0.15 ppm in the free ligand). The uncoordinated phosphorus peak is very similar to the phosphorus peak in the free ligand and also has two sets of satellites. The ratio of the two coupling constants is 1.9 compared with 1.8 in the free ligand.

The solution infrared spectrum in chloroform contains four infrared active bands for the carbonyl groups at ν_{max} 2017, 1915, 1899 and 1871 (shoulder) cm^{-1}. This is as would be expected for an octahedral metal carbonyl complex of the form [*cis*-$L_2M(CO)_4$] with local C_{2v} symmetry at the metal centre.

Venanzi and Howell reported the synthesis of [$M(CO)_3$(QP)], (M = Mo, W), in which QP acts as tridentate ligand.[11] QP coordinates to the ligand through the central phosphorus atom and through two of the tripod arms. This could be converted to [$M(CO)_2$(QP)] in which QP acts as a quadridentate ligand. Phosphorus is a smaller atom than tin suggesting that QSn should not be too sterically hindered for all three arms to coordinate to tungsten. Several attempts were made at removing one of the carbonyl groups in order to encourage the remaining arm to coordinate to the metal centre.

Venanzi and Howell carried out the mono decarbonylation reaction by heating the tri carbonyl derivatives under pressure at approximately 240 °C / 0.1 mmHg for 72 h. This method was adopted for **39**. After heating for this time, the yellow crystals had turned a dark brown colour. The brown solid was extracted with benzene to yield a dark yellow solution. Infrared analysis and NMR spectroscopy showed that the ligand had decomposed.

An alternative method to remove carbonyl groups from metal complexes is through the use of the reagent trimethylamine*N*-oxide (TMNO).[15, 16] This is a more controlled method and requires less harsh reaction conditions. The metal complex is treated with one equivalent of TMNO in DCM at room temperature and stirred in the dark for two hours. The reaction proceeds *via* the nucleophilic addition of TMNO to the most positive carbonyl carbon atom in the complex. The carbonyl group is oxidised

to carbon dioxide, which is lost from the reaction mixture, and the trimethylamine coordinates to the metal centre. The trimethylamine group coordinates only very weakly to the metal centre and so is easily displaced by other ligands.

This method was applied to **39**. The reaction was followed by solution infrared spectra analysis. The reaction proved unsuccessful, with no change in the carbonyl region, even after stirring for forty-eight hours. After this time, **39** was recovered in crystalline form.

It may be that coordination of the third arm of **36** to the metal centre is too entropically unfavourable, as proposed by Huttner.[17] Alternatively, it may be that the phosphine group of the third arm of the tripod ligand in the tetracarbonyl complex is positioned too far away from the potential binding site. Rearrangement of the ligand so that the third arm is suitably placed would require an inversion at the metal centre and the energy required to do this may be too high. The relatively high electron density on the tungsten centre will result in there being a high electron density associated with the carbonyl groups due to back donation and so the carbonyl groups will be less susceptible to nucleophilic attack by the TMNO.

6.4.1.2 Coordination to Molybdenum

The reaction between $[Mo(CO)_3(MeCN)_3]$ and **36** was carried out in DCM at 0 °C. The reaction mixture was stirred at 0 °C for one hour and then warmed to room temperature, during which time the orange solution turned red in colour. The excess solvent was removed to yield a dark orange solid. The solid was dissolved in minimal DCM and the solution filtered by cannula filtration. Red block shaped crystals, **40,** suitable for X-ray analysis were grown by vapour diffusion of diethyl ether into a DCM solution of the complex. Yellow crystals of unreacted $[Mo(CO)_3(MeCN)_3]$ and some colourless block shaped crystals of **36** also grew. Unfortunately only a small amount of material constituting the ligand bound to the metal was formed. The crystals are stable in air for a short period of time but decompose to a brown solid over 24 h. This may explain the poor CHN values, as there was a delay between the submission and analysis of the material, prior to the sensitivity of the product being known.

The structure of **40** obtained by X-ray analysis shows the complex to be $^{n}BuSn(C_6H_4PPh_2)_2$ $(C_6H_4COPPh_2)Mo(CO)_2$. This is derived by partial fragmentation of the ligand to form the fragments $Ph_2P(C_6H_4)$, **41**, and $BuSn(CO)(C_6H_4PPh_2)_2$. The structure of these two fragments is shown in Figure 6.6.

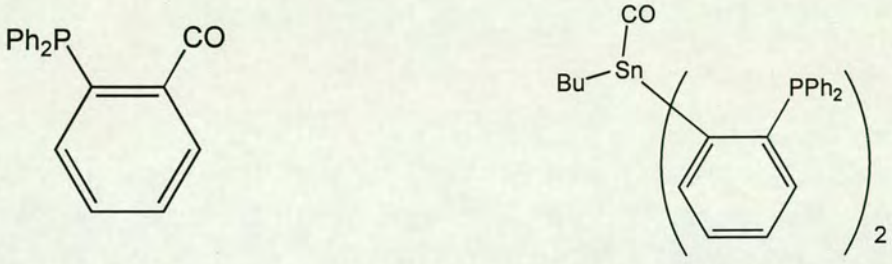

41 **42**

Figure 6.6 Ligand fragments formed upon coordination to molybdenum

41 chelates the Mo centre through the phosphorus atom and a benzyl carbonyl group formed by the nucleophilic addition to an Mo-CO ligand, while **42** coordinates to Mo *via* a Sn-Mo bond and its two phosphorus donor atoms. The Mo has one terminal carbonyl ligand and there is a second carbonyl ligand, which asymmetrically bridges the Mo-Sn bond. This represents the first example of a carbonyl group bridging a main group metal and a transition metal, as far as we are aware. A search of the X-ray crystallography database revealed no other examples. Figure 6.7 shows a plot of the entire crystal structure of **40**.

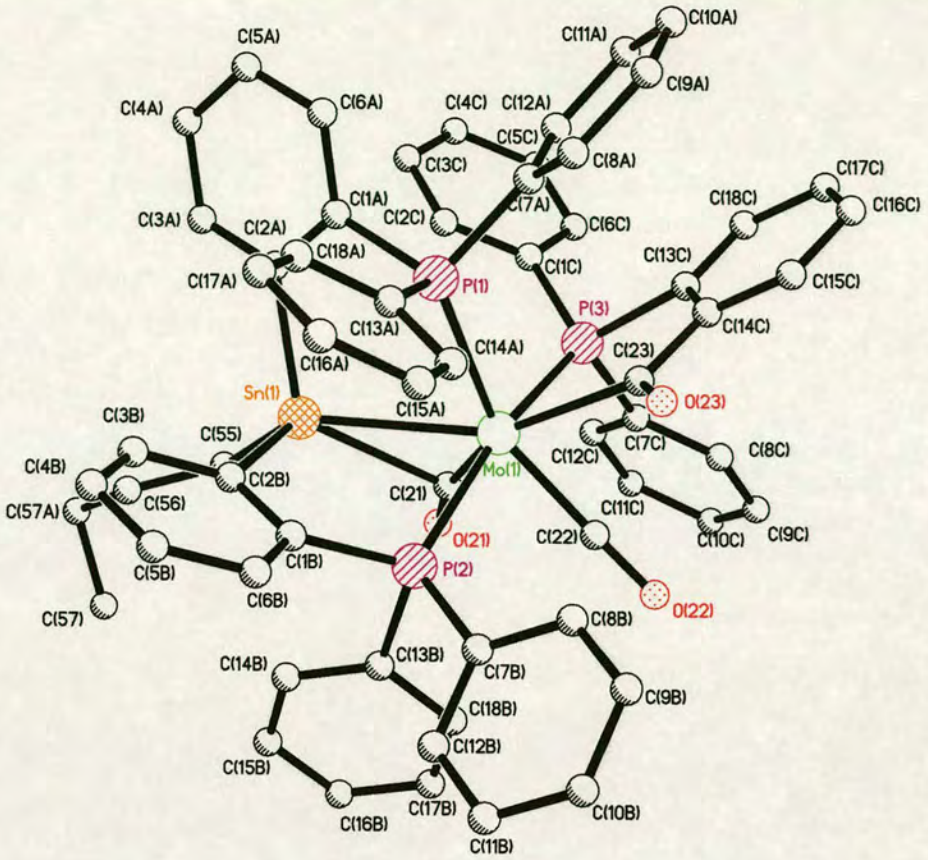

Figure 6.7 X-ray crystal structure of ^{n}BuSn($C_6H_4PPh_2$)$_2$ ($C_6H_4COPPh_2$)Mo(CO)$_2$

Figure 6.8 shows a plot illustrating the coordination environment about the tin and the molybdenum atoms and the three different types of carbonyl groups.

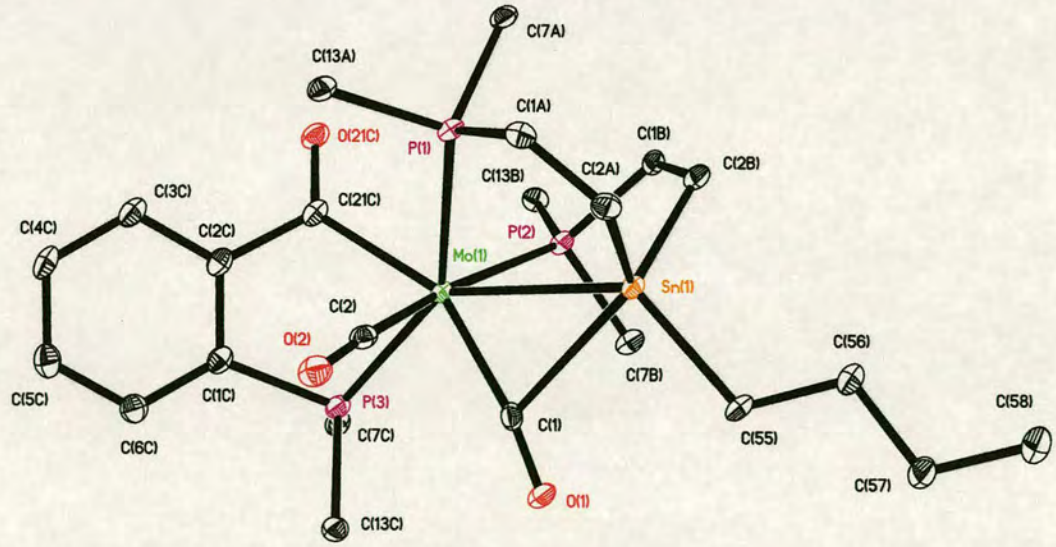

Figure 6.8 X-ray crystal structure of ^{n}BuSn($C_6H_4PPh_2$)$_2$ ($C_6H_4COPPh_2$)Mo(CO)$_2$ showing the coordination environment about Mo and Sn

Table 6.4 shows some of the bond lengths and angles in **40**. The phosphine group no longer connected to the tin ion is the most tightly bound, illustrated by the shorter P-Mo bond length (Mo(1)-P(3) = 2.4921(11) Å), compared to the phosphine groups still attached to the tin ion (Mo(1)-P(1) = 2.5882(11), and Mo(1)-P(2) = 2.6401(11) Å). The relatively large size of the tin ion enables it to support a coordination number of five. The coordination number of the molybdenum ion is now seven, which is an increase relative to the starting material.

Bond	Length / Å
Mo(1)-C(2)	1.941(4)
Mo(1)-C(1)	1.984(4)
Mo(1)-C(21C)	2.269(4)
Mo(1)-P(3)	2.4921(11)
Mo(1)-P(1)	2.5882(11)
Mo(1)-P(2)	2.6401(11)
Mo(1)-Sn(1)	2.8524(5)
Sn(1)-C(55)	2.144(4)
Sn(1)-C(2A)	2.145(4)
Sn(1)-C(2B)	2.160(4)
Sn(1)-C(1)	2.571(4)

Angle	Size / °
C(2)-Mo(1)-C(1)	83.04(17)
C(2)-Mo(1)-C(21C)	90.84(16)
C(1)-Mo(1)-C(21C)	149.92(15)
C(2)-Mo(1)-P(3)	81.47(12)
C(1)-Mo(1)-P(3)	78.07(11)
C(21C)-Mo(1)-P(3)	71.90(11)
C(2)-Mo(1)-P(1)	80.79(12)
C(1)-Mo(1)-P(1)	127.56(12)
C(21C)-Mo(1)-P(1)	79.88(11)
P(3)-Mo(1)-P(1)	146.24(4)
C(2)-Mo(1)-P(2)	170.28(12)
C(1)-Mo(1)-P(2)	90.75(12)
C(21C)-Mo(1)-P(2)	98.22(11)
P(3)-Mo(1)-P(2)	104.62(4)
P(1)-Mo(1)-P(2)	97.28(3)
C(2)-Mo(1)-Sn(1)	96.92(12)
C(1)-Mo(1)-Sn(1)	61.15(11)
C(21C)-Mo(1)-Sn(1)	148.91(11)
P(3)-Mo(1)-Sn(1)	138.98(3)
P(1)-Mo(1)-Sn(1)	71.80(3)
P(2)-Mo(1)-Sn(1)	73.49(2)
C(55)-Sn(1)-C(2A)	110.56(17)
C(55)-Sn(1)-C(2B)	108.86(16)
C(2A)-Sn(1)-C(2B)	103.61(15)
C(55)-Sn(1)-C(1)	86.98(15)
C(2A)-Sn(1)-C(1)	121.20(14)
C(2B)-Sn(1)-C(1)	123.54(14)
C(55)-Sn(1)-Mo(1)	129.38(12)
C(2A)-Sn(1)-Mo(1)	101.43(11)
C(2B)-Sn(1)-Mo(1)	100.03(11)
C(1)-Sn(1)-Mo(1)	42.51(9)

Table 6.4 Selected bond lengths / Å and bond angles / ° in $^{n}BuSn(C_6H_4PPh_2)_2(C_6H_4COPPh_2)Mo(CO)_2$

There are several examples in the literature of transition metal complexes containing a Mo-Sn bond, some of which are shown in Table 6.5.[18] The Mo-Sn bond in **40** is 2.8524(5) Å, which is longer than those shown in Table 6.5. The sum of the covalent radii for Mo and Sn is 2.70 Å, and the value of approximately 2.85 Å indicates that this is a relatively weak interaction. However, caution must be made in comparing the complexes as none of the others have a bridging μ_2-carbonyl group and they all have very different ancillary ligands.

Compound	Mo-Sn bond length / Å
$Cp_2Mo(SnPh_3)Me$	2.754
$\{(MeO)_3P\}_3(CO)_2ClMoSnBuCl_2$	2.774
$Cp_2Mo(SnPh_3)(CH_2)_4OSiMe_3$	2.769
$(MeCOC_5H_4)(CO)_3MoSnPh_2Cl$	2.736

Table 6.5 Compounds containing a Mo-Sn bond

One of the most interesting features of the crystal structure of **40** is the bridging μ_2-carbonyl group. Table 6.6 contains some selected bond lengths and angles, which describe the coordination of this carbonyl group.

Bond	Length / Å	Angle	Size / °
Mo(1)-C(1)	1.984(4)	O(1)-C(1)-Mo(1)	171.0(3)
Sn(1)-C(1)	2.571(4)	O(1)-C(1)-Sn(1)	111.2(3)

Table 6.6 Selected bond lengths / Å and bond angles / ° in 40 describing the μ_2-carbonyl group

Colton and McCormick defined an asymmetric μ_2-bridging carbonyl group as one where the two metal-carbon bond lengths are significantly different, although the C-O vector is still approximately normal to the metal-metal axis. A semi-bridging μ_2-carbonyl group is one in which the two metal-carbon bond lengths are markedly different and the two M-C-O angles are also different, such that the C-O vector is no longer perpendicular to the M-M direction.[19] The distinction between an asymmetric and a semi-bridging μ_2-carbonyl group is that provided the difference in M-C bond lengths is less than 0.3 Å and the difference in the M-C-O angles is less than 20°, the carbonyl group is referred to as asymmetric. The authors chose these values

arbitrarily. Using this distinction, the bridging carbonyl group in **40** would be described as semi-bridging.

The bridging carbonyl group in **40** is bound much more closely to the molybdenum ion compared to the tin ion. This is not surprising. Tin is a main group metal and so will not have any accessible d-electrons to donate to the carbonyl group. The lack of back bonding to the carbonyl group will result in a weaker bond, which is reflected by the longer Sn-C bond length. Carbonyl complexes of main group metals are rare due to the lack of backbonding, which results in the energy of the lone pair on the carbonyl carbon being very low. Molybdenum is able to act as a donor and an acceptor to the carbonyl group and so raises the energy of the carbonyl carbon. In the absence of the molybdenum ion, it is unlikely that the carbonyl group would be able to bond to the tin ion.

40 contains three different carbonyl groups, one terminal, one acyl and one bridging carbonyl group. Table 6.7 characterises the different types of carbonyl groups observed in the molybdenum complex.

Bond Numbering	Type	C-O Bond Length / Å (from X-ray structure)	Stretching Frequency (from infrared study) / cm^{-1}
C(1)-O(1)	Bridging	1.160(5)	1855
C(2)-O(2)	Terminal	1.166(5)	1902
O(21C)-C(21C)	Acyl	1.230(5)	1564

Table 6.7 Selected data describing the carbonyl groups in 40

The infrared spectrum in nujol showed three stretching frequencies in the carbonyl region. In comparison, the starting material has C_{3v} symmetry at the metal centre and exhibits two carbonyl stretching frequencies of 1915 and 1783 cm^{-1}.

The terminal and the bridging carbonyl groups have very similar bond lengths and stretching frequencies in the infrared spectrum. In order to conclusively confirm that the carbonyl group is indeed acting in a bridging mode, it would be useful to obtain the ^{13}C NMR spectrum, as the bridging carbonyl group would show tin satellites due to coupling to the tin atom. Unfortunately not enough of undecomposed ligand–metal

complex was available to record either the ^{13}C NMR spectrum, or the solution infrared spectrum.

6.4.2 Coordination to Manganese

There are several reports in the literature of manganese forming stable carbonyl complexes with phosphine ligands.[20, 21] For instance, the complexes *mer*-$[Mn(CO)_2L_3Br]$ and *fac*-$[Mn(CO)_3L_2Br]$, where L = PMe_2Ph or PMe_3, have been reported.[21] Following on from the relative success of obtaining metal complexes with the trisacetonitrile triscarbonyl group VI metals, it was decided to try and coordinate **36** to the manganese analogue. There are reports in the literature of phosphine and phosphite ligands substituting for the acetonitrile groups in *fac*-$[Mn(CO)_3(MeCN)_3]PF_6$, suggesting that this will be a suitable starting material. For example, two acetonitrile groups have been substituted for to give *fac*-$[Mn(CO)_3L_2(MeCN)]^+$, where L = PMe_2Ph, $P(OMe)_2Ph$ and $P(OMe)_3$; and three acetonitrile groups have been substituted for by phosphite ligands to give *fac*-$[Mn(CO)_2L_3(MeCN)]^+$.[22] However, substitution for three acetonitrile groups was not reported for phosphine ligands. This has been attributed to steric factors.

The salt *fac*-$[Mn(CO)_3(MeCN)_3]PF_6$ was easily prepared from manganese pentacarbonylbromide. $Mn(CO)_5Br$ can be synthesised as orange coloured micro crystals by treating a solution of dimanganese decacarbonyl with bromine following the procedure described by Quick *et al.*[23] *fac*-$[Mn(CO)_3(MeCN)_3]PF_6$ could then be synthesised as first reported by Reimann and Singleton.[22] $Mn(CO)_5Br$ was heated under reflux in excess acetonitrile for one hour. The desired product was then isolated in almost quantitative yield from an ethanolic solution, containing NH_4PF_6, on addition of water.

The reaction between *fac*-$[Mn(CO)_3(MeCN)_3]PF_6$ and **36** was followed by solution infrared studies. *fac*-$[Mn(CO)_3(MeCN)_3]PF_6$ shows two infrared stretching frequencies that are characteristic of complexes with C_{3v} symmetry. Progressive substitution of the acetonitrile groups will alter the local symmetry at the metal centre and so change the number of carbonyl stretches observed. Furthermore,

phosphine ligands have a better π-acceptor ability than acetonitrile groups and so a shift to higher stretching frequencies for the carbonyl groups is expected.

Reimann and Singleton reported the substitution of acetonitrile groups by phosphine ligands in *fac*-$[Mn(CO)_3(MeCN)_3]PF_6$ when a solution of the metal salt in chloroform was heated under reflux for fifteen minutes in the presence of the phosphine ligand.[22] This method, but with a longer reaction time of 1 h, was used with **36**, however no reaction took place. The reaction conditions were varied by changing the solvent system to THF and heating under reflux for four hours. Again, no reaction took place and the unreacted ligand was recovered from the reaction system. Moving to a system with a higher boiling point, the solvent was changed to diglyme. The solution was heated at 110 °C for thirty minutes. During this time, the clear yellow solution turned colourless and analysis by solution infrared showed the total disappearance of the carbonyl stretches and that the manganese complex had decomposed.

The reaction was repeated, again using chloroform as the reaction medium. This time the reaction was heated under reflux for 6 h. This was to try and achieve a balance between heating the reaction for sufficiently long enough to obtain complexation, but before the complex decomposed. Again, large colourless crystalline blocks of unreacted ligand were isolated at the end of the reaction. The unreacted ligand was removed by filtration. The clear, dark yellow solution was reduced in volume by half and layered with hexane. This resulted in the formation of small colourless crystalline blocks, $^{n}BuSn(C_6H_4PPh_2)_2Mn(CO)_3$, **41**, in extremely low yield, some of which were suitable for X-ray analysis. A plot of the crystal structure of **41** is shown in Figure 6.9.

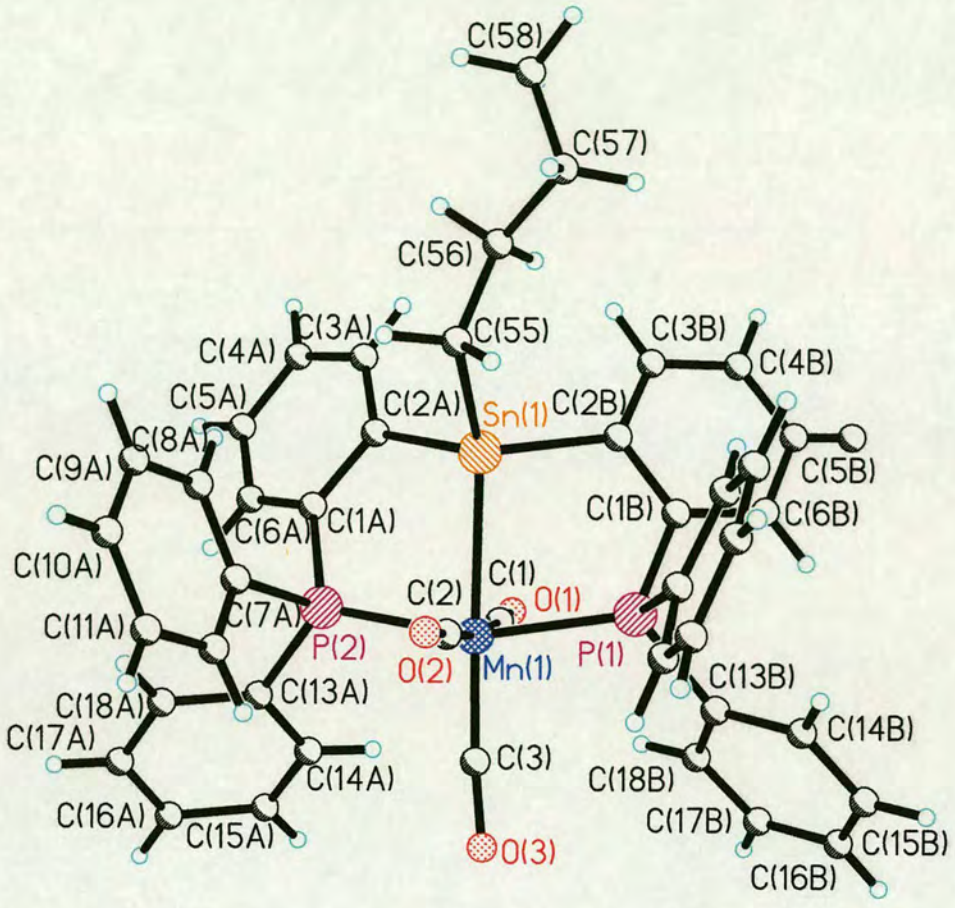

Figure 6.9 X-ray crystal structure of $^{n}BuSn(C_6H_4PPh_2)_2Mn(CO)_3$

The X-ray crystal structure of **41** shows that although a complex has formed, the ligand is no longer intact. One of the tripod arms has broken off and the ligand is coordinated to the manganese in a tridentate manner through the remaining two phosphine groups and the central tin atom. The other three coordination sites on the manganese ion remain occupied by the carbonyl groups. The two phosphine groups are coordinated trans to each other. This minimises the steric repulsion between the two sterically bulky ligand arms. The geometry at the central manganese ion is slightly distorted octahedral. The constraints of the ligand result in the octahedral geometry being slightly distorted so that the two phosphine groups lie slightly above the equatorial plane, towards the tin atom.

Bond	Length / Å
P(1)-Mn(1)	2.268(6)
P(2)-Mn(1)	2.277(6)
Mn(1)-C(3)	1.75(2)
Mn(1)-C(1)	1.85(2)
Mn(1)-C(2)	1.85(2)
Sn(1)-Mn(1)	2.570(3)
Sn(1)-C(2A)	2.125(18)
Sn(1)-C(2B)	2.162(18)
Sn(1)-C(55)	2.20(2)

Angle	Size / °
C(3)-Mn(1)-C(1)	95.9(8)
C(3)-Mn(1)-C(2)	91.4(8)
C(3)-Mn(1)-P(1)	97.5(6)
C(1)-Mn(1)-P(1)	87.1(6)
C(2)-Mn(1)-P(1)	92.7(6)
C(1)-Mn(1)-P(2)	86.3(6)
C(2)-Mn(1)-P(2)	91.7(6)
C(1)-Mn(1)-Sn(1)	84.8(5)
C(2)-Mn(1)-Sn(1)	87.9(6)
P(1)-Mn(1)-Sn(1)	80.74(15)
P(2)-Mn(1)-Sn(1)	81.59(15)
C(3A)-Mn(1)-P(2)	100.2(6)
C(2A)-Sn(1)-C(2B)	111.1(7)
C(2A)-Sn(1)-C(55)	107.6(8)
C(2B)-Sn(1)-C(55)	110.4(8)
C(2A)-Sn(1)-Mn(1)	97.9(5)
C(2B)-Sn(1)-Mn(1)	98.0(5)
C(55)-Sn(1)-Mn(1)	130.7(6)

Table 6.8 Selected bond lengths / Å and bond angles / ° in $^{n}BuSn(C_6H_4PPh_2)_2Mn(CO)_3$

Table 6.8 shows some of the bond lengths and angles around the manganese ion. Comparing these values with those for the group 6 metal carbonyl complexes, shown in Table 6.3 and Table 6.4, it can be seen that the length of the M-P bond is shorter for M = Mn than for M = Mo or W (average Mn-P = 2.273(6) Å compared with an average Mo-P = 2.5735(11) Å and W-P = 2.5483(7) Å). The environment around the tin atom is very distorted tetrahedral, however, the butyl group has large thermal parameters and is probably disordered.

The complex contains a tin – manganese bond. Complexes of transition metals in which a Group IV metal moiety acts as a donor ligand are quite common. One example is $Me_3SnMn(CO_5)$, which contains a tin – manganese bond which is 2.674(2) Å.[24] This is longer than the tin – manganese bond reported in **41**, which is 2.570(3) Å.

Table 6.9 shows some of the bond lengths and angles for the carbonyl groups in **41**. The carbonyl groups have rearranged to form the *mer* isomer. The infrared spectrum now shows three bands in the carbonyl region at ν_{max} 1988, 1925 and 1894 cm^{-1}, reflecting the decrease in symmetry. The carbonyl group coordinated *trans* to the tin atom is bound more tightly to the manganese ion than the other two carbonyl groups. This can be seen from the shorter Mn-C distance (1.75(2) Å compared with 1.85(2) Å), and the longer C-O length (1.21(2) Å compared with 1.13(2) Å and 1.119(19) Å) for the carbonyl *trans* to the tin atom. The three carbonyl groups are linearly bound to the manganese.

Bond	Length / Å
C(1)-O(1)	1.119(19)
C(2)-O(2)	1.13(2)
O(3)-C(3)	1.21(2)

Angle	Size / °
O(1)-C(1)-Mn(1)	178.3(16)
O(2)-C(2)-Mn(1)	178.3(17)
O(3)-C(3)-Mn(1)	174.1(16)

Table 6.9 Selected bond lengths / Å and angles / ° for the carbonyl groups in 41

Both the manganese ion in $[Mn(CO)_3(MeCN)_3]^+$ and the tungsten and molybdenum ions in $M(CO)_3(MeCN)_3$ (M = W, Mo) have six outer *d* electrons, however the manganese complex is positively charged and so the acetonitrile ligands will be more strongly coordinated to the metal centre and hence harder to displace. This may explain its decreased reactivity compared to the neutral carbonyl complexes.

6.4.3 Coordination to Ruthenium

There are numerous reports of ruthenium forming stable metal complexes with phosphines. Venanzi has had some success in coordinating QP to ruthenium,[25] although no X-ray structures of the resulting complexes have been reported. Ru(II) complexes of the form $[RuX_2QP]$, where X = Cl, Br, I, NCS, CN have all been synthesised. The Ru(0) complex, [Ru(CO)QP] has also been prepared. ^{31}P NMR and electronic spectra suggest that Ru(II) complexes with QP are six coordinate and have a distorted octahedral structure in which all four donor atoms of the QP ligand are coordinated to the metal, whilst the Ru(0) complex is five coordinate with a trigonal bipyramidal structure.

One method reported for the synthesis of [RuX_2QP] started from hydrated ruthenium trichloride and this same procedure was adopted for the first complexation reaction with **36**. Hydrated ruthenium trichloride was heated under reflux in ethanol, under an atmosphere of nitrogen for 24 h. During this time, the solution changed colour from dark brown, to dark green, finally turning deep blue. The exact identity of this intermediate species is not known. The solution was allowed to cool and one equivalent of **36** dissolved in DCM was added, followed by *n*-butanol. The mixture was stirred and heated gently whilst the DCM and some of the ethanol boiled off and then heated under reflux for 18 h. During this time, a very dark green solid precipitated out of solution. All attempts at obtaining this material in a crystalline form were unsuccessful. The mass spectrum (FAB+) provided some evidence for the formation of a complex with **36**, with peaks representing QSnRuCl; QSnRuCl with the loss of the butyl chain; and QSnRuCl with the loss of the butyl group and one of the tripod arms.

Venanzi used an alternative route to form the same ruthenium complex by starting from the triphenylphosphine complex $RuCl_2(PPh_3)_3$. It was hoped that the three diphenylphosphine donor groups of **36** would displace the triphenylphosphine ligands. This process is driven by the chelate effect, whereby the exchange of three monodentate ligands by one tridentate ligand is entropically favoured. A solution of [$RuCl_2(PPh_3)_3$] and one equivalent of **36** in benzene was heated under reflux under an atmosphere of nitrogen for 1 h, during which time the solution changed colour from dark brown to dark red. After cooling, the benzene was removed to leave a dark purple / brown solid. Recrystallisation from DCM and ethanol afforded colourless block shaped crystals but these were identified as unreacted ligand.

The third ruthenium starting material utilised was [(*p*-cymene)$Ru(MeCN)_3$]BF_4. This starting material could be prepared by treating the *p*-cymene ruthenium dichloro dimer [$RuCl_2$(*p*-cymene)]$_2$ with four equivalents of silver tetrafluoroborate in a solution of acetonitrile. This results in the precipitation of silver chloride out of solution, which acts as the driving force for the process. The addition of diethyl ether to the filtered solution causes the precipitation of the desired product.

It was hoped that the three arms of the tripod ligand would easily displace the three labile acetonitrile groups. To this end, one equivalent of the ligand was added to a well stirred solution of the ruthenium complex in THF. The pale green solution was heated under reflux under an atmosphere of nitrogen for 3 h. During this time, the solution turned a darker shade of green and then to brown. ^{1}H NMR analysis showed that the ligand had decomposed.

The final ruthenium starting material tried was $[RuCl_2(cod)]_n$, which is believed to have a polymeric, chloro-bridged structure. This is a useful precursor to Ru(II) complexes as the halogen bridge is easily cleaved. $[RuCl_2(cod)]_n$ is synthesised easily, following the method reported by Singleton *et al.*[26] Two equivalents of cyclooctadiene were added slowly to an ethanolic solution of ruthenium trichloride and then heated under reflux for 24 h. After this time, the product was isolated by filtration as a dark brown, highly insoluble crystalline solid.

With the aim of forming a metal complex, one equivalent of **36** was added to a suspension of $[RuCl_2(cod)]_n$ in acetonitrile. Acetonitrile was chosen as the solvent system because $[RuCl_2(cod)]_n$ is known to react with boiling acetonitrile to give $[RuCl_2(MeCN)_2(cod)]$, containing *cis*-acetonitrile ligands. It was hoped that **36** would then substitute for the labile acetonitrile groups. The dark brown suspension was heated under reflux under an atmosphere of nitrogen for 6 h but **36** remained uncoordinated.

6.4.4 Coordination to Rhodium

Rhodium metal complexes are used in various catalytic reactions, including the asymmetric hydrogenation of alkenes, as described in the introduction. With the hope of forming a catalytically active metal complex, one equivalent of **36** was added to an ethanolic solution of rhodium trichloride. The dark red solution was heated under reflux for 4 h during which time the solution turned orange and a yellow precipitate formed. The solution was filtered and the yellow precipitate washed with cold ethanol. Despite many attempts, it was not possible to obtain this material in a crystalline form.

The ^{1}H NMR spectrum of the yellow product contained a large number of peaks in the phenyl region that could not be accurately assigned. The mass spectrum (FAB+) contained peaks corresponding to a Rh(I) complex. The most intense peak of high molecular weight is at *m/z* 1098 and corresponds to [QSnRhCl]. There are also peaks at 1062 (QSnRh), 1042 (QSn(-Bu)RhCl) and at lower molecular weights, corresponding to fragments in which the tripod arms have broken down by varying extents. Unfortunately the CHN analysis does not support the formation of either the expected [$QSnRhCl_3$] or [QSnRhCl].

6.4.5 Coordination to Silver

Silver is able to support a large number of different metal geometries. With the hope of forming a tetrahedral complex in which **36** acts in a tridentate manner, one equivalent of the ligand was added to a THF solution of the silver tetrafluoroborate. The clear colourless solution was stirred overnight, under an atmosphere of nitrogen at room temperature. During this time, a white precipitate formed. This was isolated by filtration and washed with diethyl ether.

Both the CHN and the mass spectrometry results confirm the formation of a mononuclear complex [QSnAg]BF_4, **42**. Very fine needle shaped crystals could be grown by vapour diffusion of diethyl ether into an acetonitrile solution of the complex. Unfortunately they were not of suitable quality for X-ray analysis. Changing the solvent system with the aim of forming crystals of a different morphology was unsuccessful.

The ^{1}H NMR spectrum is not easily interpreted due to the similarity of the aromatic protons. The ratio of the integrals of the aromatic peaks to those in the region expected for the butyl chain are as expected for the desired product. The ^{31}P NMR spectrum suggests that **42** is mononuclear in solution. There is only one phosphorus environment, which is indicative of the ligand being coordinated to the metal through all three phosphine groups to give a C_3 symmetric complex in which all three phosphorus atoms are equivalent. The ^{31}P NMR spectrum at room temperature appears as a doublet of doublets. This is due to the presence of two NMR active Ag isotopes, occurring in similar abundances (see Table 6.10). The phosphorus chemical

shift is at 15.73 ppm. There is no central signal at this point as 100 % of the Ag is spin ½. This signal has been shifted downfield compared to the signal for the phosphine groups in the uncoordinated ligand, which resonates at –0.15 ppm.

Isotope	Spin	Abundance / %	Gyromagnetic Ratio
^{107}Ag	½	52	-1.0828
^{109}Ag	½	48	-1.2448

Table 6.10 NMR active Ag isotopes

The two coupling constants observed are $J(^{107}Ag\text{-}P)$ = 307.43 Hz and $J(^{109}Ag\text{-}P)$ = 355.01 Hz. The ratio of the coupling constants to the two isotopes is 1.15, which is equal to the ratio of their gyromagnetic ratios, as expected. The values of the coupling constants are similar to that reported for $[Ag(PPh_3)_3]BPh_4$ where $J(^{107}Ag\text{-}P)$ = 318 Hz,[27] giving further support for the formation of a mononuclear complex in which the ligand is coordinated through all three phosphine groups.

In the hope of being able to grow better quality crystals, the counter ion was exchanged for trifluoromethanesulphonate. This was achieved using silver trifluoromethanesulphonate in place of silver tetrafluoroborate. After stirring for 12 h, a grey precipitate formed. The CHN results confirmed the formation of a mononuclear complex $QSnAgCF_3SO_3$, **43**. A mixture of fine, strand like crystals and a smaller amount of colourless blocks could be grown from acetonitrile and diethyl ether. The strands were unsuitable for X-ray crystallography. A data set for the blocks was obtained but could not be refined very well, (R1 = 0.1926).

6.4.6 Coordination to Copper

Following on from the relative success of obtaining complexes with silver, the coordination of QSn to copper, another group 11 metal, was tried. Copper tetrakis(acetonitrile) tetrafluoroborate, $[Cu(MeCN)_4]BF_4$ was the starting material of choice, due to the presence of four labile acetonitrile groups. **36** was added to a well stirred solution of $[Cu(MeCN)_4]BF_4$ in acetonitrile. The clear, colourless solution was stirred under an atmosphere of nitrogen at room temperature for 48 h. Removal of the solvent resulted in the formation of a white powder. A white crystalline solid, **44,**

could be obtained from acetonitrile layered with diethyl ether. However, yet again these were not of sufficient quality for X-ray analysis.

The mass spectrum (FAB+) of **44** suggested the formation of a mononuclear copper complex, with peaks at 1024 (corresponding to QSnCu), 967 (QSn(-Bu)Cu) and further peaks corresponding to species with various extents of ligand fragmentation. The infrared spectrum was very similar to that recorded for **42**, which is also thought to be a mononuclear complex. The values obtained from the CHN analysis were lower than expected for either $[QSnCu]BF_4$ or for $[QSnCu(MeCN)]BF_4$. This can be explained by the presence of unreacted $[Cu(MeCN)_4]BF_4$ which will greatly lower the values of % C and % H and increase the % N. Due to this, it is not possible to deduce if there is still an acetonitrile group coordinated to the copper atom.

6.5 Changing the Size of the Central Ligand Atom

Attempts were made to extend this ligand system further by replacing the central tin atom with a smaller silicon atom. Various silicon trichlorides were used in the reaction with **38**. Initial attempts were made using either methyltrichlorosilane or hydridotrichlorosilane, however neither reaction yielded clean products. The success of the reaction is hard to measure by ^1H NMR analysis due to the complicated nature of the aromatic region. The protons on the central atom will come into resonance very close to zero and so will be hard to identify confidently over vacuum grease.

Phenyltrichlorosilane was also used as a starting material. The reaction was carried out in the same way as described previously and colourless crystals, $(C_6H_4)_3P(C_6H_5)$, **45**, were isolated. Although the ^1H NMR spectrum was too complex to be informative, the ^{31}P NMR spectrum showed the presence of only one phosphorus environment. The proportion of hydrogen obtained by CHN analysis was in very close agreement with the predicted values, however the percentage of carbon was not so accurate.

The X-ray analysis of **45** was most unexpected. The structure is shown in Figure 6.10.

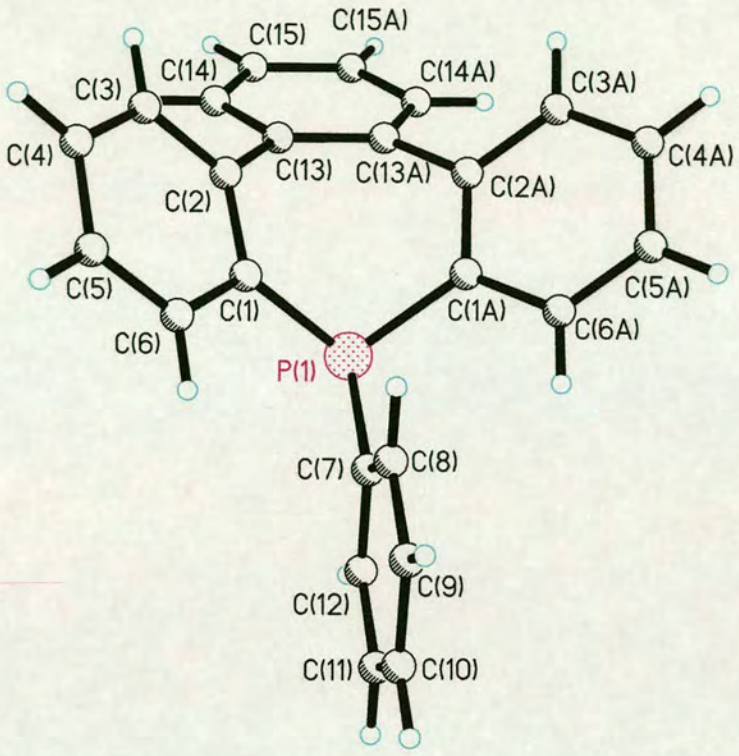

Figure 6.10 X-ray crystal structure of $(C_6H_4)_3P(C_6H_5)$

Bond	Length / Å
P(1)-C(7)	1.8310(18)
P(1)-C(1)	1.8350(13)
P(1)-C(1A)	1.8350(13)

Angle	Size / °
C(7)-P(1)-C(1)	101.90(5)
C(7)-P(1)-C(1A)	101.90(5)
C(1)-P(1)-C(1A)	99.04(8)

Table 6.11 Bond lengths / Å and angles / ° around the phosphorus atom in $(C_6H_4)_3P(C_6H_5)$

There is no silicon present. The structure is of a triphenylphosphine molecule, with two of the phenyl groups fused together, bridged by a fourth phenyl group. This results in a seven membered heterocycle. This ring is folded to minimise the strain associated with a seven membered ring and to maintain a tetrahedral like geometry at the phosphorus atom.

Table 6.1 shows the bond lengths and angles around the phosphorus atom. The three phosphorus – carbon bonds are of virtually identical length. The three C-P-C bond angles are similar, but the C(1)- P(1)-C(1A) angle, corresponding to the angle describing part of the heterocycle is smaller than the other two. There is a line of symmetry bisecting the molecule. The phosphorus phenyl ring (C(7)-C(12)) lies perpendicular to the other three phenyl rings. This will reduce the interaction between the phenyl protons.

The mass spectrum analysis of **45** contains peaks corresponding to this species, and also to the fragment corresponding to the loss of the free phenyl group. There are also several peaks corresponding to fragments with a higher molecular weight but these could not be accounted for.

In the ^{31}P NMR spectrum, the phosphorus environment is shifted upfield relative to the phosphorus atom in **36** (-15.5 ppm compared with –0.15 ppm in **36**). The ^{13}C NMR spectrum shows the presence of eleven sp^2 carbon atoms. If the structure of the crystals is representative of the whole solution, this indicates that the degree of the rotation of the phenyl ring is hindered and that the ring remains locked perpendicular to the other ring systems. This will minimise the steric interactions between phenyl protons.

The mechanism of formation for this product is not clear without further work. It is most likely a by-product of the lithiation reaction and is formed before the silicon reagent is present.

6.6 Experimental

6.6.1 Synthesis of QSn, 36

6.6.1.1 1-Bromo-2-(diphenylphosphino)benzene, 37[13]

A solution of ^{n}BuLi (1.6 M in hexane, 37 ml, 59.2 mmol) was added slowly (1ml / min) to a well stirred solution of dibromobenzene (15 g, 63.6 mmol) in 250 ml of Et_2O / THF (1 / 1) at –115 / -110 °C. The mixture was stirred at the same temperature for 40 minutes, during which time a white precipitate gradually separated out of solution. Chlorodiphenylphosphine (10.8 ml, 60.0 mmol) was slowly added at –110 / -105 °C and the resulting suspension was stirred for 15 minutes. The mixture was then allowed to warm to 20 °C and 200 ml of saturated aqueous NH_4Cl was added. The layers were separated and the aqueous layer extracted twice with Et_2O. The combined organic layers were dried over anhydrous $MgSO_4$ and the solvent was evaporated to yield a yellow oil that slowly solidified. Recrystallisation from dry ethanol afforded **37** as large white crystals. (16.24 g, 75 %).

M.P. = 78 °C

MS (+ve FAB): *m/z* 341 (M^+), 262 (M^+ - Br), 185 (M^+ - PhBr)

^{1}H NMR (250 MHz, $CDCl_3$): δ 7.51 – 7.63 (1H, m), 7.20 – 7.31 (10H, m), 7.10 – 7.14 (2H, m), 6.66 – 6.67 (1H, m)

^{13}C NMR (62.9 MHz, $CDCl_3$): δ 139.2 ($J_{P\text{-}C}$ = 12 Hz), 135.66 ($J_{P\text{-}C}$ = 10.6 Hz), 134.34, 133.90 ($J_{P\text{-}C}$ = 20.2 Hz), 132.83, 130.03, 129.69 ($J_{P\text{-}C}$ = 30.2 Hz), 128.91, 128.55 ($J_{P\text{-}C}$ = 7.1 Hz), 127.29

^{31}P NMR (101 MHz, $CDCl_3$): δ –1.2

6.6.1.2 2-(Diphenylphosphino)phenyllithium, 38[13]

A solution of ^{n}BuLi (1.6 M in hexane, 2.0 ml, 3.2 mmol) was added to one equivalent of **37** (1.08 g, 3.2 mmol) in 10 ml of diethyl ether at room temperature. After 10 minutes, the crystalline product was isolated by cannula filtration, washed twice with diethyl ether, and dried *in vacuo.* (0.65 g, 76 %).

6.6.1.3 QSn, 36

A solution of ^{n}BuLi (1.6 M in hexane, 6.0 ml, 9.5 mmol) was added to one equivalent of **37** (3.24 g, 9.5 mmol) in 30 ml of diethyl ether at room temperature. After 10 minutes, the product formed as a pale pink solid. A 78 % conversion rate was assumed. Butyl tin trichloride (0.697 g, 2.47 mmol) was placed in a Schlenk tube in the glove box. This was partially dissolved in anhydrous distilled diethyl ether. The solution of butyl tin trichloride was transferred *via* cannula to the solution of **38**. The solution changed colour from pale pink to a darker pink. The solution was stirred at –78 °C for 1 h and then warmed to room temperature. Dilute sulphuric acid (30 ml) followed by distilled water (30 ml) was added and the pale pink precipitate dissolved. The product was extracted with DCM, dried over magnesium sulphate, filtered, and the excess solvent removed *in vacuo* to yield a yellow oil that solidified. This could be recrystallised from DCM and ethanol to form **36** as colourless blocks, suitable for X-ray analysis. (1.958 g, 65 %).

M.P. = 186 °C

IR (KBr disc): ν_{max} 3048, (m), (C-H, aromatic); 2954, (m), (CH_3 antisymmetric stretch); 2919, m, (CH_2 antisymmetric stretch); 2869, (w), (CH_3 symmetric stretch); 2850, w, (CH_2 symmetric stretch); 1583, (m); 1478, (s); 1432, (vs), (P-C aromatic); 1419, (m); 1092, (s); 1025, (m); 742, (s); 694, (s), (monosubstituted benzene ring) cm^{-1}

^{1}H NMR (250 MHz, $CDCl_3$): δ 7.36, 7.12, and 7.01 (m, 42H), 1.34 (m, 4H), 0.70 (m, $CH_2CH_2C\underline{H}_2CH_3$, 2H), 0.36 (t, J = 7.38 Hz, $CH_2CH_2CH_2C\underline{H}_3$, 3H)

^{13}C NMR (62.9 MHz, $CDCl_3$): δ 154.90, 158.81, 144.06, 139.14, 138.81, 138.86, 138.16, 134.41, 133.27, 132.99, 128.46, 128.29, 128.01, 127.91, 127.82, 28.94, 27.18, 13.20, 21.70

^{31}P NMR (101 MHz, $CDCl_3$): δ –0.15 with satellite signals $J_{Sn\text{-}P}$ = 30.83 and $J_{C\text{-}P}$ = 16.94 Hz

CHN: $C_{58}H_{51}P_3Sn$ requires C 72.58, H 5.32; Found C 72.36, H 5.38.

MS (+ve FAB): *m/z* 960 (M^++1), 903 (M^++1(-Bu)), 698 ($BuSn(C_6H_4P(C_6H_5)_2)_2$), 641 ($Sn(C_6H_4P(C_6H_5)_2)_2$), 379 ($SnC_6H_4P(C_6H_5)_2$).

Crystal Data for **36**

Data were collected using Mo-Kα radiation on a colourless block of dimensions 0.25 x 0.25 x 0.17 mm on a Stoe Stadi4 diffractometer in the range $1.46 \leq 2\theta \leq 28.86°$ using the ω-θ method. Of a total of 29842 reflections collected, 11592 (R_{int} = 0.0357) were independent. The structure was solved by direct methods (SHELXS-97). Hydrogen atoms were geometrically placed with no refinement. The final difference-map extrema were 1.126 and –0.627 e $Å^{-3}$ with a final *R* of 0.0432 for 9598 parameters.

Empirical formula	$C_{58}H_{51}P_3Sn$	γ / °	90
Formula weight	959.59	Volume / $Å^3$	4840.3 (4)
Crystal system	Monoclinic	Z	4
Space group	p21/c	Temperature / K	150 (2)
a / Å	14.2296 (6)	Wavelength / Å	0.71073
b / Å	14.1239 (6)	Density calc. / Mg/m^3	1.317
c / Å	24.6325 (11)	μ(Mo-Kα) / mm^{-1}	0.664
α / Å	90	R_1 [$F>4\sigma(F)$]	0.0432
β / Å	102.1140 (0)	WR_2 (all data)	0.0970

Table 6.12 Crystallographic data for 36

6.6.2 Coordination Studies of QSn

6.6.2.1 -With Group VI Metals

6.6.2.1.1 Synthesis of Group VI trisacetonitrile triscarbonyl Complexes

$[Mo(CO)_3(MeCN)_3]$ was prepared as described by Tate and co-workers.[14]

Molybdenum hexacarbonyl (2.35 g, 8.9 mmol) was placed in a Schlenk tube. Freshly distilled anhydrous acetonitrile (50 ml) was added to give a white suspension. This was heated under reflux, under an atmosphere of nitrogen for 4 h. Over this time, the solution turned clear yellow in colour. The excess solvent was removed *in vacuo* to yield the product as a yellow microcrystalline solid. (2.52 g, 93 % yield).

IR (KBr disc) ν_{max} 1916, (m), (CO); 1784, (m); cm^{-1}

$[W(CO)_3(MeCN)_3]$ was prepared as described by Tate and co-workers.[14]

Tungsten hexacarbonyl (2.5 g, 7.1 mmol) was placed in a Schlenk tube. Freshly distilled anhydrous acetonitrile (50 ml) was added to give a white suspension. This was heated under reflux, under an atmosphere of nitrogen for 40 h. Over this time, the solution turned clear yellow in colour. The excess solvent was removed *in vacuo* to yield the product as a yellow microcrystalline solid. (2.48 g, 89 % yield).

6.6.2.1.2 Formation of $[QSnW(CO)_4]$, 39

$[W(CO)_3(MeCN)_3]$ (0.20 g, 0.52 mmol) was placed in a Schlenk tube and dissolved in freshly distilled, anhydrous benzene to give a dark yellow solution. **36** (0.50 g, 0.52 mmol) was added to the well stirred solution at room temperature. The yellow solution was heated under reflux for eight hours under an atmosphere of nitrogen. During this time, the solution turned a dark orange / red colour. The excess solvent was removed *in vacuo* to yield a mixture of dark orange and yellow coloured solids. The mixture was redissolved in the minimum volume of benzene and filtered onto a column of silica. Two yellow bands were eluted. Both fractions were collected and the excess solvent removed from each *in vacuo* to yield orange oils. These were recrystallised from benzene layered with *n*-heptane to yield pale orange crystalline materials. The first band was identified as unreacted $[W(CO)_3(MeCN)_3]$. The material from the second fraction was recrystallised from methanol and DCM to yield **39** as yellow crystals suitable for X-ray analysis.

M.P. = 210 °C

CHN: $WC_{61}H_{51}P_3SnO_3$ requires C 59.66, H 4.16; Found C 59.45, H 3.59.

^{1}H NMR (250 MHz, $CDCl_3$): δ 7.50 – 7.07 and 6.81 – 6.78 (m, 42H), 1.20 and 0.98 (m, 4H), 0.47 (m, 2H, $CH_2CH_2C\underline{H}_2CH_3$), 0.20 (t, J = 7.38 Hz, 3H, $CH_2CH_2CH_2C\underline{H}_3$)

^{13}C NMR (62.9 MHz, $CDCl_3$): δ 205.7 ($\underline{C}O$), 205.0 ($\underline{C}O$), 204.0 ($\underline{C}O$), 200.9 ($\underline{C}O$), 153.9, 152.2, 150.1, 149.1, 148.8, 147.7, 145.5, 140.7, 139.6, 136.0, 134.7, 133.0, 132.5, 129.3, 128.9, 128.7, 128.4, 128.1 ($J_{P\text{-}C}$ = 0.7 Hz), 127.8 ($J_{P\text{-}C}$ = 1.0 Hz), 126.6, 28.6 ($CH_2CH_2\underline{C}H_2CH_3$), 26.3 ($CH_2\underline{C}H_2CH_2CH_3$), 20.1 ($J_{Sn\text{-}C}$ = 21.6 Hz, $CH_2CH_2CH_2\underline{C}H_3$), 13.0 ($\underline{C}H_2CH_2CH_2CH_3$).

^{31}P NMR (101 MHz, $CDCl_3$): δ 30.59 (coordinated $\underline{P}Ph_2$), $J_{P\text{-}P}$ = 20.9, with satellite signals $J_{Sn\text{-}P}$ = 59.6 and $J_{W\text{-}P}$ = 237.2; 29.03 (coordinated $\underline{P}Ph_2$), $J_{P\text{-}P}$ = 20.8, with satellite signals $J_{Sn\text{-}P}$ = 77.8 and $J_{W\text{-}P}$ = 234.8 Hz; –4.12 (uncoordinated $\underline{P}Ph_2$) with satellite signals $J_{Sn\text{-}P}$ = 38.9 and $J_{C\text{-}P}$ = 18.5 Hz

MS (+ve FAB): *m/z* 1256 ($QSnW(CO)_4$), 1199 ($QSn(\text{-}Et)W(CO)_3$), 1170 ($QSn(\text{-}Bu)W(CO)_3$), 1114 ($QSn(\text{-}Bu)W(CO)$), 1086 ($QSn(\text{-}Bu)W$), 995, ($Sn(C_6H_4P(C_6H_5)_2)_2W(CO)_4$).

IR (KBr disc): ν_{max} 3043, (m), (C-H, aromatic); 2947, (m), (CH_3 antisymmetric stretch); 2849, m, (CH_2 antisymmetric stretch); 2067, (w); 2013, (s); 1890, (s); 179, (m); 1433, (vs), (P-C aromatic) cm^{-1}

IR (chloroform solution cell): ν_{max} (carbonyl region only) 2017, 1915, 1899, 1871 (shoulder) cm^{-1}

Crystal Data for **39**

Data were collected using Mo-Kα radiation on a colourless block of dimensions 0.29 x 0.23 x 0.15 mm on a Stoe Stadi4 diffractometer in the range $2.62 \leq 2\theta \leq 27.13°$ using the ω-θ method. Of a total of 25847 reflections collected, 10492 (R_{int} = 0.0205) were independent. The structure was solved by direct methods (SHELXS-97). Hydrogen atoms were geometrically placed and not refined. The final difference-map extrema were 0.868 and –0.489 e $Å^{-3}$ with a final *R* of 0.0256 for 9612 parameters.

Empirical formula	$C_{62}H_{51}O_4P_3SnW$	γ / °	90
Formula weight	1255.48	Volume / $Å^3$	5234.3 (5)
Crystal system	Monoclinic	Z	4
Space group	p2(1)/c	Temperature / K	150 (2)
a / Å	14.0650 (8)	Wavelength / Å	0.71073
b / Å	37.310 (2)	Density calc. / Mg/m^3	1.593
c / Å	10.7420 (6)	μ(Mo-Kα) / mm^{-1}	2.813
α / Å	90	R_1 [$F>4\sigma(F)$]	0.0256
β / Å	111.7880 (10)	WR_2 (all data)	0.0559

Table 6.13 Crystallographic data for 39

6.6.2.1.3 Formation of [QSnMo(CO)$_3$], 40

[Mo(CO)$_3$(MeCN)$_3$] (0.135 g, 0.45 mmol) was placed in a Schlenk tube and partially dissolved in freshly distilled, anhydrous DCM (15 ml). **36** (0.427 g, 0.45 mmol) was added to the dark yellow suspension at 0 °C. The solution turned a darker orange and then red in colour. The solution was stirred at 0 °C for one hour and then warmed to room temperature. The excess solvent was removed *in vacuo* to yield a dark orange solid. The solid was dissolved in minimal DCM and the solution filtered by cannula filtration. Red block shaped crystals of **40**, suitable for X-ray analysis, **36,** were grown by vapour diffusion of diethyl ether into a DCM solution of the complex. These are relatively stable in air but decomposed over 24 h to yield a brown decomposition solid.

IR (KBr disc): ν_{max} 3058, (m); 2948, (m); 2850, (m); 1902, (s), Mo-CO (terminal); 1855, (s), CO (bridging); 1591, (m), 1564, (s), CO (acyl); 1481, (m); 1433, (m); 1169, (w); 1114, (m); 1089, (m); 834, (s); 743, (s); 721, (s) cm^{-1}

MS (+ve FAB): *m/z* 1139 (QSnMo(CO)$_3$), 1112 (QSnMo(CO)$_2$), 1083 (QSnMo(CO)), 1056 (QSnMo), 1027 (QSn(-Et)Mo), 998 (QSn(-Bu)Mo), 737 (Sn(C$_6$H$_4$P(C$_6$H$_5$)$_2$)$_2$Mo).

CHN: $C_{61}H_{51}P_3SnO_3Mo$ requires C 64.27, H 4.47; Found C 60.51, H 4.26

Crystal Data for **40**

Data were collected using Mo-Kα radiation on a red block of dimensions 0.38 x 0.29 x 0.21 mm on a Stoe Stadi4 diffractometer in the range $1.13 \leq 2\theta \leq 28.80^{\circ}$ using the ω-θ method. Of a total of 22750 reflections collected, 11840 (R_{int} = 0.0368) were independent. The structure was solved by direct methods (SHELXS-97). Hydrogen atoms were geometrically placed and allowed to ride. The final difference-map extrema were 1.126 and –0.627 e Å^{-3} with a final *R* of 0.0509 for 9243 parameters.

Empirical formula	$C_{61}H_{51}MoO_3P_3Sn$	γ / °	99.275 (2)
Formula weight	1139.56	Volume / Å^3	2563.3 (5)
Crystal system	Triclinic	Z	2
Space group	P-1	Temperature / K	150 (2)
a / Å	11.5493 (13)	Wavelength / Å	0.71073
b / Å	12.4540 (15)	Density calc. / Mg/m^3	1.476
c / Å	18.581 (2)	μ(Mo-Kα) / mm^{-1}	0.872
α / Å	90	R_1 [F>4σ(F)]	0.0509
β / Å	102.1140 (0)	WR_2 (all data)	0.1204

Table 6.14 Crystallographic data for 40

6.6.2.1.4 Attempted Mono- decarbonylation of 39

39 (0.12 g, 0.096 mmol) was added to a solution of trimethylamine*N*-oxide (0.007 g, 0.096 mmol) in freshly distilled anhydrous DCM to yield a pale yellow solution. This was stirred under nitrogen for 48 h in the dark with no further change in colour. The reaction was followed by solution cell infrared analysis. The infrared solution cell spectrum of the solution was recorded after 2, 6, 10, 24 and 48 h but no change in the carbonyl region was observed. After 48 h, the excess solvent was removed *in vacuo* to yield a yellow solid. This was recrystallised from ethanol and DCM to yield the starting material as bright yellow crystals.

NMR and mass spectroscopy confirmed that the crystals were starting material.

6.6.2.2 Complexation to Manganese

6.6.2.2.1 Preparation of Bromopentacarbonyl Manganese ($Mn(CO)_5Br$)[23]

A solution of bromine (0.5 ml, 9.62 mmol) in freshly distilled anhydrous DCM (30 ml) was added slowly *via* an addition funnel to a solution of dimanganese decacarbonyl (3.0 g, 7.7 mmol) in DCM (50 ml) over a period of 30 minutes. Over this time, the pale orange solution turned bright red in colour. The solution was stirred for 1 h, under an atmosphere of nitrogen, during which time some pale yellow precipitate formed. The solution was stirred with more DCM (100 ml) and the orange / red solution was filtered to remove a small amount of yellow material. Hexane (90 ml) was added to the filtrate. The filtrate was then slowly evaporated under reduced

pressure to about 30 ml, resulting in the formation of the product as a yellow / orange microcrystalline material. The solid was isolated by filtration, washed with cold (0 °C) pentane and dried under high vacuum. (3.10 g, 73 %).

IR (KBr disc): ν_{max} 3016, (s); 2951, (s); 2328, (s), (CN); 2301, (s), (CN); 2066, (s), (CO); 1973, (s), (CO); 1424, (s); 1376, (m); 1041, (s); 838, (br); 678, (s) cm^{-1}

6.6.2.2.2 *Preparation of Bromopentacarbonyl Manganese* fac-$[Mn(CO)_3(MeCN)_3]PF_6$

$[Mn(CO)_5Br]$ (3.077 g, 0.011 mol) was dissolved in acetonitrile (20 ml) to give a pale orange solution. This was heated under reflux for 1 h. Over this time, the solution turned red and a small amount of yellow precipitate formed. The solution was filtered and reduced in volume to approximately 4 cm^3. A hot solution of NH_4PF_6 (1.85 g, 0.011 mol) in an equimolar mixture of water and ethanol (10 ml) was then added to give the required product as a yellow crystalline material that formed upon standing. This was isolated by filtration and recrystallised from DCM and ethanol, to give the product as a bright yellow crystalline material (3.598 g, 79 %).

M.P. = 130 °C, (Literature = 131 – 133 °C)

CHN: $C_9H_9O_3N_3MnPF_6$ requires C 26.55, H 2.25, N 10.35; Found C 26.12, H 2.09, N 9.98.

6.6.2.2.3 *Attempted Coordination of QSn to Manganese*

36 (0.4 g, 0.42 mmol) was dissolved in chloroform (20 ml) to yield a colourless solution. $[Mn(CO)_3(MeCN)_3]PF_6$ (0.17 g, 0.42 mmol) was added to the well stirred solution and the solution turned pale yellow. The solution was heated under reflux under an atmosphere of nitrogen, for 1 h. During this time, the solution turned a slightly darker yellow. Cold ethanol (2 ml) was added. The reaction was followed by recording the infrared solution cell spectrum. This showed no change in the carbonyl region. The solvent was removed *in vacuo* to yield a dark yellow solid. Recrystallisation resulted in clear colourless blocks of the unreacted ligand.

The reaction was repeated on the same scale using THF as the solvent system. The reaction was heated under reflux for 4 h. Again, large colourless crystalline blocks of unreacted ligand were isolated at the end of the reaction.

The reaction was repeated on the same scale using chloroform as the solvent system. The reaction was heated under reflux for 6 h. Again, large colourless crystalline blocks of unreacted ligand were isolated at the end of the reaction. The unreacted ligand was removed by filtration. The clear, dark yellow solution was reduced in volume by a half and layered with hexane. This resulted in the formation of small colourless crystalline blocks, **41**, in extremely low yield, some of which were suitable for X-ray analysis. The crystals did not refract very strongly, but it was possible to obtain a structure.

IR (KBr disc): ν_{max} 2960, (m); 2916, (s); 2848, (s); 1988, (w), (CO); 1925, (m); 1894, (m); 1473, (m); 1433, (s), (P-C aromatic); 1261, (s); 1092, (s); 1024, (s); 800, (s); 741, (m) cm^{-1}

Crystal Data for **41**

Data were collected using Mo-Kα radiation on a colourless block of dimensions 0.14 x 0.11 x 0.07 mm on a Stoe Stadi4 diffractometer in the range $1.43 \leq 2\theta \leq 20.00^{\circ}$ using the ω-θ method. Of a total of 8426 reflections collected, 3492 (R_{int} = 0.1228) were independent. The structure was solved by direct methods (SHELXS-97). Hydrogen atoms were geometrically placed. The final difference-map extrema were 1.007 and –0.939 e $Å^{-3}$ with a final *R* of 0.0938 for 2219 parameters.

Empirical formula	$C_{43}H_{37}O_3P_2SnMn$	γ / °	101.843
Formula weight	837.3	Volume / $Å^3$	1868.8(5)
Crystal system	Triclinic	Z	2
Space group	p-1	Temperature / K	150 (2)
a / Å	10.0744(16)	Wavelength / Å	0.71073
b / Å	13.355(2)	Density calc. / Mg/m^3	1.488
c / Å	14.425(2)	μ(Mo-Kα) / mm^{-1}	1.131
α / Å	94.223(3)	R_1 [$F>4\sigma(F)$]	0.0938
β / Å	98.330(4)	WR_2 (all data)	0.2155

Table 6.15 Crystallographic data for 41

6.6.2.3 Complexation to Ruthenium

6.6.2.3.1 Preparation of Ruthenium Starting Materials

6.6.2.3.1.1 Synthesis of $RuCl_2(PPh_3)_3$ [28]

Hydrated ruthenium trichloride (1.0 g, 3.8 mmol) was dissolved in methanol (250 ml). The reddish brown solution was heated under reflux under an atmosphere of nitrogen for five minutes. The solution was allowed to cool, and an excess of triphenylphosphine (6.0 g, 23 mmol) was added. The reaction mixture was heated under reflux for 3 h. During this time, very dark red shiny crystals formed. These were isolated by filtration, washed with diethyl ether (10 ml x 3) and dried under high vacuum to yield the product as an air stable crystalline solid, (2.98 g, 82 %).

MP = 131 – 132 °C, (literature = 132 – 134 °C)

6.6.2.3.1.2 Synthesis of [p-cymene $Ru(MeCN)_3$]BF_4

Silver tetrafluoroborate (1.27 g, 6.5 mmol) was added to a well stirred solution of the ruthenium dimer $RuCl_2(\eta^2\text{-}C_{10}H_{14})]_2$ (1.0 g, 1.6 mmol) in freshly distilled anhydrous acetonitrile. The dark red solution turned bright yellow and a large amount of white precipitate formed. The solution was filtered and the precipitate washed on the filter with acetone. Diethyl ether was added to the combined acetonitrile and acetone fractions to cause a dark yellow precipitate to crash out of solution. The greenish yellow solid was isolated by filtration and dried under high vacuum. (1.047 g, 72 %).

6.6.2.3.1.3 Synthesis of di-μ-chloro(η^4-1,5-cyclooctadiene)ruthenium(II) [26]

Cyclooctadiene (2.82 ml, 0.023 mol) was added slowly to a solution of ruthenium trichloride (3.0 g, 0.012 mol) in ethanol (40 ml). The solution was heated under reflux for 24 h. During this time, a brown solid precipitated from solution. After 24 h, the solution was allowed to cool and the solid was isolated by filtration, washed with diethyl ether (10 ml) and dried under vacuum to yield the product as a dark brown crystalline material. (2.44 g, 76 %).

CHN: $RuCl_2C_8H_{12}$ requires C 34.29, H 4.29; Found C 34.71, H 4.68.

6.6.2.3.2 Attempted Preparation of a Ruthenium QSn Complex

6.6.2.3.2.1 From Ruthenium Trichloride

A solution of hydrated ruthenium trichloride (0.43 g, 1.63 mmol) in ethanol (100 ml) was heated under reflux for 24 h. During this time, the solution changed colour from dark brown to dark green to deep blue. Once cooled, a solution of **36** (0.793 g, 0.83 mmol) in DCM (50 ml), followed by *n*-butanol (50 ml) was added. The mixture was heated gently whilst the DCM and some of the ethanol was boiled off. The solution was then heated under reflux for 18 h. During this time, a very dark green solid precipitated out of solution.

MS (+ve FAB): *m/z* 1095 (QSnRuCl), 1039 (QSn(-Bu)RuCl), 777 ($Sn(C_6H_4P(C_6H_5)_2)_2RuCl$).

IR (KBr disc): ν_{max} 3053, (m), (C-H, aromatic); 1571, (m); 1481, (s); 1433, (vs), (P-C aromatic); 1089, (s); 1027, (m); 909, (m); 742, (s); 695, (vs), (monosubstituted benzene ring) cm^{-1}

6.6.2.3.2.2 From $RuCl_2(PPh_3)_3$

36 (0.40 g, 0.42 mmol) was added to a solution of $[RuCl_2(PPh_3)_3]$ (0.40 g, 0.42 mmol) in benzene and the solution was heated under reflux for 1 h, during which time the solution changed colour from dark brown to dark red. The solution was allowed to cool. The benzene was removed *in vacuo* to leave a dark purple solid. Recrystallisation was attempted from DCM and ethanol. Colourless block shaped crystals grew but were identified as unreacted ligand.

6.6.2.3.2.3 From [*p*-cymeneRu(MeCN)$_3$]BF_4

36 (0.216 g, 0.2 mmol) was added to a well stirred solution of [*p*-cymene $Ru(MeCN)_3BF_4$] (0.1 g, 0.2 mmol) in THF (20 ml). The pale green solution was heated under reflux under an atmosphere of nitrogen for 3 h. During this time, the solution turned a darker shade of green and then to brown. ^1H NMR showed that the solution had decomposed.

6.6.2.3.2.4From di-μ-chloro(η^4-1,5-cyclooctadiene)ruthenium(II)

36 (0.125 g, 0.13 mmol) was added to a suspension of di-μ-chloro(η^4-1,5-cyclooctadiene)ruthenium(II) (0.041 g, 0.13 mmol) in acetonitrile (15 ml). The dark brown suspension was heated under reflux under an atmosphere of nitrogen for 6 h but no reaction took place.

6.6.2.4 Complexation to Rhodium

36 (0.455 g, 0.474 mmol) was added to a dark red solution of rhodium trichloride in ethanol (50 ml). The solution was stirred at room temperature under an atmosphere of nitrogen for 2 h. After this time, there was no change in colour of the solution so it was heated under reflux under an atmosphere of nitrogen for 4 h. The solution turned orange and a yellow precipitate formed. The solution was filtered and the yellow precipitate washed with cold ethanol. Despite many attempts, it was not possible to obtain this material in a crystalline form.

MS (+ve FAB): *m/z* 1098 (QSnRhCl), 1077 (QSn(-Bu)$RhCl_2$), 1062 (QSnRh), 1042 (QSn(-Bu)RhCl), 1005 (QSn(-Bu)Rh), 887 ($Sn(C_6H_4P(C_6H_5))_2(C_6H_4P(C_6H_5))RhCl$), 779, ($Sn(C_6H_4P(C_6H_5))_2RhCl$).
CHN: $C_{58}H_{51}P_3N_3SnRhCl_3$ requires C 59.56, H 4.36; $C_{58}H_{51}P_3N_3SnRhCl$ requires C 63.44, H 4.65; Found C 60.61, H 2.05.

6.6.2.5 Complexation to Silver

6.6.2.5.1 Formation of [QSnAg]BF_4, 42

36 (0.2 g, 0.21 mmol) was added to a solution of silver tetrafluoroborate (0.041 g, 0.21 mmol) in THF (20 ml). The clear colourless solution was stirred at room temperature under an atmosphere of nitrogen for 24 h. During this time, a white precipitate formed. The white precipitate was isolated by filtration and washed on the filter with diethyl ether (2 x 5 ml). The residue was dried under high vacuum for 3 h to yield **42** as a white powder (0.198 g, 82 %).

IR (KBr disc): ν_{max} 3055, (m); 2962, (w); 2926, (w); 1479, (m); 1435, (s); 1274, (s); 1223, (s); 1148, (s); 1034, (s); 998, (s); 745, (s); 694, (s); 636, (s) cm^{-1}

CHN: $C_{58}H_{51}P_3SnAgBF_4$ requires C 60.30, H 4.40; Found C 59.48, H 4.08.

MS (+ve FAB): *m/z* 1068 (QSnAg), 805 ($BuSn(C_6H_4P(C_6H_5)_2)_2Ag$), 749 ($Sn(C_6H_4P(C_6H_5)_2)_2Ag$), 379 ($SnC_6H_4P(C_6H_5)_2$).

^{31}P NMR (101 MHz, $CDCl_3$): δ 15.73 with Ag satellites $J(^{107}Ag\text{-}P)$ = 307.43 and $J(^{109}Ag\text{-}P)$ = 355.01 Hz

The ^{1}H spectrum is very complicated to interpret due to the large number of phenyl protons. However, it is possible to ascertain that the ratio of aromatic protons to alkyl chain protons is as expected for a mononuclear complex containing one equivalent of **36**. I.e. 0.214.

6.6.2.5.2 Formation of $QSnAgCF_3SO_3$, 43

36 (0.4 g, 0.42 mmol) was added to a solution of silver trifluoromethanesulphonate (0.107 g, 0.42 mmol) in THF (20 ml). The clear colourless solution was stirred at room temperature under an atmosphere of nitrogen for 24 h. During this time, the solution turned cloudy due to the formation of a grey precipitate. The solid was isolated by filtration and washed on the filter with diethyl ether (2 x 5 ml). The residue was dried under high vacuum for 3 h to yield **43** as a pale grey powder (0.356 g, 70 %).

IR (KBr disc): ν_{max} 3047, (m); 2927, (m); 2860, (m); 1478, (m); 1446, (m); 1435, (s); 1291, (s); 1241, (s); 1094, (m); 1028, (s); 744, (s); 714, (m); 693, (s); 635, (s) cm^{-1}

CHN: $C_{58}H_{51}P_3SnAgCF_3SO_3$ requires C 58.22, H 4.19; Found C 58.35, H 4.26.

6.6.2.6 Complexation to Copper

6.6.2.6.1 Formation of $[QSnCu(MeCN)_4]BF_4$, 44

36 (0.25 g, 0.26 mmol) was added to a clear colourless solution of copper tetra(acetonitrile) tetrafluoroborate (0.082 g, 0.26 mmol) in acetonitrile. The solution was stirred at room temperature for 48 h under an atmosphere of nitrogen. After this time, the solution was removed *in vacuo* to yield a white crystalline solid. This could

be recrystallised from ethanol and diethyl ether to give a white crystalline solid, **44**. Unfortunately this was not suitable for X-ray analysis.

MS (+ve FAB): *m/z* 1024 (QSnCu), 967 (QSn(-Bu)Cu), 705 ($Sn(C_6H_4P(C_6H_5)_2)_2Cu$). **IR** (KBr disc): ν_{max} 3050, (m), (C-H, aromatic); 2956, (m), (CH_3 antisymmetric stretch); 2925, m, (CH_2 antisymmetric stretch); 1480, (m); 1436, (vs), (P-C aromatic); 1261, (m); 1052, (s); 801, (m); 743, (s); 694, (s); 519, (s); 499, (s) cm^{-1}
CHN: $C_{58}H_{51}P_3SnCuBF_4$ requires C 62.76, H 4.60; $C_{60}H_{54}P_3NSnCuBF_4$ requires C 62.60, H 4.70, N 1.21; Found C 55.32, H 4.51, N 0.18.

6.6.3 Attempted Synthesis of Ligands With a Central Silicon Atom

6.6.3.1 -Using Hydridotrichlorosilane as a Starting Material

A solution of ^{n}BuLi (1.6 M in hexane, 7.3 ml, 0.012 mol) was added to one equivalent of **37** (4.0 g, 0.012 mol) in 20 ml of diethyl ether at room temperature. After 10 minutes, the product formed as a pale pink solid. A 78 % conversion rate was assumed. Hydridotrichlorosilane (0.31 ml, 0.003 mol) was added slowly to the solution of **38**. The solution changed colour from pale pink to a darker pink. The solution was stirred at –78 °C for 1 h and then warmed to room temperature. Dilute sulphuric acid (20 ml) followed by distilled water (20 ml) was added and the pale pink precipitate dissolved. The product was extracted with DCM, dried over magnesium sulphate, filtered, and the excess solvent removed *in vacuo* to yield a yellow oil. The addition of diethyl ether caused the precipitation of a fine white powder. Attempts at recrystallising the material were unsuccessful.

^{1}H NMR ($CDCl_3$, 200 MHz) showed a large number of peaks in the aromatic region, but no conclusive evidence of the presence of a silicon hydride.

6.6.3.2 -Using Methyltrichlorosilane as a Starting Material

A solution of ^{n}BuLi (1.6 M in hexane, 4.0 ml, 6.4 mmol) was added to one equivalent of **37** (2.16 g, 6.4 mmol) in 20 ml of diethyl ether at room temperature.

After 10 minutes, the product formed as a pale pink solid. A 78% conversion rate was assumed. Methyltrichlorosilane (0.2 ml, 1.66 mmol) was added to the solution of **38**. The solution changed colour from pale pink to a darker pink. The solution was stirred at –78 °C for 1 h and then warmed to room temperature. Dilute sulphuric acid (15 ml) followed by distilled water (15 ml) was added and the pale pink precipitate dissolved. The product was extracted with DCM, dried over magnesium sulphate, filtered, and the excess solvent removed *in vacuo* to yield an intractable yellow oil.

6.6.3.3 -Using Phenyltrichlorosilane as a Starting Material

A solution of ^{n}BuLi (1.6 M in hexane, 2.6 ml, 4.2 mmol) was added to one equivalent of **37** (1.414 g, 4.15 mmol) in 15 ml of diethyl ether at room temperature. After 10 minutes, the product formed as a pale pink solid. A 78% conversion rate was assumed. Phenyltrichlorosilane (0.2 ml, 1.1 mmol) was added to the solution of **38**. The solution changed colour from pale pink to a darker pink. The solution was stirred at –78 °C for 1 h and then warmed to room temperature. Dilute sulphuric acid (10 ml) followed by distilled water (10 ml) was added and the pale pink precipitate dissolved. The product was extracted with DCM, dried over magnesium sulphate, filtered, and the excess solvent removed *in vacuo* to yield a white solid. This was recrystallised from DCM and ethanol to yield colourless crystals, **45**.

MP = 188 °C

CHN: $C_{60}H_{47}P_3Si$ requires C 81.08, H 5.29; $C_{24}H_{17}P$ requires C 85.62, H 5.05; Found C 82.12, H 5.16.

MS (+ve FAB): *m/z* 614, 488, 474, 460, 443, 353, 336 ('M^+'), 289, 273, 259 ('M^+'-Ph), 228 ('M^+'-PPh)

^{1}H NMR (250 MHz, $CDCl_3$): δ 7.87 (m), 7.55 (dt, J = 1.3, 4.7 Hz), 7.37 – 7.42 (m), 7.20 (td, J = 6.5, 1.6 Hz), 7.09 (tt, J = 7.2, 1.3 Hz), 7.05 (ddd, J = 1.1, 3.4, 6.7 Hz)

^{13}C NMR (62.9 MHz, $CDCl_3$): δ 142.53 ($J_{P\text{-}C}$ = 16.29 Hz), 142.18 ($J_{P\text{-}C}$ = 6.42 Hz), 140.68, 138.85, 138.44, 130.99, 130.25, 128.96, 128.81, 127.74, 127.61, 127.54, 126.58

^{31}P NMR (101 MHz, $CDCl_3$): δ -15.5

Crystal data for **45**

Data were collected using Mo-Kα radiation on a colourless lath of dimensions 0.61 x 0.19 x 0.10 mm on a Stoe Stadi4 diffractometer in the range $2.31 \leq 2\theta \leq 28.83^{\circ}$ using the ω-θ method. Of a total of 11472 reflections collected, 2230 (R_{int} = 0.0297) were independent. The structure was solved by direct methods (SHELXS-97). Hydrogen atoms were geometrically placed. The final difference-map extrema were 0.385 and –0.226 e $Å^{-3}$ with a final *R* of 0.0388 for 1825 parameters.

Empirical formula	$C_{48}H_{34}P_2$	γ / °	90
Formula weight	672.69	Volume / $Å^3$	1714.37 (11)
Crystal system	Orthorhombic	Z	2
Space group	Pnma	Temperature / K	150 (2)
a / Å	17.6263 (6)	Wavelength / Å	0.71073
b / Å	13.0087 (5)	Density calc. / Mg/m^3	1.303
c / Å	7.4767 (3)	μ(Mo-Kα) / mm^{-1}	0.163
α / Å	90	R_1 [$F>4\sigma(F)$]	0.0388
β / Å	90	WR_2 (all data)	0.1082

Table 6.16 Crystallographic data for 45

6.7 References

1. I. V. Howell, S. A. J. Pratt and L. M. Venanzi, *J.Chem. Soc.*, 1961, 3167

2. J. G. Hartley, L. M. Venanzi and D. C. Goodall, *J.Chem. Soc.*, 1963, 3930

3. J. W. Dawson and L. M. Venanzi, *J. Am. Chem. Soc.*, 1968, **90**, 7229

4. J. G. Hartley, D. G. E. Kerfoot and L. M. Venanzi, *Inorg. Chim. Acta*, 1967, **1**, 145

5. A. Orlandini and L. Sacconi, *Inorg. Chem.*, 1976, **15**, 78

6. L. M. Venanzi, *Angew. Chem. Int. Ed.*, 1964, **3**, 453

7. B. R. Higginson, C. A. McAuliffe and L. M. Venanzi, *Helv. Chim. Acta*, 1975, **58**, 1261

8. A. Orlandini and L. Sacconi, *Inorg. Chim. Acta*, 1976, **19**, 61

9. M. T. Halfpenny, J. G. Hartley and L. M. Venanzi, *J. Chem. Soc. A*, 1967, 627

10. J. W. Dawson, D. G. E. Kerfoot, C. Preti and L. M. Venanzi, *Chem. Commun.*, 1968, 1687

11. I. V. Howell and L. M. Venanzi, *Inorg. Chim. Acta*, 1968, **3**, 121

12. I. V. Howell and L. M. Venanzi, *J. Chem. Soc. A*, 1967, 1007

13. S. Harder, L. Brandsma, J. A. Kanters, A. Duisenberg and J. H. Van Lenthe, *J. Organomet. Chem.*, 1991, **420**, 143

14. D. P. Tate, W. R. Knipple and J. M. Augl, *Inorg. Chem.*, 1962, **1**, 432

15. D. B. Snyder, S. J. Schauer, D. P. Eyman, J. L. Moler and J. J. Weers, *J. Am. Chem. Soc.*, 1993, **115**, 6718

16. W. L. Ingham and N. J. Coville, *Inorg. Chem.*, 1992, **31**, 4084

17. A. Jacobi, G. Huttner, U. Winterhalter and S. Cunskis, *Eur. J. Inorg. Chem.*, 1998, 675

18. H. K. Sharma, I. Haiduc and K. H. Pannell, *Transition Metal Complexes of Ge, Sn & Pb*, in *The Chemistry of Organic Germanium, Tin and Lead Compounds*, Z. Rappoport, Editor. 2002, John Wiley & Sons Ltd

19. R. Colton and M. J. McCormick, *Co-ord. Chem. Rev.*, 1980, **31**, 1

20. E. W. Abel and G. Wilkinson, *J. Chem. Soc.*, 1959, 1501

21. R. H. Reimann and E. Singleton, *J.Chem. Soc., Dalton. Trans.*, 1973, 841

22. R. H. Reimann and E. Singleton, *J.Chem. Soc., Dalton. Trans.*, 1974, 808

23. M. H. Quick, R. J. Angelici, K. J. Reimer and A. Shaver, *Inorg. Synth.*, 1990, **28**, 156

24. R. F. Bryan, *J.Chem. Soc. (A)*, 1968, 696

25. M. T. Halfpenny and L. M. Venanzi, *Inorg. Chim. Acta*, 1971, **5**, 91

26. M. O. Albers, T. V. Ashworth, H. E. Oosthuizen and E. Singleton, *Inorg. Synth.*, 1989, **26**, 68

27. M. Camalli and F. Caruso, *Inorg. Chim. Acta*, 1987, **127**, 209

28. T. A. Stephenson and G. Wilkinson, *J. Inorg. Nuclear Chem.*, 1966, **28**, 945

7 Conclusions

The aim of this thesis was to investigate the design, synthesis and coordination chemistry of novel tripodal ligands. The ligands were designed to impose C_3 symmetry on a metal centre, which would render the complex suitable for use in asymmetric catalysis.

This thesis has described the synthesis of six novel tripodal ligand systems. The tripods all have the generic structure illustrated in Figure 7.1.

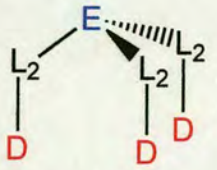

E Central atom
L Linker atom
D Donor atom

Figure 7.1 Generic structure of tripodal ligands described in this thesis

The ligands all have two atoms linking the three donor atoms to the central (bridgehead) atom. This design approach was taken because tridentate coordination of the ligand to a metal results in the formation of three eight membered chelate rings. The three rings are predicted to twist to relieve the strain associated with the large chelate rings, resulting in a C_3 symmetric complex.

The systems vary in terms of the central atom; the donor atom; and the flexibility of the tripod arms, which is partially dictated by the nature of the linker atoms. The nature of these variables for the ligand systems are shown in Table 7.1.

Chapter	Ligand System	Central Atom	Donor Atom	Linker Atoms
2	$OP(2\text{-}SHC_6H_4)_3$	P	S	2 sp^2 C
2	$OP(2\text{-}OHC_6H_4)_3$	P	O	2 sp^2 C
3	$HOC(C_5H_4NO)_3$	C	O	1 sp^2 C, 1 sp^2 N
4	$CH_3N(CH_2N_2C_6H_4)_3$	N	N	1 sp^2 C, 1 sp^3 C
5	$N(CH_2CH^iPrNRMe)_3$	N	N	2 sp^3 C
6	$^tBuSn(C_6H_4PPh_2)_3$	Sn	P	2 sp^2 C

Table 7.1 Novel ligand systems described within this thesis

Unfortunately none of the ligands were shown to coordinate to the metal through all three of the tripod arms to produce complexes of the desired C_3 symmetry.

It was not possible to form metal complexes with the ligands $OP(2\text{-}SHC_6H_4)_3$, **4**, and $OP(2\text{-}OHC_6H_4)_3$, **9**, described in Chapter 2. It is most likely that there are energetically more favourable side reactions taking place, preventing the desired mode of coordination from occurring. For **4**, the ligand probably dimerises *via* the formation of a disulphide bridge, limiting the coordination to metals. In the case of **9**, polymeric species may be formed through phenolate bridging. Alternatively, the coordination of the phosphorus oxide oxygen to the metal will leave at least one of the tripod arms free for coordination, possibly to another metal.

The third ligand system, $HOC(C_5H_4NO)_3$, **15**, which contains 2-pyridyl-*N*-oxide donors, has a similar basic framework to **4** and **9** but with different atoms. This ligand also contains a substituent on the bridgehead atom that is able to coordinate to a metal centre. Again, it is likely that this unfavourable process occurs due to the formation of a more stable chelate ring than when the ligand coordinates through the three tripod arms. Unfortunately time constraints and the lengthy synthesis of this ligand limited the extent of the coordination studies carried out with this system. More work could be carried out to replace the remaining substituent on the central atom with a non-coordinating one. This would remove the possibility of alternative chelate rings forming.

The synthesis of the alkylated benzimidazole system proved to be extremely difficult. Many different approaches were taken to alkylate the central nitrogen atom, none of which were satisfactory. In retrospect, the desired alkylated ligand could have formed in small quantities. It may be that the alkyl group is bonded only weakly to the central nitrogen atom, and upon metal complex formation it is easily lost, allowing the central nitrogen atom to bond to the metal. This will result in the formation of three five-membered chelate rings, conferring greater stability on the metal complex. However the resulting complex possesses C_{3v} symmetry and is therefore achiral.

It was not possible to synthesise $N(CH_2CH^iPrNRMe)_3$ (R = phosphorus-2,2'-binaphthol). It is likely that the phosphoramidite substituents would make this ligand too sterically hindered to coordinate to a metal ion through all three arms.

QSn, **36**, described in chapter 6 is the most sterically bulky of the ligand systems studied, due to the presence of phenyl rings on the donor atoms. There are two sp^2 carbon linker atoms, making this a highly rigid system. A number of novel complexes were obtained with QSn, three of which were characterized by X-ray crystallography. None of the complexes show the desired coordination of the ligand to the metal through all three tripod arms. Comparing the metal complexes obtained with W, Mo and Mn, it appears that the smaller the metal, the more unfavourable the formation of a tridentate complex. QSn coordinates to tungsten, the largest of the three metals, through two of the arms with the remaining arm uncoordinated. Coordination to the smaller molybdenum results in coordination of two of the arms and partial fragmentation of the ligand. Complexation to manganese, the smallest of the three metals results in two of the ligand arms coordinating to the metal and complete fragmentation of the third arm. The structures obtained with the different metals are very varied, implying that the combination of ligand and metal would have to be finely controlled to synthesise a complex with C_3 symmetry, if this is even feasible. The formation of tin-transition metal bonds *via* activation of one of the Sn-C bonds in this ligand appears to be a relatively facile process leading to a range of unusual structures. This tendency should be reduced for the silicon centred ligand 'QSi' given the greater Si-C bond strength, however this system proved to be inaccessible using the route used for QSn.

The extreme difficulty in synthesising tridentate metal complexes of C_3 symmetry using the tridentate ligand systems described within this thesis suggests that this is a non-trivial route to form novel asymmetric catalysts. The results suggests that the ligands may be too rigid to coordinate to metals to form tridentate complexes. It may be that more flexible ligands containing sp^3 linker atoms would be better suited to tridentate coordination. However, the thermodynamics of tripod ligand coordination is favoured by reducing the flexibility of the free ligand to reduce the loss of entropy on coordination. There is thus a delicate balance between this factor and the need to provide a favourable geometry to maximise the enthalpy of coordination. The work illustrates the high degree of control the ligand design has on its coordination properties.